UNIVERSITY OF CALIFORNIA, MERCED

High-throughput Analysis of WNT Signaling Pathway in Osteoblasts

A dissertation submitted in partial satisfaction of the requirements for the degree Doctor of Philosophy

in

Quantitative and Systems Biology

by

Aimy Sebastian

Committee in charge:

Dr. Suzanne S. Sindi, Chair
Dr. David H. Ardell
Dr. Gabriela G. Loots
Dr. Jennifer O. Manilay

2016

The Dissertation of Aimy Sebastian is approved, and it is acceptable in quality and form for publication on microfilm and electronically:

Gabriela G. Loots

Jennifer O. Manilay

David H. Ardell

Suzanne S. Sindi, Chair

Date

University of California, Merced

2016

Table of Contents

Signature Page iii

Table of Contents iv

List of Figures vi

List of Tables viii

Acknowledgements ix

VITA x

Abstract xiii

Chapter 1: Introduction 1

1.1. WNT proteins 1

1.2. WNT signaling pathways 2

1.3. Overview of bone development and metabolism 5

1.4. WNT signaling in bone development and homeostasis 10

1.5. Objectives of the study 23

Chapter 2: High-throughput Sequencing to Study Gene Expression and Gene Regulation 27

2.1. Introduction 27

2.2 High-throughput sequencing technologies 27

2.3. Profiling gene expression changes with RNA-seq 28

2.4. Studying transcription regulation with ChIP-seq 37

2.5. Summary 41

Chapter 3: WNT Co-receptors LRP5 and LRP6 Differentially Mediate WNT3A Signaling in Osteoblasts 43

3.1. Introduction 43

3.2. Methods 43

3.3. Results 46

3.4. Discussion 57

Chapter 4: Integrative Analysis of ChIP-seq and RNA-seq Experiments Identifies WNT3A Inducible Regulatory Elements in Osteoblasts 97
4.1. Introduction 97
4.2. Methods 98
4.3. Results 100
4.4. Discussion 106
Chapter 5: WNT16 Regulates the Expression of Canonical and Non-canonical WNT Targets in Osteoblasts 121
5.1. Introduction 121
5.2. Methods 122
5.3. Results 123
5.4. Discussion 129
Chapter 6: Conclusion 148
References 151

List of Figures

1. Figure 1.1: Dendrogram of mouse WNT proteins 1
2. Figure 1.2: Canonical WNT signaling 3
3. Figure 1.3: Non-canonical WNT pathways 4
4. Figure 1.4: Structure of a long bone 6
5. Figure 1.5: Osteoblast differentiation 7
6. Figure 1.6: Bone formation 8
7. Figure 1.7: Bone remodeling 9
8. Figure 1.8: Osteoporotic bone 10
9. Figure 1.9: Cell type specific promoters commonly used to drive transgene or Cre-recombinase expression in rodent animal models 11
10. Figure 2.1: Fastq file format 29
11. Figure 2.2: RNA-seq data analysis workflow 30
12. Figure 2.3: Low and high quality RNA-seq data 31
13. Figure 2.4: Read mapping 33
14. Figure 2.5: RNA-seq data before and after filtering 34
15. Figure 2.6: RNA-seq data before and after normalization 35
16. Figure 2.7: Heatmap representation of differentially expressed genes 36
17. Figure 2.8: ChIP-seq experimental workflow 38
18. Figure 2.9: Enhancers 39
19. Figure 2.10: Osteoblast enhancers 41
20. Figure 3.1: Experimental design 47
21. Figure 3.2: qPCR analysis of known WNT targets 48
22. Figure 3.3: Enriched GO terms associated with WNT3A targets 49
23. Figure 3.4: Expression profiles of WNT3A targets during the differentiation of early pre-osteoblast to mature osteoblasts (Day 2 to Day 18) 51
24. Figure 3.5: Osteoblast proliferation assay 52
25. Figure 3.6: Calvarial injection 53
26. Figure 3.7: Histology and µ-CT data 54
27. Figure 3.8: Venn diagrams of sets of genes differentially expressed in $Lrp5^{-/-}$, $Lrp6^{-/-}$ and $Lrp5^{-/-}$;$Lrp6^{-/-}$ osteoblasts compared to respective controls 56
28. Figure 3.9: Venn diagrams of significantly differentially expressed genes in WNT3A-treated WT, $Lrp5^{-/-}$, $Lrp6^{-/-}$ and $Lrp5^{-/-}$;$Lrp6^{-/-}$ osteoblasts. 57
29. Figure 4.1: TCF/LEF binding sites in Axin2 promoter 101
30. Figure 4.2: Distribution of overlapping H3K4me1 and H3K27ac peaks 102
31. Figure 4.3: Overlapping H3K4me1 and H3K27ac peaks 102
32. Figure 4.4: Enriched ontology terms associated with osteoblast enhancers 103
33. Figure 4.5: Putative WNT inducible enhancer in Ptch1 intronic region 104
34. Figure 4.6: Enhancer validation 105

35. Figure 4.7: AP-1 binding motif.....105
36. Figure 5.1: qPCR validation of canonical WNT targets in WNT5A treated osteoblasts.....124
37. Figure 5.2: Enriched GO terms associated with WNT16 targets.....126
38. Figure 5.3: Expression profiles of WNT16 targets during the differentiation of pre-osteoblast to mature osteoblasts (Day 2 to Day 18) 127
39. Figure 5.4: Venn diagrams of genes differentially expressed in WNT16, WNT3A and WNT5A treated osteoblasts compared to sham-treated osteoblasts 128

List of Tables

1. Table 1.1: Human skeletal disorders associated with mutations in key WNT pathway members 24
2. Table 1.2: Mouse phenotypes associated with key WNT pathway members.....24
3. Table 3.1: List of qRT-PCR primers.....59
4. Table 3.2: Genes differentially expressed inWNT3A treated WT, $Lrp5^{-/-}$, $Lrp6^{-/-}$ and $Lrp5^{-/-}$;$Lrp6^{-/-}$ osteoblasts compared to sham treated controls 59
5. Table 3.3: WNT3A targets with bone metabolism phenotypes.....75
6. Table 3.4: Enriched signaling pathways associated with genes up- and down-regulated by WNT3A in WT osteoblasts.....77
7. Table 3.5: Expression profiles of WNT3A targets during osteoblasts differentiation 78
8. Table 3.6: Genes differentially regulated in *Lrp5*$^{-/-}$, *Lrp6*$^{-/-}$ and *Lrp5*$^{-/-}$*;Lrp6*$^{-/-}$ osteoblasts compared to sham treated controls.....82
9. Table 4.1: WNT3A activated genes with TCF/LEF binding sites in their promoter.....107
10. Table 4.2: WNT inducible enhancers identified near WNT3A targets 108
11. Table 5.1 List of qRT-PCR primers 130
12. Table 5.2: Genes differentially regulated by WNT16 and WNT5A.....130
13. Table 5.3: Expression profiles of WNT16 targets during osteoblasts differentiation.....144

Acknowledgements

First, I would like to thank my parents Mary and Devassy for their guidance, sacrifices and endless love and my husband Basil for being a source of inspiration and positive energy in my life. I would also like to express my deepest gratitude to my sister Anu who has always been by my side.

I am deeply grateful to my advisor Dr. Gaby Loots for her invaluable guidance and support. She has been an inspiring and attentive mentor, indispensable in providing stimulating and nurturing scientific environment enriched with helpful comments, ideas and insights throughout my time at her lab. Without her contributions, none of this work would have been possible.

I have been fortunate to work with a group of very talented and motivated colleagues. I would like to express my deepest gratitude to Nicholas Hum and Deepa Murugesh for all their help with animal work and cell culture experiments. Additionally, I would like to thank other members of the Loots lab, Cristal Yee, Jiun Chang, Kelly Martin and Melanie Mendez for their support and friendship.

I would like to extend my gratitude to my committee members, Dr. Suzanne Sindi, Dr. Jennifer Manilay and Dr. David Ardell for their guidance and advice on the projects that are presented in this dissertation.

I also wish to thank Dr. Aris Economides and Dr. Sarah Hatsell (Regeneron) for all the help with RNA sequencing and Dr. Blaine Christiansen (UC Davis) for helping me with μCT analysis.

For this study, Deepa Murugesh performed animal breading, genotyping and calvarial injections. Nicholas Hum performed osteoblast isolation and culture, cell culture based assays, RNA-isolation and sequencing. Part of the sequencing was performed at Regeneron. Dr. Blaine Christiansen performed the μCT scans and analysis. The dissertation author performed the experimental design with guidance from Dr. Gaby Loots, analyzed the RNA-seq, ChIP-seq and other experimental data, performed functional annotation, data interpretation and synthesis.

VITA

EDUCATION

Ph.D. Quantitative and Systems Biology **2012-present**
University of California, Merced

M.Sc. Bioinformatics **2008**
Amrita University, India

B.Sc. Bioinformatics **2005**
Punjab Technical University, India

Certificate Course in Information Technology **2004**
National Institute of Information Technology, India

PUBLICATIONS

- **Sebastian, A.**, Hum, N. R., Murugesh, D. K., Hatsel, S., Economides, A. N. and Loots G. G. Wnt co-receptors Lrp5 and Lrp6 differentially mediate Wnt3a signaling in osteoblasts (in preparation).
- Chang, J. C., Christiansen, B. A., Collette, N. M., **Sebastian, A.**, Murugesh, D. K., Hum, N. R., Hatsell, S., Economides, A. N., Blanchette, C. D. and Loots G. G. SOST/Sclerostin reduces the severity of post traumatic osteoarthritis by inhibiting MMP2/3(in preparation).
- **Sebastian, A.** and Loots, G.G. Genomic Profiling in Bone. *Genetics of Bone Biology and Skeletal Disease*. Edited by R. V. Thakker. (in press)
- **Sebastian, A.** and Loots, G.G. Transcriptional Control of *Sost* in Bone. *Bone*. DOI: 10.1016/j.bone.2016.10.009 (2016)
- Chang, J. C.*, **Sebastian, A.***, Murugesh, D. K., Hatsell, S., Economides, A. N., Christiansen, B. A. and Loots, G. G. Global molecular changes in a tibial compression induced ACL rupture model of post-traumatic osteoarthritis. *Journal of Orthopaedic Research*. DOI: 10.1002/jor.23263 (2016). ***Equal contribution***.
- **Sebastian, A**., Hum, N. R., Hudson, B. D. and Loots, G. G. Cancer–Osteoblast Interaction Reduces Sost Expression in Osteoblasts and Up-Regulates lncRNA MALAT1 in Prostate Cancer. *Microarrays*, 4(4):503-519 (2015).
- Hudson, B. D., Hum, N. R., Thomas, C. B., Kohlgruber, A., **Sebastian, A**., Collette, N. M., Coleman, M. A., Christiansen, B. A. and Loots G. G. SOST inhibits prostate cancer invasion. *PLOS ONE*, 10(11):e0142058 (2015).
- Collette, N. M., Yee, C. S. N., Murugesh, D. K., **Sebastian, A**., Taher, L., Gale, N. W., Economides, A. N., Harland, R. and Loots, G. G. Sost and its Paralog Sostdc1 coordinate digit number in a Gli3-dependent manner. *Developmental Biology*. 383(1), 90-105 (2013).
- **Sebastian, A.** and Ramakrishnan, V. Computational Biology Applications. *Nutri - horticulture*. Edited by K V Peter. ISBN: 9788170357766.

- **Sebastian, A.**, Bender, A. and Ramakrishnan, V. Virtual Activity Profiling of Bioactive Molecules by 1D Fingerprinting, *Molecular Informatics*, 29(11), 773–779 (2010).
- Prasad, T. S. K., Goel, R., Kandasamy, K., Keerthikumar, S., Kumar, S., Mathivanan, S., Telikicherla, D., Raju, R., Shafreen, B., Venugopal, A., Balakrishnan, L., Marimuthu, A., Banerjee, S., Somanathan, D. S., **Sebastian, A.**, Rani, S., Ray, S., Kishore, C. J. H., Kanth, S., Ahmed, M., Kashyap, M., Mohmood, R., Ramachandra, Y. L., Krishna, V., Rahiman, A. B., Mohan, S., Ranganathan, P., Ramabadran, S., Chaerkady, R. and Pandey, A. Human Protein Reference Database - 2009 update. *Nucleic Acids Research*, 37, D767-D772 (2009).

CONFERENCE PRESENTATIONS

1. **Sebastian, A.,** Chang, J. C., Christiansen, B. A., Murugesh, D. K., Hatsel, S., Economides, A. N. and Loots G. G. Differential regulation of post-traumatic osteoarthritis associated genes in STR/ort, MRL/MpJ and C57BL/6 Mice. *Bone-omics: Translating Genomic Discoveries into Clinical Applications symposium 2016, Atlanta, Georgia***.**
2. **Sebastian, A.,** Hum, N. R., Murugesh, D. K., Hatsel, S., Economides, A. N. and Loots G. G. Igfbp2, Inhbb and Sema4f are Wnt3a-inducible in osteoblasts, independent of Lrp5/6 receptors. *The American Society for Bone and Mineral Research Annual Meeting 2016, Atlanta, Georgia***.**
3. **Sebastian, A.,** Chang, J. C., Christiansen, B. A., Murugesh, D. K., Hatsel, S., Economides, A. N. and Loots G. G. Differential regulation of post-traumatic osteoarthritis associated genes in STR/ort, MRL/MpJ and C57BL/6 Mice. *The American Society for Bone and Mineral Research Annual Meeting 2016, Atlanta, Georgia***.**
4. **Sebastian, A.**, Martin, K.A., Pan, C.X., Ma, A., deVere White, R. and Loots, G.G. Transcriptome analysis of patient-derived bladder cancer xenografts identifies genes associated with chemoresistance. *Quantitative and Systems Biology retreat 2016, University of California, Merced, California.*
5. **Sebastian, A.,** Yee, C.S., Murugesh, D. K., Hatsel, S., Economides, A. N., Robling, A.G. and Loots G. G. Transcription factor Mef2C has both an anti-anabolic and a pro-catabolic function in bone. *The Orthopaedic Research Society Annual Meeting 2016, Orlando, Florida.*
6. **Sebastian, A**., Martin, K.A., Pan, C.X., Ma, A., deVere White, R. and Loots, G.G. Transcriptome analysis of patient-derived bladder cancer xenografts identifies genes associated with chemoresistance. *The American Association for Cancer Research Annual meeting 2016, New Orleans, Louisiana.*
7. **Sebastian, A.,** Hum, N. R., Murugesh, D. K., Hatsel, S., Economides, A. N. and Loots G. G. Integrative analysis of RNA-seq and ChIP-seq data identifies Wnt3a inducible genes and regulatory elements in osteoblasts. *The American Society for Bone and Mineral Research Annual Meeting 2015, Seattle, Washington.*
8. **Sebastian, A.,** Murugesh, D. K., Robling A. G., Hatsel S., Economides, A. N. and Loots G. G. Mef2C targets energy metabolism genes in bone. *The American*

Society for Bone and Mineral Research Annual Meeting 2015, Seattle, Washington.

9. **Sebastian, A.**, Hum, N. R., Christiansen, B. A. and Loots G.G. SOST inhibits prostate cancer invasion by repressing long noncoding RNA MALAT1. *UC Davis Comprehensive Cancer Center Annual Cancer Research Symposium 2015, Sacramento, California.*
10. **Sebastian A.,** Hum, N. R., Murugesh, D. K., Hatsel, S., Economides, A. N. and Loots G.G. Global gene expression analysis to identify Wnt targets in osteoblasts. *Quantitative and Systems Biology retreat 2014, University of California, Merced, California.*

HONORS AND AWARDS

- The American Society for Bone and Mineral Research travel award, 2016
- 2nd place, poster competition, Annual Cancer Research Symposium 2015, UC Davis Comprehensive Cancer Center, Sacramento, California.
- Summer research fellowship 2015, University of California, Merced.
- Summer research fellowship 2013, University of California, Merced.
- 1st Rank, M.Sc. Bioinformatics, Amrita University, India: Achieving the highest GPA among all Amrita university Bioinformatics graduate students.

Abstract

High-throughput Analysis of WNT Signaling Pathway in Osteoblasts

by

Aimy Sebastian

Doctor of Philosophy

University of California, Merced, 2016

Dr. Suzanne S. Sindi, Chair

Dr. David H. Ardell

Dr. Gabriela G. Loots

Dr. Jennifer O. Manilay

Multiple signaling pathways have been shown to regulate bone development and metabolism, and the WNT signaling pathway is emerging as one of the most crucial contributors. Several WNT ligands, receptors and WNT antagonists are expressed in bone and play a role in maintaining postnatal bone homeostasis. However, specific functions of individual WNT pathway members in bone are only beginning to be elucidated. Investigating the role of WNT signaling in bone development and metabolism will provide important implications for the treatment of fractures and bone thinning disorders such as osteoporosis and osteopenia. The focus of my thesis is to elucidate the functions of three out of nineteen WNT ligands and WNT co-receptors LRP5 and LRP6 in osteoblasts (bone forming cells).

In this thesis, I investigated the role of WNT ligands WNT3A, WNT5A and WNT16 in osteoblasts to identify the target genes regulated by these WNTs and to understand the molecular mechanism by which these WNTs regulate bone metabolism. Gene expression analysis of neonatal osteoblasts treated with recombinant WNTs identified more than 1000 genes regulated by WNT signaling in osteoblasts and suggested that WNT3A and WNT16 positively regulate early stages of osteoblast differentiation and inhibit osteoblast maturation/mineralization.

I also studied the role of WNT co-receptors LRP5 and LRP6 in mediating canonical WNT signaling. LRP5 and LRP6 are two WNT co-receptors that have been linked to bone development and metabolism. Both LRP5 and LRP6 are required for normal postnatal bone homeostasis. However, their specific roles are not well understood. To determine the roles of LRP5 and 6 in mediating canonical WNT signaling, osteoblasts lacking *Lrp5*, *Lrp6* and both *Lrp5* and *6* were treated with recombinant WNT3A. The RNA isolated from all WNT3A treated samples were sequenced and analyzed to identify genes regulated through LRP5 and LRP6 and genes that do not require LRP5/6 for WNT3A induced transcriptional regulation. This study revealed that LRP6 plays a dominant role in mediating WNT3A signaling in osteoblasts.

Canonical WNTs such as WNT3A regulate target gene expression by activating TCF/LEF family transcription factors. These transcription factors bind to promoters and/or enhancers of target genes to induce gene transcription. To identify direct targets of canonical WNT signaling, using ChIP-seq, I identified TCF/LEF binding sites near WNT3A targets. More than 80% WNT3A targets had TCF/LEF binding sites in their promoter and/or enhancers. This study also identified more than 500 putative WNT inducible enhancers in osteoblasts. A subset of predicted WNT inducible enhancers was validated experimentally to confirm WNT3A inducible enhancer activity.

My findings expand our current understanding of the role of WNT signaling pathway in regulating osteoblast differentiation and function, as well as contribute to the knowledge of the WNT signaling pathway itself. The WNT target genes identified in this study may be further explored for their therapeutic potential in treating osteoporosis and other bone disorders.

Chapter 1

Introduction

1.1 WNT proteins

The WNTs constitute a large family of highly conserved secreted signaling proteins of about 40 kDa in size [1]. At least 19 WNT proteins are expressed in mammals (Figure 1.1), corresponding to 19 distinct genetic loci [2]. The name 'WNT' is derived from the first two members of the family discovered: *Wingless* (*Wg*), a gene involved in embryonic development of fruit fly and *Int-1*, an oncogene activated by mouse mammary tumor virus in virally induced murine mammary carcinomas, which later was identified as a homolog of *Wg* [1]. Since the discovery of the first WNT gene more than three decades ago, great advances have been made in understanding the molecular events regulated by WNTs (reviewed in [3]). The WNT signaling pathway has been shown to play a major role in regulating diverse processes during embryogenesis and adult tissue homeostasis including stem cell renewal, cell proliferation, differentiation, migration, and apoptosis. Dysregulation of WNT signaling leads to multiple diseases including cancer and degenerative disorders [3-6]. Knockout studies in mice have shown that germline deletion of several WNTs including *Wnt1*, *Wnt3*, *Wnt3a*, *Wnt4*, *Wnt5a*, *Wnt7b*, *Wnt9a*, *Wnt9b*, and *Wnt11* leads to lethality (reviewed in [7]), highlighting the importance of WNT signaling in development.

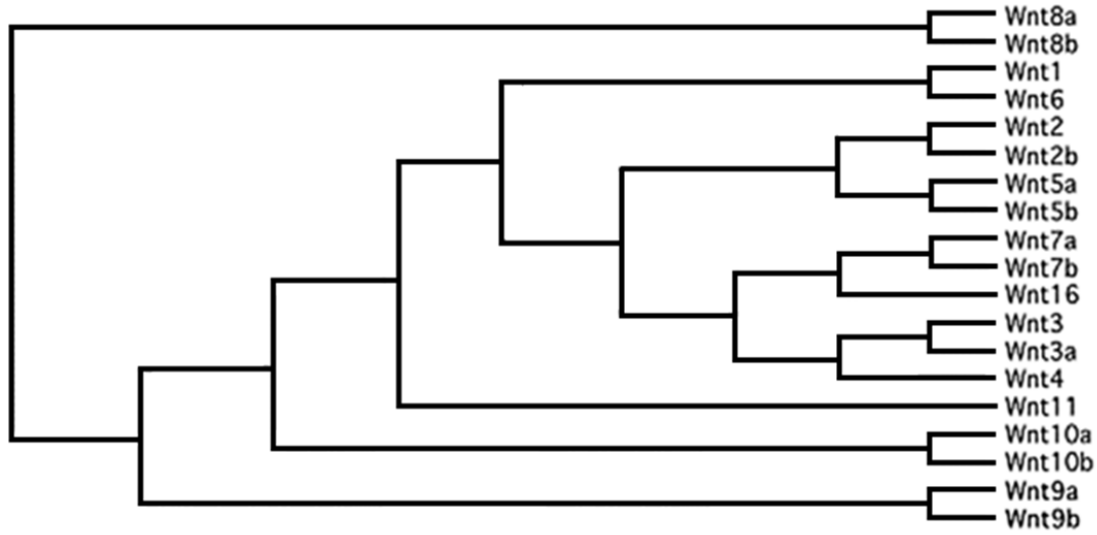

Figure 1.1: Dendrogram of mouse WNT proteins*. Dendrogram shows 19 WNT proteins expressed in mouse.*

WNT signaling plays a major role in regulating skeletal development and postnatal bone homeostasis and it is emerging as a therapeutic target for skeletal diseases such as osteoporosis and treating bone fracture [8,9]. However, very little is known about the specific roles played by different WNT ligands, WNT receptors/co-receptors and other pathway members in bone development, repair and remodeling. The major goal

of my thesis work is to increase our understanding of the molecular mechanisms by which WNT signaling pathway regulate bone metabolism. In my thesis work, I studied the role of three WNT ligands WNT3A, WNT5A and WNT16 and WNT co-receptors LRP5 and LRP6 in osteoblasts (bone forming cells) and identified the target genes regulated by these WNTs.

In the following sections, I will provide an overview of WNT signaling and bone metabolism, and a review of studies conducted in the past to understand WNT signaling in the context of bone development and metabolism. Finally, I will discuss the objectives of my study.

1.2. WNT signaling pathways

WNT proteins activate multiple intracellular signaling cascades to perform their functions (see Figure 1.2/1.3 and discussion below). Based on early studies WNT signaling pathways are classified as either canonical or non-canonical pathways [10].

1.2.1 Canonical WNT signaling

The best understood WNT signaling pathway is the 'canonical' or β-catenin-dependent signaling pathway (reviewed in [10]). In the absence of WNT ligands, cytoplasmic β-catenin forms a complex with adenomatous polyposis coli (APC), Axin, glycogen synthase kinase 3β (GSK3β) and casein kinase 1 (CK1). This multi-protein complex is called the β-catenin destruction complex. APC and Axin act as scaffold proteins which facilitate the amino-terminal phosphorylation of β-catenin *via* the kinases GSK3β and CK1. Phosphorylated β-catenin is recognized by the beta-transducin repeat containing E3 ubiquitin protein ligase (β-Trcp) and is subsequently polyubiquitinated [11] and degraded by the proteasome, thereby maintaining low levels of β-catenin in the cytoplasm and nucleus. The WNT ligands activate this signaling pathway by interacting with cell surface receptors of Frizzled (FZD) family and low-density lipoprotein receptor-related protein (LRP) co-receptors. This induces the phosphorylation and subsequent activation of Dishevelled (DVL/DSH) proteins. Activated DVL recruits the β-catenin destruction complex to plasma membrane which subsequently leads to inactivation of the destruction complex and β-catenin stabilization. Stabilized β-catenin translocates to the nucleus where it interacts with members of the T-cell factor/lymphoid enhancer factor (TCF/LEF) family of transcriptional activators and initiates transcription of WNT-responsive genes (Figure 1.2) [1,10,12]. Beyond these interactions, very little is currently known about the nature of WNT-responsive genes in different cellular contexts.

1.2.2 Non-canonical WNT Signaling

Non-canonical WNT signaling encompasses those pathways that do not use LRP and β-catenin–TCF/LEF module for downstream signaling; however, FZD and DVL play a role in non-canonical WNT signaling pathways as well [13]. Major non-canonical WNT pathways include the planar cell polarity (PCP) pathway (Figure 1.3A) and WNT/Ca^{2+} pathway (Figure 1.3B). In the PCP pathway, WNTs bind to FZD and activate DVL. DVL then signals through Dishevelled associated activator of morphogenesis 1 (DAAM1) to activate Rho or Rac GTPases. Rho GTPase activates Rho-associated protein kinase (ROCK) to regulate cytoskeletal changes and Rac activates c-Jun amino-terminal

kinase (JNK) which subsequently leads to the activation of AP-1 family transcription factors [14]. Several transmembrane proteins including receptor tyrosine kinase-like orphan receptor (ROR), Receptor-Like Tyrosine Kinase (RYK) and protein tyrosine kinase 7 (PTK7) were implicated as co-receptors of FZD in the PCP pathway (reviewed in[10]).

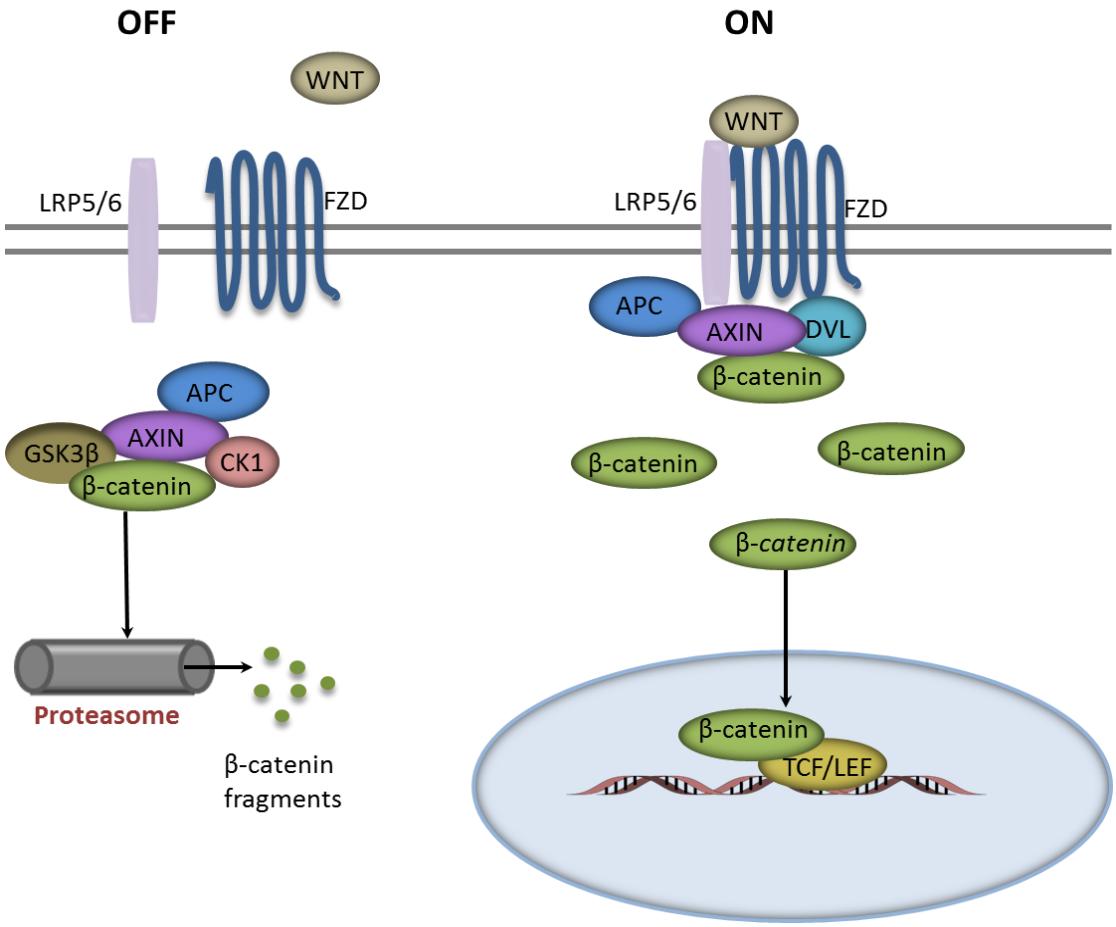

Figure 1.2: Canonical WNT signaling. *In the absence of WNT signaling a multi-protein complex called the β-catenin destruction complex is formed which consists of β-catenin, Axin, APC, GSK3β and CK1. Subsequently, β-catenin gets phosphorylated by GSK3β and CK1 and undergoes proteasomal degradation. WNT proteins activate canonical signaling by interacting with FZD receptors and co-receptors LRP5/6. Activation of WNT signaling leads to inactivation of the destruction complex and β-catenin stabilization. Stabilized β-catenin translocates to the nucleus and interacts with TCF/LEF family of transcriptional activators and activates gene transcription*

In the WNT/Ca^{2+} pathway, WNT-FZD binding activates phospholipase C (PLC) which then hydrolyzes membrane-bound phosphatidyl-inositol-4,5-bisphosphate (PIP2), generating inositol triphosphate (IP3) and diacylglycerol (DAG). IP3 binds to its receptors causing the release of intracellular calcium which results in the activation of

calcineurin (CaN)-NFAT pathway and Ca^{2+}/calmodulin dependent protein kinase II (CamKII). DAG activates protein kinase C (PKC) and mitogen-activated protein kinases (MAPKs). The WNT/Ca^{2+} pathway is involved in the regulation of several cellular processes including cell adhesion and migration [10, 14, 15]. Unlike the WNT/β-catenin signaling, many of the downstream components of non-canonical WNT pathways such as JNK/AP-1 and Ca^{2+}/NFAT are not exclusive to WNT signaling but, activated by several other signaling molecules [16, 17].

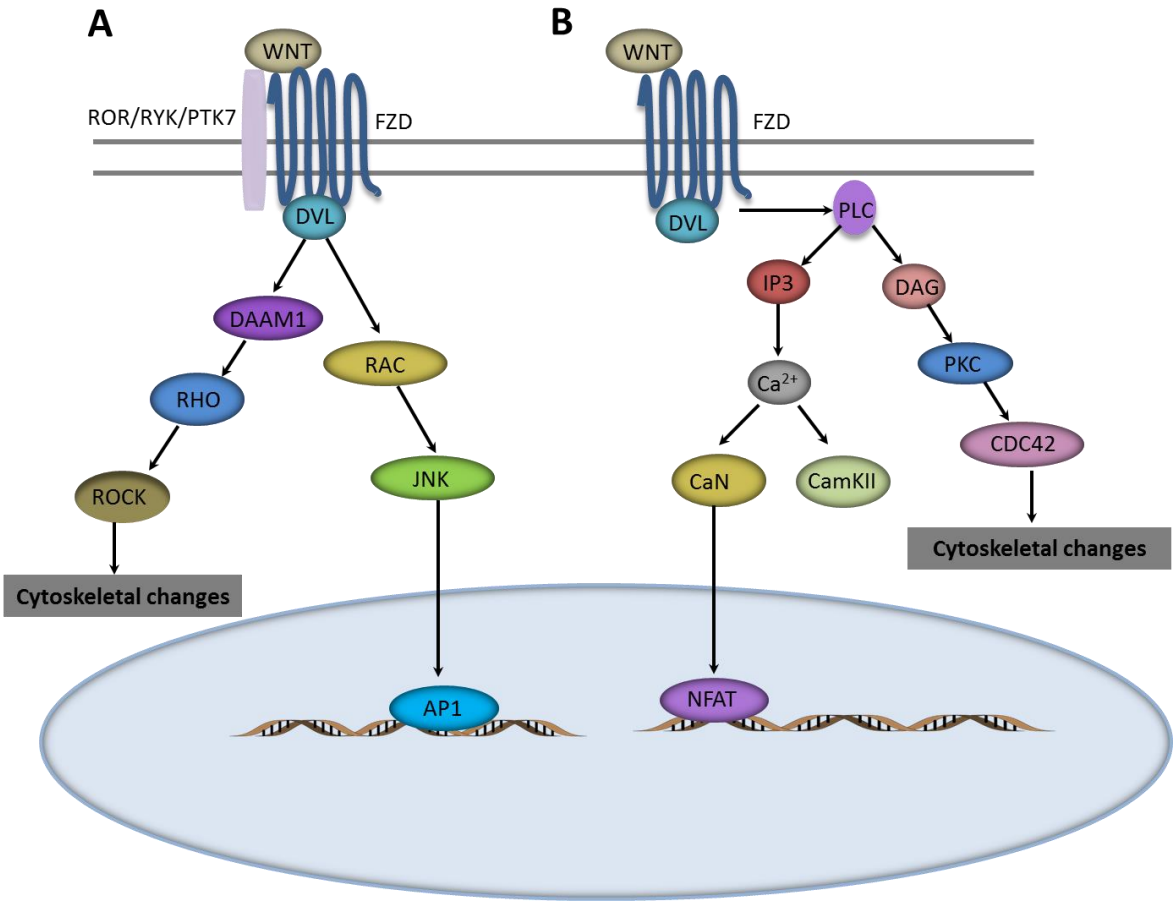

Figure 1.3: Non-canonical WNT pathways. ***A)*** *In the PCP pathway, WNTs interact with FZD and co-receptors such as ROR, RYK and PTK7 and activate RHO-ROCK signaling to regulate cytoskeletal changes or JNK pathway to regulate gene transcription.* ***B)*** *In the WNT/Ca^{2+} pathway, WNT-FZD interaction activates PLC. PLC hydrolyzes PIP2 generating IP3 and DAG. IP3 activates CaN/NFAT signaling and CAMKII signaling. DAG activates PKC signaling and regulates cytoskeletal changes.*

Canonical and non-canonical WNT pathways have been shown to inhibit each other reciprocally, thereby regulating each other's down-stream effects [18]. Secreted antagonists including secreted frizzled-related proteins (SFRP), WNT-inhibitory factor 1 (WIF1), Dickkopf (DKK) proteins, Sclerostin (SOST) and sclerostin domain containing 1 (SOSTDC1) also play a major role in modulating WNT signaling output. These secreted

proteins regulate WNT signaling either by binding directly to the WNT ligands (SFRPs and WIF1), inhibiting both canonical and non-canonical signaling pathways or by binding to the WNT co-receptors LRP5/6 (DKKs, SOST and SOSTDC1), inhibiting canonical signaling (reviewed in [3]).

The WNTs perform their diverse functions by selectively activating canonical or non-canonical pathways. Mechanisms by which WNTs selectively activate different signaling pathways are not fully understood. Few earlier studies described this as intrinsic properties of WNT ligands and suggested that some WNTs (WNT1, WNT3A, WNT8, WNT10B etc.) activate canonical signaling while others (WNT4, WNT5A, WNT11 etc.) have a preference for non-canonical pathways. However, some recent studies have shown that the WNTs activate canonical or non-canonical signaling pathways in a context dependent manner [19-21], suggesting that generalizations about WNT functions may lead to misleading assumptions in specific cell types or organ systems. Several factors including ligand concentration, WNT-receptor specificity and the presence of other modulators have been shown to play a role determining WNT signaling specificity [18, 21, 22]. These findings suggest that the current classifications of WNTs as “canonical” WNTs (WNT1, WNT3A, WNT8, WNT10B etc.) and “non-canonical” WNTs (WNT4, WNT5A, WNT11 etc.) may be revised in future studies. Future studies aiming at determining the exact mechanism by which different WNTs activate specific intracellular signaling cascades is essential to understand how WNTs perform their diverse functions.

1.3. Overview of bone development and metabolism

Bone is the main component of the skeleton and performs several important physiological functions including: (1) to provide structural support to the body, (2) to protect internal organs from injury, (3) to permit movement and locomotion, (4) to maintain mineral homeostasis, and (5) to serve as a storage depot for growth factors and cytokines [23]. Based on their architectural structure, long bones such as the femur and tibia are classified into cortical (or compact) bone and trabecular (cancellous or spongy) bone (Figure 1.4). Cortical bone is dense and solid and forms the outer layer of bones. Cortical bone has an outer periosteal surface and an inner endosteal surface. Trabecular bone is composed of porous, honeycomb-like structures and found in the epiphysis and along the marrow (medullary) cavities. The human skeleton is composed of approximately 80% cortical bone and 20% trabecular bone [23, 24].

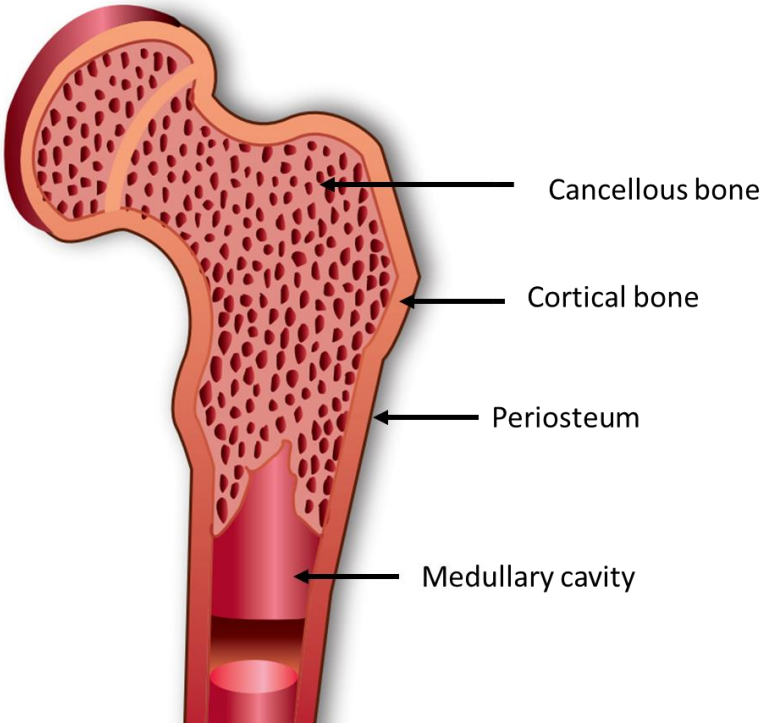

Figure 1.4: Structure of a long bone. *Long bone mainly consists of cortical bone, cancellous (trabecular) bone, an outer covering periosteum and medullary (marrow) cavity.*

There are mainly three types of cells present in bone: osteoclasts, osteoblasts and osteocytes. Osteoclasts are bone-resorbing cells of hematopoietic origin. These cells break down or enzymatically dissolve the bone matrix. Osteoblasts are bone-forming cells derived from mesenchymal stem cells (MSCs). In addition to making osteoblasts, MSCs also have the ability to differentiate into other lineages including cartilage (chondrocytes), fat (adipocytes) and muscle (myocytes) (Figure 1.5A). During osteogenic differentiation, MSCs give rise to osteoprogenitors which subsequently differentiate into pre-osteoblasts and then to mature osteoblasts [25] (Figure 1.5B). Osteocytes are terminally differentiated osteoblasts that have been spared apoptosis and remain embedded in the bone matrix [26, 27] (Figure 1.5B). Recent studies have also suggested that chondrocytes can trans-differentiate into osteoblasts in the growth plate [28]; however, the mechanism contributing to this phenomenon has yet to be determined.

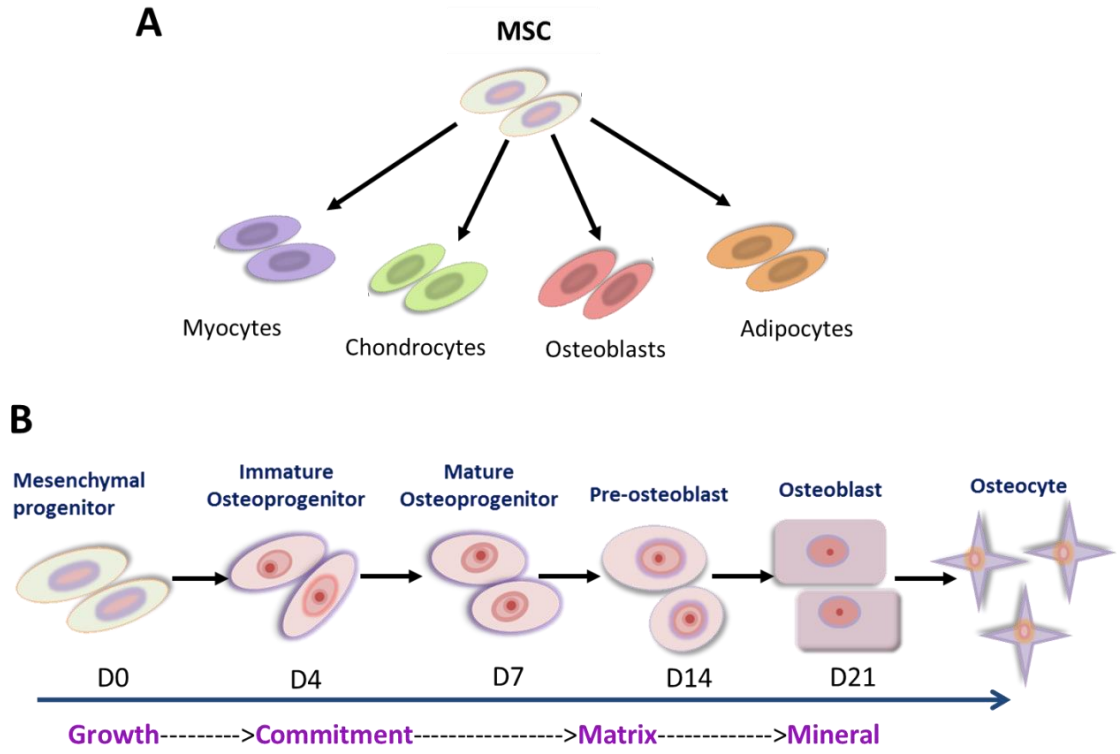

***Figure 1.5**: **Osteoblast differentiation**. **A**) MSCs can differentiate into different lineages including myocytes, chondrocytes, osteoblasts and adipocytes. **B**) During osteogenesis MSCs differentiate into to osteoprogenitors by day 4 (D4) which subsequently differentiate into pre-osteoblasts and start secreting the bone matrix (D14) and then to mature osteoblasts by day 21 and mineralize the matrix by secreting calcium phosphate (D21). Osteoblasts that get entrapped in the bone matrix will turn into osteocytes.*

1.3.1 Bone formation

During embryogenesis, bone is formed through two major mechanisms: endochondral and intramembranous bone formation. Long bones such as the femur are formed *via* endochondral bone formation during which mesenchymal progenitor cells condense and differentiate into chondrocytes to form a cartilaginous template of the future bone. After the formation of the cartilaginous template, chondrocytes in the center terminally differentiate into hypertrophic chondrocytes and secrete extracellular matrix (ECM) which then undergoes calcification. The hypertrophic chondrocytes are then eliminated by apoptosis and the calcified cartilage is invaded by blood vessels. Simultaneously, osteoblasts migrate to this region and replace calcified cartilaginous matrix by bone matrix (Figure 1.6A). Flat bones such as cranial bones are formed by intramembranous ossification (Figure 1.6B). In this process, mesenchymal progenitor cells condense and differentiate directly into osteoblasts which then deposit bone matrix [23, 24, 29]. Intramembranous ossification does not require a cartilage template.

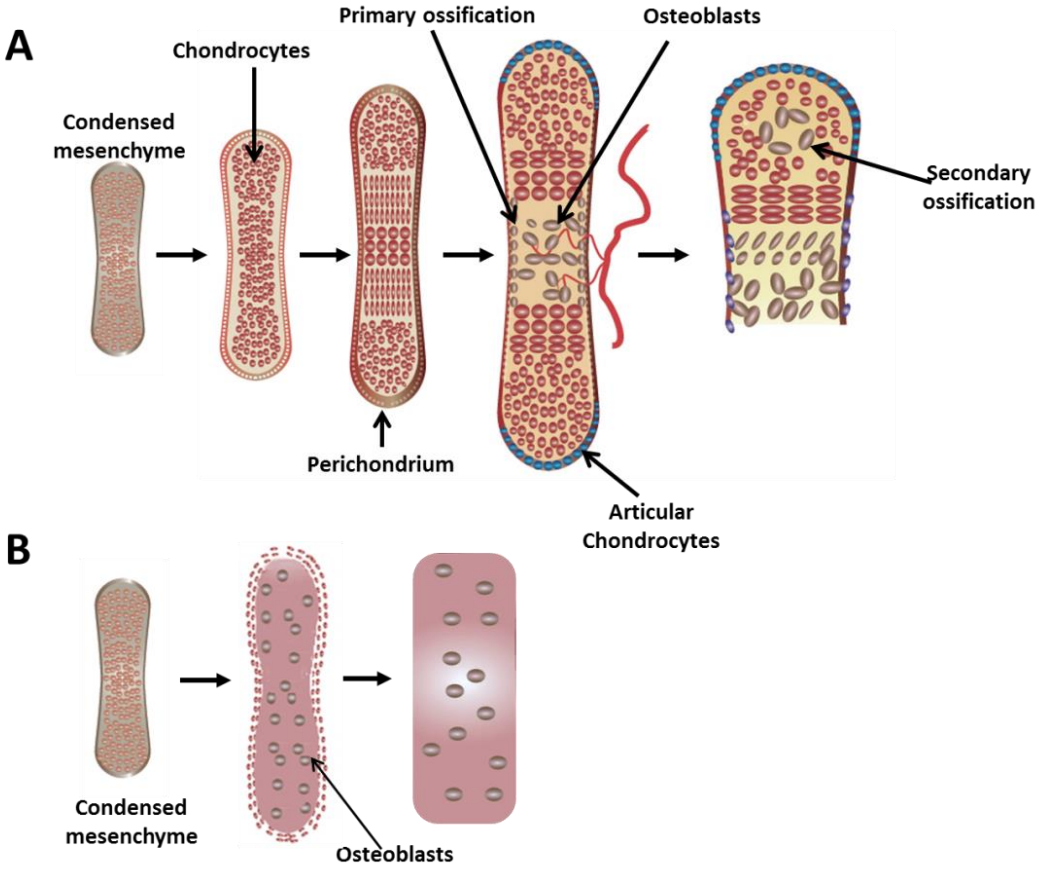

Figure 1.6: Bone formation*. **A)** During endochondral ossification, mesenchymal cells differentiate into chondrocytes and first make a cartilage template. Chondrocytes in the center stop proliferating and undergo hypertrophy. Hypertrophic chondrocytes mineralize their matrix and undergo apoptosis, attracting blood vessels and osteoblasts that remodel the template into bone. **B)** During intramembranous ossification, mesenchymal cells differentiate directly into osteoblasts and make bone.*

1.3.2 Bone remodeling

Living bone is a highly metabolically active organ; it undergoes constant remodeling to maintain its structure and strength. Bone remodeling involves removal of old or damaged bone and replacing it with new, mechanically stronger bone (Figure 1.7). During bone remodeling, mononuclear osteoclast precursor cells migrate to the site of remodeling, differentiate into active multinucleated osteoclasts and resorb bone by acidification and proteolytic degradation of the mineralized bone matrix. At the completion of bone resorption, osteoblasts recruited to the reabsorbed area synthesize a collagenous matrix which then mineralizes to form new bone [23, 27]. Osteoblasts that get trapped in the bone matrix during bone formation become osteocytes. Osteocytes form a network of thin canaliculi which allows them to communicate among themselves and with other cells present on the bone surfaces. It has been proposed that osteocytes act as mechanosensors that regulate the activity of both osteoblasts and osteoclasts in response to bone tissue strain and biomechanical load (reviewed in [30]). Osteocytes are

the most abundant cells (~90-95%) in the bone, they are long lived and become phagocytized and digested during bone resorption [27].

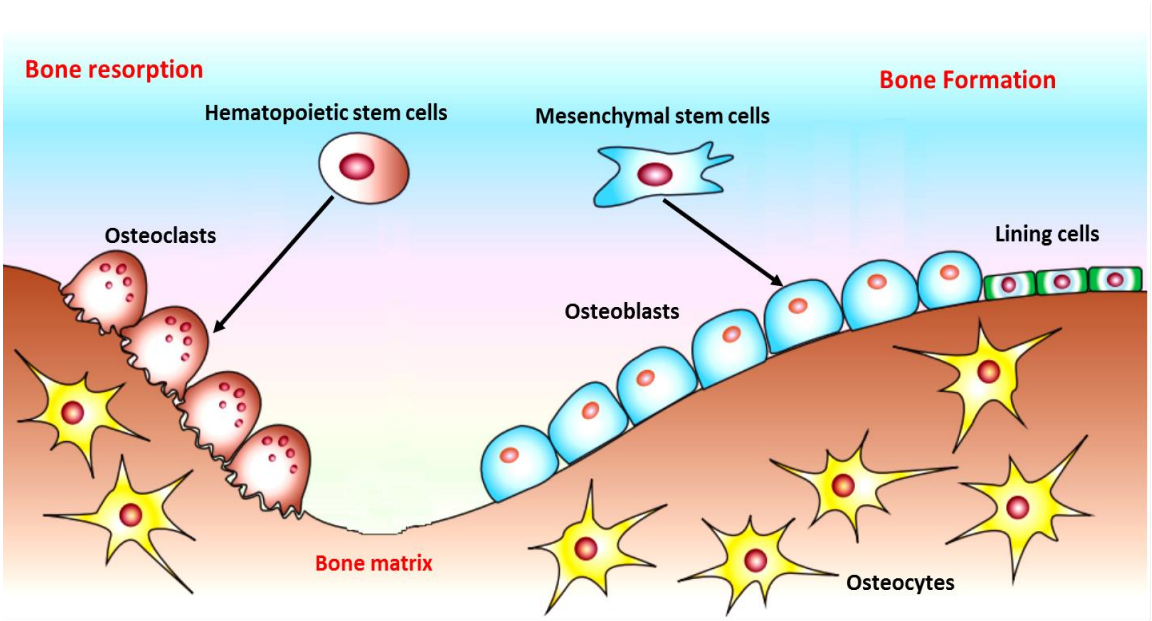

Figure 1.7: Bone remodeling*. During bone remodeling osteoclasts, derived from hematopoietic stem cells, resorb old and damaged bone. At the completion of bone resorption, osteoblasts recruited to the reabsorbed area make new bone [31].*

Bone resorption and bone formation are coupled through several factors (reviewed in [27]). Osteoclast formation and bone resorption are controlled by the ratio between two proteins, receptor activator of NF-κB ligand (RANKL) and osteoprotegerin (OPG) expressed by osteoblast lineage cells. RANKL stimulates osteoclast differentiation through interacting with its receptor, RANK, expressed on the surface of osteoclast precursors. OPG is a secreted protein that belongs to the TNF receptor family which acts as a decoy receptor for RANKL thereby regulating osteoclast mediated bone resorption [27, 32]. Osteoclasts secrete factors such as cardiotrophin-1, sphingosine-1-phosphate (S1P), CTHRC1 and complement factor 3a (C3a) to promote osteoblast precursor recruitment and differentiation [33]. Other proposed coupling factors include bone matrix-derived factors such as TGF-β, IGFs, BMPs, PDGF and FGFs released during resorption [23, 33].

A balance between bone formation and resorption is required for healthy bone and an imbalance in remodeling can lead to the development of bone thinning disorders such as osteoporosis and osteopenia. Osteoporosis is a disease characterized by decreased bone mass due to increased resorption, increased bone fragility, and increased risk of fractures [34] (Figure 1.8). Osteoporosis is highly prevalent among elderly and women. Osteoporotic fractures cause large numbers of disabilities, deaths, and huge health care cost through hospitalization and rehabilitation expenses. Currently available pharmacological agents are not very effective in treating osteoporosis. Most of the

currently used therapeutics prevents osteoclasts from resorbing more bone (examples: bisphosphonates, denosumab). However, none of these treatment options can help to replace already lost bone. The only anabolic drug approved by the Federal and Drug Administration (FDA) is parathyroid hormone (PTH) which stimulates bone formation when administered intermittently [34]. However, prolonged use of PTH increases the risk of developing osteosarcoma [34]. Treatment strategies aiming at decreasing bone resorption along with stimulating bone formation may help to treat osteoporosis successfully. This makes WNT signaling pathway an attractive target for therapeutic intervention in treating osteoporosis as WNTs promote bone formation and inhibit bone resorption.

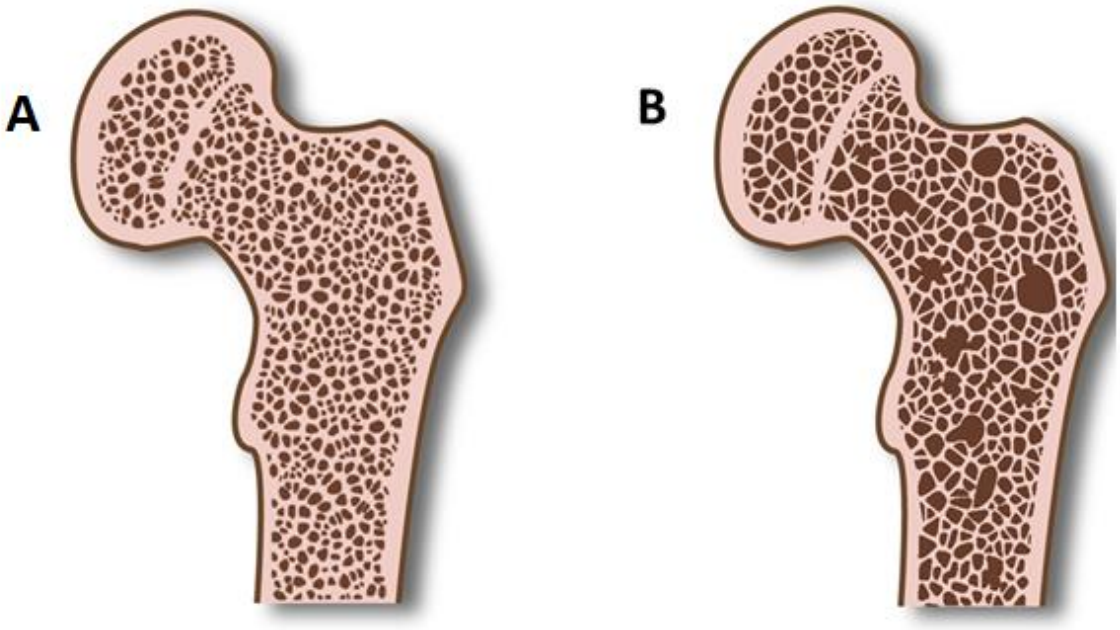

***Figure 1.8**: **Osteoporotic bone**. Normal bone is strong and dense (**A**) and osteoporotic bone is porous, fragile and brittle (**B**).*

1.4. WNT signaling in bone development and homeostasis

The WNT signaling pathway regulates almost all aspects of bone development and metabolism. Mutations in several WNT pathway members have been shown to cause skeletal defects in human. Loss-of-function mutations in WNT co-receptors LRP5 and LRP6 are associated with low bone mass (LBM) and conditions such as osteoporosis, whereas activating mutations in LRP5 are associated with high bone mass (HBM) [35-39]. Inactivation of the secreted WNT antagonist SOST results in HBM associated with two human dysplasias: sclerosteosis and van Buchem disease [40, 41]. These discoveries have led to extensive research on the role WNT signaling in bone and this pathway has emerged as a key regulator of skeletal development and adult bone homeostasis.

1.4.1 WNT proteins in skeletal development and metabolism

Several WNT ligands are expressed in bone. Spencer *et al.* measured WNT expression in a range of osteoblast-like cells (MG-63, SaOS-2 and TE85) and primary

human osteoblasts, and detected the expression of *WNT2*, *WNT2B*, *WNT3A*, *WNT4*, *WNT5A*, *WNT10A* and *WNT11* [42]. Witte *et al.* evaluated the expression of all WNT ligands during mouse limb development and observed expression of *Wnt2*, *Wnt2b*, *Wnt3*, *Wnt5a*, *Wnt5b*, *Wnt6*, *Wnt7a*, *Wnt7b*, *Wnt9a*, *Wnt9b*, *Wnt10a*, *Wnt10b*, *Wnt11* and *Wnt16* in the developing limb [43]. They also found that the WNT expression is spatially and temporally regulated during limb development [43]. Using *in situ* hybridization, Tan *et al.* evaluated WNT expression in neonatal calvaria and detected high levels of *Wnt10b*, *Wnt5a*, *Wnt5b*, *Wnt9a*, *Wnt11*, *Wnt4* and *Wnt16*, moderate expression of *Wnt1*, *Wnt2*, *Wnt2b*, *Wnt3a*, *Wnt7a*, *Wnt7b*, *Wnt8a*, *Wnt8b*, and *Wnt9a*, *Wnt3*, *Wnt6* and *Wnt9b* in low levels [44]. They also found that WNTs displayed distinct expression patterns in different parts of the bone. For example, *Wnt7b* showed a high expression in the perichondrium than the trabecular and cortical bone regions whereas *Wnt10b* was broadly expressed throughout the bone [44]. Mak *et al.* found that the expression levels of *Wnt2*, *Wnt2b*, *Wnt4*, *Wnt5a*, *Wnt10b*, and *Wnt11* were higher in mature osteoblasts compared to their progenitors [45]. These studies showed that the WNT expression is highly regulated in the skeleton, suggesting that not all WNTs are functionally redundant.

Mutation analysis in humans (Table 1.1) and transgenic overexpression or Cre-recombinase mediated deletion of WNTs in animal models using cell- and developmental stage-specific promoters (Figure 1.9) have suggested that the WNT ligands perform both overlapping and non-redundant functions during bone development and metabolism [24,46].

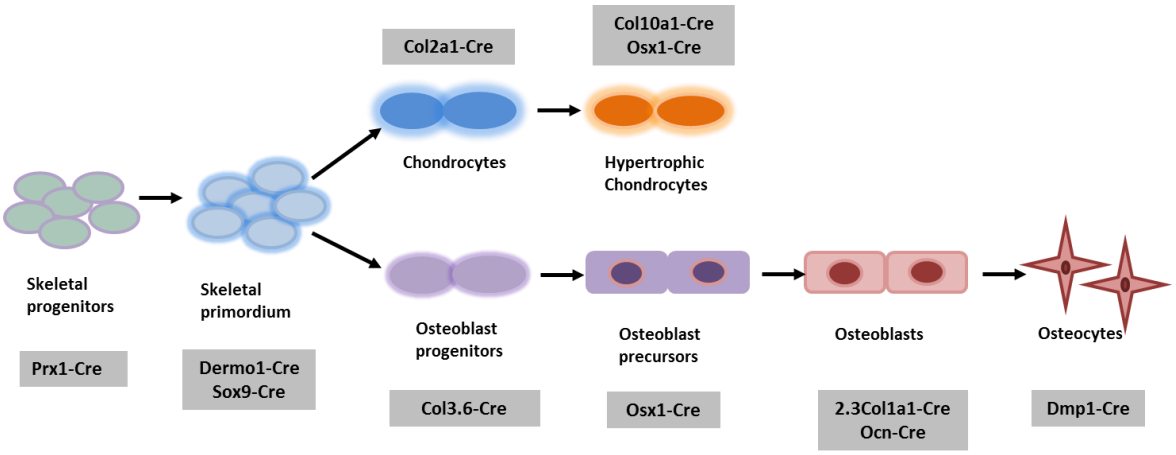

***Figure 1.9**: **Cell type specific promoters commonly used to drive transgene or Cre-recombinase expression in rodent animal models.** Various promoters indicated at the top and bottom of the diagram in gray boxes are used to drive transgene or Cre-recombinase expression in osteoblasts at various stages of their maturation.*

In humans, mutations in the *WNT1* gene cause osteogenesis imperfecta, a congenital disorder characterized by reduced bone mass, dramatically increased bone fragility and recurrent fractures [47, 48]. Recombinant WNT1 significantly increased differentiation of bone marrow stromal cells into osteoblasts [49]. Moreover, WNT1 stimulated mineralization of MC3T3 osteoblastic cells [50]. Weivoda *et al.* recently

showed that Transforming growth factor beta (TGF-β) receptor signaling in osteoclasts induces WNT1 secretion and couples bone resorption to formation [51]. These studies together suggest that WNT1 plays a key role in regulating bone development and metabolism.

Mutation in *WNT3* causes tetra-amelia, a rare genetic disorder characterized by complete absence of all four limbs and other abnormalities including craniofacial and urogenital defects [52]. *WNT3* has also been identified as a candidate gene associated with altered bone mineral density (BMD) in humans [53]. WNT3 shows ~84% amino acid identity to WNT3A [54]. Heterozygous deletion of *Wnt3a* in mice resulted in decreased BMD and trabecular bone mass [55]. WNT3A enhanced proliferation of osteoprogenitors, osteoblast differentiation and survival, and suppressed osteoclastogenesis [56-61]. WNT3A has also been shown to suppress osteogenic differentiation of uncommitted MSCs [56] suggesting that WNT3A treatment inhibits/promotes osteogenesis in a context dependent manner. Although WNT3A is considered a canonical WNT ligand, it has been reported that WNT3A also activates non-canonical signaling pathways to regulate osteogenesis and osteoclastogenesis [60-63].

Genome-wide association studies have identified *WNT4* as a gene linked to BMD in humans [53]. Mice overexpressing *Wnt4* in osteoblasts exhibited high bone mass, which was associated with enhanced bone formation, decreased osteoclast formation and decreased bone resorption [64]. *In vitro*, WNT4 stimulated osteoblastic differentiation of MSCs and inhibited RANKL-induced osteoclast formation [64, 65]. WNT4 regulated osteogenesis and osteoclastogenesis independent of β-catenin [64, 65].

WNT5A mutations are associated with autosomal dominant Robinow syndrome, a skeletal dysplasia characterized by short stature, limb shortening, genital hypoplasia, and craniofacial abnormalities [66]. Homozygous deletion of *Wnt5a* in mice caused severe skeletal abnormalities including dwarfism, facial abnormalities, shortened limbs and tails, as well as missing digits; these mice died during the perinatal period [66-68]. *Wnt5a* heterozygous knockout mice did not display any gross abnormalities during skeletal development but, exhibited low bone mass, and a reduction in osteoclast number, osteoblast number and bone formation parameters [69]. Osteoblast lineage specific deletion of *Wnt5a* using a Cre recombinase transgene driven by the osterix promoter (*Osx1-Cre)* resulted in reduced trabecular bone mass, impaired bone formation and decreased osteoclastogenesis, suggesting that WNT5A secreted by osteoblast-lineage cells is crucial in osteoclastogenesis and maintaining normal postnatal bone homeostasis [69]. *In vitro*, WNT5A significantly enhanced osteoclast differentiation and osteogenic differentiation of mouse embryonic stem cell (ESC) [59, 70]. It is believed that WNT5A preferentially signals through non-canonical pathways. However, WNT5A has also been shown to positively regulate the expression of *Lrp5/6* and enhance WNT/β-catenin signaling in osteoblast lineage cells [71]. WNT5B is the closest relative of WNT5A with ~80% amino acid identity. Transgenic mice overexpressing *Wnt5b* in chondrocytes displayed several skeletal defects including an open skull, shortened long bones and reduced ossification in the limb, and smaller rib cages [72]. Recombinant WNT5B

enhanced osteoclast differentiation [59]. WNT5B has also been identified as a gene associated with altered BMD [53].

WNT7A plays a key role in limb patterning [73]. A homozygous missense mutation in WNT7A has been linked to tetra-amelia [74]. WNT7A is most similar to WNT7B, with ~77% amino acid identity [75]. Deletion of *Wnt7b* in skeletal progenitors using a *Cre* recombinase transgene expressed by the dermo1 promoter (*Dermo1-Cre)* resulted in defects in bone formation [62]. Overexpression of *Wnt7b* in osteoblast lineage using either an *Osx1* or a *Col1* promoter resulted in high bone mass mainly due to increased osteoblast number and activity [76]. Overexpression of *Wnt7b* induced osteogenic differentiation of ST-2 mouse bone marrow stromal cell line and multipotent mouse embryonic mesenchymal cell line C3H10T1/2 [62, 76, 77]. The effect of WNT7B on osteoblast function was found to be independent of β-catenin [62, 76].

WNT10A and its closest relative WNT10B (64.5% amino acid identity) [78] inhibited adipogenesis and stimulated osteoblastogenesis *in vitro* through a β-catenin-dependent mechanism [79-81]. In mice, overexpression of *Wnt10b* using either the osteocalcin (*Ocn)* promoter or the *Fabp4* promoter resulted in high trabecular bone mass and increased bone strength [81,82]. However, no significant differences were detected in the cortical bone. The high bone mass observed in *Wnt10b* transgenic mice was a result of increased osteoblastogenesis [81]. *Wnt10b*$^{-/-}$ mice displayed reduced trabecular bone mass, which was associated with decreased osteogenesis rather than an increased number of osteoclasts or an increase in the bone resorption rate [81, 83]. WNT10B also plays an important role in the maintenance of mesenchymal progenitor cells [83]. Mutations in WNT10B have been detected in individuals with Split-hand/foot malformation (SHFM), a rare limb developmental malformation [84] and Oligodontia, a dental abnormality characterized by the absence of six or more teeth [85].

Overexpression of *Wnt11* in bone marrow-derived MSCs inhibited proliferation of MSCs and stimulated chondrogenic differentiation [86]; however, *Wnt11* overexpression in MC3T3E1 pre-osteoblasts enhanced osteoblast maturation and mineralization [87]. It is likely that the effect of WNT11 is dependent on the developmental stage of the cell.

Polymorphisms in the WNT16 gene are associated with low bone mineral density, cortical thickness and fracture risk [88, 89]. Mice lacking *Wnt16* developed spontaneous fractures as a result of decreased cortical thickness and high cortical porosity; however, the trabecular bone parameters were not altered in these mice [90]. Consistent with these findings *Wnt16* was found to be highly expressed in mice cortical bone [90]. The reduced cortical thickness was not due to reduced bone formation, but a result of increased bone resorption. WNT16 inhibited osteoclastogenesis both directly by acting on osteoclast progenitors and indirectly by increasing OPG expression in osteoblasts [90]. Osteoblast-lineage specific inactivation of *Wnt16* phenocopied global deletion of *Wnt16* and displayed lower cortical thickness, higher cortical porosity, spontaneous fractures at cortical bone sites and lower mechanical strength of the cortical bone. In contrast, the trabecular bone was unaffected [90], suggesting that lack of WNT16 affects only cortical

bone. However, transgenic mice overexpressing human WNT16 in osteoblasts exhibited a significant increase in both cortical and trabecular bone mass [91].

1.4.2 Porcupine and Wntless in skeletal development and homeostasis

The WNTs are post-translationally lipid modified by Porcupine (PORCN), a membrane-bound-O-acyltransferase localized to the endoplasmic reticulum (ER) [92]. Lipid modification is necessary for WNT secretion as well as binding to the FZD receptors on the target cells [92]. Loss of PORCN function causes WNTs to accumulate in the ER [93]. Mutations in PORCN cause X-linked dominant syndrome focal dermal hypoplasia (Goltz syndrome) with a multisystem birth defect, and in utero lethality in males [94]. In mouse, *Porcn* hemizygous male embryos died during early embryogenesis, while heterozygous females exhibited limb, skin and body patterning abnormalities, and high levels of perinatal lethality [95, 96]. Conditional inactivation of *Porcn* in limb mesenchyme using *Prx1-Cre* or in limb ectoderm using *Msx2-Cre* also resulted in severe limb defects [95, 96].

Wntless (WLS) is a multi-pass transmembrane protein essential for WNT secretion [93, 97]. Polymorphisms in WLS locus were shown to be associated with altered BMD [98, 99]. In mice, homozygous deletion of *Wls* resulted in embryonic lethality [100]. Mice lacking *Wls* in limb mesenchyme displayed reduced size and severe limb defects, and the majority of them died at the weaning stage due to a failure of food and water intake caused by the limb abnormality [101]. *Msx2-Cre* mediated deletion of *Wls* in limb ectoderm also resulted in limb defects along with other abnormalities including defective intramembranous ossification in the skull [101]. Osteoblast lineage specific deletion of *Wls* with *Col1-Cre* resulted in defective skull ossification and vertebral organization, and a dramatic reduction in cortical and trabecular bone mass which was associated with defective osteoblastogenesis and enhanced osteoclastogenesis [102]. The majority of these mutant mice died at one to two weeks of age [102]. Deletion of *Wls* preferentially in mature osteoblasts using *Ocn-Cre* also resulted in defective osteoblast differentiation and mineralization, increased osteoclast activity, and a significant reduction in both trabecular and cortical bone mass [103]. These mutants had spontaneous fractures and a high frequency of premature lethality at around 2 months of age [103].

These studies suggest that defects in osteoblastic WNT secretion severely impact bone development and metabolism and WNTs from neighboring tissues do not compensate for the loss of osteoblastic WNTs.

1.4.3 WNT receptors and co-receptors in bone development and metabolism

Several members of the FZD family receptors and co-receptors such as LRP5/6, ROR and RYK are expressed in bone and were shown to differentially modulate WNT signaling output.

1.4.3a FZDs

The FZDs are seven-transmembrane domain receptors that contribute to activation of both canonical and non-canonical signaling pathways. The FZD family

comprises of ten members (FZD1-FZD10) in mammals [104]. FZD contains a conserved ~120-amino-acid cysteine-rich domain (CRD) at the N-terminus that directly interacts with the WNT ligands. Our current understanding of the WNT specificity and affinity of FZD is very limited. However, some WNT-FZD combinations were shown to be favored over others in certain contexts [104]. Several FZDs including *Fzd2*, *Fzd3*, *Fzd4*, *Fzd5*, *Fzd6*, *Fzd8* and *Fzd9* are expressed in bone cells [42,105,106]. Deletion of several FZD receptors including *Fzd2*, *Fzd3*, *Fzd4* and *Fzd5* resulted in embryonic or postnatal lethality [7]. Mice lacking *Fzd8* displayed osteopenia with normal bone formation and increased osteoclastogenesis [105]. Deletion of *Fzd9* in mice resulted in low bone mass as a result of impaired bone formation, and osteoblasts lacking *Fzd9* displayed defects in bone matrix mineralization [107]. Canonical WNT signaling was unaffected in *Fzd9*$^{-/-}$ osteoblasts [107]. Not much is known about specific functions of other FZD receptors in bone.

1.4.3b LRP5/6

LRP5 and LRP6 are single transmembrane receptors that belong to the low-density-lipoprotein receptor-related proteins (LDLR) family [108]. LRP5 and LRP6 share ~71% homology. These two proteins show different patterns of expression during development where LRP6 is widely expressed in developing embryos and LRP5 shows a restricted expression pattern [109]. Loss-of-function mutations in *LRP5* were found to be associated with osteoporosis and osteoporosis pseudoglioma syndrome (OPPG) and *LRP5* gain-of-function mutations cause autosomally dominant high bone mass trait [35,37,39,110]. Mice lacking *Lrp6* display severe developmental defects and die shortly after birth [111] whereas *Lrp5*$^{-/-}$ mice have no developmental defects but acquire a low bone mass phenotype postnatally [112]. Mechanical loading induced bone formation was significantly reduced in Lrp5$^{-/-}$ mice and in mice lacking *Lrp5* selectively in osteocytes [113] whereas mice harboring HBM-causing *Lrp5* mutations exhibited increased osteogenesis in response to mechanical loading [114]. Heterozygous deletion of *Lrp6* resulted in low bone mass without any obvious skeletal abnormalities [115]. *Lrp6*$^{+/-}$; *Lrp5*$^{+/-}$ and *Lrp6*$^{+/-}$; *Lrp5*$^{-/-}$ mice displayed limb abnormalities and significantly lower bone mass than *Lrp6*$^{+/-}$ [115]. Deletion of both *Lrp5* and *Lrp6* in the embryonic mesenchyme using *Dermo1-Cre* resulted in severe skeletal defects and these mice exhibited absence of osteoblasts, and died shortly after birth [116]. Mice lacking either *Lrp5* or *Lrp6* selectively in mature osteoblasts displayed a significant reduction in BMD, and mice lacking both *Lrp5* and *Lrp6* in osteoblasts developed severe osteopenia with a significant reduction in both osteoblast and osteoclast number [109]. *Ocn-Cre* mediated deletion of *Lrp5* in osteoblasts also exhibited marked increases in body fat with corresponding reductions in whole-body energy expenditure whereas mice lacking *Lrp6* in osteoblasts did not display these phenotypes [117]. Interestingly, deletion of both *Lrp5* and *Lrp6* in the early osteoclast precursors using *Rank-Cre* resulted in reduced osteoclast and osteoblast number and decreased trabecular bone mass [61], suggesting that LRP5 and LRP6 play a role in osteoclasts as well.

Comprehensively, these findings suggest that LRP5 and LRP6 may have overlapping and distinct functions in bone and that both LRP5 and LRP6 are required for

normal postnatal bone homeostasis. In addition to LRP5 and 6, recent studies have identified LRP1, LRP4 and LRP8 as regulators of WNT signaling [118,119,120,121]

1.4.3c ROR1/2

The ROR receptors are transmembrane tyrosine kinases that bind to WNT ligands with their CRD [122]. ROR preferentially activate non-canonical WNT signaling [123,124]. In mammals, the ROR family contains two members, ROR1 and ROR2 and both have been shown to mediate WNT signaling [122]. ROR2 mutations are linked to skeletal disorders brachydactyly type B and Robinow syndrome [125-127]. *Ror2*$^{-/-}$ mice die shortly after birth exhibiting skeletal and cardiac abnormalities [128,129]. Although *Ror1*-deficient mice did not exhibit any severe skeletal or cardiac defects [130] they displayed postnatal growth deficiency and minor skeletal defects including abnormal ossification in the spine [131]. Mice lacking both *Ror1* and *Ror2* displayed significantly enhanced skeletal and cardiac abnormalities compared to *Ror2* mutants, suggesting that *Ror1* and *Ror2* may genetically interact during skeletal and cardiac development [130]. *Ror2*$^{+/-}$ mice exhibited high bone mass and decreased osteoclast number [69]. It has been shown that WNT5A enhances osteoclastogenesis through ROR2 expressed in osteoclast precursors [69]. Deletion of *Ror2* in osteoclast precursors using *Rank-Cre* resulted in reduced osteoclast number and increased trabecular bone mass whereas osteoclast specific deletion of *Ror2* using *Ctsk-Cre* resulted in increased bone mass because of a reduction in bone resorption with no change in osteoclast numbers [69]. ROR2 has also been shown to promote osteoblast differentiation and *ex vivo* bone formation [132].

1.4.3d RYK

RYK is receptor tyrosine kinase with an extracellular domain resembling WIF protein [122,133]. *Ryk*-null mice exhibited distinctive craniofacial appearance, shortened limbs and postnatal lethality [134]. In a recent study Andre *et al*. showed that RYK transduces WNT5A signaling by forming a complex with Van Gogh-like protein 2 (VANGL2), a core PCP pathway component, and that RYK regulates the PCP pathway at least in part by promoting VANGL2 stability [135]. *Ryk*$^{-/-}$*; Vangl2*$^{+/-}$ mice displayed severe developmental defects including open neural tube and shortened long bones in the limbs [135].

1.4.4 Intracellular regulators of canonical WNT signaling

Key intracellular regulators of canonical WNT signaling include DVL (DVL1/2/3), β-catenin, AXIN, APC, GSK3B, CK1 and TCF/LEF family transcription factors. The majority of the intracellular mediators of non-canonical WNT signaling are not specific to WNT signaling, but involved in several other signaling pathways. Therefore the functions of those molecules in bone development and metabolism are not discussed here. DVL plays a role in both canonical and non-canonical pathways; however, none of the DVL family members have been directly linked to any human skeletal disorders and no severe skeletal abnormalities were reported for *Dvl1, Dvl2* or *Dvl3* knockout mice [7].

1.4.4a β-catenin

β-catenin is a widely expressed 90-kDa protein with dual functions in cell-cell adhesion and regulation of gene transcription. There are mainly two pools of β-catenin in the cell; one is tethered to cadherins at the cell junctions and another pool that is "free" in the cytosol/nucleus. The cytoplasmic pool is involved in WNT mediated transcription regulation [136]. Genome-wide association studies have identified β-catenin as a gene linked to altered BMD in humans [53]. Global inactivation of β-catenin in mice resulted in embryonic lethality [137]. Conditional inactivation of β-catenin in mesenchymal progenitor cells resulted in severe skeletal defects characterized by defective osteoblast differentiation, ectopic chondrocyte differentiation and perinatal lethality [138,139]. Overexpression of a stabilized form of β-catenin in osteoblast precursors using *Osx1-Cre* resulted in excessive premature ossification and the mutants died at birth [140]. Conditional deletion of β-catenin in the osteoblast lineage using *Col1-Cre*, *Ocn-Cre* or *Dmp1-Cre* resulted in low bone mass with a striking increase in osteoclast numbers [137,141,142], whereas constitutive activation of β-catenin in osteoblasts resulted in high bone mass with reduced osteoclast formation [141]. Mice lacking β-catenin in osteoblasts/osteocytes exhibited a significant reduction in OPG levels whereas constitutive activation of β-catenin in osteoblasts increased OPG expression suggesting that osteoblastic β-catenin regulate osteoclast formation and bone resorption by activating OPG expression [137,141,142]. *In vitro*, osteoblasts lacking β-catenin exhibited elevated RANKL expression, diminished OPG expression and impaired maturation and mineralization [137]. In a recent study, Chen *et al.* removed β-catenin in *Osx1*-expressing early-stage osteoblast-lineage cells by administering tamoxifen temporarily to postnatal mice and found that bone formation activity of the targeted osteoblasts was greatly reduced [143]. These findings suggest that β-catenin promotes bone formation and suppresses bone resorption. Interestingly, β-catenin deletion from *Dmp*1-expressing osteocytes/osteoblasts postnatally did not reduce mechanical loading induced periosteal bone formation despite the fact that WNT/LRP5 signaling in osteocytes is critical for load-induced bone formation [144,145].

Wei *et al.* recently showed that during osteoclastogenesis, β-catenin was highly expressed in the proliferating osteoclast precursors; however, it was downregulated when the progenitors started to differentiate along the osteoclastic lineage [146]. They also showed that β-catenin deletion in the osteoclast precursors causes HBM by preventing precursor proliferation whereas constitutively active β-catenin blocked osteoclast differentiation, also resulting in HBM [146]. These findings suggest that β-catenin regulates osteoclastogenesis through a direct effect on osteoclast lineage cells and indirectly through osteoblastic OPG.

A recent study by Li *et al.* revealed that bone remodeling level in trabecular bone is more readily affected by changes in the β-catenin levels than cortical bone [147]. These findings suggest that β-catenin plays a critical role in skeletal development and postnatal bone homeostasis and the functions of β-catenin signaling may vary depending on the skeletal cell type, developmental stage of the cell and specific location.

1.4.4b Axin

Axin acts as a scaffold protein for the components of β-catenin destruction complex. There are two *Axin* genes in vertebrates, *Axin1* and *Axin2* [148]. *Axin1* is ubiquitously expressed, while *Axin2* has a more restricted expression pattern and is a direct target of the canonical Wnt signaling pathway [149]. *Axin1* has been identified as a gene associated with BMD in human [53]. Homozygous *Axin1* mutant mice die *in utero*; however, heterozygous *Axin1* mutants survived with no obvious abnormalities [150]. Inactivation of *Axin2* in mice resulted in a runt phenotype, accelerated chondrocyte maturation, enhanced osteoblast differentiation and mineralization, accelerated intramembranous ossification and premature suture closure [148,150]. Adult $Axin2^{-/-}$ mice displayed high bone mass, increased osteoblast differentiation and activity, and decreased osteoclast formation [151]. Compared to $Axin2^{-/-}$ mice the $Axin1^{+/-}$; $Axin2^{-/-}$ mice displayed more profound abnormalities including significantly reduced size, deformities of the vertebrae and ribs and incomplete calvarial formation [150], suggesting that both *Axin1* and *Axin2* are required for normal skeletal development.

1.4.4c APC

APC, also known as deleted in polyposis 2.5 (DP2.5), is classified as a tumor suppressor gene. APC plays a key role in normal β-catenin degradation. APC has been identified as a gene associated with altered BMD [152,153]. Global inactivation of *Apc* resulted in embryonic lethality [154]. Conditional inactivation of *Apc* in *Col2a1*-expressing cells resulted in high level of β-catenin in skeletal precursors leading to greatly impaired skeletal development and perinatal lethality [155]. The majority of the skeletal precursor cells lacking *Apc* failed to differentiate into chondrocytes or osteoblasts suggesting that *Apc*-mediated regulation of β-catenin levels is essential for differentiation of skeletal precursors [155]. Conditional deletion of *Apc* in osteoblasts with the *Ocn-Cre* resulted in dramatic increase in bone deposition, disappearance of osteoclasts and early postnatal lethality [137].

1.4.4d GSK3

Glycogen synthase kinase 3(GSK3) is a serine/threonine kinase that phosphorylates numerous substrates including transcription factors, structural proteins, and signaling proteins [156]. GSK3 has two highly conserved isoforms, GSK3α and GSK3β. GSK3-mediated phosphorylation triggers β-catenin destabilization. Homozygous deletion of GSK3β results in embryonic lethality [157]. $GSK3\beta^{+/-}$ mice showed normal skeletal development; however, $GSK3\alpha^{-/-}$; $GSK3\beta^{+/-}$ mice exhibited dwarfism with significantly shortened long bones and vertebra [158]. Adult $Gsk3\beta^{+/-}$ mice exhibited high bone mass accompanied by significant increases both bone formation and resorption parameters [159,160]. Furthermore, treatment with GSK3β inhibitor lithium chloride enhanced osteoblast differentiation and bone formation [42,161,162].

1.4.4e TCF/LEF family transcription factors

The TCF/LEF family includes four members, TCF1 (*Tcf7*), TCF3 (*Tcf7l1*), TCF4 (*Tcf7l2*) and LEF1 (*Lef1*). Full-length TCF1 and LEF1 often function as activators of WNT target genes whereas TCF3 seems to act as a transcription repressor. Full-length TCF4 also sometimes functions as transcriptional repressor [163]. *Tcf7*-null mice

developed normally but, displayed a low bone mass phenotype which was associated with an increase in bone resorption [141]. *Lef1*-null mice exhibited several developmental defects and perinatal lethality [159]. *Lef1*$^{+/-}$ female mice exhibited decreased osteoblast activity and significantly reduced trabecular bone mass [159]. However, bone mass was unaffected by *Lef1* haploinsufficiency in male mice [159]. LEF1 is expressed in pre-osteoblasts but, LEF1 expression decreases as osteoblasts mature [164]. LEF1 overexpression inhibited osteoblast differentiation whereas overexpression of Lef1ΔN, a short isoform of LEF1 that lacks the first 113 amino acids and a high affinity β-catenin binding domain, in differentiating osteoblasts induced osteoblast maturation [164-166]. Transgenic expression of *Lef1ΔN* in osteoblasts resulted in increased trabecular bone mass which was associated with enhanced osteoblast maturation and bone formation [167].

1.4.4f WTX

Wilms Tumor gene on the X chromosome (*WTX*) is a tumor suppressor gene located on the X chromosome [168]. Cytoplasmic WTX physically associates with components of the β-catenin destruction complex promoting the ubiquitination and proteasomal degradation of β-catenin [169,170]. Mutations in *WTX* cause Osteopathia striata with cranial sclerosis (OSCS) where the affected females exhibit sclerotic striations on the long bones, cranial sclerosis and craniofacial dysmorphism, and males display a more severe phenotype with high incidence of lethality [171,172]. *Wtx* deletion in mice resulted in neonatal lethality [169]. *Wtx*-null neonates revealed several abnormalities affecting bones, kidneys, heart, spleen, and adipose tissue [169]. Inactivation of *Wtx* in mesenchymal progenitors using *Prx1-Cre* resulted in bone overgrowth due to increased commitment toward osteoblastogenesis, and decreased adipocyte content in long bones. Mesenchymal progenitor cells lacking *Wtx* showed increased total and activated β-catenin levels [169]. Deletion of *Wtx* in osteoblast precursors using *Osx1-Cre* resulted in increased mineralization of the cortical and trabecular bone [169]. In contrast, *Wtx* deletion in mature osteoblasts using *Ocn-Cre* did not result in any gross differences in the neonatal or adult skeleton. These findings suggest that WTX has stage specific functions during osteogenesis.

1.4.5 WNT inhibitors in bone development and homeostasis

Several secreted WNT antagonists including SFRPs, DKKs, SOST and SOSTDC1 have been shown to regulate WNT signaling in bone.

1.4.5a SFRPs

The SFRPs are ~300 amino acid long secreted glycoproteins that share high homology to the FZD receptors. Mammals encode five members of the SFRP (*SFRP1-5*) family. SFRPs antagonize WNT signaling by binding to the WNTs directly, thereby preventing their functional association with FZDs on the target cell surface [3]. SFRPs may also bind to the FZD receptors [173]. All SFRPs are expressed in bone cells and may perform diverse functions during bone development and remodeling [43, 46]. *Sfrp1*$^{-/-}$ mice exhibited increased trabecular bone mass without any change in cortical bone [174]. Increase in bone mass was mainly due to reduced apoptosis of osteoblast lineage cells although proliferation was also modestly enhanced by deletion of *Sfrp1* [174].

Overexpression of *Sfrp1* in mice resulted in decreased trabecular bone mass and attenuated the bone anabolic effects of PTH [175]. SFRP1 has also been shown to inhibit osteoclastogenesis *in vitro* [174,176]. *In vitro*, SFRP2 suppressed BMP2 induced osteoblast differentiation and inhibition of SFRP2 significantly restored mineralized nodule formation [177]. *Sfrp3*$^{-/-}$ mice exhibited increased cortical bone density and thickness [178]. *Sfrp3*$^{-/-}$ mice also displayed an increased periosteal anabolic response to mechanical loading [178]. Overexpression of *Sfrp4* in osteoblasts from *Col1*-promoter resulted in significant reduction in trabecular bone mass which was associated with suppressed osteoblast proliferation and decreased bone formation [179]. Recombinant SFRP4 inhibited osteoblast proliferation *in vitro* [180]. Mice lacking *Sfrp4* displayed increased trabecular bone mass which was associated with excessive bone deposition and suppression of bone resorption; however, cortical bone mass and thickness were decreased [181]. Polymorphisms in *SFRP4* were found to be associated with altered BMD in humans [53]. Collectively, these data demonstrate that SFRPs negatively regulate bone formation through the inhibition of WNT signaling in a location dependent manner**.**

1.4.5b DKKs

The DKK family is comprised of four (DKK1-4) 255–350 amino acids long secreted proteins. Three members of the DKK family DKK1, DKK2, and DKK4 were identified as potent inhibitors of the WNT/β-catenin pathway [182]. DKKs interact with LRP5/6 and prevent WNT-induced FZD–LRP complex formation, thereby inhibiting WNT signaling. Deletion of *Dkk1* in mice resulted in severe developmental abnormalities including limb defects and the mutants died at birth [183]. *Dkk1*$^{+/-}$ mice showed an increase in bone formation, with no changes in bone resorption, leading to a significant increase in bone mass [184]. Overexpression of *Dkk1* selectively in osteoblasts using the *Col1*-promoter resulted in a significant reduction in bone mass which was associated with reduced bone formation [185]. Recombinant DKK1 inhibited osteoblast differentiation *in vitro* and DKK1-neutralizing antibody enhanced bone formation when injected into mice [186,187]. *Dkk2*-null mice displayed a low bone mass phenotype and osteoblast cultures derived from *Dkk2*$^{-/-}$ mice mineralized at a slower rate than wildtype cells [188]. *Dkk*2 suppressed osteogenesis in the absence of WNT7B, but induced terminal osteoblast differentiation after peak endogenous *Wnt7b* expression [188], suggesting that the effect *Dkk*2 on osteoblasts may vary depending on cellular context. *Dkk2* deficiency also led to a substantial increase osteoclast number [188]. Inhibition of *Dkk4* promoted osteoblast proliferation and differentiation, and suppressed osteoblast apoptosis [189]. DKK3 is a divergent member of the DKK family and does not seem to play a significant role in WNT signaling [182]; however, DKK3 inhibited BMP2 induced bone formation [190].

1.4.5c SOST

SOST is a 190-amino acid long secreted glycoprotein of DAN family that is primarily expressed in bone. Like DKK, SOST also binds to LRP5/6 co-receptors and antagonizes the canonical WNT signaling [191]. In humans, mutations in the SOST gene locus are associated with Sclerosteosis and Van Buchem disease (VB), two rare skeletal disorders characterized by excessive bone growth [41,192]. Mice lacking *Sost* displayed increased bone formation and bone strength whereas transgenic mice overexpressing

Sost/SOST showed decreased bone mass [193-195]. Mechanical loading induced bone formation was greatly reduced in transgenic mice that constitutively express high levels of *Sost* whereas *Sost*$^{-/-}$ mice did not lose bone mass after unloading [196,197], suggesting that mechanical loading promotes bone formation at least in part through down-regulation of *Sost*. Furthermore, the anabolic effect of intermittent PTH administration is also mediated at least in part by downregulation of SOST [198]. The anabolic effect of PTH was blunted in SOST deficient mice as well as in mice overexpressing SOST [199]. *In vitro*, SOST inhibited proliferation and differentiation and stimulated apoptosis of osteogenic cells [200,201]. SOST has also shown to promote osteoclastic bone resorption by modulating RANKL:OPG ratio in osteocytes [202].

1.4.5d SOSTDC1

SOSTDC1 is another secreted factor that belongs to the DAN family of proteins [203], which inhibits WNT activity by binding to LRPs [204,205]. *Sostdc1* deficient mice did not show any obvious developmental skeletal defects, but *Sost*$^{-/-}$*; Sostdc1*$^{-/-}$ mice exhibited preaxial polydactyly [206]. *Sostdc1*-null mice also displayed significantly enhanced cortical bone formation, increase in cortical BMD and decreased trabecular bone mass [207]. SOSTDC1 polymorphisms were associated with low bone-mass phenotype in Chinese women [208]. These findings suggest that SOSTDC1 may also play a significant role in skeletal development and remodeling by antagonizing WNT signaling.

1.4.5e NOTUM

NOTUM is a lipase that inhibits WNT signaling by removing a palmitoleoylate moiety that is essential for the WNT activity [209]. Inhibiting NOTUM leads to an increase in bone mass [210] suggesting that NOTUM plays a role in bone metabolism. However, more studies are required to understand the precise role of this protein in skeletal development and homeostasis.

1.4.6 Other WNT pathway modulators

Apart from the key pathway members discussed above several other proteins including Kremen (KRM), R-spondins (RSPO) and VANGL1/2 may also modulate WNT signaling in bone.

1.4.6a KRMs

The KRMs (KRM1 and KRM2) are single-pass transmembrane proteins that act as co-receptors for DKK1. KRM2 is predominantly expressed in bone whereas as KRM1 has a wide expression pattern [211]. KRMs form a ternary complex with DKK1 and LRP6, and induce rapid endocytosis and removal of LRP6 from the cell membrane thereby blocking canonical WNT signaling [212]. Transgenic overexpression of *Krm2* in osteoblasts using *Col1* promoter resulted in severe osteoporosis whereas *Krm2*$^{-/-}$ mice displayed a high bone mass phenotype at 24 weeks of age [211]. However, *Krm2*$^{-/-}$ mutants did not show any differences in bone mass at younger ages [213]. Mice lacking both *Krm1* and *Krm2* displayed defective limb development which was found to be further enhanced in *Krm1*$^{-/-}$*; Krm2*$^{-/-}$*; Dkk1*$^{+/-}$ triple mutant mice, suggesting that *Dkk1* and *Krm1/2* genes genetically interact during limb development [213]. Double mutant

Krm1$^{-/-}$; *Krm2*$^{-/-}$ mice also displayed increased bone volume and bone formation parameters postnatally [213].

1.4.6b RSPOs and LGR4/5

The RSPOs (RSPO1-4) are a family of secreted proteins that promote β-catenin stabilization [214]. RSPOs interfere with DKK1/KRM-mediated internalization of LRP6 through an interaction with KRM, resulting in increased LRP6 levels on the cell surface [215]. RSPO1 has been shown to act synergistically with WNT3A to induce osteoblast differentiation of uncommitted mesenchymal C2C12 cells [216]. Mice lacking *Rspo2* gene exhibited severe skeletal defects including mandibular hypoplasia, and maxillary and mandibular skeletal deformation [217]. In ovariectomized mice, exogenous RSPO2 rescued the bone loss and improved the microarchitecture of bone [218]. Furthermore, in MC3T3 pre-osteoblastic cells, WNT11 promoted osteoblast maturation and mineralization through RSPO2 [87]. Variation in RSPO3 was found to be associated with low BMD and fracture risk [219]. Leucine-rich repeat containing G protein-coupled receptor LGR4 and LGR5 are required for RSPO signaling [220,221]. In MC3T3 cells, LGR4 acted as the key receptor for RSPO2 to promote osteoblast differentiation and shRNA mediated silencing of LGR4 disrupted RSPO2-induced osteoblast maturation and mineralization [218]. *Lgr4*-null mice exhibited delayed embryonic bone formation, decreased body size and bone length, and increased perinatal lethality [222]. Postnatally, *Lgr4*$^{-/-}$ mice displayed reduced bone mass with severe defect in bone formation and enhanced osteoclastic bone resorption [222]. Together, these data suggest that RSPOs and LGR4/5 play a key role in modulating WNT signaling in bone.

1.4.6c VANGL1/2

VANGL1 and VANGL2 are four-pass transmembrane proteins acting as scaffolding proteins in the PCP pathway. Alterations to VANGL2 result in more severe developmental defects than VANGL1, suggesting that VANGL2 plays a more central role in development [223]. Homozygous *Vangl2* loop-tail mutant mice (*Vangl2*$^{Lp/Lp}$) harboring a loss-of-function point mutation displayed severe skeletal defects. *Wnt5a*$^{+/-}$; *Vangl2*$^{Lp/Lp}$ mutants displayed a more severe phenotype suggesting a genetic interaction between *Wnt5a* and *Vangl2* [224]. VANGL2 has recently been shown to play a key role in transducing WNT5A/RYK signaling [135]. Osteoblasts from heterozygous *Vangl2* loop-tail mutant mice displayed impaired orientation of division in response to strain. Bones from *Vangl2* loop-tail heterozygous mice displayed altered bone architecture and disorganized bone-forming surfaces [225]. Together these findings suggest that VANGL proteins play a key role in mediating the WNT/PCP pathway in bone.

The studies reviewed above (summarized in Table 1.1 and 1.2) clearly show that the WNT signaling pathway is a key regulator of bone development and homeostasis. These studies also suggest that targeting WNT pathway could be an effective strategy in treating metabolic bone disorders such as osteoporosis. However, these studies only provide a glimpse into the complex world of WNT signaling in bone. We still know very little about redundant and non-redundant functions of different WNTs in bone, the target genes regulated by these WNTs and about the molecular mechanisms by which different WNTs perform their functions. To develop therapeutics that target the WNT signaling

pathway efficiently, with minimal adverse effects, it is important to understand the specific mechanism by which different WNTs regulate bone metabolism.

Performing large scale gene expression studies after overexpressing different WNT ligands in osteoblast lineage cells will allow us to identify the target genes regulated by these WNTs during bone formation and understand the molecular mechanism by which these WNTs regulate bone metabolism. Such studies will also lead to the identification of novel therapeutic targets for bone diseases.

1.5. Objectives of the study

The goal of my thesis work is to better understand the molecular interactions along the WNT signaling pathway in the context of bone metabolism. Herein I used high-throughput sequencing technologies to gain insights into the molecular mechanisms by which WNT ligands WNT3A, WNT5A and WNT16 regulate osteoblasts differentiation and to elucidate the role of WNT co-receptors LRP5 and LRP6 in mediating WNT signaling in osteoblasts. I selected these WNT ligands for my study because of their known ability to regulate osteoblast differentiation [216,226] and the availability of active recombinant proteins, which made my study possible. Both LRP5 and LRP6 play a role in postnatal bone homeostasis [110]. I studied these co-receptors to understand their specific functions in osteoblasts and their role in mediating WNT3A signaling. Major objectives of my study included:

1) Understand the specific roles of WNT3A and canonical WNT co-receptors LRP5 and LRP6 in osteoblasts. Previous studies have suggested that canonical WNT ligand WNT3A regulates osteoblast differentiation [216]; however, the target genes regulated by WNT3A in osteoblasts or the molecular mechanism by which WNT3A regulate osteoblast differentiation is not known. To study the role of WNT3A in osteoblasts, using RNA sequencing (RNA-seq), I performed gene expression profiling of wildtype calvarial osteoblasts treated with recombinant WNT3A and identified the genes regulated by WNT3A. To gain more insights into the molecular mechanisms by which WNT3A regulate osteoblast differentiation I also performed a functional analysis of WNT3A targets. Next, I hypothesized that canonical WNT co-receptors LRP5 and LRP6 perform non-redundant functions in mediating WNT signaling in osteoblasts. To test this hypothesis, using RNA-seq, I identified genes regulated by WNT3A in osteoblasts lacking *Lrp5*, *Lrp6* and both *Lrp5* and 6 co-receptors. These results are discussed in Chapter 3.

2) Identification and validation of WNT3A inducible regulatory elements in osteoblasts. Canonical WNTs activate transcription factors of TCF/LEF family to induce gene transcription. To identify direct targets of canonical WNT signaling and WNT inducible regulatory elements, using Chromatin immunoprecipitation (ChIP) followed by deep sequencing (ChIP-seq), I identified TCF/LEF binding sites near target genes activated by WNT3A. TCF/LEF binding sites were detected in both promoters of WNT targets and in enhancer regions. A subset of enhancers with TCF/LEF binding sites was validated experimentally to confirm WNT3A inducible enhancer activity. These results are discussed in Chapter 4.

3) Identification and functional annotation of WNT16 targets in osteoblasts. WNT16, a WNT ligand highly expressed in osteoblasts, regulates both bone formation and bone resorption [90,226]. To identify the target genes regulated by WNT16 in osteoblasts and to understand the mechanisms by which WNT16 regulate bones metabolism, calvarial osteoblasts isolated from neonatal mice were treated with recombinant WNT16 and gene expression changes were quantified using RNA-seq. WNT16 target genes in osteoblasts were identified by comparing gene expression in WNT treated samples to sham treated samples. I performed a functional analysis of these targets to gain a better understanding of the molecular mechanisms by which WNT16 regulate bone metabolism. I also identified non-canonical WNT5A targets in osteoblasts and compared WNT16 targets to canonical WNT3A and non-canonical WNT5A targets. My study showed that WNT16 activates both canonical and non-canonical WNT targets. These results are discussed in Chapter 5.

***Table 1.1**: Human skeletal disorders associated with mutations in key WNT pathway members.*

Gene	***Human Diseases***	***References***
WNT1	*Osteogenesis imperfecta*	*[47]*
WNT3	*Tetra-amelia*	*[52]*
WNT5A	*Robinow syndrome*	*[66]*
WNT7A	*Tetra-amelia*	*[74]*
WNT10B	*Split-hand/foot malformation*	*[84]*
	Oligodontia	*[85]*
LRP5	*Osteoporosis pseudoglioma*	*[35]*
	Osteoporosis	*[37]*
ROR2	*brachydactyly type B*	*[125]*
	Robinow syndrome	*[125]*
WTX	*Osteopathia striata with cranial sclerosis*	*[171]*
SOST	*Sclerosteosis*	*[40]*
	Van Buchem disease	*[41]*

***Table 1.2**: Mouse phenotypes associated with key WNT pathway members.*

Gene	***Skeletal phenotype***	***References***
$Apc^{fl/fl}$,Ocn-Cre	*High bone mass, increased osteoblastogenesis, reduced osteoclastogenesis*	*[137]*
Axin2 KO	*High bone mass, increased osteoblastogenesis, reduced osteoclastogenesis*	*[151]*
Col1-Sfrp4 (GOF)	*Increased trabecular bone mass*	*[180]*

Ctnnb1$^{fl/fl}$; Col1-Cre	*Low bone mass, increased osteoclastogenesis*	*[141]*
Ctnnb1$^{fl/fl}$;Dmp1-cre	*Low bone mass, increased osteoclastogenesis*	*[142]*
Ctnnb1$^{fl/fl}$;Ocn-Cre	*Low bone mass, increased osteoclastogenesis*	*[137]*
Dkk1$^{+/-}$	*High bone mass*	*[184]*
Fzd9$^{-/-}$	*Low bone mass*	*[107]*
Gsk3β$^{+/-}$	*Increased bone formation*	*[160]*
Krm2$^{-/-}$	*High bone mass at 24 weeks of age*	*[211]*
Lef1$^{+/-}$	*Low bone mass in females, decreased osteoblast function*	*[159]*
Lgr4$^{-/-}$	*Low bone mass, increased bone resorption, reduced bone formation*	*[222]*
Lrp5$^{-/-}$	*Low bone mass*	*[112]*
Lrp5$^{fl/fl}$;Ocn-Cre	*Low bone mass*	*[109]*
Lrp6$^{+/-}$	*Low bone mass*	*[115]*
Lrp6$^{fl/fl}$;Ocn-Cre	*Low bone mass*	*[109]*
Osx-Wnt7b (GOF)	*High bone mass, increased osteoblast number and activity*	*[76]*
Ror2$^{+/-}$	*High bone mass and decreased osteoclast number*	*[69]*
Sfrp1$^{+/+}$	*Increased trabecular bone mass*	*[174]*
Sfrp3$^{+/+}$	*Increased cortical bone mass*	*[178]*
Sost$^{+/+}$	*High bone mass*	*[193]*
Sostdc1$^{-/-}$	*Increased cortical bone mass, decreased trabecular bone mass*	*[207]*
Tcf1$^{-/-}$	*Low bone mass, increased osteoclastogenesis*	*[141]*
Wls$^{fl/fl}$;Col1-Cre	*Low bone mass, increased osteoclastogenesis , reduced osteoblastogenesis*	*[102]*
Wls$^{fl/fl}$;Ocn-Cre	*Low bone mass, increased osteoclastogenesis , reduced osteoblastogenesis*	*[103]*
Wnt10b$^{-/-}$	*Low bone mass, reduced bone formation*	*[81]*
Wnt16$^{-/-}$	*Low cortical bone mass, increased bone resorption*	*[90]*
Wnt3a$^{+/-}$	*Low bone mass*	*[55]*

Wnt5a$^{fl/fl}$;Ocn-Cre	*Reduced trabecular bone mass, impaired bone formation and reduced osteoclastogenesis*	*[69]*
Wtx$^{fl/fl}$;Osx1-Cre	*Increased mineralization*	*[169]*
GOF : Gain of function		

Chapter 2

High-throughput Sequencing to Study Gene Expression and Gene Regulation

2.1 Introduction

The advances in Next Generation Sequencing (NGS) technologies have revolutionized genomic research by allowing us to acquire genome-wide data using massively parallel sequencing approaches [227]. With high-throughput sequencing approaches it is now possible to characterize all the genes expressed in a particular cell/tissue, identify single nucleotide polymorphisms (SNPs), small insertions or deletions (indels), larger structural variations and copy number variations, and detect DNA methylation patterns, chromatin modifications and binding sites of DNA-binding proteins such as transcription factors, with high accuracy [227-229] .

In my dissertation, I used several distinct high-throughput sequencing approaches to study the role of WNT signaling pathway in osteoblasts. RNA-seq was used to profile WNT signaling induced transcriptional changes and ChIP-seq was used to identify WNT inducible regulatory elements. This chapter provides a general introduction to high-throughput sequencing and briefly describes how sequencing technologies were applied to study the role of WNT signaling in osteoblasts.

2.2 High-throughput sequencing technologies

During the past decade, impressive progress has been made in the field of NGS technologies. Currently, several sequencing platforms are available including the ones developed by Illumina (Genome Analyzer/HiSeq/NextSeq/MiSeq), Roche (454) and ThermoFisher (ABI SOLiD/Ion) [228]. These NGS platforms use different sequencing technologies. For example, Illumina uses a method called sequencing by synthesis. First, the genomic DNA is broken into small fragments and universal adaptors are ligated to the ends, allowing these templates to be amplified with common PCR primers. These templates are then immobilized to a flow cell surface and amplified using a method called bridge amplification and subsequently sequenced to identify the nucleotide sequences. Fluorescent labeled deoxynucleoside triphosphates (dNTP) are added onto the flow cell during each sequencing cycle. The nucleotide label serves as a terminator for the polymerization reaction. After removing the unbound nucleotides, the fluorescent dye is imaged to identify the base and then enzymatically cleaved to allow incorporation of the next nucleotide [228,230]. Roche 454 uses pyrosequencing technology which relies on the detection of pyrophosphate released during the incorporation of a nucleotide into the DNA molecule and Ion uses semiconductor sequencing technology which is a method based on the detection of protons released during nucleotide incorporation [231].

The growing power and reducing cost have made NGS technologies very popular over the past few years and high-throughput sequencing is becoming the standard technology to study gene expression and gene regulation.

2.3 Profiling gene expression changes with RNA-seq

For several years DNA microarrays have been the technology of choice for large-scale gene expression studies. RNA-seq avoids several limitations of microarrays such as the dependence on predesigned probes, high background noise due to non-specific probe binding and inability to accurately measure genes with high expression due to signal saturation. RNA-seq also possesses several other advantages over microarrays including the ability to detect novel transcripts, allele-specific expression and indels.

In this study, RNA-seq was used to identify genes regulated by the WNT signaling in osteoblasts. Osteoblasts isolated from neonatal mice were treated with recombinant WNTs and gene expression changes were profiled using RNA-seq. The RNA-seq experiments involve two main steps: a) Library preparation and sequencing and b) computational analysis of RNA-seq data to identify transcriptional changes. The RNA-seq experimental workflow is briefly discussed below.

2.3.1 Library preparation and sequencing

RNA sequencing involves several steps, from RNA isolation to sequencing millions of short fragments.

a) RNA isolation and quality check: The first step is RNA extraction. Here, the RNA was harvested from osteoblast cultures. The quality and quantity of the starting RNA material plays a huge role is generating high quality sequencing data. About 1µg of the total RNA was used for each library. RNA quality was checked using a Bioanalyzer (Agilent) and RNA with RNA integrity number (RIN) $\geq$ 9 (on a scale of 1-10) was considered as good quality RNA.

***b) mRNA enrichment*:** This step ensures that we enrich for the RNA population of interest. Several RNA enrichment methods including rRNA depletion and poly-A selection are available for RNA enrichment [232]. In this study, poly-A selection was used to enrich for mRNA population. Poly-T oligo-attached magnetic beads were used to select for RNA population with poly-A tail.

c) RNA fragmentation: Most sequencing platforms require the RNA/DNA molecules about to be sequenced to be of relatively short length. In this step, the mRNA was fragmented to generate short fragments.

d) Reverse transcription and amplification: In this step, the RNA fragments were converted to cDNA. Adapters were ligated to fragment ends, reverse transcribed and PCR amplified to generate cDNA constructs. Next, a library validation was performed to make sure that the cDNA fragments are of appropriate size.

e) Sequencing: Samples were sequenced using Illumina HiSeq 2000 or NextSeq 550 and at least 20 million reads were generated for each library. Once the sequencing run was complete, the data was converted to fastq files which include for each read: a unique identifier, the nucleotide sequence and the Phred quality score per base [233] (Figure 2.1). The Phred quality score Q is defined as $Q = -10log_{10}(P)$, where P is the probability of the base call being incorrect [233,234].

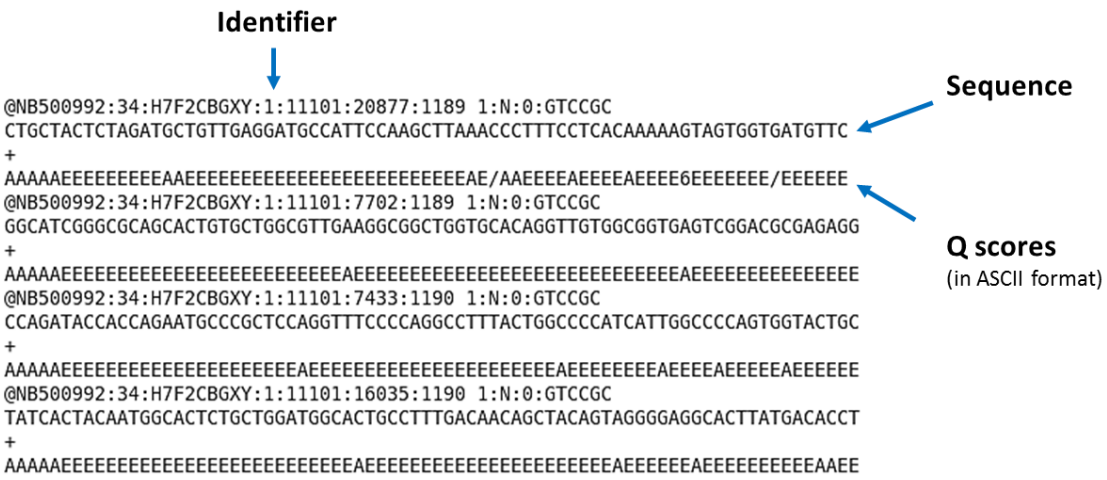

Figure 2.1: Fastq file format*. Each read has a unique identifier, nucleotide sequence and the Phred quality score (Q) per base.*

2.3.2 RNA-seq data analysis

RNA-seq data analysis involved six key steps (Figure 2.2). As the first step, quality of the data was verified. After this, the reads were mapped to the mouse genome. Then, the expression level was estimated for each gene. The expression data was then filtered to remove genes with low expression and normalized using statistical approaches. Subsequently, genes differentially expressed between experimental conditions were identified. Finally, the biological significance of the data was determined.

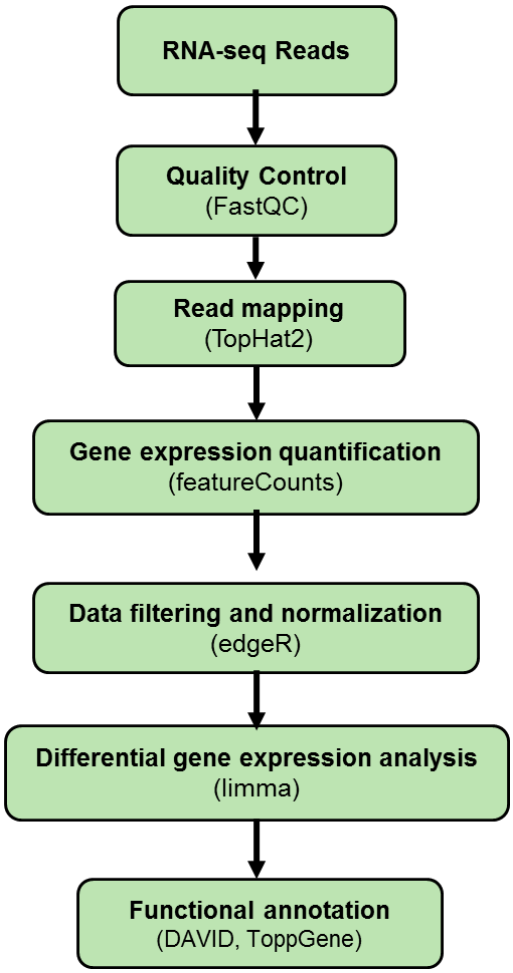

Figure 2.2: RNA-seq data analysis workflow. *The figure shows a general workflow used for carrying out RNA-seq data analysis.*

***a) Quality control*:** Before data analysis, a quality check must be performed to verify the quality of the data. Problems in the library preparation or sequencing can lead to poor data quality. Low data quality can affect the downstream analysis and interpretation, producing inaccurate results. Quality check generally involves the analysis of base quality, adapter contamination, GC content, *k*-mer content and sequence duplication levels [235]. Several tools such as RSeQC [236], RNA-SeQC [237] and FastQC [238, 239] have been developed for data quality check. In this study, I used FastQC for sequencing data quality check. FastQC is an effective and widely used quality assessment tool [239,235,240]. FastQC takes raw sequence data as input and generates a quality control report that tells whether the data has any problems of which we should be aware before doing any downstream analysis, such as low read quality and adapter contamination. In this study, samples with Phread score of 20 (base call accuracy: 99%) or above at all base positions were considered as high quality samples (Figure 2.3). FastQC result showed that our samples are of high quality. Also, no adapter contamination was detected in our data. For each library, FastQC also checks the GC

content distribution of the reads. The GC content bias within a library could be an indication of library contamination. FastQC did not detect GC bias in our data. However, our data showed sequence duplication. In RNA-seq, this does not necessarily indicate a problem as high abundance of a small number of genes may lead to high number of duplicate reads and is ignored if the duplication level is consistent across the samples [235]. If the data do not pass quality checks it should be processed to remove low quality bases, adapter sequences and other contaminating sequences. Data preprocessing mainly involves trimming low quality bases and contaminating sequences such as adapters, and removing short reads from the data. Several tools including Trimmomatic [241], FASTX-toolkit (http://hannonlab.cshl.edu/fastx_toolkit/), and Cutadapt (https://pypi.python.org/pypi/cutadapt) are available for data preprocessing. After preprocessing the data is ready for downstream analysis. Given the high quality of our data (Phred score > 20) (Figure 2.3) and lack of adapter contamination no additional preprocessing was performed.

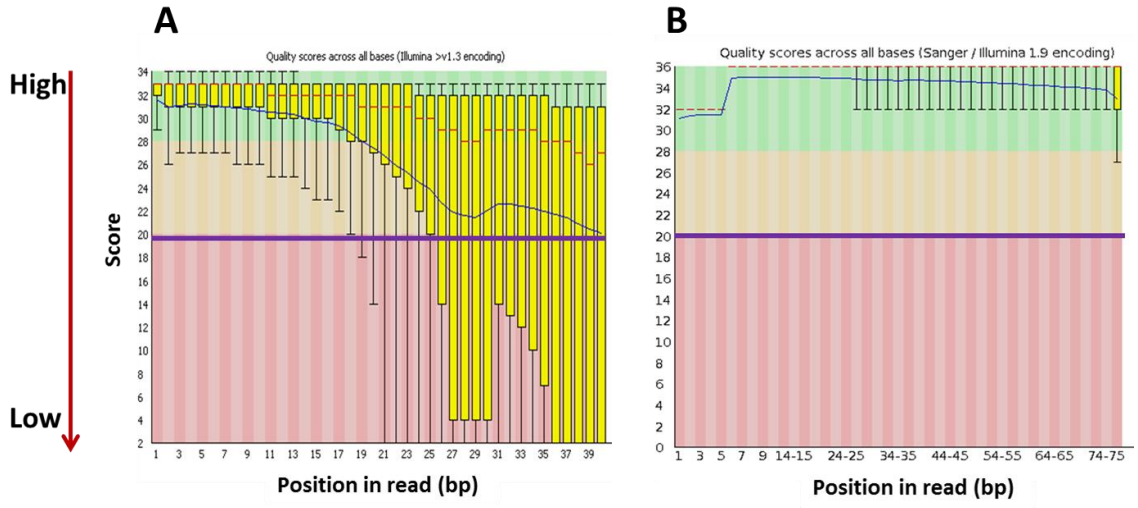

***Figure 2.3**: **Low and high quality RNA-seq data**. FastQC results showing low quality data with Phred score <20 (**A**) and high quality data (**B**). Box plots in these figures show range of quality scores at each base position in a sample. The blue line represents the mean quality. Data with base quality less than 20 (purple line) at any base position is considered as low quality data.*

***b) Read mapping*:** Mapping involves aligning reads onto a reference genome or transcriptome to find their locations with respect to the reference. To date several read mapping algorithms have been developed, including Bowtie [242], BWA [243], Subread [244], TopHat [245], STAR [246], GSNAP [247] and MapSplice [248]. Mapping tools take sequencing data as input and for every read it will try to find a (possibly unique) location in the reference that matches the read; however, some reads may map to multiple locations or fail to map to the reference genome. A large number of unmapped reads indicate low data quality or library contamination.

Because of the large size of the reference genome, finding optimal alignment for millions of reads in the sequencing data is a computationally challenging problem, both in terms of time taken for mapping and computing resources required [249]. Therefore, most alignment methods avoid seeking an optimal global alignment [250] in an attempt to improve the mapping speed and make the process less computationally intensive, and these tools may miss some true alignments in the process.

Aligning RNA-seq reads to the genome has several advantages over aligning to the transcriptome including the discovery of novel genes and novel isoforms. However, it requires the ability to detect splice sites in the reads and align reads spanning exon-exon junctions (Figure 2.4). Read aligners such as Subread [244], TopHat2 [251], STAR [246], GSNAP [252] and MapSplice [248] are capable of aligning reads across splice junctions (Figure 2.4). In my study, I used TopHat2 [251], for read alignment. In a recent study, Engström *et al*. performed a systematic evaluation of 26 RNA-seq alignment protocols based on 11 programs including TopHat2, STAR, GSNAP and MapSplice on real and simulated human and mouse transcriptome data. Overall, GSNAP, MapSplice and STAR showed a better performance than other methods [253]. TopHat2 protocol using transcriptome annotation also showed a comparable performance. With transcriptome annotation data TopHat2 performed better than most other methods in producing spliced alignments and detecting long insertions and was ~3 times faster than GSNAP and MapSplice [253]. However, TopHat2 displayed a low tolerance for mismatches and failed to map a large proportion of low quality reads, suggesting that TopHat2 may not be ideal for aligning data with low base quality. STAR was much faster than GSNAP, MapSplice and TopHat2 [253]; however, the memory requirement was much higher than TopHat2 [246]. Overall, TopHat2 performed well as a spliced aligner.

In my study, along with the RNA-seq data and the reference genome, a transcriptome annotation file was also provided as input to TopHat2. The annotation file was obtained in GTF format (mouse genome version: mm10) from UCSC genome browser [254]. When a transcriptome annotation file is provided, TopHat2 first maps the reads against the transcriptome. The transcriptome mapping improves the sensitivity and accuracy of the mapping and increases the alignment speed [251]. The remaining reads will be then mapped to the genome. TopHat2 uses Bowtie in the first stage of alignment. In this study, Bowtie was used to align short reads (≤50bp) and Bowtie 2 was used to align long reads (>50bp). After the initial Bowtie alignment, TopHat2 determines potential splice sites in the reads and aligns reads spanning exon-exon junctions. For all samples analyzed in this study, TopHat2 was able to align >90% of the reads back to the genome, with less than 10% reads mapping to multiple locations in the genome.

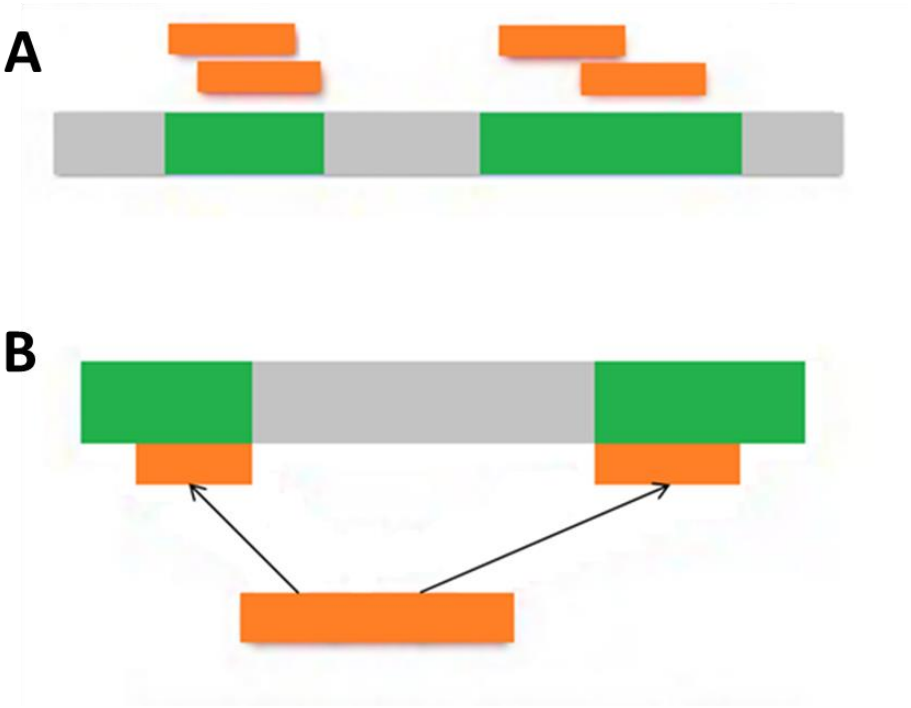

***Figure 2.4**: **Read mapping**. (**A**) Aligning reads spanning single exon to the reference. (**B**) Spliced alignment. For reads spanning splice junctions, the splice sites are determined and the reads are mapped to the candidate exons.*

***c) Gene expression quantification*:** Read alignments are used to quantify gene expression levels. A number of methods have been developed for read quantification or gene/transcript abundance calculation, including Cufflinks [255], HTSeq [256], featureCounts [257], IsoEM [258] and RSEM [259]. Tools such as HTSeq and featureCounts take alignment files as input and summarize read counts at the gene level, by counting all reads that overlap any exon of a gene whereas methods such as Cufflinks assemble reads to transcripts and calculate transcript level abundance. Several commonly used differential expression analysis tools including DESeq [260], edgeR [261] and limma [262] use read counts to estimate differential gene expression. Here, I used featureCounts to generate gene level read counts. The algorithms featureCounts and HTSeq are comparable in terms of counting results. However, featureCounts is significantly faster and memory efficient compared to HTSeq [257].

Gene level read counts provide a summary of the gene expression levels but, do not distinguish between a gene's isoforms. Reads can be assigned to genes with high confidence, but estimating isoform level expression is difficult as different isoforms of a gene generally have significant genomic overlap [257]. Methods such as Cufflinks [255] and RSEM [259] attempt to identify isoforms level expression for each gene, by leveraging information from reads aligned to regions where the isoforms differ. In my study, I did not investigate the changes in isoform expression levels.

d) Data filtering and normalization: Removing genes that are not expressed in any experimental condition at a biologically meaningful level will reduce the number of statistical tests that need to be performed downstream to identify differentially expressed genes. After calculating the read counts, the data was filtered to remove low expressed genes and the genes with counts per million (CPM) ≥ 2 in at least three samples were retained. Density plots were used to assess the data distribution before and after filtering (Figure 2.5). The limma method I used for differential expression analysis works with log2 CPM values [263]. For limma's best performance it is recommended to filter low expressed genes [264]. Therefore, the data was filtered based on CPM values [264] to remove genes with low expression values. The filtering cut-off values are usually chosen based on the data under consideration [263], with a goal of removing genes with no expression or extremely low expression across the samples. Here, the filtering cut-off value was chosen arbitrarily and with the chosen cut-off I could remove majority of genes with unreliable expression (Figure 2.5).

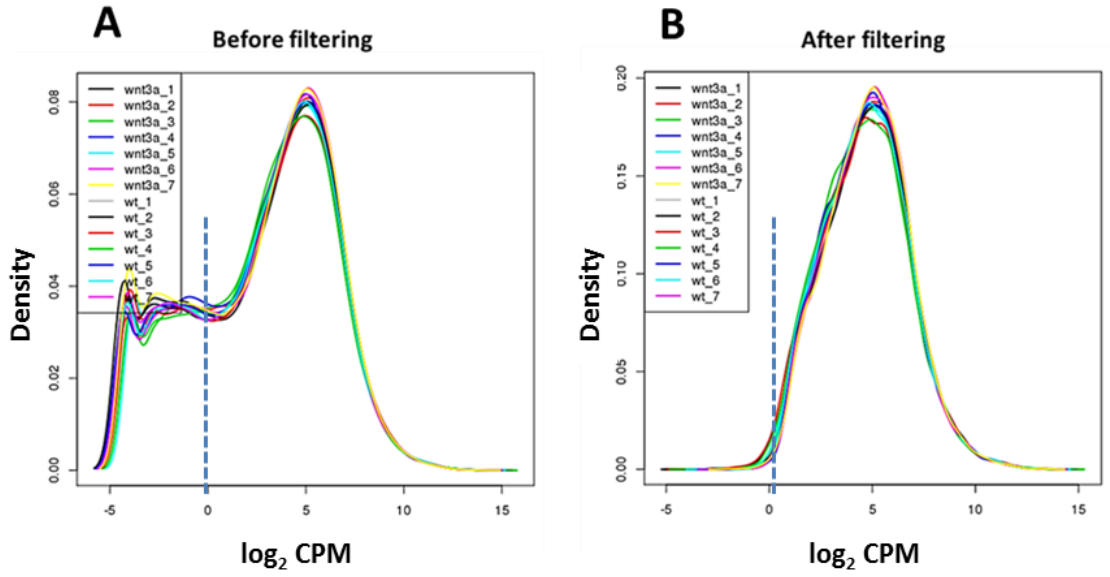

***Figure 2.5**: **RNA-seq data before and after filtering**. The density of log_2 CPM values for un-filtered (**A**) and filtered (**B**) data. Dotted vertical lines mark the log_2 CPM of zero. Filtering removed majority of genes with extremely low expression.*

In an RNA-seq experiment, all samples are expected to have a similar range and distribution of gene expression values. During the RNA-seq sample preparation and sequencing, several factors that are not of biological interest can affect the gene expression levels in each sample, leading to unwanted variations [265]. Data normalization removes these unwanted variations. Several methods including Total Count (TC) [266], Upper Quartile (UQ) [266], Median (Med) [266], Trimmed Mean of M values (TMM) [267] and the Reads Per Kilobase per Million mapped reads (RPKM) normalization [255] are available for RNA-seq data normalization. In recent study, Dillies *et al*. compared 7 normalization methods including RPKM, TC, UQ, Med, DESeq

[260] and TMM using Illumina RNA-seq datasets and showed that RPKM and TC are ineffective in normalizing RNA-seq data [266]. Normalization methods UQ, Med, DESeq and TMM performed comparably on the datasets tested, both in terms of the qualitative characteristics of the normalized data and the results of differential expression analysis [266]. In my study, using edgeR [261], I performed the UQ normalization to normalize the data. The UQ normalization is a scaling method in which scaling factors are calculated from the 75% quantile of the counts for each library, after removing transcripts with zero expression in all libraries [266,268]. The expression distributions of un-normalized and normalized data were assessed using boxplots (Figure 2.6). Our samples had a very similar expression distribution and the normalization had very little effect on the data (Figure 2.6).

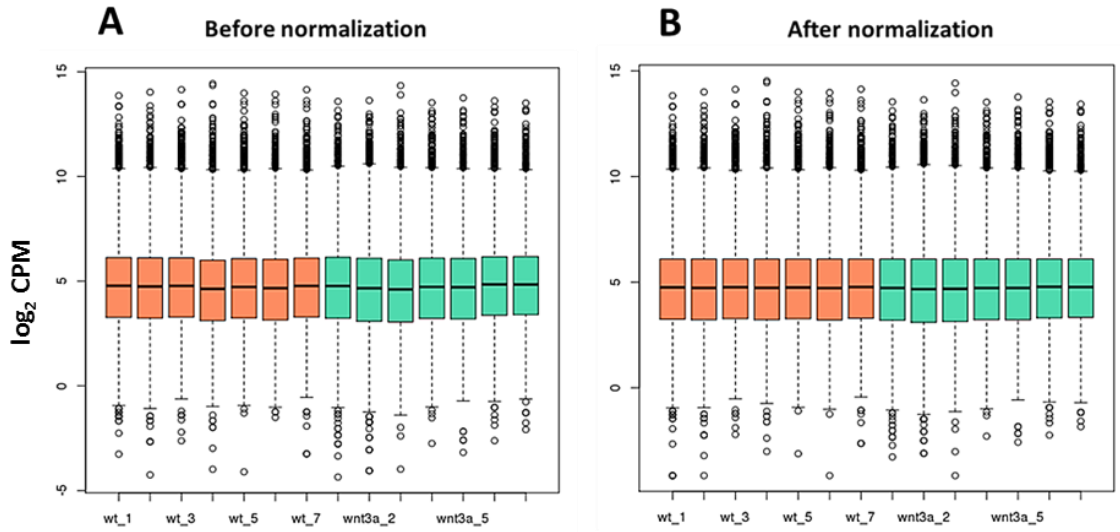

***Figure 2.6**: **RNA-seq data before and after normalization**. Boxplots of log_2 CPM values showing expression distributions for un-normalized (**A**) and normalized (**B**) data. Orange and green indicate two experimental conditions, WNT3A treated osteoblasts (wnt3a) and wildtype controls (wt).*

e) Differential gene expression analysis: Many algorithms have been developed to identify differentially expressed genes (Figure 2.7) from RNA-seq data, including DESeq [260], edgeR [261], Cuffdiff [255], baySeq [269] and limma [262]. In a recent study, Seyednasrollah *et al*. [270] compared the performance of eight differential expression analysis tools including Cuffdiff 2 [255], edgeR [261], DESeq [260], baySeq [269], NOIseq [271] and limma [262]. In their study, no single method emerged as favorable in all the comparisons they made. DESeq, limma and Cuffdiff 2 showed the lowest rate of false positive discoveries. EdgeR and limma were computationally fastest among all the tools tested. Tools such as DESeq, edgeR and limma contain features for handling complex experimental designs with multiple experimental variables and to adjust for unwanted variations due to experimental batch effects, which are important features for my study. In my study, I used limma for differential expression analysis. The limma method was originally designed for microarrays; however, the limma is designed in such

a way that, after proper data preprocessing and normalization, the same analysis pipeline can be used for different types of expression data including RNA-seq and microarray data. In my study, differentially expressed genes were identified using limma after voom normalization [262]. Genes with fold change ≥1.5 and false discovery rate (FDR) [272] corrected *p*-value <0.05 were considered to be significantly differentially expressed. The FDR is the expected proportion of false rejections of the null hypothesis among all rejections when simultaneously testing a family of hypotheses. The FDR correction enables control of the expected false discovery rate. [272]. Here, the Benjamini–Hochberg procedure was used for FDR correction [272]. Finally, we experimentally validated a subset of differentially expressed genes using quantitative real-time PCR.

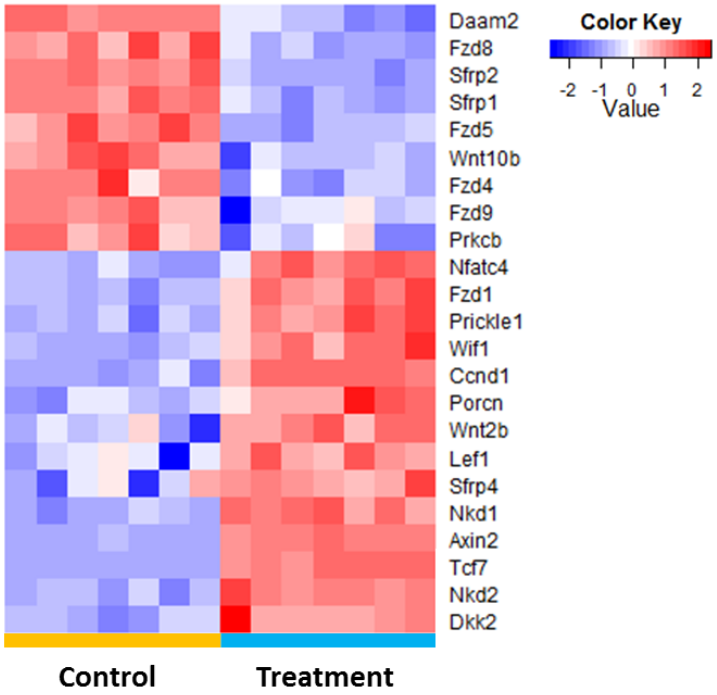

***Figure 2.7**: **Heatmap representation of differentially expressed genes.** Each column in the heatmap corresponds to a sample and each row corresponds to a gene. Change in blue to red indicates increase in expression values.*

f) Functional annotation: After identifying differentially expressed genes, a functional enrichment analysis is generally performed to understand the biological contexts of these genes. Several functional enrichment analyses tools including DAVID [273], GSEA [274], GOrilla [275], STEM [276] and ToppGene [277] have been developed for this purpose. For a given set of genes, using knowledge available in biological databases such as KEGG [278] and Gene Ontology [279], these tools test for enrichment of each annotated biological function. This increases the chance of detecting biological functions that are most relevant to the experimental system. In this study, DAVID [273] and ToppGene [277] were used to identify enriched biological processes and phenotypes associated with differentially expressed genes. DAVID is one of the most widely used

functional enrichment analysis tool which has certain features that are not available in most other functional enrichment analysis tools such as the pathway visualization module. I found ToppGene particularly useful in my study as it identifies enriched mouse phenotypes associated with differentially expressed genes, which is not a feature available in many other ontology analysis tools including DAVID.

RNA-seq allowed the identification of hundreds of genes regulated by the WNT signaling pathway in osteoblasts. These findings are discussed in detail in Chapters 3 and 5.

2.4 Studying transcription regulation with ChIP-seq

The identification of chromatin modifications and protein-DNA interactions allows us to gain a detailed understanding of gene regulatory networks that control transcription. ChIP-seq enables the genome-wide detection of protein-DNA binding events and chromatin modifications [280].

2.4.1 ChIP-seq experimental workflow

A ChIP-seq workflow differs depending on the type of interaction of interest. To detect binding sites of DNA-binding proteins such as transcription factors, the protein of interest is crosslinked to the DNA by treating cells with formaldehyde. The DNA is then fragmented using sonication. Antibodies specific to the protein of interest are used to enrich for the DNA-protein complex [280] (Figure 2.8). To identify nucleosome positions or histone modifications, micrococcal nuclease (MNase) digestion without prior crosslinking is more commonly used to fragment the DNA as it removes linker DNA more efficiently than sonication. The immunoprecipitated DNA is subsequently sequenced and mapped back to the reference genome to identify transcription factor binding sites or chromatin modifications (Figure 2.8).

To identify significant transcription factor binding sites or chromatin modifications, generally a control experiment is also performed either using input DNA from the ChIP experiment or DNA fragments derived using an unspecific antibody. Only regions that show statistically significant signal enrichment in the experimental sample compared to the control are regarded as significant binding sites.

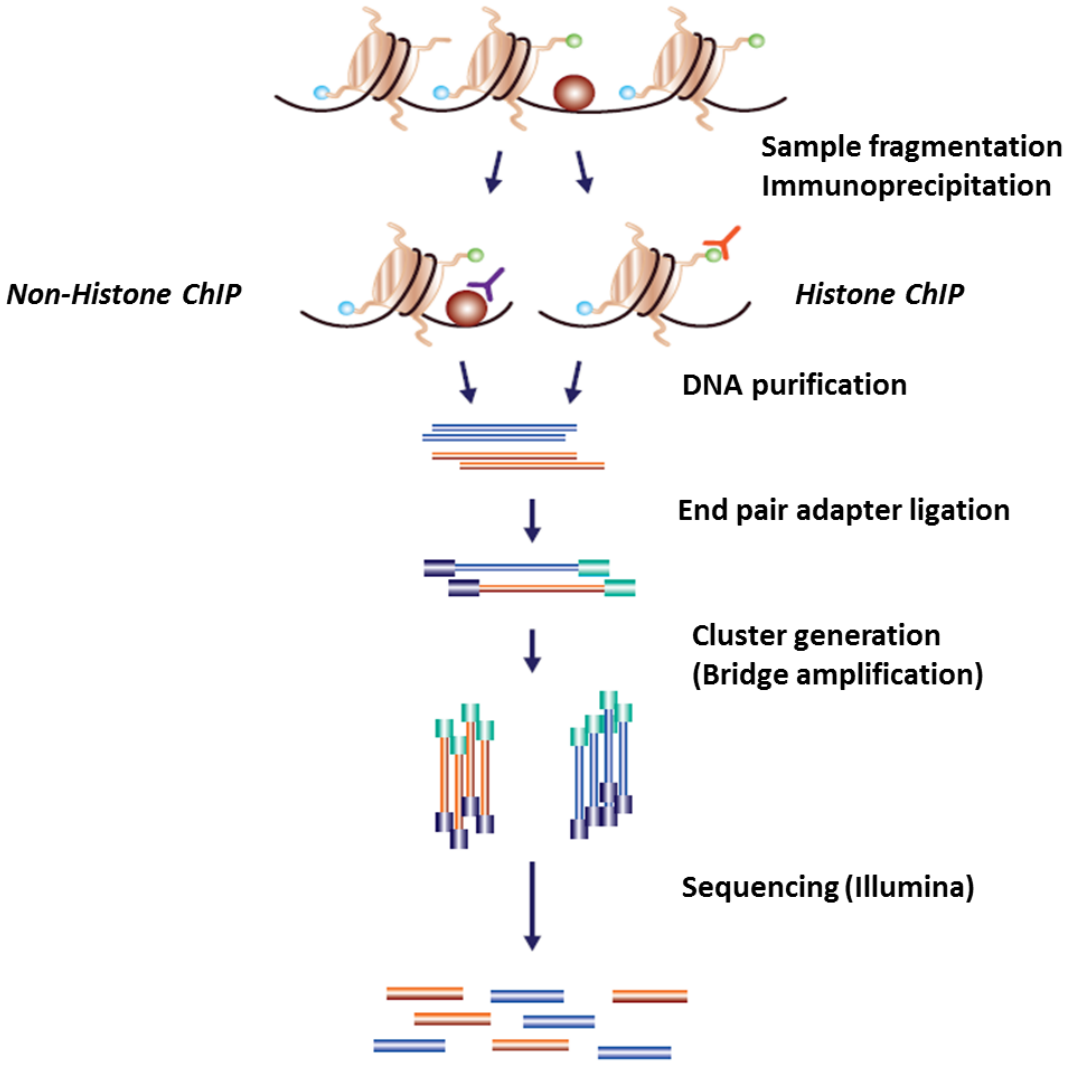

Figure 2.8: ChIP-seq experimental workflow. *The ChIP process enriches crosslinked DNA-protein complexes or modified nucleosomes of interest using antibodies specific to the protein or the histone modification. The DNA is then purified and sequenced using high-throughput sequencing technologies. In this study, the ChIP DNA was sequenced using Illumina sequencing technology. Common adaptors were ligated to the purified ChIP DNA and clusters of clonal sequences were generated by bridge amplification, and sequenced using Illumina NextSeq 550.*

In my thesis work, ChIP-seq was used to identify targets of WNT activated transcription factors TCF/LEF and WNT inducible enhancers in osteoblasts. Canonical WNT signaling activates TCF/LEF family transcription factors to regulate gene expression. These transcription factors bind to the promoter or enhancers of target genes to regulate their expression. TCF/LEF target genes were discovered by mapping TCF/LEF binding sites identified using publically available ChIP-seq datasets to the nearest genes.

Enhancers are cis-regulatory elements to which transcription factors bind to increase gene transcription (Figure 2.9) [281]. Consortia such as ENCODE [282] and the Roadmap [283] have extensively mapped enhancers across multiple cell lines and tissues, advancing our understanding of gene regulation in these tissues. Histone modification H3K4me1 (monomethylation of histone H3 lysine 4) together with H3K27ac (acetylation of Lysine 27 of histone H3) has been widely used to identify active enhancers [281]. In this study, ChIP was performed using antibodies targeting histone modifications H3K4me1 and H3K27ac. Subsequently, ChIP-isolated DNA fragments were sequenced using Illumina NextSeq 550 (Figure 2.8). The data was analyzed computationally to identify osteoblast enhancers.

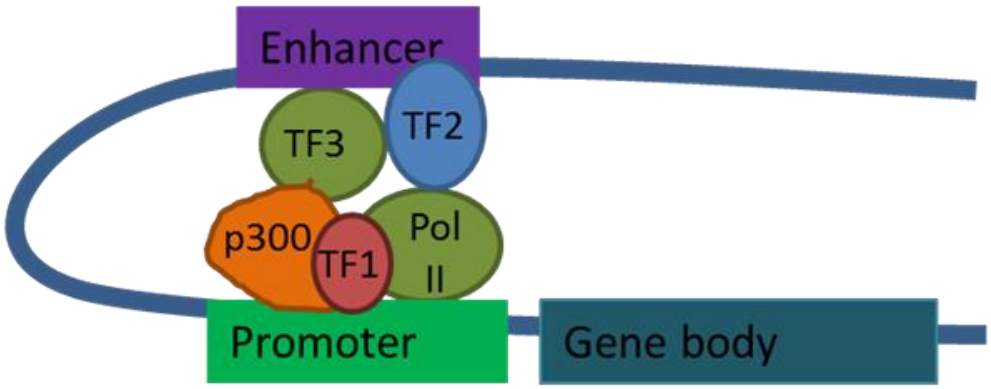

Figure 2.9: Enhancers. *Enhancers are regulatory DNA sequences that, when bound by specific transcription factors (TF), enhance the transcription of an associated gene.*

2.4.2 ChIP-seq data analysis

ChIP-seq data analysis involves three major steps: read mapping, peak calling and downstream analysis to aid biological discovery. The downstream analysis depends on the biological process under study. The downstream analysis could include identification of regulatory elements such as enhancer, functional annotation of regulatory elements using tools such as GREAT [284], annotation of peaks to known genomic features using tools such as ChIPseeker [285] and HOMER [286] or transcription factor binding motif identification using algorithms such as MEME [287], MDscan [288], HOMER [286] and PscanChIP [289].

***a) Read mapping*:** ChIP-seq produces DNA sequences that can be aligned to the genome using DNA sequence aligners such as Bowtie [242] and BWA [243]. In a recent study, Hatem *et al*. compared nine alignment tools including Bowtie, Bowtie 2 [242] and BWA. Their study did not find any tool that outperforms all other tools in all the tests they performed [290]. Among the tools they tested, GSNAP [252] and SOAP2 [291] showed highest mapping error percentage. Novoalign correctly mapped the largest percentage of reads; however, it had the lowest throughput [290]. Bowtie, Bowtie 2 and BWA showed comparable mapping percentages. Bowtie and Bowtie 2 had the best throughput for most

of the tests they performed and BWA performed better for longer reads [290]. Developers of Bowtie recommend Bowtie to align short reads(≤ 50 bp) and Bowtie 2 to align long reads (>50 bp) to the genome[292]. Based on this recommendation, Bowtie and Bowtie 2 were used in my study to align short reads and long reads respectively.

***b) Peak calling*:** After obtaining the read alignment, the next step is to find the genomic regions that have been enriched with aligned reads in the experimental samples compared to the control samples. Several tools ('peak callers') including MACS [293], PeakSeq [294], SISSRS [295], QuEST [296] and SICER [297] have been developed for this purpose. For each experimental sample, the peak callers calculate the number of reads aligned to different regions in the reference genome and the enrichment relative to the number of reads in the control sample. Wilbanks *et al*. compared eleven peak callers including MACS, SISSRS, PeakSeq and QuEST using multiple transcription factor ChIP-seq datasets and found that these programs have similar performance with regards to sensitivity and specificity; however, MACS showed a better performance than most algorithms in estimating precise binding location of transcription factors [298]. In my study MACS was used to identify significantly enriched H3K4me1, H3K27ac and TCF/LEF peaks (p-value <0.00001).

***c) Peak annotation*:** After peak calling, significant peaks were assigned to genomic features using ChIPseeker [285]. ChIPseeker takes peak files as input and assigns peaks to different genomic features such as promoter, exon, 5' UTR, 3' UTR, intron, and intergenic regions. Functional annotation of significant peaks was performed using GREAT [284]. Functional annotation identified enriched gene ontology [279] terms associated with the peaks. Most functional annotation tools are gene based. GREAT takes genomic coordinates of the peaks as input and associates these genomic regions with nearby genes and applies the gene annotations to the regions. GREAT performs a binomial test to determine significantly enriched ontology terms. Peaks were run against whole genome background with genome assembly mm10 and ontology terms with a binomial p-value < 10^{-5} were identified.

d) Enhancer identification: Osteoblast enhancers were identified by finding regions with overlapping H3K4me1 and H3K27ac peaks that are more than 3 kilobases (kb) away from the transcription start sites (TSS) (Figure 2.10). For every gene, the region within ±3kb of the TSS was considered as the promoter as in other published studies [299,300]. BEDOPS [301] was used to calculate the distance between H3K4me1 and H3K27ac peaks. BEDOPS takes two peak files as input and for each peak in file 1, it identifies the nearest peak in file 2 and the distance to the nearest peak. H3K4me1 and H3K27ac peaks with a distance 0 were considered as overlapping peaks. Putative WNT inducible enhancers in osteoblasts were identified by finding enhancers (H3K4me1+; H3K27ac+ regions) with TCF/LEF binding sites. Subsequently, a list of high confidence WNT inducible enhancers was generated by integrating gene expression and ChIP-seq data such that putative WNT inducible enhancers identified near WNT target genes were considered as high confidence WNT inducible enhancers.

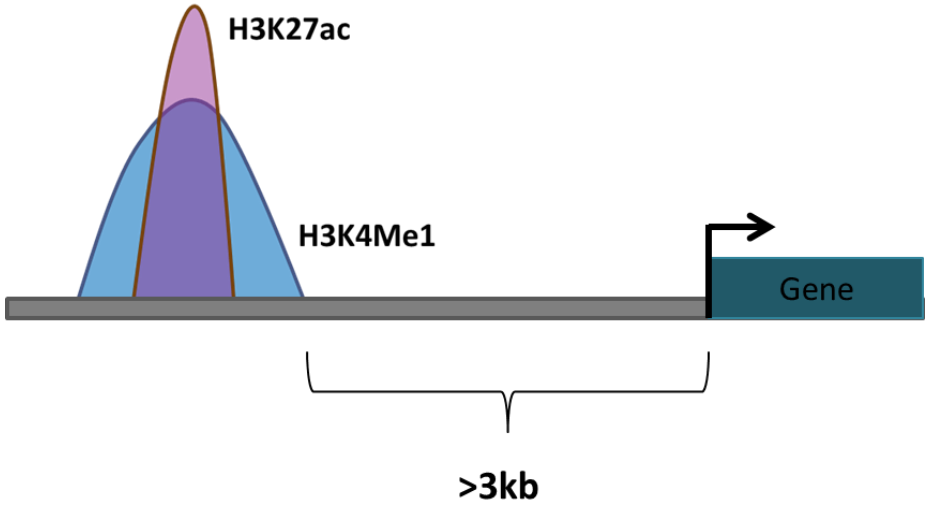

Figure 2.10: Osteoblast enhancers. *Regions with overlapping H3K4me1 and H3K27ac peaks that are more than 3kb away from TSS were identified as osteoblast enhancers.*

***e) Identification of enriched transcription factor binding sites*:** Enhancers commonly contain recognition sites for multiple transcription factors. For putative WNT inducible enhancers, HOMER [286] was used to identify enriched transcription factor binding sites in those regions. Unlike many other motif enrichment analysis tools that require genomic sequences as input [302,303], HOMER can takes genomic coordinates obtained from peak callers as input. HOMER identifies known motifs enriched in the input using a library of previously determined transcription factor binding motifs. HOMER also discovers novel transcription factor binding motifs.

This study allowed the identification of TCF/LEF target genes, putative WNT inducible enhancers and transcription factors that may bind to these enhancers and cooperate with TCF/LEF to activate the transcription of WNT target genes. These findings are discussed in Chapter 4.

2.5 Summary

RNA-seq and ChIP-seq are widely being used to profile gene expression changes and to identify transcriptional regulatory elements, respectively. Several studies have used RNA-seq to study gene expression changes in bone. Ayturk *et al.* employed RNA-seq to profile the transcriptome of *Lrp5* wildtype ($Lrp5^{+/+}$), *Lrp5* knock-out ($Lrp5^{-/-}$), and HBM-causing ($Lrp5^{p.A214V/+}$) knock-in alleles and identified genes and molecular mechanisms altered in these genotypes [304]. In another study, using RNA-seq, Kelly *et al.* investigated transcriptional changes in cortical and cancellous bone in response to mechanical loading [305]. A number of studies have successfully used ChIP-seq to understand epigenetic changes during osteoblast differentiation [306-308].

In my thesis work, using RNA-seq, I identified several novel genes regulated by canonical and non-canonical WNT ligands in osteoblasts. Integrating gene expression measures with ChIP-seq provides additional insights into the mechanisms by which

chromatin modifications and protein-DNA interactions regulate gene expression. By combining ChIP-seq and RNA-seq data I also identified several putative WNT inducible regulatory elements in osteoblasts (see Chapters 3-5). Altogether, this study provides novel insights into the WNT signaling pathway in osteoblasts using cutting edge technologies.

Chapter 3

WNT Co-receptors LRP5 and LRP6 Differentially Mediate WNT3A Signaling in Osteoblasts

3.1 Introduction

Several studies have identified the β-catenin-dependent canonical WNT signaling pathway as a key regulator of bone development and homeostasis. Canonical WNT signaling promote osteoblast differentiation from mesenchymal stem cells (MSCs), inhibit adipogenic and chondrogenic differentiation of MSC, enhance osteoblast proliferation, maturation and mineralization, and inhibit osteoblast apoptosis [309]. Canonical WNT signaling has also been shown to inhibit osteoclast differentiation [61]. WNT3A preferentially activate canonical WNT signaling and has been shown to play a key role in regulating bone metabolism [63,216]. However, very little is known about the molecular mechanism by which WNT3A regulate osteoblast differentiation or target genes regulated by these WNTs during this process.

WNT proteins activate canonical signaling by binding to transmembrane receptors FZD and co-receptors LRP5/6. Previous studies have suggested that both LRP5 and LRP6 are essential for normal postnatal bone homeostasis [112,117]. However, not much is known about their specific roles in mediating canonical WNT signaling and target genes regulated through these co-receptors.

To understand how WNT3A mediated canonical signaling modulates osteoblastic gene expression and to identify the role of LRP5 and LRP6 in mediating WNT3A signaling in osteoblasts, neonatal calvarial osteoblasts isolated from C57Bl6/J (*WT*) and osteoblasts lacking *Lrp5* (*Lrp5*$^{-/-}$), *Lrp6* (*Lrp6*$^{-/-}$) and *Lrp5/6* (*Lrp5*$^{-/-}$;*Lrp6*$^{-/-}$) were treated with WNT3A for 24 hours and gene expression changes were quantified by RNA-Seq. We found that WNT3A up-regulated the expression of several key regulators of osteoblast proliferation/ early stages of differentiation while inhibiting genes involved in osteoblast maturation/mineralization. Our study also showed that LRP6 is the key mediator of WNT3A signaling in osteoblasts and loss of LRP5 had minimal effect on WNT3A signaling.

3.2 Methods

3.2.1 Generation of knockout animals

All animal experimental procedures were conducted in accordance with guidelines under the institutional animal care and use committees at Lawrence Livermore National Laboratory. Osteoblasts from C57Bl6/J (*WT*) and *Lrp5*$^{-/-}$ and osteoblasts lacking *Lrp6* and both *Lrp5* and *6* were used in this study. *Lrp5*$^{-/-}$ mice have been described previously [115]. To generate *Lrp6* and *Lrp5/6* deficient osteoblasts, floxed mice were crossed with UBC-Cre-ERT2 and Cre-recombinase expression was induced by treating osteoblasts with hydroxytamoxifen (TMX) *in vitro*. *Lrp5/6* deletion efficiency was quantified by quantitative real-time PCR (qRT-PCR).

3.2.2 Osteoblast isolation and culture

Osteoblasts were isolated from calvaria of neonates (4-5 days old) by serial digestion in Collagenase 1 and ethylenediaminetetracetic acid (EDTA) solutions [310]. Osteoblast enriched fractions were centrifuged, washed with phosphate-buffered saline (PBS), plated in 12 well plates at 2.6×10^5 cells/well to ensure high cell number and subconfluency at the time of RNA collection. These cells were cultured in DMEM/F12 supplemented with 10% fetal bovine serum (FBS) and 1% penicillin/streptomycin (P/S) at 37 °C. Following a 24 hour incubation, the media was changed to remove digestion debris and non-viable cells. These cultures were treated with 100ng/µl of recombinant WNT3A (R&D systems). The RNA was isolated from these cultures after incubating the cells for another 24 hours. For *Lrp5*$^{-/-}$*;Lrp6*$^{-/-}$and *Lrp6*$^{-/-}$ cells, following isolation of osteoblasts, cells were plated at $1x10^5$ cells/well, cultured for 24 hours in DMEM+FBS+P/S media, followed by a 48 hour treatment with DMEM+FBS+P/S with 1 uM hydroxytamoxifen (Sigma) prior to 24 hour WNT3A treatment.

3.2.3 Quantitative Real-time PCR

Total RNA was purified using RNeasy Mini Kit (QIAGEN) according to manufacturer's protocol. Superscript III First-Strand Synthesis System (Invitrogen) was used with oligodT primers for reverse transcription according to manufacturer's protocol. Real time quantitative PCR was then performed with SYBR Select Master Mix (Applied Biosystems) using a Applied Biosystems 7900HT Fast Real-Time PCR System with the following cycling conditions: 50°C for 2 min for SYBR then 95 °C for 3 min (2 min for SYBR), followed by 40 cycles of 95 °C for 3 s (10 s for SYBR) and 30 s at 60 °C. Data was normalized to control gene (Gapdh) and fold changes were calculated using the comparative Ct method [311]. Three independent replicates were analyzed per condition. Primers used qRT-PCR are given in Table 3.1.

3.2.4 Osteoblast Proliferation assay

Osteoblast proliferation was assessed by Carboxyfluorescein Diacetate Succinimidyl Ester (CFSE) staining using CellTrace™ CFSE Cell Proliferation Kit (Molecular Probes). MC3T3 pre-osteoblastic cells were incubated in 5uM CFSE for 20 min at 37°C, then incubated in media with or without 100ng/µl recombinant WNT3A (R&D systems) added to serum media for 8 days. Media was changed every 2-3 days. Stained cells were analyzed using a FACSCalibur flow cytometer (Becton Dickinson). The cell cycle distributions were analyzed with Modfit LT software (version 4.1).

3.2.5 RNA-isolation and sequencing

Total RNA was purified using RNeasy Mini Kit (QIAGEN) according to manufacturer's protocol. RNA integrity was assessed using Bioanalyzer (Agilent). Poly(A)+-enriched cDNA libraries were generated using the TruSeq Sample Preparation kit (Illumina) and checked for quality and quantity using Bioanalyzer (Agilent). RNA-seq was performed on a HiSeq 2000 or a NextSeq 550 sequencer (Illumina). At least three replicates were sequenced for each condition.

3.2.6 RNA-seq data analysis

Data quality was checked using FastQC (version 0.11.4) software. All the samples were found to have high quality (Phred score > 20). Sequence reads were aligned to the mouse reference genome (mm10) using TopHat2 (version 2.0.11) [245,251]. After read mapping, 'featureCounts' from Rsubread package (version 1.22.2) [257] was used to perform summarization of reads mapped to RefSeq genes and generate gene-wise read counts. Subsequently, genes were filtered from downstream analysis if they did not have a CPM (counts per million mapped fragments) value ≥2 in at least three libraries. Density plots were used to analyze the distribution of unfiltered and filtered data. Subsequently, 'upper quartile' normalization was performed using the calcNormFactors function in edgeR (version 3.14.0) [261]. Normalization effects were assessed using boxplots. Differentially expressed genes were identified using 'limma' (version 3.28.12) after 'voom' [263] normalization. Multi-dimensional scaling (MDS) plots were used to assess whether samples cluster according to the treatments rather than batch effects. Experimental batch effects were adjusted for by including experimental batch as a covariate in the statistical model. A gene is called significantly differentially expressed when its false discovery rate (FDR) [272] adjusted *p*-value is less than 0.05 and fold change is ≥1.5.

We also analyzed a published RNA-seq dataset profiling gene expression changes during osteoblast differentiation, starting with early pre-osteoblast stage through to mature osteoblasts [312]. This dataset was then used to assess how the expression of WNT3A targets change during osteoblast differentiation. After aligning the RNA-seq reads to the mouse genome with TopHat2 (version 2.0.11), gene expression values were calculated using Cuffnorm from Cufflinks (version 2.2.1). From this data, we obtained the expression values of WNT3A targets at all stages of osteoblast differentiation. This data was then clustered using hierarchical clustering, in R (version 2.15.2). Hierarchical clustering method groups data points into clusters based on their similarity. Clusters of genes with similar expression profiles were obtained using the 'cutree' function in R (version 2.15.2). After clustering, the temporal expression profiles of these genes were visualized using heatmaps. Heatmaps were generated using heatmap.2 function in gplots (version 2.11.0) R package.

3.2.7 Functional Annotation

The functional analysis of differentially expressed genes was performed using functional annotation tools DAVID (version 6.7) [313] and ToppGene [277]. Enriched biological processes and pathways were identified using DAVID. Ontology terms [279] with a *p*-value less than 0.01 were considered significant. ToppGene was used to identify genes associated with bone metabolism phenotypes.

3.2.8 Calvarial injection

Four to six week old C57Bl6/J mice were injected with 100 ng of recombinant WNT3A protein (R &D systems) in 0.01% CHAPS/PBS or 0.01% CHAPS/PBS (vehicle control) in a volume of 20 µl. The protein or vehicle control was injected subcutaneously over mouse calvaria above the sagittal suture between the parietal bones once daily for

five days followed by a two day gap. This seven day procedure was then repeated. Mice were anesthetized briefly with Isoflurane for the injections. Fourteen days after the start of injection, the mice were euthanized and the calvarias were dissected.

3.2.9 Histology and micro computed tomography (μCT)

Calvarias were cut along the sagittal plane where one half was processed for hematoxylin and eosin (H&E) staining and the other half for μCT. First, one half of the calvaria sections were fixed in 10% neutral buffer formalin for 24-48 hours and then decalcified in 14% EDTA for ~7 days. Calvaria samples were embedded in paraffin blocks, sectioned (5-μm) on microscope slides and baked at 42°C overnight. Samples were de-waxed and stained with hematoxylin and counterstained with eosin, then mounted with Permount. ImagePro Plus (version 7.0) and a CCD QIClick camera were used for imaging. All the images were taken at 20X resolution.

The remaining half of the calvaria sections were stored in 70% EtOH at 4°C for μCT. Specimens were processed blindly to reduce bias, and labels were matched to treatment only after all the scanning and image analyses were complete. Calvarias were measured and analyzed for bone parameters ($n \geq 5$ per group) (μCT 35, SCANCO, Brüttisellen, Switzerland) according to the guidelines for μCT analysis of rodent bone structure [314]. Quantification of bone parameters was done using the tools provided by the manufacturer. Significant differences between experimental conditions were probed using two sample *t*-tests (*p*-value <0.05).

3.3 Results

3.3.1 Gene expression analysis of WNT3A-treated osteoblasts

To investigate how WNT3A signaling modulates osteoblastic gene expression, neonatal calvarial osteoblasts were treated with recombinant WNT3A for 24 hours and the gene expression changes were profiled using RNA-seq (Figure 3.1). Before performing RNA-seq, a qRT-PCR analysis was conducted on a limited number of known WNT target genes *Axin2*, *Lef1*, *Igfbp2* and *Ibh* to confirm that the experimental conditions were appropriate (Figure 3.2).

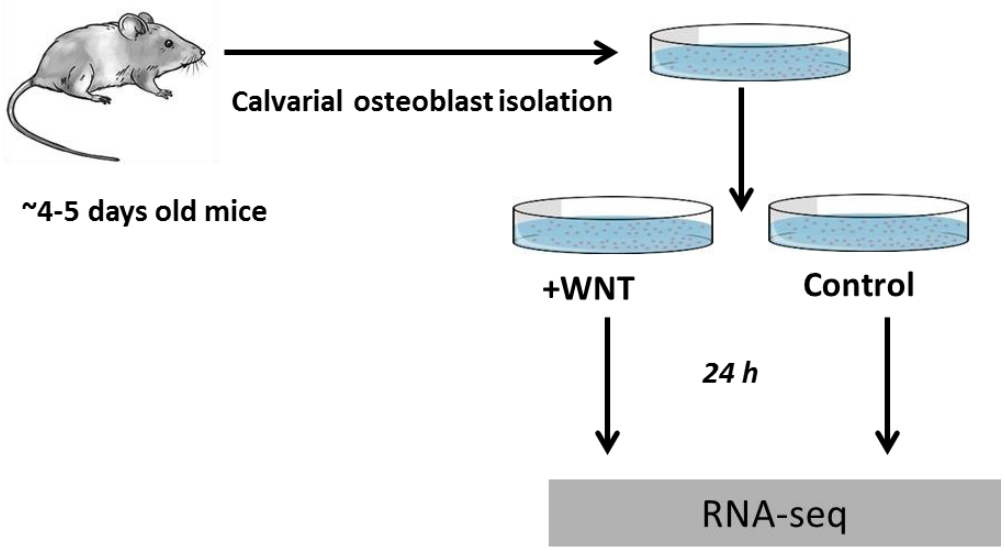

Figure 3.1*: *Experimental design. *Calvarial osteoblasts isolated from 4-5 days old mice were treated with recombinant WNT3A for 24 hours (h). RNA was then isolated from WNT3A treated and control samples and sequenced using Illumina HiSeq 2000 or a NextSeq 550.*

By comparing gene expression data from WNT3A treated *WT* osteoblasts to sham treated *WT* osteoblasts, we identified 278 up-regulated genes and 510 down-regulated genes in WNT3A treated samples (Table 3.2). Several members of WNT signaling pathway including *Porcn*, *Fzd1*, *Lef1*, *Tcf7* and *Axin2* were found to be up-regulated and *Sfrp1*, *Sfrp2*, *Fzd4, Fzd9*, *Rspo2*, *Rspo3* and *Lgr4* were found to be down-regulated in WNT3A treated osteoblasts. We also identified a number of known canonical WNT target genes as either up-regulated (*Nkd1*, *Nkd2*, *Bmp4*, *Fgf18*, *Grem1*, *Cyr61*, *Ccnd1*, *Tnfrsf19* etc.) or down-regulated (*Jag1*, *Vcan*, *Sfrp2* etc.) in response to WNT3A treatment.

WNT3A down-regulated the expression of *Pparg*, the master regulator of adipocyte differentiation [315] and *Sox9*, a key regulator of chondrocyte differentiation [316]. Previous studies have demonstrated that knockdown of *Pparg* induces spontaneous osteoblast differentiation in ST2 cells, a progenitor cell that possesses both osteogenic and adipogenic potential [58]. In mice, overexpression of *Sox9* in osteoblasts from a 2.3-kb *Col1a1* promoter resulted in dwarfism and osteopenia, with a significant reduction in bone volume, osteoblasts number and bone formation rate. These studies suggest that WNT3A mediated down-regulation of *Pparg* and *Sox9* may promote osteogenic differentiation and bone formation.

We also identified several genes associated with altered bone metabolism phenotypes in mice as WNT3A targets in osteoblasts. Thirty three genes including *Bmp2*, *Fosl2* and *Cthrc1* with known bone metabolism phenotypes were up-regulated while 42 genes with bone metabolism phenotypes including *Spp1*, *Fzd9* and *Sfrp1* were down-regulated in response to WNT3A treatment (Table 3.3). WNT3A has previously been

shown to induce the expression of the osteoblast differentiation marker alkaline phosphatase (*Alp*). However, we did not observe a significant change in the expression of *Alp* or other osteoblast markers such as *Col1a1* or *Bglap* in WNT3A treated osteoblasts.

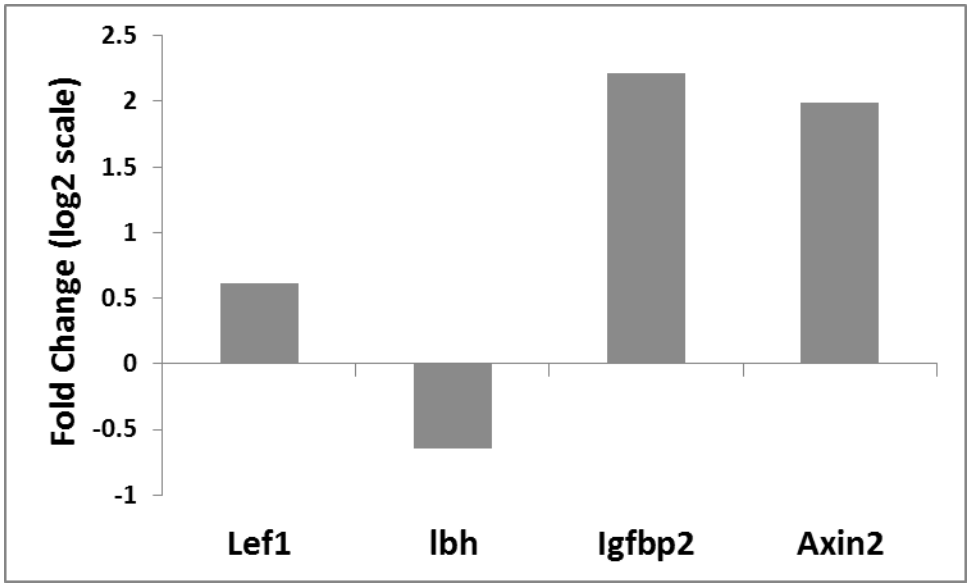

***Figure 3.2**: **qRT-PCR analysis of known WNT targets**. The qRT-PCR analysis was conducted on known WNT targets to confirm that the WNT3A treatment worked as expected. Fold change values (WNT3A treated vs. Control) are shown.*

A gene ontology analysis with DAVID identified biological processes including '*regulation of cell proliferation*', '*mesenchymal cell differentiation*', '*cell motion*', '*positive regulation of cell differentiation*' and '*skeletal system development*' as enriched for up-regulated genes (Figure 3.3A). For down-regulated genes, gene ontology categories corresponding to '*immune response*', '*cell adhesion*', '*vasculature development*', '*regulation of cell death*', '*ossification*' and '*response to hypoxia*' were identified as enriched (Figure 3.3B). '*Regulation of cell proliferation*' was the most significantly enriched term for up-regulated genes with 39 genes including *Bmp2*, *Bmp4*, *Tgfb2*, *Pdgfa*, *Fosl2*, and *Hbegf* in that category. Surprisingly, for down-regulated genes '*immune response*' was identified as the most significantly enriched category with 43 genes. Immune response related genes down-regulated by WNT3A include genes such as *Cxcl12*, *Ccl5*, *Tlr3*, *Tlr4* and *Tlr7*. *Cxcl12* signaling in osteoblasts has been shown to regulate the mesenchymal stem cell and osteoclast lineage populations [317]. TLR signaling may also play a role in regulating osteogenic differentiation [318,319]. Further studies are required to understand the roles of other immune response related genes in osteoblasts.

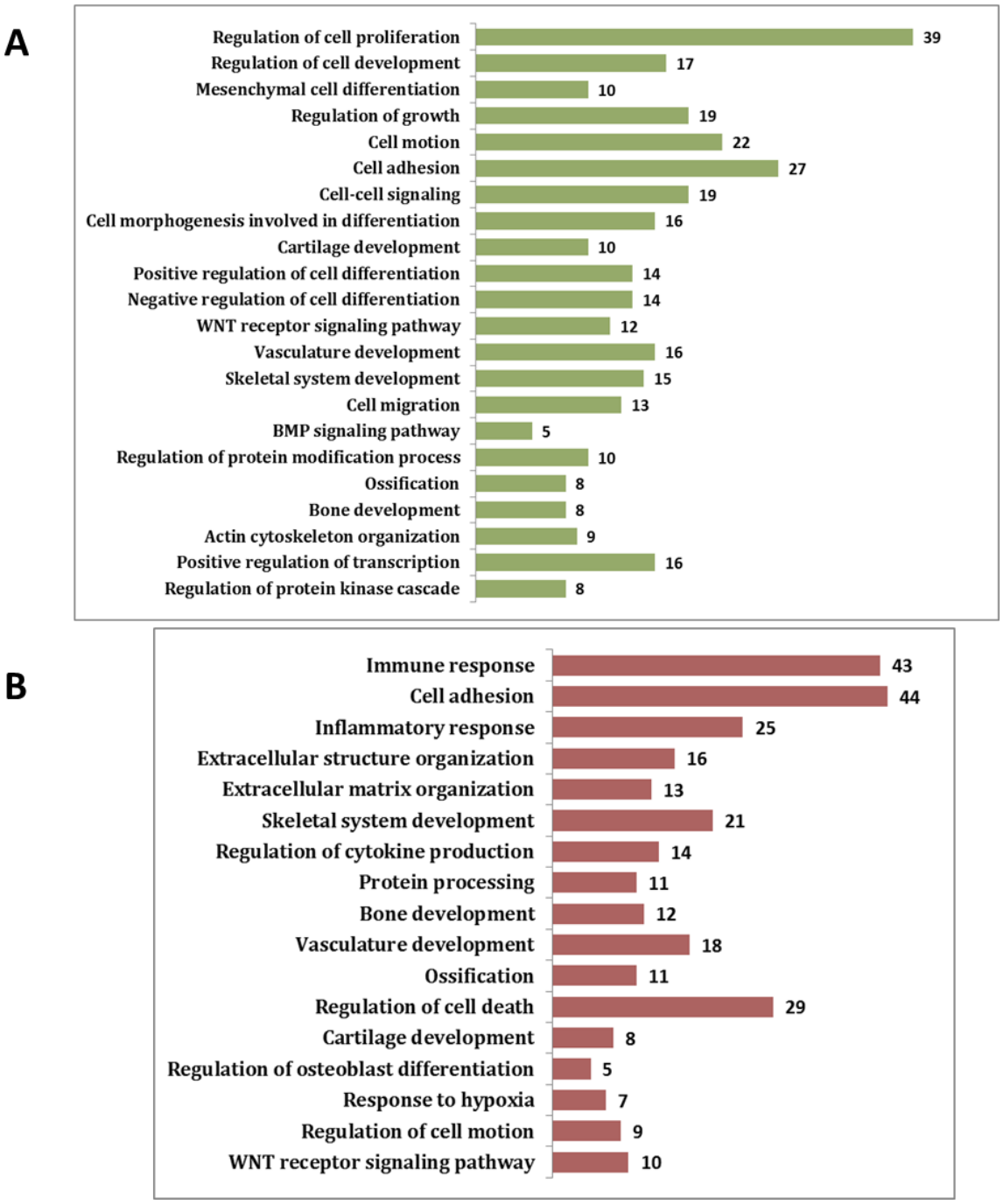

***Figure 3.3**: **Enriched GO terms associated with WNT3A targets**. Enriched biological processes associated with genes up (**A**) and down-regulated (**B**) by WNT3A in WT osteoblasts. Enriched biological processes (p-value <0.01) associated with differentially expressed genes were identified using DAVID. Number of genes associated with each ontology term is shown in the figure. Categories are arranged in the order of increasing p-values (from top to bottom).*

A pathway analysis with DAVID identified '*WNT signaling pathway'*, '*TGF-beta signaling pathway'*, '*MAPK signaling pathway'*, '*p53 signaling pathway'* and '*Cytokine-cytokine receptor interaction'* as enriched signaling pathways associated with genes up-regulated by WNT3A and '*Complement and coagulation cascades'* and '*Toll-like receptor signaling pathway'* as enriched signaling pathways associated with down-regulated genes (Table 3.4). This data suggest that WNT signaling may cooperate with TGF-beta signaling pathway and MAPK signaling pathway, two other key regulators of skeletal development and metabolism, to regulate osteoblast differentiation.

3.3.2 WNT3A activated genes associated with osteoblast proliferation and inhibited genes associated with osteoblast maturation/mineralization

To better understand the temporal regulation and function of WNT3A targets during osteogenesis, we analyzed their expression changes during differentiation of early pre-osteoblasts to mature osteoblasts (day 2 to day 18), using a publicly available dataset [312]. We reanalyzed the public data as described in Section 3.2.6 and examined the changes in the expression of WNT3A targets as pre-osteoblasts differentiate to mature osteoblasts. Our analysis revealed that a large number of genes up-regulated by WNT3A are normally expressed at high levels during early stages of osteogenic differentiation (Table 3.5 and Figure 3.4A) and a majority of the genes down-regulated by WNT3A are highly expressed during late stages of osteoblast differentiation (Table 3.5 and Figure 3.4B). This suggests that WNT3A treatment promotes the expression of genes involved in osteoblast proliferation or early stages of differentiation, while inhibiting genes involved in osteoblast maturation and mineralization.

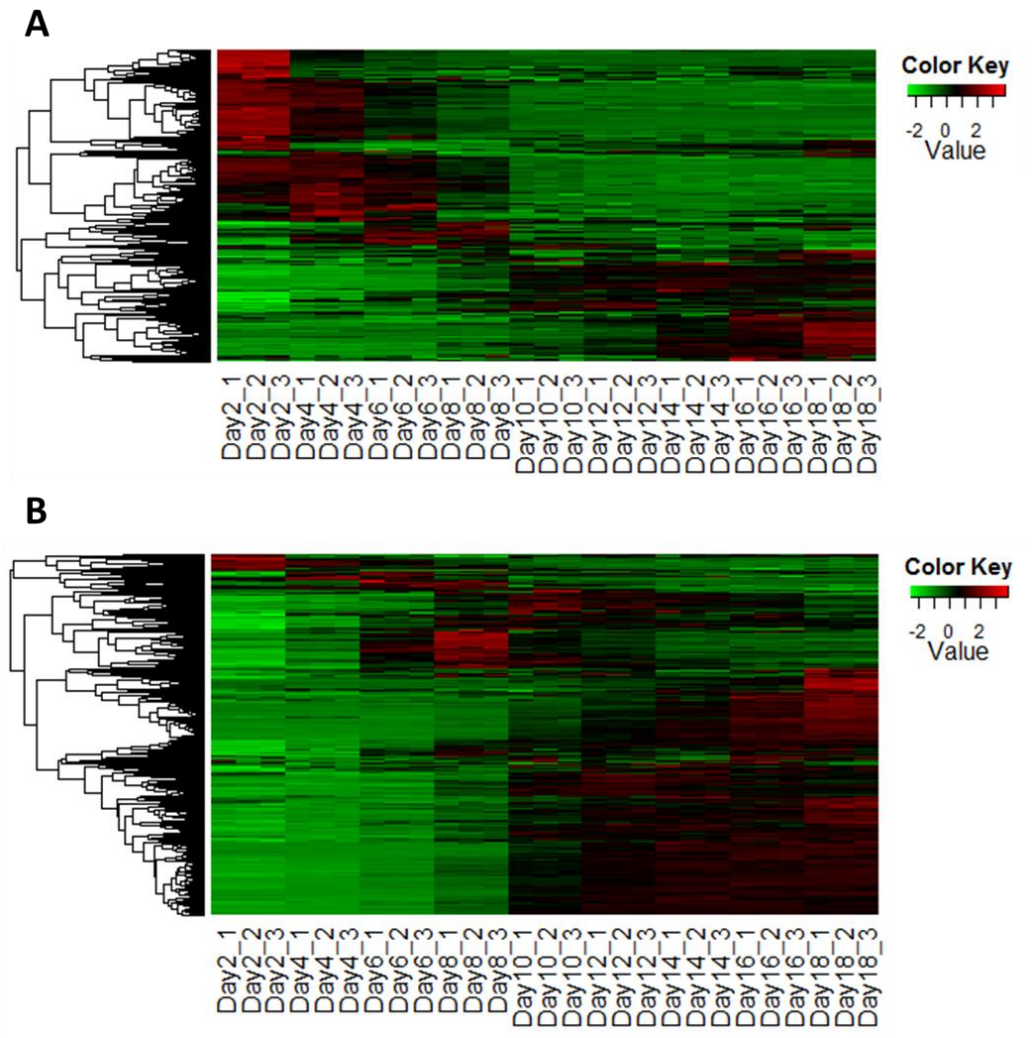

Figure 3.4: ***Expression profiles of WNT3A targets during the differentiation of early pre-osteoblast to mature osteoblasts (Day 2 to Day 18)***. *Expression levels of WNT3A targets at different stages of osteoblast differentiation were determined using a public dataset as described in Section 3.2.6. Genes were clustered using hierarchical clustering and heatmaps were generated using gplots 2.11.* ***A****) Expression profiles of genes up-regulated by WNT3A. A large number of genes up-regulated by WNT3A are highly expressed in early stage osteoblasts.* ***B****) Expression profiles of genes down-regulated by WNT3A. Majority of the genes down-regulated by WNT3A are highly expressed in late stage osteoblasts.*

Previous studies have also suggested that WNT3A increases cell proliferation [56,320]. To confirm the role of WNT3A in osteoblast proliferation, MC3T3 pre-osteoblastic cells were treated with recombinant WNT3A and cell proliferation was measured using CFSE staining. MC3T3 cells treated with WNT3A displayed a significant increase in proliferation rate (Figure 3.5) compared to un-treated cells. By day

8, the majority of WNT3A treated cells were in generation 5 and 6 whereas the majority of sham treated cells were in generation 3 and 4 (Figure 3.5). This suggests that WNT3A treated cells proliferated significantly faster than controls.

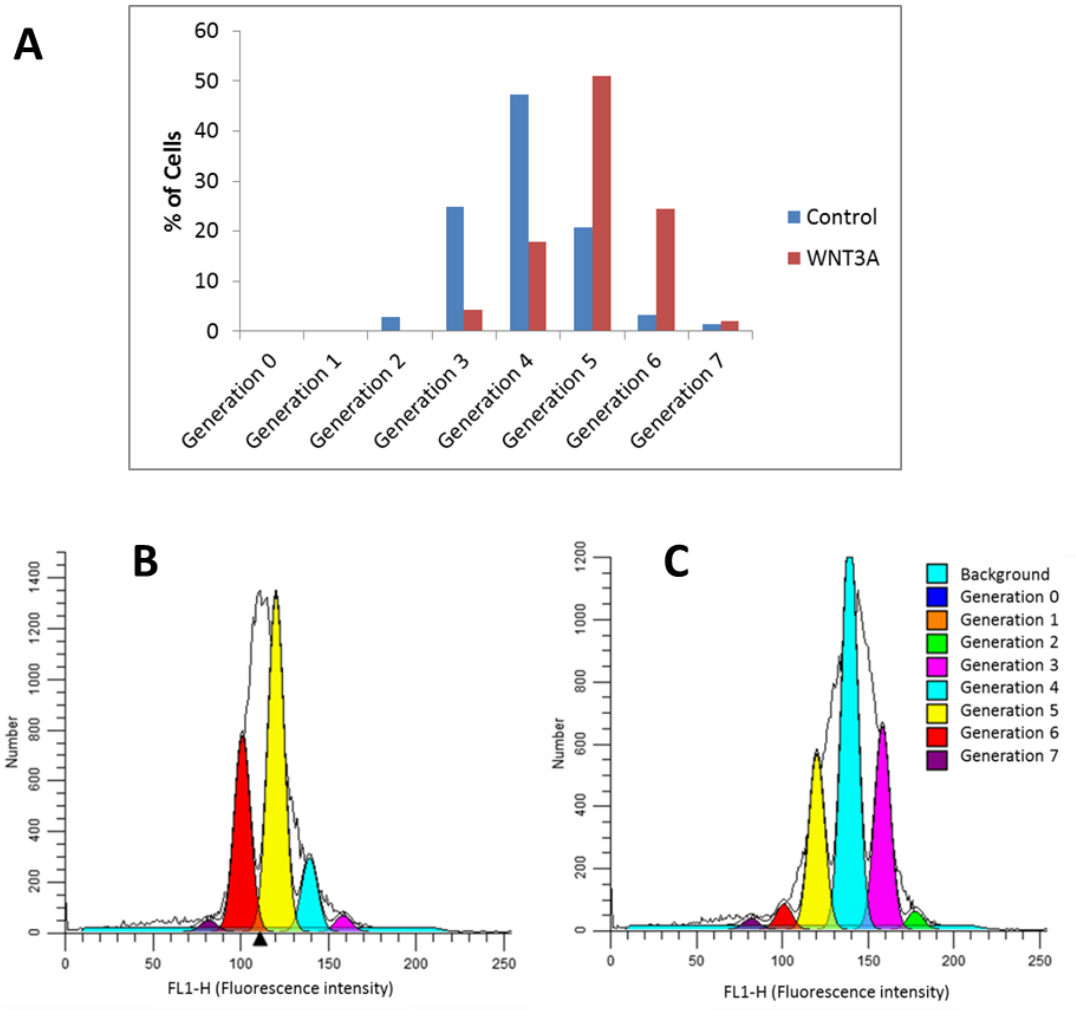

Figure 3.5: Osteoblast proliferation assay*. CFSE cell proliferation assay showed that by day 8 majority of WNT3A treated cells were in generation 5 and 6 (**A** and **B**) and majority of sham treated cells were in generation 3 and 4 (**A** and **C**).*

To understand how WNT3A regulates osteogenesis *in vivo*, we injected 4-6 week old mice with recombinant WNT3A or PBS. All mice received recombinant WNT3A/PBS injection subcutaneously on the calvaria as described in Section 3.2.8 (Figure 3.6).

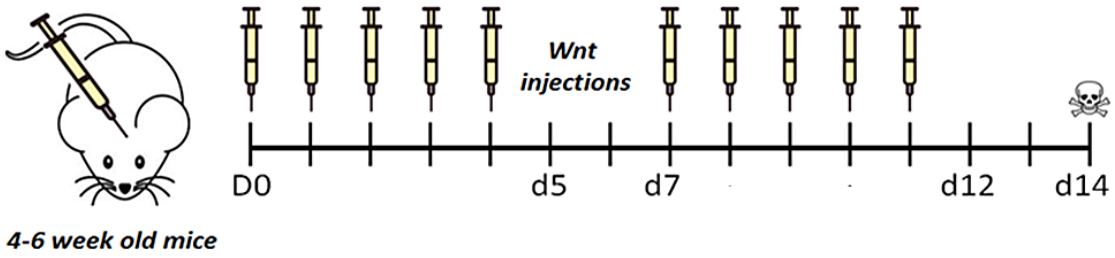

***Figure 3.6**: **Calvarial injection**. Four to six week old mice received recombinant WNT3A/PBS injections subcutaneously on the calvaria as described in Section 3.2.8. After 14 days, the calvarias were isolated and analyzed using histology and µCT.*

Fourteen days after the treatment, calvarias were isolated and examined using histology and µCT to see the changes in bone formation. Histology analysis revealed that WNT3A treated calvaria was significantly thicker than PBS treated calvaria (Figure 3.7 A, B). A µCT analysis showed that treatment with WNT3A resulted in significant reduction in calvarial BMD (Figure 3.7 D). However, µCT also showed that WNT3A treated calvarias were slightly thicker than PBS treated calvarias (*p*-value =0.053). These results together suggest that WNT3A treatment increased osteoblast proliferation/early differentiation and decreased osteoblast maturation/mineralization.

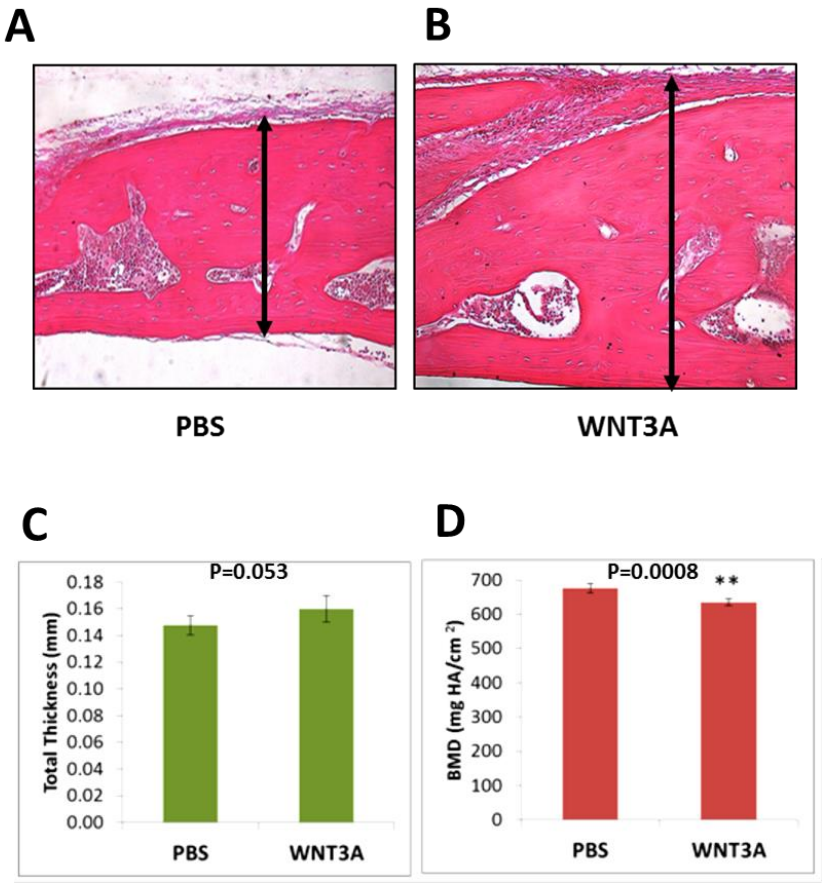

***Figure 3.7**: **Histology and µCT data**. Histology of PBS (**A**) and WNT3A (**B**) treated calvarias. H&E staining showed that WNT3A treated calvaria was significantly thicker than PBS treated calvaria. µCT of WNT3A and PBS treated calvarias (**C** and **D**). WNT3A treated mice showed increased calvarial thickness (p-value = 0.053) and a significant reduction in calvarial BMD (p-value = 0.0008). Statistical significance was determined using a two sample t-test.*

3.3.3 Ablation of Lrp5 and Lrp6 had different effects on osteoblastic gene expression

Next, we investigated the role of WNT co-receptors LRP5 and LRP6 in osteoblasts. Osteoblasts lacking *Lrp5* (*Lrp5*$^{-/-}$), *Lrp6* (*Lrp6*$^{-/-}$) and *Lrp5/6* (*Lrp5*$^{-/-}$;*Lrp6*$^{-/-}$) were generated for this purpose. *Lrp5*$^{-/-}$ osteoblasts were isolated from neonatal *Lrp5*$^{-/-}$ mice as described in Section 3.2.2. Since *Lrp6*$^{-/-}$ mice are embryonically lethal *Lrp6*$^{-/-}$ osteoblasts and *Lrp5*$^{-/-}$;*Lrp6*$^{-/-}$ osteoblasts were generated by treating *Lrp6*$^{fl/fl}$;*UBC-Cre ERT2* osteoblasts and *Lrp5*$^{fl/fl}$;*Lrp6*$^{fl/fl}$;*UBC-Cre ERT2*, respectively, with TMX *in vitro*.

By comparing gene expression in *Lrp5*$^{-/-}$ osteoblasts to *WT* osteoblasts we identified 172 up-regulated genes and 77 down-regulated genes in *Lrp5*$^{-/-}$ osteoblasts (Table 3.6). Seven genes induced by WNT3A in *WT* osteoblasts including *Sfn*, *Ahr*, *Ankrd1*and *Ahrr* showed down-regulation in *Lrp5*$^{-/-}$ osteoblasts while 32 genes down-regulated by WNT3A in *WT* osteoblasts including *Cxcl12*, *Dcn*, *Mmp13*, *Chrdl1* and *Mt2* showed an increased expression in *Lrp5*$^{-/-}$ osteoblasts relative to *WT* osteoblasts.

To account for the effects TMX may have on osteoblastic gene expression, *Lrp6*$^{-/-}$ and *Lrp5*$^{-/-}$*;Lrp6*$^{-/-}$osteoblasts were compared to TMX treated controls. By comparing *Lrp6*$^{-/-}$ (*Lrp6*$^{fl/fl}$*;UBC-Cre ERT2* +TMX) to TMX treated controls (*Lrp6*$^{fl/fl}$+TMX) we identified 200 up-regulated genes and 81 down-regulated genes in *Lrp6*$^{-/-}$ (Table 3.6). Five genes induced by WNT3A in *WT* osteoblasts including *Grem1*, *Ndnf*, and *Dynap* showed a down-regulation in *Lrp6*$^{-/-}$ osteoblasts while 73 genes down-regulated by WNT3A in *WT* osteoblasts including *Comp*, *Fzd9*, *Mmp13* and *Chrdl1* showed higher expression in *Lrp6*$^{-/-}$ osteoblasts relative to controls.

We identified 262 up-regulated genes and 87 down-regulated in *Lrp5*$^{-/-}$*;Lrp6*$^{-/-}$ (*Lrp5*$^{fl/fl}$*;Lrp6*$^{fl/fl}$*;UBC-Cre ERT2*+TMX) osteoblasts compared to TMX treated controls (*Lrp5*$^{fl/fl}$*;Lrp6*$^{fl/fl}$ + TMX*)* (Table 3.6). Seventeen genes induced by WNT3A in *WT* osteoblasts including *Axin2*, *Ndnf*, *Nkd1* and *Tnfrsf19* showed a down-regulation in *Lrp5*$^{-/-}$*;Lrp6*$^{-/-}$ osteoblasts while 84 genes down-regulated by WNT3A in *WT* osteoblasts showed an enhanced expression in *Lrp5*$^{-/-}$*;Lrp6*$^{-/-}$osteoblasts relative to controls.

Of the 249 genes differentially expressed in *Lrp5*$^{-/-}$ osteoblasts, 28 and 27 genes overlapped with genes differentially expressed in *Lrp6*$^{-/-}$ and *Lrp5*$^{-/-}$*;Lrp6*$^{-/-}$ osteoblasts, respectively (Figure 3.8). Eighty nine genes differentially expressed in *Lrp6*$^{-/-}$ compared to controls overlapped with genes differentially expressed between *Lrp5*$^{-/-}$*;Lrp6*$^{-/-}$ osteoblasts and controls (Figure 3.8). Nine genes including *Pou3f4*, *Ntrk2*, *Parp10*, *Siglec1*, *Irgm2*, *Trim30d* and *Lgals3bp* were differentially expressed in all three genotypes compared to respective controls.

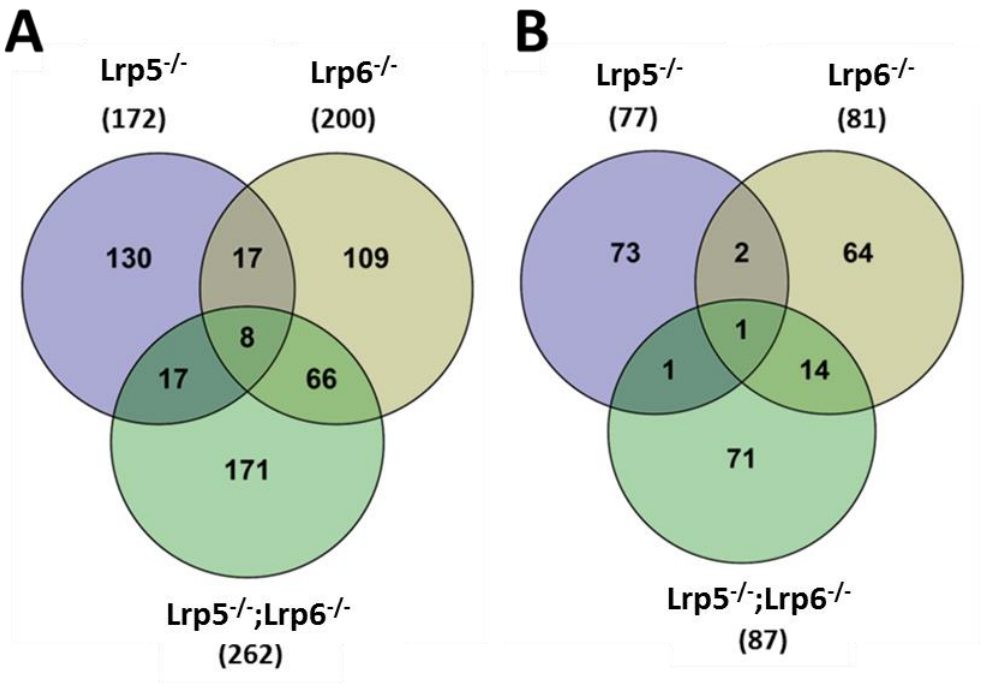

Figure 3.8: Venn diagrams of sets of genes differentially expressed in Lrp5$^{-/-}$, Lrp6$^{-/-}$ and Lrp5$^{-/-}$;Lrp6$^{-/-}$ osteoblasts compared to respective controls*. **A**) Up-regulated genes. **B**) Down-regulated genes.*

3.3.4 Ablation of Lrp6, but not Lrp5, significantly impaired WNT3A signaling in osteoblasts

To study the role of LRP5 and LRP6 in modulating WNT3A signaling we quantified gene expression changes in WNT3A treated *Lrp5*$^{-/-}$, *Lrp6*$^{-/-}$ and *Lrp5*$^{-/-}$;*Lrp6*$^{-/-}$ osteoblasts compared to respective sham treated controls. By comparing WNT3A treated *Lrp5*$^{-/-}$ osteoblasts to sham treated *WT* osteoblasts we identified 1,067 genes differentially expressed in WNT3A treated *Lrp5*$^{-/-}$ osteoblasts. This included 440 up- and 627 down-regulated genes. ~73% (575/788) of the WNT3A targets identified in *WT* osteoblasts were ≥1.5 fold up or down-regulated in *Lrp5*$^{-/-}$ osteoblasts in response to WNT3A treatment, suggesting that WNT3A mediated signaling is largely unaffected by the loss of *Lrp5* in osteoblasts (Figure 3.9 and Table 3.2).

By comparing WNT3A treated *Lrp6*$^{-/-}$ osteoblasts to sham treated controls (*Lrp6*$^{fl/fl}$+TMX) we identified 352 genes up- or down-regulated in *Lrp6*$^{-/-}$ osteoblasts in response to WNT3A treatment. Only ~14% (111/788) of which were found to be WNT3A targets in *WT* OB, suggesting that the lack of *Lrp6* significantly impaired WNT3A signaling in osteoblasts (Figure 3.9 and Table 3.2).

Three hundred and fifty eight genes were differentially expressed between WNT3A treated *Lrp5*$^{-/-}$;*Lrp6*$^{-/-}$ osteoblasts and sham treated controls (*Lrp5*$^{fl/fl}$;*Lrp6*$^{fl/fl}$ + TMX*).* However, only 52 (~7%) of the WNT3A target genes were found to be ≥1.5 fold

up or down-regulated in WNT3A treated *Lrp5*$^{-/-}$*;Lrp6*$^{-/-}$ osteoblasts compared to control osteoblasts, suggesting that 93% of WNT3A targets in mature osteoblasts are transcriptionally modified *via* LRP5/6 co-receptor-dependent activation (Figure 3.9 and Table 3.2).

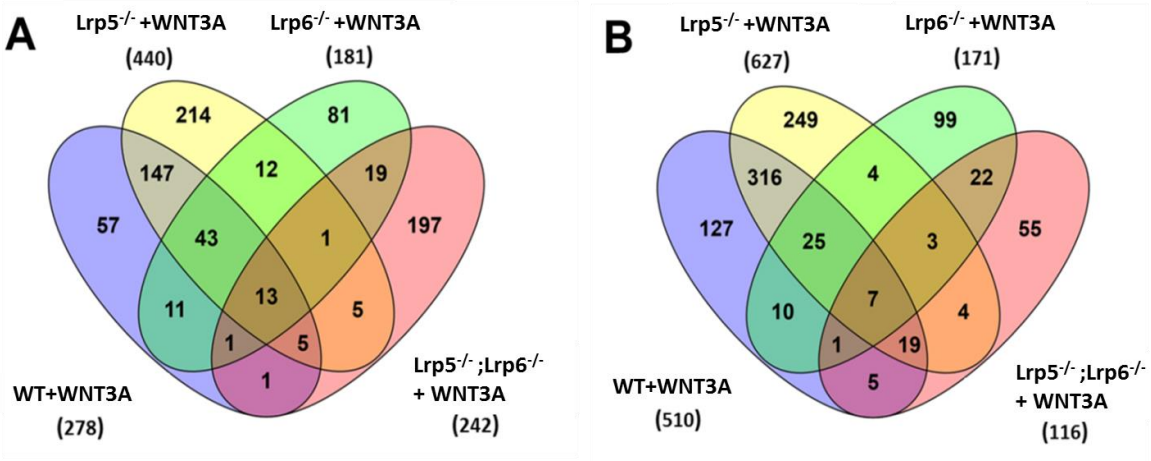

Figure 3.9: Venn diagrams of significantly differentially expressed genes in WNT3A-treated WT, Lrp5*$^{-/-}$*, Lrp6*$^{-/-}$ *and Lrp5*$^{-/-}$*;Lrp6*$^{-/-}$ *osteoblasts*. A)*** *Significantly up-regulated genes.* ***B)*** *Significantly down-regulated genes.*

3.4 Discussion

WNT3A is a major canonical WNT ligand that has been shown to promote bone formation [321]. Although numerous WNT3A target genes have been identified in different cell types including pluripotent mesenchymal cell line C3H10T1/2 [322] and stromal cell line ST2 [58], very little is known about the target genes regulated by WNT3A in osteoblasts. This study provides the first account of WNT3A regulated transcriptome in primary osteoblasts.

Previous gene expression studies have identified a number of canonical WNT targets in different cell and tissue types. We found that several of these known WNT targets including *Nkd1*, *Nkd2*, *Bmp4*, *Grem1*, *Cyr61*, and *Tnfrsf19* are differentially expressed in osteoblasts in response to WNT3A treatment. *Bmp4*, *Cyr61* and *Tnfrsf19* have previously been identified as major positive regulators of osteoblast differentiation [323-325]. This study also identified several members of WNT signaling pathway as WNT3A targets, suggesting a feedback regulation of WNT signaling in osteoblasts. WNT3A also regulated the expression of members of other signaling pathways including TGF-β/BMP signaling, MAPK signaling and several transcription factors including *Tcf4*, *Vdr* and *Nfatc4*. So, it is possible that some of the genes identified in this study are regulated indirectly by WNT3A.

Examination of the temporal expression patterns of WNT3A targets during osteoblastogenesis, revealed that a large number of the genes up-regulated by WNT3A

are highly expressed during the early stages of osteogenic differentiation and majority of the genes down-regulated by WNT3A are highly expressed in mature osteoblasts. This suggests that WNT3A promotes osteoblast proliferation or early stages of differentiation and inhibits osteoblast maturation/mineralization. This is in line with previous findings showing that WNT3A enhances proliferation of MSCs, pre-osteoblast cell lines and mouse primary osteoblasts [56,320]. WNT3A has also been shown to promote and inhibit the osteogenic differentiation of MSCs [56,320,326]. Our study confirmed that WNT3A promotes proliferation of pre-osteoblastic cells. We also found that continuous WNT3A treatment inhibits bone mineralization *in vivo*, suggesting that WNT3A is a positive regulator of early stage osteogenesis and a negative regulator of osteoblast maturation/mineralization.

LRP5 and LRP6 are key mediators of β-catenin dependent WNT signaling. However, very little is known about their specific roles in mediating canonical WNT signaling. Our study shows that LRP5 and LRP6 regulate different target genes in osteoblasts. Only ~11% (28/249) of genes differentially expressed in *Lrp5*$^{-/-}$ osteoblasts compared to controls overlapped with genes differentially expressed in *Lrp6*$^{-/-}$ osteoblasts. We also found that WNT3A regulated >73% of its target genes independent of LRP5, whereas lack of LRP6 significantly impaired the ability of WNT3A to regulate its target genes. This suggests that LRP6 is the key mediator of WNT3A signaling in osteoblasts. However, it is known that loss of LRP5 greatly impairs bone formation [35, 39], suggesting that LRP5 has a significant role in mediating WNT signaling in bone. It is likely that LRP5 may play a major role in mediating signaling by other canonical WNT ligands such as WNT1 and WNT10B. Alternatively, LRP5 may have a context dependent function in bone.

This study revealed that the number of genes suppressed by WNT3A in osteoblasts was significantly higher than the number of WNT3A activated genes (510 versus 278 genes). Interestingly, we also found that a large number of genes suppressed by WNT3A were up-regulated in sham treated *Lrp5*$^{-/-}$, *Lrp6*$^{-/-}$ and *Lrp5*$^{-/-}$*;Lrp6*$^{-/-}$ osteoblasts compared to sham treated controls. However, only a few genes up-regulated by WNT3A were down-regulated in these receptor knockouts compared to controls. This suggests that transcription repression is a major mechanism by which canonical WNTs perform their functions. In a recent study Karner *et al.* showed that WNT3A inhibit gene expression by suppressing histone acetylation in an LRP5/6 dependent, but β-catenin independent manner [58]. Our study identified histone deacetylase 9 (*Hdac9*) as a gene activated by WNT3A in osteoblasts. Previous studies have shown that *Hdac9* inhibits *Pparg* expression [327], suggesting that *Hdac9* may play a role in WNT3A mediated transcription repression. Further studies are required to understand whether HDAC9 plays a role in suppressing gene expression in osteoblasts in a WNT responsive manner.

Altogether, this study has identified several novel WNT target genes and provides new insights into LRP5/6 dependent WNT signaling in osteoblasts. These results enhance our understanding of the role of the canonical WNT signaling pathway in the regulation

of osteoblast differentiation and function, as well as our general knowledge of the WNT signaling pathway.

Table 3.1: List of qRT-PCR primers

	Forward	**Reverse**
Axin2	ATGAGTAGCGCCGTGTTAGTG	GGGCATAGGTTTGGTGGACT
Igfbp2	CAGACGCTACGCTGCTATCC	CTCCCTCAGAGTGGTCGTCA
Lef1	ATCACCTACAGCGACGAGCAC	TGGACATGGAAGTGTCGCCTG
Ibh	CTGCTCTGACTATCTGAGATCGG	CAGCAACGGTCAAAGTCTGAT

Table 3.2: ***Genes differentially expressed inWNT3A treated WT, Lrp5$^{-/-}$, Lrp6$^{-/-}$ and Lrp5$^{-/-}$;Lrp6$^{-/-}$ osteoblasts compared to sham treated controls.*** *Fold changes are given in log2 scale (log2 FC). All genes have an FDR corrected p-value < 0.05.*

GENE	**WT+WNT3A (log2 FC)**	**Lrp5$^{-/-}$+WNT3A (log2 FC)**	**Lrp6$^{-/-}$+WNT3A (log2 FC)**	**Lrp5$^{-/-}$;Lrp6$^{-/-}$ +WNT3A (log2 FC)**
Bex1	4.393	4.134		
Slc13a4	4.080			
Fgfbp1	3.853			
Sema4f	2.994	2.665	1.492	0.673
Sstr2	2.842			
Nell2	2.841	2.762	1.408	1.088
Ndnf	2.784	3.031	0.803	
Axin2	2.709	2.568	1.833	0.623
Ntf3	2.482	2.450		
Tmem100	2.290	2.191	0.983	
Colec10	2.177	1.567		
Igfbp2	2.176	1.658	0.698	
C430002N11Rik	2.086	2.251		
Aqp5	2.081	2.127		
Grik3	2.062	2.266		
Syt13	2.051	2.028	1.196	0.981
Hhip	2.028	1.768	0.955	
Tnfsf15	2.012	1.464	1.584	0.606
Nkd2	1.968	2.231		
Dio2	1.963	2.659		
Slc1a2	1.937	1.859		
Tgfb2	1.909	1.729	1.022	
Bmper	1.909	1.934		
Grem1	1.882	1.638		
Inhbb	1.866	1.764	1.118	0.696
Dpp4	1.854	1.984		
Lypd6	1.820	1.539		

Iyd	1.794	1.759		
Ccbe1	1.783	1.851		
Pamr1	1.776	1.533	0.851	0.792
Cdh17	1.757	1.234	1.176	
Nebl	1.746		1.161	
Bmp7	1.719	0.939	0.876	
Car8	1.690	1.361		
Apcdd1	1.686	1.429		
Kcnj2	1.678	2.138	0.789	
Col7a1	1.675	1.110	0.638	0.625
Eva1a	1.613	1.711		
Gm12505	1.591	2.430		
Tnfrsf19	1.585	1.463	1.017	
Dynap	1.583	2.189	0.769	0.758
Herc3	1.567	1.556	0.921	
Timp3	1.532	1.115	0.931	
Enpp2	1.529	1.752	0.893	
Prss46	1.510	1.418		0.623
Rgcc	1.488	1.526		
Tceal5	1.451	1.258		
Etv4	1.439	1.504		
Gjb2	1.416	0.835	1.294	0.830
Fhod3	1.391	1.408	0.996	
Gadd45g	1.388	1.175	0.724	
Atp1a2	1.380	1.084		
Arl4c	1.380	1.323	0.587	
Slitrk6	1.378	2.151	1.221	
Itga8	1.378	1.095		
Grem2	1.367	1.272		
Ngf	1.351	1.159		0.648
Aldh1a2	1.318	1.778		-0.927
Ctnnd2	1.309	0.751		0.933
Mrgprf	1.282	1.155		
C1ql3	1.277	1.159		
Sfn	1.262	-0.989	1.878	0.727
Cnn1	1.261		0.797	
Fam180a	1.241			
Lif	1.230	0.847	0.815	
Specc1	1.220	1.159		
Cap2	1.215	1.298		
Tcf7	1.198	1.194		
Plat	1.198	1.203	0.615	
Pmaip1	1.186	1.197	0.733	
Piezo2	1.180	0.811		
E030011O05Rik	1.169	1.113	0.784	0.954
Hck	1.152		0.856	
Gabrb3	1.140	1.004		
Col26a1	1.130	0.991	1.183	
Tec	1.128	0.981	0.938	

Ddah1	1.125	1.322		
Pdgfa	1.110	0.921		
Nkd1	1.107	0.774		
Has2	1.101	1.478		
Stc1	1.100	1.822	0.687	
D6Ertd527e	1.098	1.097		
Slc20a1	1.097	0.990		
Noct	1.097	1.235		
Ahr	1.095	0.704	0.977	
Zfp503	1.092	0.952		
Ptgs2	1.085	1.490	1.078	0.701
Aldh1a7	1.078		0.751	
Nov	1.075	0.650		
Rdh10	1.059			
Ier3	1.054	1.350	0.929	
Scube1	1.050	1.150	0.887	
Ahrr	1.040			
Lrrc15	1.026	0.631		
Ptch1	1.026	0.866		
Tspyl5	1.025	1.102		
Rerg	1.020	0.904	0.700	
Fam101a	1.008		0.770	
5430421F17Rik	1.006			
Pcdh10	1.006			
Arxes2	1.005	0.975		
Cdc42ep3	1.004	0.891		
Insc	1.004	0.823		
Murc	0.992	1.020		
Lurap1l	0.990	0.681	-0.585	
Hdac9	0.985	1.987	1.231	
Cxadr	0.984	0.851	1.127	
Errfi1	0.984	1.076	1.251	
Ankrd1	0.982			
Nrcam	0.978	1.515	1.041	
Thsd4	0.977	0.911		
Tiparp	0.968	0.836		
Fgf21	0.964	0.795		-0.616
Syn1	0.956	0.895		
Fam101b	0.952			
Spry1	0.943	1.025		
Tgfb3	0.935	0.648		
Creld1	0.927	1.005		
Adamts8	0.927	0.888		
Plcxd2	0.926	0.867		
Fzd1	0.919	0.946		
Filip1l	0.916	0.680		
Fam185a	0.914	0.712		
Moxd1	0.913		1.040	
Wif1	0.911	0.971	0.840	

Rgs16	0.909	1.233		
Crabp1	0.906	1.339		
Prickle1	0.904	0.978		
Bmp3	0.895			
Nipal4	0.892			
Cdkn2a	0.890	0.851		
Cxcl14	0.885	1.978		
Lrrc32	0.885	0.911		
Dusp1	0.881	0.722	0.798	
Fgf18	0.881		0.789	
Pgf	0.880	0.845		
Fmnl2	0.878	0.811		
5930412G12Rik	0.872			
Fam198b	0.870	0.872		
Smim3	0.870	0.923		
Galnt16	0.867	0.878		
Kank1	0.866	0.778		
Ppfibp2	0.856	0.777		-0.728
Itga4	0.855	0.906		
Fbln5	0.854	0.857		
Hbegf	0.853	0.834		
Ror1	0.845	1.042		
Cyp26b1	0.841	1.087		
Serpine1	0.830	1.207		0.937
Galnt3	0.828	0.775		
Lef1	0.824			
Ccnd1	0.822	0.651		
Slc16a3	0.821	1.064	0.780	
Nog	0.817	0.678		
Aif1l	0.810			
Prg4	0.809	1.792		
Scn3a	0.808	0.607	1.110	0.758
Bmpr1b	0.803	1.241		
Bmp2	0.802	0.729		
Spire2	0.799	0.740		
Fam131a	0.796	0.598	0.685	
Lepr	0.795	0.684		0.628
Arsi	0.792			
Hspa4l	0.792	0.779		
Cyr61	0.792	0.888	0.886	
Wbscr17	0.787	0.613		
Cd24a	0.779	0.631	0.715	
Fgf13	0.776			
Tes	0.775	0.799		
Irx3	0.772	0.729		
Hunk	0.771			
Elfn1	0.770	0.799	0.647	
Pard6b	0.768	0.795		
Actg2	0.764			

Phldb2	0.762			
Ch25h	0.757	1.023	1.304	
Pdxp	0.755	0.923		
Sema3f	0.755			
Trp53i11	0.755		0.789	
Tmem26	0.746	0.838		-0.752
Sema5a	0.745	1.100	0.615	
Pmepa1	0.745	0.657		
Osbpl3	0.744	0.688		
Arxes1	0.743			
Sh3rf1	0.742	0.692		
Rras2	0.739	0.690		
Cdo1	0.738	0.846		
Cacna1g	0.737	0.592		
Sync	0.734	0.769		
Inhba	0.733			0.903
Dpep1	0.730	0.616		
Svip	0.723	0.917		
Fam184a	0.722			
Prrx2	0.721	0.913		
Map6	0.721			
Porcn	0.717	1.033		-0.705
Dpt	0.717	0.889		
Rnf122	0.716	1.003		
Gpn2	0.711			
Cacnb4	0.710	0.947		
Csrp1	0.709	0.640		
Fosl2	0.700	0.858		
Rnd3	0.700		0.603	
Tagln	0.700			
Foxn3	0.699			
Dkk2	0.699	0.869		
Jak2	0.695	0.943		
Tnfaip6	0.692	1.093		
Nrp2	0.692			
Qpct	0.688	0.700		
Nav3	0.688	0.849		
Fam84b	0.687		0.799	
Efemp1	0.684	0.888		
Klhdc8a	0.683			
Artn	0.683	0.879		
Robo2	0.683	0.727		
Eef1e1	0.681	0.728		
Adrb2	0.674	0.629		
Stambpl1	0.674	0.796		
Plaur	0.672			
Egln3	0.669	0.987		-0.613
Mrto4	0.668	0.713		
Lin7a	0.662	0.873		-0.959

Gdnf	0.660	0.901		
Kctd11	0.658			
Pfkfb1	0.657			
Fgfr1	0.657			
Tcf4	0.653			
Kcnj15	0.651	1.485	1.037	
Unc13b	0.650	0.613		
Pitpnc1	0.645			
Zfp462	0.639			
Fam65b	0.638	0.690		
Mllt3	0.637			
Sh3bp4	0.637			
Adk	0.634			
Tnfrsf12a	0.633			
Tpd52	0.631	0.724		
Coq10b	0.630			
Nedd9	0.627	0.588		
Bmp4	0.627			
Pxylp1	0.626	0.809		
Nfatc4	0.624	0.706		
Ddit4l	0.621	1.012		
Vgf	0.621	1.266		
Itm2a	0.620	0.589	0.703	
Rapgef3	0.619	0.602		
Cthrc1	0.618	0.678		
Wnt2b	0.618		0.766	
Adamts4	0.617	0.616		
Hes1	0.617			
Sgms1	0.614			
Mtus1	0.614			
Lims2	0.614			
Col23a1	0.613			-0.743
Glipr1	0.612	0.762		
Fjx1	0.612	0.814		
Dbf4	0.611	0.639		
Sfrp4	0.611	1.144	0.849	
Itgb1	0.609	0.619		
Maff	0.609	0.634		
Pim1	0.608			
Arhgap6	0.604	0.643		
Timm8a1	0.604	0.828		
Stard13	0.603			
Phlda1	0.602			
Limk2	0.602			
Wdr92	0.601	1.052		
Acta2	0.601			
Slc2a3	0.599	1.018		
Sorbs1	0.598			
Chst1	0.598			

Itga3	0.596			
Suox	0.595			
Rb1	0.594	0.632		
Irx5	0.594			
Il16	0.588	0.767	0.949	
Arhgdig	0.586	0.749		
Aff3	-0.587	-0.787		
Sytl2	-0.587	-0.690		
Bcar3	-0.587			
Rida	-0.587	-0.636		
Vill	-0.588	-0.681		
Bbs1	-0.590	-0.612		
Zfp811	-0.590	-0.652		
Thra	-0.592	-0.621		
Fam43a	-0.592			
Camk1d	-0.592	-0.659		
A4galt	-0.592			
Acss3	-0.593			
3632451O06Rik	-0.593	-0.637		
Rnf144b	-0.594	-0.647		
Adamtsl3	-0.594	-0.645		
Igsf10	-0.596			
Ankrd44	-0.597			
Heph	-0.597			
H2-T10	-0.598			
Smpdl3b	-0.598	-1.041		
Lgals9	-0.599			
Fzd8	-0.599			
Ldb2	-0.600	-0.814		
Tlr4	-0.601			
Pik3ip1	-0.601	-0.827		
Msrb2	-0.601	-0.661		
Klhl13	-0.604			
Fry	-0.606	-0.874		
Cd82	-0.607	-0.692		
Pnmal2	-0.607	-0.643		
Ganc	-0.607			
Parp9	-0.610			0.843
Slc7a8	-0.610	-0.622		
Cd1d1	-0.611	-0.596		
Daam2	-0.611	-0.951		
B230118H07Rik	-0.611	-0.680		
Lpin1	-0.612	-0.772		
AI429214	-0.613			
Col18a1	-0.613	-0.689		
Trim12c	-0.613	-0.657		0.867
Icam1	-0.614			
Arhgef6	-0.614			
Coq8a	-0.614			

Bicc1	-0.616			
4933431E20Rik	-0.616			
Mamld1	-0.617	-0.700		
Slitrk5	-0.617			
Rab32	-0.618			
Thy1	-0.619			
Mar8	-0.620	-0.701		
Prkaa2	-0.621	-0.624	0.731	
Sema3e	-0.621	-0.788		
H2-T22	-0.623			
Dync2li1	-0.623	-0.861		
Efna5	-0.625			
Rab27b	-0.625			
BC052040	-0.628	-0.718		
Pik3ap1	-0.628			0.924
Zfp872	-0.628			
Fmo5	-0.630	-1.175		
Lmo1	-0.630			
Egfr	-0.631			
Ostn	-0.631			-0.799
Tbxa2r	-0.633	-1.088		
Tro	-0.634			
Drp2	-0.634	-0.590		
Smarca1	-0.635	-0.752		
Plekha4	-0.635	-0.732		
Heg1	-0.635	-0.706		
Trim12a	-0.637	-0.809		0.813
Pde3a	-0.637	-0.657		
3425401B19Rik	-0.637	-0.702		
1110032A03Rik	-0.640	-0.586		
Ank1	-0.643			
Galk2	-0.643			
Irak3	-0.644			
Rsph9	-0.644	-0.682		
Slc27a6	-0.646	-0.851		
Lrrn4cl	-0.649	-0.749		
Neat1	-0.649			
H2-T24	-0.650			1.311
Cdk14	-0.650	-0.629		
Nrp1	-0.650			
Rbp4	-0.651	0.681	1.228	
Sema6d	-0.652			
Tlr7	-0.653			0.716
Dpp7	-0.653			
Ccl7	-0.656			
Tlcd2	-0.656			
Cep126	-0.658			
Cited2	-0.659	-0.643		
Ppfia4	-0.659			

Mxd4	-0.661	-0.623		
Cobl	-0.661	-0.703		
Npas2	-0.663			
Cdnf	-0.664			
Ephb6	-0.664	-1.092		
Ecm2	-0.664	-0.872		
Gstm1	-0.664	-0.826		
Acot11	-0.665	-0.607		
Hivep3	-0.665	-0.683		
Col2a1	-0.665	-1.193		0.676
Podn	-0.666	-0.766		
Prrg3	-0.666	-0.688		
Cadm1	-0.666	-0.809		
Tha1	-0.667	-0.591		
Nr2f1	-0.667	-0.667		
Aldh3b1	-0.668			
Mme	-0.668			
Rgag4	-0.669	-1.021		
Ly6e	-0.671			
Lama2	-0.672			
S100a13	-0.675	-0.731		
Exoc3l4	-0.676	-0.762		
Nid2	-0.677	-0.658		
F3	-0.678			
Fam134b	-0.679	-0.659		
Ppp1r3c	-0.679		-0.968	
Tox	-0.680	-1.005		
Sesn3	-0.680	-0.664		
Zbtb7c	-0.680			
Cd55	-0.681			
Capn6	-0.681			
Mcc	-0.682	-0.750		
Epyc	-0.682		0.978	
Spa17	-0.682	-0.775		
Dock10	-0.683			
Stat1	-0.684	-0.814		0.898
Atp10d	-0.684			
Rnf144a	-0.685	-0.761		
Fst	-0.687	-0.606		
Itih2	-0.687			
Epha5	-0.688	-0.748		
Meox1	-0.689		-0.930	-1.085
Prrt2	-0.689			
Ypel2	-0.690			
Lum	-0.692			
Fam124a	-0.692			
Trim34a	-0.692	-0.667		0.884
Rab3il1	-0.693	-0.834		
Emb	-0.696			

Tor3a	-0.696	-0.870		0.591
Tapbpl	-0.697	-0.788		
Tns2	-0.698	-0.806		
Igf1	-0.698			
Il11ra1	-0.699			
Chn2	-0.701			-0.855
Ccdc30	-0.701	-1.008		
Tap1	-0.702			0.774
Tceal3	-0.705	-0.954		
Frmd4b	-0.705			0.629
Kctd12	-0.706	-0.770		
Larp6	-0.707			
Dlk1	-0.708	-0.995	-0.985	
Brinp1	-0.709			
Tet1	-0.710			
Ppp1r3b	-0.710			
Tapbp	-0.713	-0.675		
Cdkl2	-0.714			
Amigo2	-0.715	-0.746		
Col22a1	-0.716	-0.870		
Plekhg5	-0.719	-0.737		
Dapk1	-0.719	-0.702		
Pcdhga1	-0.720	-0.600		
Eya1	-0.723	-0.719		
Col27a1	-0.723	-0.918		
Gbp7	-0.723	-1.015		1.290
Pag1	-0.725			
Scn2a1	-0.726	-0.801		
Ptpn13	-0.726			
Idi1	-0.728	-0.814		
Rtp4	-0.730	-0.738		1.333
F13a1	-0.731		0.773	
S1pr3	-0.731	-0.871	-0.600	
Pmp22	-0.734			
Igsf3	-0.735	-0.642		
Tbx18	-0.736			
Rnasel	-0.738	-0.885		
Aig1	-0.742	-0.707		
Gca	-0.742			
Tmem169	-0.744	-0.773		
Mylip	-0.747	-0.773		
Gpc6	-0.747	-0.708		
Ccdc74a	-0.747	-0.803		
Lmcd1	-0.749	-0.731		
Dtx3l	-0.749	-0.759		0.879
S100a4	-0.750			
Irgm2	-0.750			1.153
Bfsp1	-0.751	-0.967		
Hspa12a	-0.752	-0.708		

Pcyt1b	-0.752	-0.832		
Dleu2	-0.752	-0.899		-0.882
Lbh	-0.753		-0.613	
Prune2	-0.753	-0.669		
Dync1i1	-0.753	-0.854		
Ebf1	-0.753	-0.655		
Plagl1	-0.755	-0.874		
Parp10	-0.756	-0.624		0.675
Vcan	-0.758			
Slc1a3	-0.759		-1.189	
Epha3	-0.759			
Prkcb	-0.762			
Tap2	-0.762			
Gbp2	-0.763	-0.961		1.148
Gnao1	-0.765	-0.813		
Slc38a6	-0.766	-0.586		
C1rl	-0.768	-0.742		
Fmod	-0.768	-0.758		
Wdr5b	-0.769	-0.914		
Col9a1	-0.772	-1.272	0.855	
Vdr	-0.773			
Trim21	-0.776	-0.957		0.930
Rassf2	-0.776	-0.822		
AW551984	-0.778	-0.671		
L1cam	-0.779			
Asap3	-0.780			
Il18	-0.782	-0.971		
Elovl6	-0.784	-0.875		
Ebf3	-0.785	-0.986		
Pdgfra	-0.786	-0.629		
Wnt10b	-0.786	-0.828		
Trpv4	-0.787	-0.941		
9530077C05Rik	-0.788	-0.865		
Dlg2	-0.789			-0.741
Chrna7	-0.790	-0.756		
Pstpip2	-0.791	-0.725		
Lgr4	-0.792	-0.782		
Nfasc	-0.792		0.978	
Uba7	-0.800	-0.670		0.683
Pde7b	-0.801			
Hs3st3a1	-0.801	-0.600		
Oas1b	-0.802			1.249
Sfrp1	-0.802			-0.806
Cdh6	-0.803	-0.989		
Plxnd1	-0.804	-0.676		
Adam5	-0.805	-1.471		
Eps8l2	-0.807	-1.470		
Sybu	-0.807			
Il7	-0.808	-0.703		

Epha4	-0.809	-0.811		
Slamf7	-0.810			
Rnf125	-0.811	-0.590		
Pdzd2	-0.812	-0.880		
Thsd7a	-0.817	-0.670		
BC030870	-0.820			
Ptx3	-0.823			
Tcea3	-0.824	-1.389		
Ednra	-0.826	-0.764		
Serpina3n	-0.827		0.747	
Fzd5	-0.828	-0.860		
Sepp1	-0.832			
AW011738	-0.833	-1.017		1.280
Ang	-0.834	-0.825		
Serpina3g	-0.836			
Id4	-0.839	-1.132		
Bhlhe41	-0.839			
Dhrs9	-0.840	-0.947		
S1pr1	-0.840			
Bcl2l11	-0.841	-0.990		
Fam160a1	-0.852	-0.816		
Plscr2	-0.855	-0.920		
Sept1	-0.859	-0.772		
Sp110	-0.860			1.099
Prelp	-0.860	-1.003		
Angpt2	-0.862	-0.862		
Pm20d2	-0.862	-0.661		
Enpp5	-0.865	-0.829		
Ephx2	-0.865	-0.833		
Apod	-0.865	-0.853		0.742
Fam46a	-0.867	-0.672		
Mab21l1	-0.868	-0.957		
Ifih1	-0.875	-0.746	0.713	1.191
Fbln7	-0.876	-1.356		
Sorl1	-0.876	-0.842		
Ecscr	-0.876	-0.614		
Lgals3bp	-0.877			0.896
Slc16a4	-0.878	-1.277		
Slfn8	-0.884	-0.942		1.279
Sp100	-0.886			1.115
Fgd4	-0.889	-0.739		
Npr3	-0.892	-0.862		
Trim30a	-0.894			1.839
AA467197	-0.895			
Kcna6	-0.895	-0.756		
Fzd4	-0.896		-1.156	
Hapln1	-0.896	-1.262		
Mnda	-0.897			0.911
Snx32	-0.898	-0.878		

Cd34	-0.898	-0.585	-0.751	
Herc6	-0.899	-0.775		0.971
Agtr1a	-0.900			
Pappa2	-0.901	-0.685		
Rnf150	-0.901	-0.613		
Cd200	-0.902	-0.937		
Endod1	-0.902	-0.855		
Ssc5d	-0.907	-0.858		
Srsf12	-0.909	-1.071		
Igfbp6	-0.910	-0.753	-0.960	
Epas1	-0.916			
Scrn1	-0.918	-1.174		
Dhx58	-0.919	-0.812		1.258
Hr	-0.920	-0.983		
Tlr2	-0.922			
Sntb1	-0.922		-0.724	
Ednrb	-0.922		-1.065	
Naalad2	-0.923		-0.873	
Col5a3	-0.923	-0.902	-0.811	-0.840
Tshz2	-0.924	-0.985		
Scn8a	-0.929			
Lgr5	-0.929			
Rcsd1	-0.931	-1.308		
Dlx5	-0.935	-1.002		
Cdk15	-0.939	-1.077		
Gbp6	-0.940	-1.202	1.305	1.136
Megf10	-0.941		-1.001	
Igtp	-0.942	-0.870		1.033
Dcn	-0.943			
Smpdl3a	-0.943			
Mest	-0.944	-1.561		
Cfb	-0.946			0.802
Plpp3	-0.948	-0.894		
Enpep	-0.948	-0.767		-0.736
Sorbs2	-0.948	-1.301		
Serpinb9	-0.951	-0.806		
Cpxm1	-0.953	-0.773		
Gxylt2	-0.954	-0.946		
Gfra2	-0.955	-1.287		-0.689
Plscr4	-0.957	-1.049		
Plac8	-0.958			
1810041L15Rik	-0.959			
Cadm3	-0.964	-0.946	-0.802	
Atp1b1	-0.966	-0.792		
Susd2	-0.969	-1.241		
Abca6	-0.973	-2.101		
Iqgap2	-0.975	-0.753		
Il1rn	-0.977	-0.785		-0.665
Mt2	-0.978			

Clec11a	-0.980	-1.131		-0.754
Itgb3	-0.981	-1.091		
1500015O10Rik	-0.982	-0.944		
Podnl1	-0.984	-0.938		
Jag1	-0.984	-0.889		
Sec16b	-0.985	-0.819		
Rab11fip4	-0.986			
Nlrc5	-0.993	-0.773	0.694	1.071
Pcp4l1	-0.994	-1.000		
Asb13	-0.994	-1.152		
Shisa3	-0.997	-0.648		
Tlr3	-0.997	-0.873		0.800
Mylk	-0.999	-0.873		
Psmb8	-0.999	-0.707		0.722
Clstn3	-1.001	-1.245		
Dhrs3	-1.002	-0.829		
Mybpc1	-1.002	-1.397		
Fgfr3	-1.003	-0.848		
H2-Q4	-1.003			0.805
Srgn	-1.009	-0.720		
Smoc2	-1.010	-1.112		
Rnf213	-1.011	-0.946		1.507
Zfp423	-1.014	-1.130		
Spns2	-1.018	-0.975		
St3gal6	-1.019	-1.366		
Fam13c	-1.020	-1.141		
Spp1	-1.021	-0.717		
Cd74	-1.024	-0.746		
Slc7a2	-1.025	-0.719		
Nrk	-1.027	-1.018		
Psmb9	-1.028	-0.791		
F8	-1.032	-1.183		
Adamts3	-1.033	-0.612		
Fap	-1.033			
Ube2l6	-1.036	-1.170		
Rab36	-1.043	-0.853		
Gas6	-1.053	-1.265		
Peg3	-1.054	-1.422		
Abca9	-1.057	-0.976		
Enpp3	-1.059	-0.821		
Slc4a10	-1.060	-0.819		
Slfn5	-1.063	-0.914		1.307
Fxyd1	-1.065			-0.730
Lpl	-1.066	-1.038	-0.771	
Tmem8	-1.066	-1.317		
Bche	-1.077	-0.967		
Lrrc75b	-1.079	-1.415		
Bmf	-1.097	-1.169	-0.601	
Aspg	-1.098	-1.217		

Klf12	-1.108	-1.057		
Ifi204	-1.112	-0.803		1.270
Cfh	-1.115			
Ptprv	-1.115	-1.257		
Kazald1	-1.126	-1.349	-0.687	-0.683
Gpr88	-1.126	-0.925		-0.759
Map2k6	-1.127	-1.065		
Ptgfr	-1.128	-0.587		-1.396
Ptgir	-1.129	-0.911	-1.022	
Traf1	-1.131	-0.799		
Islr	-1.131	-1.173		
Pdgfd	-1.134	-0.664	-0.661	
Pycard	-1.136	-0.904	-0.690	
Fgf7	-1.148	-0.728		
Ccl5	-1.153	-1.329		1.214
Phf11d	-1.158	-0.850		1.081
Tnmd	-1.159	-1.244		
Serping1	-1.162			
Meox2	-1.162		-1.135	
Gm4951	-1.173	-1.011		
Apol6	-1.182	-0.606		
Gm12250	-1.183			0.898
S100b	-1.185	-1.329		
Hpgd	-1.194		-0.929	
C1ra	-1.197	-1.168		
Limch1	-1.204	-1.798	-0.802	
Adamts18	-1.205	-1.581		
Col13a1	-1.207	-1.137		
Klf15	-1.208	-1.133		-0.686
Ifi44	-1.218			1.210
Abca8b	-1.224	-1.013		
Dock8	-1.227	-1.119		
Aoc3	-1.228	-0.591	-0.840	
Gbp3	-1.237	-1.434	1.093	1.497
Crispld1	-1.242	-1.218		
Col9a3	-1.243	-2.090		0.612
Parp14	-1.244	-1.141		1.263
Cygb	-1.263	-1.415	-0.825	
Tle2	-1.272	-1.110		
Col8a2	-1.275	-1.835		
Vit	-1.276	-1.201	-0.749	
Palm3	-1.285	-1.960		
Sparcl1	-1.288	-1.369	-0.873	-0.730
Gpx3	-1.298	-1.118	-0.607	
Rassf4	-1.317	-0.851		
C1s1	-1.318	-0.950		
Glt8d2	-1.320	-1.397		
Chil1	-1.328	-0.986		
Mterf4	-1.331	-1.101		

Pdzrn4	-1.336	-1.009		
Olfml2a	-1.338	-1.906		
Zim1	-1.345	-2.168		
Saa3	-1.365	-1.068		
Negr1	-1.383	-1.469		-0.757
Gfra1	-1.403	-0.820		
Synm	-1.426	-1.427		
Olfml1	-1.434	-1.319		-0.893
Ptn	-1.439	-1.328	-0.621	
Esm1	-1.440	-0.933	-0.839	
Xylt1	-1.447	-1.430		
Col9a2	-1.460	-2.148		
C4b	-1.461	-1.077	0.789	
Tmtc1	-1.473	-1.389		
Elmo1	-1.481	-1.301		
Adam23	-1.494	-1.163		
Galnt5	-1.505	-1.147		
Cdkn1c	-1.509	-1.771	-0.596	-0.597
Aim1	-1.515	-1.379		1.296
Lcn2	-1.526	-1.144		
Mmp13	-1.534	-0.778		
Gdf10	-1.542	-1.640		-0.994
Cp	-1.557	-0.745		
Gbp5	-1.564	-1.482		1.222
C3	-1.565	-1.312		
Kcns1	-1.572	-1.669		
Clu	-1.584	-1.327		
Cntn1	-1.585	-1.749		
Cmya5	-1.588	-1.025		
Steap4	-1.594	-0.716		
Cacna1d	-1.599			
Gsta4	-1.601	-1.595	-1.067	-0.775
Egfl6	-1.609	-0.925	-0.629	-0.719
Lbp	-1.614	-1.362		
Lrrc4	-1.639	-2.373		-0.664
Col11a2	-1.659	-2.088	0.662	
Diras2	-1.674	-1.771		
Lgals4	-1.675	-1.179		
Calml4	-1.678	-1.228		-0.887
Cxcl9	-1.682	-1.873		
Ifi27l2a	-1.726			1.019
Susd5	-1.730	-1.640		
Penk	-1.737	-1.202		
Sned1	-1.798	-1.573		
Abi3bp	-1.849	-1.982	-0.902	-0.735
Ggt5	-1.856	-1.436		
Col14a1	-1.856	-1.430		-0.647
Mfi2	-1.866	-2.928	0.628	
Sept4	-1.882			

Sorcs1	-1.943	-1.760		
Sox9	-1.952	-2.266		
Chrdl1	-1.986	-1.129		-0.741
Fzd9	-2.014	-1.626		
Pparg	-2.049	-1.745	-1.162	
Dner	-2.090	-1.729	-0.881	
Palmd	-2.115	-1.066		-0.664
Comp	-2.124	-1.727		
Smoc1	-2.146	-1.640		
Hp	-2.166	-2.162		
Cxcl12	-2.179	-1.680		
Dio3	-2.198	-1.581	-1.125	
Entpd3	-2.226	-2.135		
Serpinb1a	-2.336	-1.886		-0.653
Matn4	-2.382	-2.182		
Rspo3	-2.399	-1.633	-0.668	
Rspo2	-2.491	-1.935	-1.130	
Sfrp2	-2.615	-2.183	-0.717	
Scara5	-2.706	-2.905		-1.132
Hgf	-2.791	-2.034	-0.963	
Lect1	-2.863	-3.846		0.666
Angpt1	-3.013	-2.428		
Gprin3	-3.026	-2.629	-1.529	0.715
Fmo1	-3.533	-2.991		-1.072
Stk32b	-4.095	-2.941		
Ucma	-4.577	-4.745		

Table 3.3: WNT3A targets with bone metabolism phenotypes*. Fold changes are given in log2 scale (log2 FC). All genes have an FDR corrected p-value <0.05.*

Gene	log2 FC
Axin2	2.71
Bmp7	1.72
Col7a1	1.68
Grem2	1.37
Cnn1	1.26
Lif	1.23
Slc20a1	1.10
Ptgs2	1.08
Nov	1.07
Ptch1	1.03
Fam101b	0.95
Prickle1	0.90
Bmp3	0.90
Fgf18	0.88
Galnt3	0.83
Nog	0.82
Bmpr1b	0.80

Bmp2	0.80
Lepr	0.79
Sema3f	0.76
Osbpl3	0.74
Cdo1	0.74
Prrx2	0.72
Fosl2	0.70
Dkk2	0.70
Efemp1	0.68
Adrb2	0.67
Fgfr1	0.66
Mllt3	0.64
Bmp4	0.63
Cthrc1	0.62
Sgms1	0.61
Itgb1	0.61
Thra	-0.59
Tlr4	-0.60
Daam2	-0.61
Egfr	-0.63
Irak3	-0.64
Hivep3	-0.66
Col2a1	-0.67
Cadm1	-0.67
Aldh3b1	-0.67
Stat1	-0.68
Igf1	-0.70
Ebf1	-0.75
Plagl1	-0.75
Gnao1	-0.76
Fmod	-0.77
Vdr	-0.77
Rassf2	-0.78
Pdgfra	-0.79
Sfrp1	-0.80
Id4	-0.84
Npr3	-0.89
Epas1	-0.92
Tlr2	-0.92
Ednrb	-0.92
Dlx5	-0.94
Dcn	-0.94
Itgb3	-0.98
Clstn3	-1.00
Dhrs3	-1.00
Fgfr3	-1.00
Spns2	-1.02
Spp1	-1.02
Xylt1	-1.45

Mmp13	-1.53
C3	-1.56
Col14a1	-1.86
Sox9	-1.95
Fzd9	-2.01
Pparg	-2.05
Rspo2	-2.49
Sfrp2	-2.62
Lect1	-2.86

Table 3.4: Enriched signaling pathways associated with genes up- and down-regulated by WNT3A in WT osteoblasts. *Differentially expressed genes associated with these pathways are also given.*

Enriched pathways : up-regulated genes	**Genes**
WNT signaling pathway	NKD1, TCF7, NKD2, FZD1, LEF1, PORCN, WNT2B, DKK2, CCND1, PRICKLE1, SFRP4, WIF1, NFATC4, AXIN2
TGF-beta signaling pathway	BMP4, INHBB, INHBA, NOG, BMP2, TGFB3, BMPR1B, BMP7, TGFB2
MAPK signaling pathway	FGF18, FGFR1, NTF3, PDGFA, TGFB3, FGF13, FGF21, CACNB4, TGFB2, DUSP1, RRAS2, GADD45G, CACNA1G, NFATC4, NGF
Cytokine-cytokine receptor interaction	BMP2, TNFRSF12A, PDGFA, LEPR, TGFB3, TNFSF15, TGFB2, INHBB, LIF, INHBA, CXCL14, TNFRSF19, BMPR1B, BMP7
Regulation of actin cytoskeleton	FGFR1, FGF18, LIMK2, PDGFA, RRAS2, ITGA8, FGF13, ITGA3, FGF21, ITGA4, ITGB1
p53 signaling pathway	CCND1, CDKN2A, GADD45G, SERPINE1, PMAIP1, SFN
Cell cycle	CCND1, CDKN2A, DBF4, GADD45G, TGFB3, RB1, SFN, TGFB2
Enriched pathways : down-regulated genes	**Genes**
Complement and coagulation cascades	C1RA, CD55, C3, C4B, CFB, F13A1, F3, F8, CFH, SERPING1
Toll-like receptor signaling pathway	CXCL9, TLR2, TLR3, TLR4, LBP, CCL5, STAT1, TLR7, MAP2K6, SPP1
Focal adhesion	EGFR, IGF1, COL2A1, HGF, ITGB3, COL5A3, PRKCB, LAMA2, COMP, PDGFRA, PDGFD, COL11A2, MYLK, SPP1
Axon guidance	EPHA5, EPHA4, EPHB6, NRP1, SEMA6D, SEMA3E, L1CAM, EFNA5, CXCL12, EPHA3

Table 3.5: Expression profiles of WNT3A targets during osteoblasts differentiation. *WNT3A targets showing high and low expression at early (day 2-day 6) and late stages (day 8-day 18) of osteoblast differentiation are shown in the table. Gene expression was profiled during differentiation of early pre-osteoblasts to mature osteoblasts.*

Up-regulated genes with high expression at early stages				
Bex1	Pgf	Suox	Tiparp	Ankrd1
Sema4f	Hbegf	Fgfbp1	Creld1	Nrcam
Ntf3	Cyp26b1	Nell2	Filip1l	Thsd4
Colec10	Serpine1	Grem1	Fam185a	Tgfb3
Grik3	Lef1	Specc1	Wif1	Plcxd2
Syt13	Slc16a3	Cap2	Cxcl14	Rgs16
Tnfsf15	Nog	Plat	Lrrc32	Nipal4
Nebl	Lepr	Zfp503	Fam198b	Dusp1
Car8	Cyr61	5430421F17Rik	Smim3	Pim1
Eva1a	Elfn1	Fam101b	Aif1l	Arhgap6
Gm12505	Actg2	Spry1	Prg4	Timm8a1
Dynap	Phldb2	Moxd1	Scn3a	Phlda1
Herc3	Pmepa1	Crabp1	Bmpr1b	Wdr92
Prss46	Arxes1	Cdkn2a	Spire2	Acta2
Gjb2	Rras2	Ccnd1	Hspa4l	Slc2a3
Gadd45g	Inhba	Fam131a	Cd24a	Chst1
Grem2	Prrx2	Ch25h	Tes	Lif
Ngf	Map6	Sync	Pard6b	Pmaip1
Ctnnd2	Gpn2	Fam184a	Osbpl3	Gabrb3
Sfn	Fosl2	Rnd3	Sh3rf1	Ddah1
Cnn1	Tagln	Dkk2	Svip	Has2
Tcf7	Jak2	Nrp2	Csrp1	Ahrr
E030011O05Rik	Plaur	Fam84b	Klhdc8a	Lrrc15
Hck	Egln3	Adrb2	Artn	Cxadr
Tec	Gdnf	Cthrc1	Eef1e1	Glipr1
Pdgfa	Kctd11	C430002N11Rik	Stambpl1	Dbf4
Slc20a1	Fam65b	Aqp5	Mrto4	Stard13
Ptgs2	Mllt3	Nkd2	Kcnj15	Limk2
Ier3	Sh3bp4	Bmper	Pitpnc1	Sorbs1
Ptch1	Adk	Inhbb	Zfp462	Itga3
Arxes2	Tnfrsf12a	Iyd	Tpd52	Rb1
Cdc42ep3	Vgf	Cdh17	Coq10b	Arhgdig
Insc	Hes1	Col7a1	Pxylp1	
Murc	Lims2	Etv4	Rapgef3	

Lurap1l	Itgb1	Arl4c	Wnt2b	
Errfi1	Maff	C1ql3	Sgms1	
Up-regulated genes with low expression at early stages				
Slc13a4	Itga8	Fmnl2	Cacnb4	Rgcc
Sstr2	Aldh1a2	Galnt16	Foxn3	Tceal5
Ndnf	Mrgprf	Kank1	Tnfaip6	Fhod3
Axin2	Fam180a	Ppfibp2	Qpct	Atp1a2
Tmem100	Piezo2	Itga4	Nav3	Slitrk6
Igfbp2	Col26a1	Fbln5	Efemp1	Adamts8
Hhip	Nkd1	Ror1	Robo2	Fzd1
Dio2	Stc1	Galnt3	Lin7a	Prickle1
Slc1a2	D6Ertd527e	Bmp2	Pfkfb1	Bmp3
Tgfb2	Ahr	Arsi	Fgfr1	Fgf18
Dpp4	Aldh1a7	Wbscr17	Tcf4	Cacna1g
Lypd6	Nov	Fgf13	Unc13b	Dpep1
Ccbe1	Rdh10	Irx3	Nedd9	Porcn
Pamr1	Scube1	Hunk	Bmp4	Dpt
Bmp7	Tspyl5	Pdxp	Nfatc4	Rnf122
Apcdd1	Rerg	Sema3f	Ddit4l	Fjx1
Kcnj2	Fam101a	Trp53i11	Itm2a	Sfrp4
Tnfrsf19	Pcdh10	Tmem26	Adamts4	Irx5
Timp3	Hdac9	Sema5a	Mtus1	Il16
Enpp2	Syn1	Cdo1	Col23a1	
Down-regulated genes with high expression at late stages				
Aff3	Aldh3b1	Wdr5b	Cdk15	Klf15
Sytl2	Mme	Col9a1	Gbp6	Abca8b
Bcar3	Rgag4	Trim21	Megf10	Dock8
Vill	Ly6e	Rassf2	Igtp	Aoc3
Bbs1	Exoc3l4	AW551984	Dcn	Gbp3
Zfp811	Nid2	Asap3	Smpdl3a	Crispld1
Thra	Fam134b	Il18	Mest	Col9a3
Fam43a	Ppp1r3c	Elovl6	Cfb	Parp14
A4galt	Tox	Ebf3	Enpep	Cygb
Acss3	Sesn3	Pdgfra	Sorbs2	Tle2
3632451O06Rik	Zbtb7c	Trpv4	Serpinb9	Col8a2
Adamtsl3	Cd55	9530077C05Rik	Cpxm1	Vit
Igsf10	Capn6	Dlg2	Gxylt2	Palm3
Ankrd44	Mcc	Chrna7	Gfra2	Sparcl1
Heph	Epyc	Pstpip2	Plscr4	Gpx3
H2-T10	Spa17	Nfasc	1810041L15Rik	Rassf4

Smpdl3b	Dock10	Uba7	Atp1b1	C1s1
Lgals9	Stat1	Pde7b	Susd2	Glt8d2
Fzd8	Atp10d	Hs3st3a1	Abca6	Chil1
Ldb2	Rnf144a	Oas1b	Iqgap2	Pdzrn4
Tlr4	Fst	Sfrp1	Il1rn	Olfml2a
Pik3ip1	Itih2	Plxnd1	Mt2	Zim1
Msrb2	Epha5	Adam5	Clec11a	Negr1
Klhl13	Meox1	Sybu	Itgb3	Gfra1
Fry	Prrt2	Epha4	1500015O10Rik	Synm
Cd82	Ypel2	Slamf7	Jag1	Olfml1
Pnmal2	Lum	Rnf125	Sec16b	Ptn
Ganc	Trim34a	Pdzd2	Rab11fip4	Esm1
Parp9	Rab3il1	Tcea3	Nlrc5	Xylt1
Slc7a8	Emb	Ednra	Asb13	Col9a2
Cd1d1	Tor3a	Serpina3n	Shisa3	C4b
Daam2	Tapbpl	Fzd5	Tlr3	Tmtc1
B230118H07Rik	Igf1	Sepp1	Mylk	Elmo1
Lpin1	Il11ra1	AW011738	Psmb8	Adam23
AI429214	Chn2	Ang	Clstn3	Galnt5
Col18a1	Ccdc30	Serpina3g	Dhrs3	Cdkn1c
Trim12c	Tceal3	Bhlhe41	Mybpc1	Aim1
Icam1	Frmd4b	Dhrs9	Fgfr3	Lcn2
Arhgef6	Kctd12	S1pr1	H2-Q4	Mmp13
Bicc1	Larp6	Bcl2l11	Srgn	Gdf10
4933431E20Rik	Dlk1	Fam160a1	Smoc2	Cp
Mamld1	Brinp1	Plscr2	Zfp423	Gbp5
Slitrk5	Tet1	Sp110	Spns2	C3
Rab32	Ppp1r3b	Prelp	St3gal6	Kcns1
Prkaa2	Tapbp	Angpt2	Fam13c	Clu
Dync2li1	Cdkl2	Pm20d2	Cd74	Cntn1
Efna5	Amigo2	Enpp5	Slc7a2	Cmya5
Rab27b	Col22a1	Ephx2	Nrk	Steap4
BC052040	Plekhg5	Apod	Psmb9	Cacna1d
Pik3ap1	Dapk1	Fam46a	F8	Gsta4
Zfp872	Pcdhga1	Mab21l1	Adamts3	Egfl6
Fmo5	Eya1	Ifih1	Fap	Lbp
Lmo1	Col27a1	Fbln7	Ube2l6	Lrrc4
Egfr	Gbp7	Sorl1	Rab36	Col11a2
Ostn	Pag1	Lgals3bp	Gas6	Diras2
Tbxa2r	Scn2a1	Slc16a4	Peg3	Lgals4

Drp2	Ptpn13	Slfn8	Abca9	Calml4
Smarca1	Rtp4	Sp100	Slc4a10	Cxcl9
Plekha4	F13a1	Fgd4	Slfn5	Ifi27l2a
Heg1	S1pr3	Npr3	Fxyd1	Susd5
Trim12a	Pmp22	Trim30a	Lpl	Penk
Pde3a	Igsf3	Kcna6	Tmem8	Sned1
3425401B19Rik	Tbx18	Fzd4	Bche	Abi3bp
1110032A03Rik	Rnasel	Hapln1	Lrrc75b	Ggt5
Ank1	Aig1	Snx32	Bmf	Col14a1
Irak3	Gca	Cd34	Aspg	Mfi2
Rsph9	Tmem169	Herc6	Klf12	Sorcs1
Slc27a6	Mylip	Agtr1a	Cfh	Sox9
Lrrn4cl	Gpc6	Pappa2	Ptprv	Chrdl1
Cdk14	Ccdc74a	Rnf150	Kazald1	Fzd9
Rbp4	Lmcd1	Cd200	Gpr88	Pparg
Sema6d	Dtx3l	Endod1	Map2k6	Palmd
Tlr7	Irgm2	Ssc5d	Ptgfr	Comp
Dpp7	Bfsp1	Srsf12	Traf1	Smoc1
Tlcd2	Hspa12a	Igfbp6	Islr	Hp
Ppfia4	Pcyt1b	Epas1	Pdgfd	Cxcl12
Mxd4	Dleu2	Scrn1	Pycard	Dio3
Cobl	Prune2	Dhx58	Ccl5	Entpd3
Npas2	Dync1i1	Hr	Phf11d	Matn4
Cdnf	Ebf1	Tlr2	Tnmd	Rspo3
Ephb6	Plagl1	Sntb1	Serping1	Rspo2
Ecm2	Parp10	Ednrb	Meox2	Sfrp2
Gstm1	Slc1a3	Naalad2	Gm4951	Scara5
Hivep3	Epha3	Col5a3	Gm12250	Hgf
Podn	Prkcb	Tshz2	S100b	Lect1
Prrg3	Tap2	Scn8a	Hpgd	Angpt1
Cadm1	Gbp2	Lgr5	C1ra	Gprin3
Tha1	Gnao1	Rcsd1	Limch1	Fmo1
Nr2f1	C1rl	Dlx5	Adamts18	Stk32b
Fmod	Col13a1	Ucma		
Down-regulated genes with low expression at late stages				
Camk1d	Col2a1	Wnt10b	Podnl1	Cited2
Rnf144b	Lama2	Lgr4	Pcp4l1	Acot11
Thy1	S100a13	Cdh6	Spp1	Vdr
Sema3e	F3	Eps8l2	Enpp3	L1cam
H2-T22	Fam124a	Il7	Ifi204	Plac8

Tro	Tap1	Thsd7a	Ptgir	Cadm3
Galk2	Idi1	Ptx3	Fgf7	Ccl7
Neat1	S100a4	Id4	Apol6	Slc38a6
H2-T24	Lbh	Ecscr	Ifi44	Mnda
Nrp1	Vcan	AA467197	Dner	Serpinb1a

Table 3.6: Genes differentially expressed in Lrp5$^{-/-}$, Lrp6$^{-/-}$ and Lrp5$^{-/-}$;Lrp6$^{-/-}$ osteoblasts compared to sham treated controls. *Fold changes are given in log2 scale (log2 FC). All genes have an FDR corrected p-value <0.05. .*

Gene	Lrp5$^{-/-}$ (log2 FC)	Lrp6$^{-/-}$ (log2 FC)	Lrp5$^{-/-}$;Lrp6$^{-/-}$ (log2 FC)
H2-T23	0.95	0.61	0.83
Irgm2	0.96	1.33	1.56
Lgals3bp	0.73	0.62	0.87
Ntrk2	1.01	1.54	0.77
Parp10	0.62	0.79	0.99
Pou3f4	2.01	1.95	1.6
Siglec1	0.96	0.86	0.89
Trim30d	0.77	1.03	1.39
Adgre1	0.67	0.63	
Bst1	0.81	0.66	
Cd53	0.88	0.64	
Chrdl1	0.61	0.59	
Eno1b	5.19	0.64	
Fam19a2	0.88	0.78	
Fbxo2	0.93	0.8	
Gbp2b	5.67	0.67	
Hdac9	1.1	0.92	
Il33	0.84	0.61	
Mmp13	0.75	0.69	
Mmp9	1.09	0.6	
Mpeg1	1.53	0.62	
Nell1	0.94	0.92	
Otor	1.81	2.04	
Palmd	1.02	0.6	
Rbp4	1.08	1.33	
AI607873	0.79		1.51
Alpk1	0.96		0.6
Cfb	1.19		0.62
Coch	0.69		0.59
Ddx60	0.95		1.77
Fcgr1	1.02		1.37
Hgf	0.96		0.67
Ifi27l2a	1.12		0.82
Mnda	0.93		1.14

Mndal	1.29		0.85
Ms4a6c	1.01		0.77
Psmb9	0.84		0.89
Slc37a2	0.61		0.69
Slfn10-ps	0.67		1.17
Sp110	0.86		1.48
Wdfy1	1.14	-0.61	1.26
Zbp1	0.9		2.28
1810037I17Rik	4.66		
A930005H10Rik	1.26		
A930033H14Rik	0.97		
AA467197	0.89		
Abca5	0.76		
Acp5	1.7		
Adh1	0.8		
Adi1	0.83		
Adra2a	0.64		
AI506816	0.73		
Aldh3a1	1.95		
Atp6ap2	0.63		
Atp6v0b	0.63		
BC002163	4.51		
BC022687	1.68		
C1qa	1.22		
C1qc	0.78		
Cacna1d	0.67		
Car6	0.6		-0.73
Casp4	0.76		
Ccl2	0.74		
Ccl7	0.67		
Ccr1	0.7		
Cd47	0.72		
Cfh	0.6		
Chd3os	0.74		
Col3a1	0.62		
Cp	0.66		
Crip1	0.62	-0.59	
Crip2	0.69		
Ctsc	0.61		
Ctsk	0.69		
Ctss	0.65		
Cuedc1	0.7		
Cxcl1	0.91	-1.26	
Cxcl12	0.76		
Cxcl14	1.6		
Cxcl5	0.95	-0.63	
D430020J02Rik	0.83		
Dcn	0.67		
Ddx4	0.7		

Dio2	1.1		
Dynlt1b	1.13		
Ednrb	1.26		
Efcab7	1.46		
Egfl6	0.68		
Eif3f	0.6		
F830016B08Rik	0.92		
Faap20	0.61		
Fabp4	0.84		
Fabp5	1.01		
Fam65c	0.72		
Fbln1	0.6		
Fbxo27	0.95		
Fcer1g	0.63		
Fmo1	0.6		
Fth1	0.69		
Fxyd1	0.76		
Gatm	0.72		
Gfra1	0.65		
Glrx	0.69		
Gm12505	1.16		
Gm4924	1.01		
Gm4951	0.9		
Gm8909	5.4		
Gm9855	6.25		
Grik3	0.68		
H2-D1	0.92		
H2-K2	3.32		
Herpud2	0.6		
Hk3	0.66		
Hpgd	0.87		
Ibsp	0.6		-1.09
Igfbp3	0.88		-0.66
Il15ra	0.6		
Il6	1.39		
Ism1	0.69		
Kcnj15	1.11		
Kcnj2	0.94		-0.71
Klhl41	1.15		
Lgr5	0.68		
Mir22hg	0.65		
Mmp3	1.01		
Ms4a6d	1.09		
Ms4a7	1.37		
Mt1	0.81		
Mt2	1.13		
Nrcam	0.72		
Pcsk5	1.23		
Pde1a	0.82	-0.6	

Pla2g7	0.6		
Ppif	0.61		
Prg4	0.93		
Prok2	2.78		
Ptger4	1.05		
Pttg1	0.59		
Rabac1	0.65		
Rpl22l1	0.79		
Rps12	0.85		
Rps19-ps3	1.39		
Rspo3	0.6		
S100a16	0.87		
Serpina3h	4.76	-1.66	
Serpina3i	2.16		
Serpine2	0.61		
Serping1	0.69		
Shtn1	0.65		
Slc13a3	0.71		
Slc9b2	1.11		
Slirp	0.59		
Slitrk6	0.75		-0.67
Snai1	0.59		
Snhg6	0.61		
Srgn	0.9		
Stk32c	0.88		
Sycp3	1.18		
Tex15	0.73		
Tifa	0.85		
Tmem176a	0.6		
Tmem181b-ps	1.06		
Tnfaip6	0.75		
Tnfsf11	0.82		
Trappc2	0.6		
Ttr	4.81		
Ubiad1	0.64		
Ulbp1	0.89		
Vgf	0.82		
Wnt16	0.78		
Xdh	0.86		
Yy2	0.67		
Bst2		0.94	1.26
C4b		1.01	0.78
Cd24a		0.67	0.64
Cd80		0.63	0.88
Cemip		0.68	0.77
Clca3a1		1.06	1.16
Col11a2		1.4	0.97
Col2a1		0.99	0.9
Col9a1		1.35	0.76

Col9a2	-0.67	1.32	1.2
Col9a3	-0.74	1.23	1.13
Comp		0.97	0.62
Cxcl10		2.96	1.7
D630003M21Rik		0.75	0.62
Dhx58		1.19	1.47
Dtx3l		0.63	1.14
Fgd4		0.61	0.66
Frzb		1.53	1.42
Gbp3		1.76	1.93
Gbp6		1.64	1.81
Gbp7		1.46	1.66
H2-Q4		0.65	0.94
Hal		0.72	0.91
Helz2		0.61	1.21
Ifi44		2.04	1.46
Ifih1		1.25	1.43
Ifit1		3.54	2
Ifit3		2.88	2.14
Igtp		1.59	1.52
Iigp1		2.81	1.98
Irf7		2.12	1.66
Irf9		0.73	0.72
Irgm1		1	1.36
Isg15		2.77	1.99
Klhdc7a		1.05	1.14
Lect1	-0.68	1.4	1.31
Nfasc		0.85	0.64
Nlrc5		0.82	1.34
Oasl2		1.99	1.93
Parp14		1.06	1.59
Parp9		0.77	1.06
Psmb8		0.88	0.95
Rnf213		0.75	1.74
Rtp4		2.03	1.56
Samd9l		0.62	1.27
Scn3a		0.83	0.75
Sema3d		1.51	0.85
Serpinb6b		0.69	0.63
Serpinb9b		0.61	1.18
Slfn8		1.49	1.66
Stat1		0.65	1.26
Stat2		0.72	1.08
Tap1		0.64	1
Tgfa	-0.8	1.05	0.63
Tlr3		0.66	1.26
Trim12c		0.62	1.02
Trim21		0.75	1.31
Trim30a		1.62	2.11

Trim34a		0.87	1.14
Uba7		0.65	0.98
Usp18		2.24	1.95
Veph1		0.88	0.79
Vnn1		0.74	1.05
Xaf1		0.96	1.2
Xist		6.32	1.78
Zim1	-0.66	0.74	0.8
6530402F18Rik		0.59	
Aldh1a7		0.68	
Apobec3		0.62	
Apoe		0.68	
Arhgap22	-0.74	0.72	
Arhgap30		0.75	
Atp1b1		0.61	
Atp6v0a4		0.83	
Bmp5		0.63	
C3		0.65	
Car3		4.01	
Ccdc125		0.71	
Cdkl5		0.63	
Clec12a		0.72	
Clec3a		1.3	
Clec4n		0.64	
Clu		1.08	
Col26a1		1.1	
Crct1		0.63	
Cybb		0.62	
Cys1		0.76	
Dock8		0.6	
Efcab11	-1	0.91	
Elmo3		0.76	
Enpp5		0.59	
Epha5		0.67	
Epyc		1.19	
F13a1		0.88	
F5		0.98	
Fam101a		0.98	
Fam13a		0.67	
Fam46b		0.62	
Fam84b		0.63	
Fbln7		0.88	
Fermt3		0.59	
Foxd1		0.63	
Fzd9		1.05	
Gdf10		0.81	-0.69
Gjb2		1.41	
Gm5617		0.63	
Ifitm10		0.81	

Igfbp2		0.61	
Igfbp5		0.72	
Il1rn		0.7	
Itga2		1.11	
Itgb4		0.59	
Itih2		0.61	
Kcns1		0.79	
Klc3		0.68	
Krt7		1.03	-0.63
Krt8		2.34	
Lama1		0.68	
Lbp		0.9	
Lcp2		1.11	
Lilr4b		0.61	
Matn3		1.4	
Matn4		1.14	
Mdfi		0.66	
Mecom		0.8	
Mfi2	-0.95	1.27	
Mia		1.33	
Mmp12		0.65	
Moxd1	-0.72	0.8	
Mrc1		0.68	
Nptx1		0.8	
Ntn3		0.76	
Ntrk3		0.65	
Ogdhl		0.59	
Olfml2a		0.8	
Pantr1		0.66	
Phex		0.68	
Prdm6		0.64	
Prkcb		0.63	
Rab11fip4		1.14	
Rasgef1b		0.69	
Rdh12		0.66	
S100b		0.65	
Scara5		0.66	
Serinc2		0.79	
Serpina3n		1.06	
Serpinb9		0.73	
Sfn	-2.15	1.56	
Sfrp4		0.7	
Shroom1		0.62	
Slc16a4		0.73	
Slc2a12		0.59	
Slc4a10		0.64	
Slc5a5		0.97	
Slitrk5		0.69	
Smoc1		1.03	

Sorl1		0.6	
Spock3		1.14	
Syt8		1.06	
Tfcp2l1		0.77	
Tmem8		0.72	
Tmtc1		0.88	
Tpd52l1		0.65	
Trnp1	-1.06	0.92	
Trp63		1.11	
Trpm6		0.67	
Tspan13		0.96	
Unc5a		0.71	
Wfikkn2		0.66	
Zfhx2		0.65	
Zfp429		1.03	
Zfp612		0.63	
Zfp951		0.61	
Zic3		0.77	
Zic4		0.71	
1700007K13Rik			0.89
1700024P16Rik			0.66
2010300F17Rik			0.73
4930470H14Rik			0.68
9230114K14Rik			0.61
A630089N07Rik			0.68
Acan	-0.64		0.77
Ackr4			1.11
Adamts6			0.6
Adar			0.76
Adrbk2			0.68
Aim1			1.44
Aldh1l1			0.66
Angpt2			0.63
Ano3			1.07
Apod			0.89
Apol6			0.78
Apol7a			0.84
Apol9a			0.98
Apol9b			1.49
Apold1			0.73
AW011738			1.85
BC005561			0.67
C130083M11Rik			0.6
C3ar1			0.61
C920009B18Rik			0.59
Cacna1h			0.66
Ccl5			1.44
Cd180			0.69
Cd274			1.33

Cd300a			0.67
Cd300lb			0.82
Cd55			0.72
Cd93			0.59
Celf5			0.8
Clcn5			0.62
Cmpk2			1.67
Col8a1			0.61
Cpeb4			0.73
Crispld1			0.62
Ctgf			0.67
D830031N03Rik			0.63
Ddx58			1.06
Dhrs9			0.76
Dnah8			0.64
Dner			0.61
E030011O05Rik			0.65
Eda2r			0.73
Eif2ak2			1.1
Elovl7			0.62
Epas1			0.67
Fam212b			0.65
Fat1			0.78
Fat4			0.67
Fcgr2b			0.75
Fibcd1			0.65
Flrt2			0.6
Flt4			0.67
Frmd4b			0.64
Gata2			0.7
Gbp2			1.57
Gbp5			2.07
Gbp9			1.97
Gdf6			0.63
Gm12250			1.89
Gm6548			0.91
Gprin3			1.02
H2-T22			0.66
H2-T24			1.26
Havcr2			0.73
Herc6			1.27
Hmgcll1			0.64
Ifi202b			1.99
Ifi203			2.07
Ifi204			1.44
Ifi35			0.77
Ifi47			1.57
Ifit2			0.88
Ifit3b			2.15

Igsf9b			1.14
Il18bp			0.93
Inhba			0.8
Isg20			0.59
Kcnq1ot1			0.76
Klhl11			0.59
Krt19			0.81
Lama2			0.63
Lgr6			0.98
Lnpep			0.6
Malat1			0.93
Masp1			0.61
Mctp2			1.05
Mgat5			0.69
Miat			0.6
Mocos			0.63
Mx1			2.15
Mx2			2.35
Nav2			0.76
Nbeal1			0.59
Npr3			0.9
Oas1a			1.75
Oas1b			1.52
Oas1c			1.01
Oas2			2.22
Oasl1			1.66
P2rx7			0.6
Pamr1			0.62
Pappa			0.85
Parp12			0.78
Pdgfd			0.81
Pdk4			0.88
Peg3			0.76
Perp			0.84
Phf11d			1.54
Pik3ap1			1.22
Pik3r5			0.73
Pisd-ps2			0.66
Plin4			0.84
Pml			0.6
Ppbp			0.78
Prrg4			1.06
Ptk2b			0.6
Ptpn7			0.6
Ptprc			0.83
Rasgrp3			0.79
Rassf4			0.69
Rgs17			1.4
Rgs4			0.85

Rgs5			1.11
Rsad2			2.21
Rtn4rl1			0.64
Serpinb2		-0.65	1.07
Serpine1			0.67
Slc16a13			0.66
Slc26a7			0.83
Slc2a9			0.74
Slc43a2			0.61
Slc6a17	-1.34		0.65
Slfn2			1.22
Slfn5			1.69
Slfn9			0.84
Sncg			0.63
Sox5			0.68
Sp100			1.39
Srsf12			0.73
St3gal6			0.69
Styk1			0.66
Susd5			0.85
Syndig1			0.61
Tbc1d2			0.91
Tbx18			0.66
Tdrp			0.79
Tfap2b			1.36
Thsd7a			0.71
Tlr13			0.6
Tlr7			0.79
Tmem200a			0.73
Tor3a			0.88
Trim12a			1.06
Trim25			0.86
Trp53inp1			0.66
Ube2l6			0.69
Uprt			0.61
Vat1l			0.8
Wnt2			0.86
Xrn1			0.61
Xylt1			0.83
Zbed6			0.64
Zbtb20			0.79
Zfp369			0.6
Znfx1			0.7
Sept1	-0.96		
1190007I07Rik	-1.78		
1700030C10Rik	-2.6		
2200002D01Rik	-0.8		
2610035D17Rik	-1.13		
2610507I01Rik	-0.8		

4732491K20Rik	-0.62		
9430038I01Rik	-1.33		
AA388235	-0.91		
Abca6	-1.48		
Ablim3		-0.77	
Acta1		-0.72	-0.79
Actc1		-1.13	-1.11
Actn2		-1.08	-0.74
Ahdc1	-0.88		
Ahnak2	-0.67		
Ahr	-1.05		-0.81
Ahrr	-0.68		
Aldh1a2			-1.37
Amz2	-0.97		
Angptl6			-0.77
Ankrd1	-0.79		
Anxa8		-0.62	
Aoc3		-0.71	
Arc	-0.61		
Arl4d	-0.63		
Arpp21		-1.12	
Artn			-0.64
Atp2a1			-0.73
Aunip	-1.3		
Aurkaip1	-0.61		
Avpr1a		-0.78	
Axin2			-0.96
Barx1		-0.84	
BC100451	-1.21		
Cacna1s		-0.59	
Cadm4			-1.51
Casq2		-0.69	
Ccdc109b	-1.13	-0.83	
Ccdc40	-1.72		
Cd74			-0.69
Cdh3	-0.63		
Cfap69		-0.69	
Ch25h			-0.65
Chchd10			-0.71
Chrng		-0.88	
Cnn1	-0.77		
Col15a1	-0.74	-1.1	-1.12
Col5a3			-0.65
Col7a1	-0.79		
Coq8b	-0.74		
Cox6a2			-0.68
Cth	-1.12		
Cxcr6		-0.61	
Ddx3y		-0.86	

Des		-0.66	
Dlx1		-0.76	
Dlx2		-0.73	
Dubr	-0.65		
Dynap		-1.45	
Eepd1			-0.69
Egln3			-0.79
Eif2s3y		-0.89	
Eln			-0.91
Emx2		-0.82	
Emx2os		-0.84	
Eps8l2	-0.63		
Erbb3		-0.64	
Fam177a	-0.93		
Fblim1	-0.61		
Fgf21			-0.9
Flt1		-0.64	
Fndc1			-1.06
Foxl2			-0.83
Frrs1	-0.67		
Gas1			-0.61
Gas7			-0.64
Gfra2			-0.6
Gm13889			-0.68
Gm15645		-0.79	
Gpr141		-0.72	
Gpr27			-0.61
Grem1		-0.84	
Gsta4			-0.64
Gsto1		-0.62	
H1fx			-0.66
H2-DMb1	-1.38		
Has1		-0.85	
Hhipl1	-0.67		
Hsd17b1			-0.66
Ier2			-0.83
Insc			-0.79
Irx1			-0.8
Kdm5d		-0.79	
Kitl		-1	
Krt10	-0.66		
Lgals4	-0.71		
Lgi2			-0.72
Limch1	-0.63		
Lin7a			-1.02
Lipt1			-0.61
Lmod1	-0.84		
Lrrn1		-0.63	-0.76
Lurap1l		-0.6	

Lypd6		-0.7	
Macrod1			-0.62
Megf10		-0.74	
Meox1			-0.86
Meox2		-0.75	
Mgarp			-0.6
Miip	-0.61		
Mina	-0.77		
Moap1	-0.9		
Ms4a4d		-0.72	
Msi2	-0.84		
Mybph		-0.91	-0.98
Myh3		-0.97	-0.73
Myl4		-0.7	-0.89
Mylk4		-0.66	
Mylpf			-0.6
Myo7a	-1.12		
Myod1		-1.21	
Myog		-1.1	-1.1
Myom2		-0.59	
Nacad	-0.61		
Ncmap	-0.79		
Ndnf		-0.77	-0.87
Ndst3	-1.12		
Ndufa3	-0.81		
Ndufa4l2			-1.24
Neb		-0.92	
Ngef			-0.64
Ngfr			-1.5
Nkd1			-0.62
Nmrk1	-0.73		
Nrep			-0.64
Nxph4			-0.89
Obscn		-0.66	
Omd			-0.69
Pax9		-0.66	
Pcdh20		-0.72	
Pde1b			-0.61
Pdpn	-0.93		
Pea15a	-0.59		
Pgm5			-0.75
Phka2	-0.77		
Pitx1		-1.44	
Plp1			-0.89
Pop4	-0.86		
Porcn			-0.82
Prr7			-0.61
Ptgfr			-0.84
Rab6b	-1.91	-0.65	

Ramp1	-0.84		
Rcor2			-0.67
Rdm1			-0.75
Rem1		-0.7	
Shox2		-1.24	
Siglecg		-0.84	
Sim2			-1.33
Slc16a3			-0.66
Slc25a29			-0.67
Slc26a11	-0.67		
Slc6a15		-0.65	
Slmo1			-0.61
Smyd1		-0.94	
Sod3			-0.71
Sostdc1		-0.67	
Spon2			-1.27
Spry1			-0.69
Spry4	-0.62		
Synpo2l		-0.89	-0.63
Tbx2		-0.78	
Tbx3		-1.24	
Thbs4		-0.61	
Tmeff2		-0.62	
Tmem203			-0.59
Tmem204			-0.7
Tmem88	-1.19		
Tmem8c		-0.88	-0.74
Tnfrsf19			-1.35
Tnfrsf1b	-0.61		
Tnnc1		-0.79	
Tnnc2		-0.77	-0.77
Tnni1		-0.76	-0.92
Tnnt2		-0.83	-1.07
Tnnt3			-0.84
Tprn			-0.68
Trim72		-0.91	
Tspan18	-0.74		
Ttn		-0.77	
U90926		-0.98	
Uty		-0.77	
Wdr54			-0.72
Wdr60	-0.63		
Xirp1		-0.71	
Zcchc5			-0.67
Zfp472	-0.79		
Zfp984	-1.08		

Chapter 4

Integrative Analysis of ChIP-seq and RNA-seq Experiments Identifies WNT3A Inducible Regulatory Elements in Osteoblasts

4.1 Introduction

The WNT/β-catenin signaling or the canonical WNT pathway is a major regulator of several key biological processes including cell proliferation, differentiation and apoptosis. To initiate canonical WNT signaling the extracellular WNT ligand binds to the FZD receptor and LRP5/6 co-receptor on the cell surface. This prevents Axin, APC and GSK3 mediated degradation of cytoplasmic β-catenin. As a consequence, β-catenin accumulates in the cytoplasm and translocates to the nucleus, where it is recruited to WNT-responsive elements (WRE) bound by TCF/LEF family transcription factors. In the absence of β-catenin, TCF/LEF transcription factors bind to Groucho/TLE proteins and act as transcriptional repressors. Nuclear β-catenin displaces Groucho/TLE from TCF/LEF and activates transcription of WNT targets [328].

Osteoblasts are bone-forming cells that are responsible for the synthesis and mineralization of the bone matrix. The WNT/β-catenin signaling is a key regulator of osteoblast differentiation and function [309,329]. Thus, deciphering the mechanism by which WNT/β-catenin signaling regulate osteoblastic gene expression is paramount to understanding WNT mediated transcription regulation in osteoblasts. To identify direct WNT/β-catenin target genes in osteoblasts it is necessary to map the binding sites for TCF/LEF transcription factors across the genome. Recently, ChIP-seq has successfully been used to identify binding sites for several transcription factors on a genome-wide scale [330-333]. Previous ChIP-seq experiments have suggested that not all transcription factor binding events correlate with active transcription [334]. Therefore, it is important to perform an integrative analysis incorporating both ChIP-seq and gene expression data to identify functionally relevant transcription factor binding events.

Transcription factors bind to promoters and enhancers to activate gene expression. Enhancers are distal-acting DNA elements that bind transcription factors to increase gene transcription [330]. Genomic studies have identified numerous key biochemical features of functional enhancer elements. For example, active enhancer elements correlate with the location of mono-methylated lysine 4 of histone H3 (H3K4me1) and acetylated lysine 27 of histone H3 (H3K27ac). Several studies have used H3K27ac marks in combination with H3K4me1 to identify active enhancers in different cell types [335-337]. Genome-wide mapping of WNT inducible enhancers in osteoblasts will greatly improve our understanding of WNT mediated transcription regulation in osteoblasts.

In this study, we employed an integrative genomics approach to examine the mechanisms of WNT3A-target gene regulation in osteoblasts. First, using ChIP-seq, we

identified active osteoblast enhancers by finding regions with overlapping H3K4me1 and H3K27ac (H3K4me1+, H3K27ac+) marks. To find WNT3A targets activated *via* the β-catenin dependent pathway, we mapped TCF/LEF binding sites identified using ChIP-seq to the genes activated by WNT3A and identified genes with TCF/LEF binding sites in their promoter and/or enhancers. We found that >80% WNT3A activated genes harbor TCF/LEF binding sites in their promoter region or enhancers. This study also identified several putative WNT inducible enhancer elements (H3K4me1+, H3K27ac+, TCF/LEF+) near WNT3A target genes. Subsequently, we validated a subset of predicted WNT inducible enhancers and confirmed their WNT3A dependent enhancer activity. Taken together, this study identified several TCF/LEF targets and putative WNT-inducible regulatory elements in osteoblasts.

4.2 Methods

4.2.1 Osteoblast isolation and culture

Osteoblasts were isolated from calvaria of neonatal (4-5 days old) mice by serial digestion in Collagenase 1 and EDTA solutions, as described in Chapter 3. Osteoblast enriched fractions were cultured in DMEM/F12 supplemented with 10% fetal bovine serum and 1% penicillin/streptomycin at 37 °C for 3 days to get a sufficient number of cells. Subsequently, these cultures were treated with 100ng/µl of recombinant WNT3A (R&D systems) for 24 hours.

4.2.2 ChIP-seq

H3K4me1 (AM#39298, ActiveMotif) and H3K27ac (AM#39133, Active Motif) ChIP library preparation was performed at Active Motif (Carlsbad, CA) according to proprietary methods. Libraries were validated for integrity using the Agilent Bioanalyzer (Agilent Technologies) and sequenced on the NextSeq 550 sequencer (Illumina). The input DNA without antibody immunoprecipitation was also sequenced and used as the control.

4.2.3 ChIP-seq data analysis

H3K4me1 and H3K27ac ChIP-seq data and the input control were aligned to the mouse genome (mm10) using Bowtie 2 (version 2.1.0) [242]. Peak calling was performed by MACS software (version 1.4.2) and the H3K4me1 and the H3K27ac peaks significantly enriched over the input DNA (p-value < 10^{-5}) were identified.

TCF/LEF binding peaks were identified using 16 publically available ChIP-seq datasets from 12 human cell lines (K562, LOVO, GM12878, LS180, HELA, HePG2, HCT116, PANC1, HEK293, MCF7, U937 and MDA-MB-453). Twelve TCF4/LEF ChIP-seq datasets were downloaded from the following ENCODE [282] experiments: ENCSR000EVE, ENCSR000EVF, ENCSR000EWT, ENCSR000EUV, ENCSR000EUY, ENCSR000EVQ, ENCSR000EXL, ENCSR501DKS, ENCSR863KUB, ENCSR888XZK, ENCSR444LIN and ENCSR343ELW. From ENCODE the peak files were downloaded in BED format. The remaining four TCF4/LEF datasets were obtained from the following NCBI GEO [338] experiments: GSM722426, GSM1099033, GSM791409 and GSM1208689. Datasets in SRA format were converted into fastq

format using NCBI SRA toolkit (version 2.4.5). Data quality was checked using FastQC (version 0.11.5) software. Trimmomatic (version 0.32) [241] was used for data preprocessing. Using Trimmomatic, the reads were scanned with a 4-base wide sliding window, cutting when the average base quality drops below 15. Reads with length <25 bases after preprocessing were discarded. TCF/LEF ChIP-seq data was aligned to the human genome (hg19) using Bowtie (version 1.0.1) [242] and binding peaks were identified using MACS (version 1.4.2) [293]. TCF/LEF peaks in hg19 coordinates were converted into mm10 coordinates using UCSC liftover [339].

4.2.4 Peak annotation

ChIPseeker (version 1.10) [285] was used to annotate peaks to different genomic features such as promoter (±3kb of the TSS), downstream (the region that was downstream of the transcription termination site), exon, 5' UTR, 3' UTR, intron, and intergenic. ChIPseeker was also used to calculate the distance from the peak to the nearest TSS.

Gene ontology [279] analysis was performed using the online tool GREAT (version 3.0.0) [284] and enriched biological processes associated with the peaks were obtained (p-value < 10^{-5}).

4.2.5 WNT inducible enhancer identification

Osteoblast enhancers were identified by intersecting H3K4me1 and H3k27ac peaks using BEDOPS (version 2.4.8) [301] and identifying regions with overlapping (distance between peaks = 0) H3K4me1 and H3K27ac peaks. Subsequently, BEDOPS was used to calculate the distance between TCF/LEF peaks and H3K4me1+, H3K27ac+ enriched regions and H3K4me1+, H3K27ac+ elements with TCF/LEF peaks near them (distance < 1kb) were identified. These H3K4me1+, H3K27ac+, TCF/LEF+ regions were considered as candidate WNT inducible enhancers.

Enhancers were visualized using IGV (version 2.3.16) [340] and the ECR browser [341]. The ECR Browser provides a graphical interface that allows users to visualize and analyze Evolutionary Conserved Regions (ECRs) in genomes of sequenced species including human and other model organisms such as mouse, rat and zebrafish.

4.2.6 WNT inducible Enhancer validation

Putative enhancer regions were amplified using Phusion High-Fidelity DNA Polymerase (New England Biolabs) according to manufacturer's protocol with EcoRI recognition sites added to the 5' end of all primers. TCF binding sites isolated from Topflash reporter plasmid (a reporter plasmid containing multiple copies of wildtype TCF-binding sites) were used as positive control [342]. Amplicons were then cloned into the EcoRI site of the pGLuc Mini-TK 2 vector (New England Biolabs) upstream of both the thymidine kinase promoter and Gaussia luciferase. Subconfluent MC3T3 cells were co-transfected with pGLuc Mini-TK 2 enhancer plasmids and pSV40-CLuc control plasmid with Cypridina luciferase at a ratio of 10:1 using Lipofectamine 3000 (Life Technologies) according to manufacturer's protocol. Following a 24 hour incubation,

culture media was changed to either control media (DMEM/F12, 10% FBS, 1% Penicillin/Streptomycin) or WNT media (control media plus 100ng/µl recombinant WNT3A (R&D systems)). After additional 24 hour incubation, media was collected and assayed for luciferase activity using BioLux Gaussia Luciferase Assay Kit and BioLux Cypridina Luciferase Assay Kit (New England Biolabs) on a Modulus II plate reader (Turner Biosystems). For analysis, Gaussia luciferase relative light unit (RLU) values were normalized to Cypridina luciferase RLU for each well.

4.2.7 Transcription factor binding motif analysis

Promoters of WNT target genes and WNT inducible enhancers were analyzed using HOMER (version 4.7.2) [286] and enriched transcription factor binding motifs were identified (p value < 0.001).

4.3 Results

4.3.1 Analysis of TCF/LEF ChIP-seq data identified genes with WREs in their promoter

WNT activated transcription factors TCF/LEFs bind to WREs in the promoter and enhancers to activate WNT target genes. Using 16 publically available ChIP-seq datasets we identified 161824 TCF/LEF binding peaks in 12 different cell lines. To identify genes with TCF/LEF peaks in their promoters, we mapped the TCF/LEF peaks to genomic features using ChIPseeker and identified 11798 protein coding and non-coding RNA genes with TCF/LEF binding sites in their promoter. Next, we analyzed WNT3A activated genes identified in Chapter 3 for the presence of TCF/LEF peaks and found that 65% (181/278) of the genes activated by WNT3A have TCF/LEF binding sites in their promoter region. These genes include *Tcf7*, *Lef1*, *Axin2*, *Ndnf*, *Inhbb*, *Tnfrsf19* and *Nkd1*. Figure 4.1 shows TCF/LEF ChIP-seq peaks from multiple cell types mapping to *Axin2* promoter. A complete list of WNT3A activated genes with TCF/LEF binding sites in their promoter are given in Table 4.1.

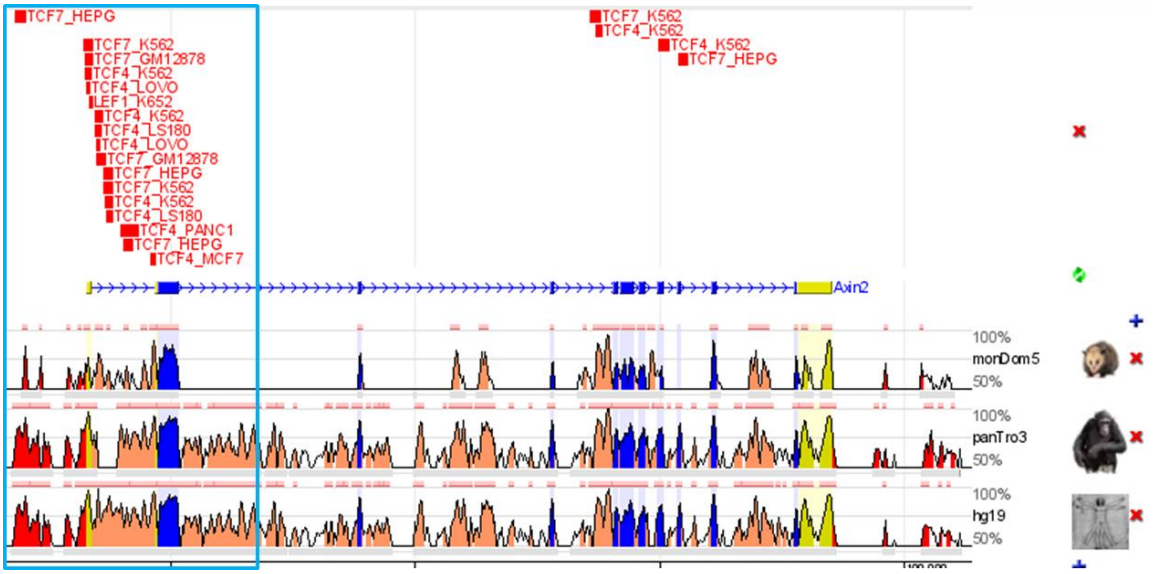

Figure 4.1: TCF/LEF binding sites in Axin2 promoter. *Multiple TCF/LEF binding peaks (red solid rectangles) from different cell lines mapped to Axin2 promoter region. The data was visualized using ECR browser. Genomic regions are color coded as follows: exons (blue); introns (salmon); intergenic regions (red). The height of the conservation plot at each position represents the number of nucleotides conserved in a windows of 100 nucleotides centered on that position.*

4.3.2 Distribution of enhancer-associated histone marks across the osteoblast genome

H3K4me1 and H3K27ac together mark active enhancer regions. By mapping H3K4me1 and H3K27ac ChIP-seq data to the mouse genome we identified 85788 H3K4me1 and 54080 H3K27ac peaks. This included 49635 elements with overlapping H3K4me1 and H3K27ac (H3K4me1+, H3K27ac+) peaks. A large number (61%) of these H3K4me1+, H3K27ac+ elements were located in intronic or intergenic regions. Figure 4.2 shows the distribution of H3K4me1+, H3K27ac+ regions in osteoblasts. We further separated H3K4me1+, H3K27ac+ regions into proximal and distal regions, relative to the TSS. The regions within ±3kb of the TSS were defined as proximal regions and the rest as distal regions. The distal regions were considered as osteoblast enhancers. This included 36178 elements. A prime example of overlapping H3K4me1 and H3K27ac ChIP-seq peaks is evident at the *Inhbb* genomic region (Figure 4.3)

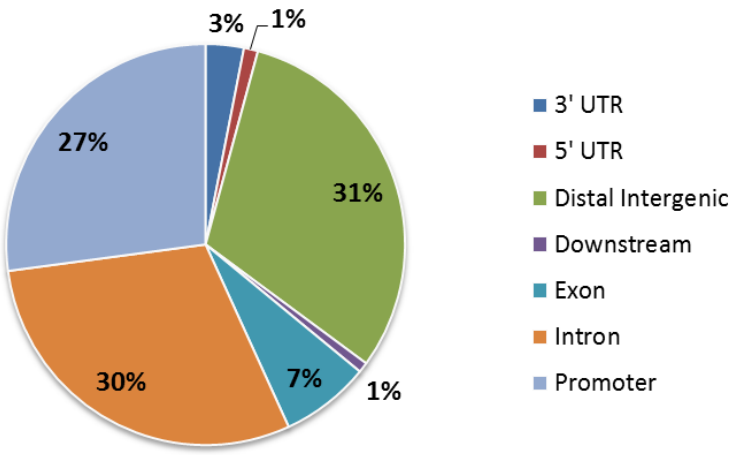

Figure 4.2: Distribution of overlapping H3K4me1 and H3K27ac peaks. *The majority of H3K4me1+, H3K27ac+ regions mapped to intronic or intergenic regions.*

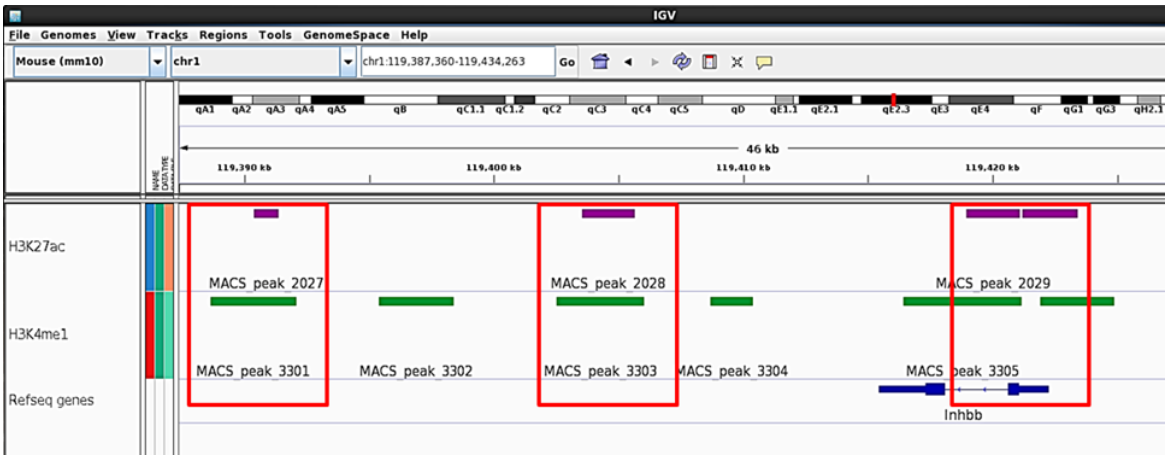

Figure 4.3: Overlapping H3K4me1 and H3K27ac peaks*. Overlapping H3K4me1 (green) and H3K27ac (purple) peaks identified near Inhbb promoter and distal intergenic regions. Overlapping H3K4me1 and H3K27ac peaks are highlighted in red boxes. The data was visualized using IGV.*

Functional annotation of osteoblast enhancers was performed using GREAT annotation software. GREAT identified several key ontology terms associated with bone development and metabolism including '*extracellular matrix organization*', '*positive regulation of mesenchymal cell proliferation*' and '*positive regulation of canonical WNT receptor signaling pathway*' as enriched for these osteoblast enhancers. Figure 4.3 shows the top 25 enriched biological processes identified by GREAT.

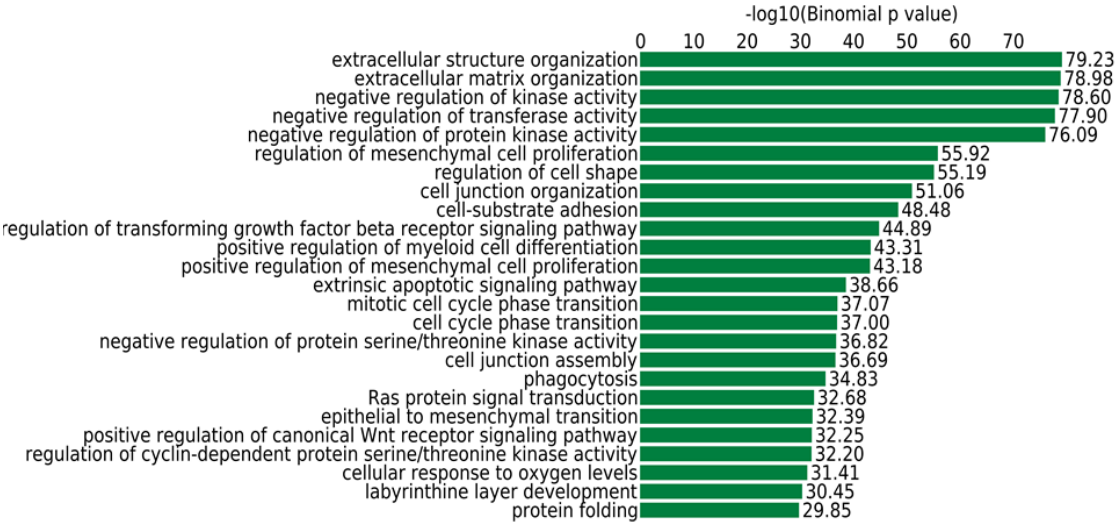

Figure 4.4: Enriched ontology terms associated with osteoblast enhancers. *The top 25 biological processes identified by GREAT are shown. Ontology terms with binomial p-value < 10^{-5} were considered as significant. The ontology terms are arranged in the order of increasing binomial p-value (top to bottom). The p-values are given in –log10 scale.*

4.3.3 Comparative analysis of ChIP-seq and RNA-seq data predicts WNT inducible enhancers

Next, we mapped TCF/LEF binding peaks to distal H3K4me1+,H3K27ac+ elements and identified 12479 H3K4me1+, H3K27ac+ elements with TCF/LEF binding peaks near (less than ±1kb) them. These regions were defined as candidate WNT inducible enhancers. These putative WNT inducible enhancers were assigned to the nearest genes using ChIPseeker and identified 5614 genes with WNT inducible enhancers in their vicinity. This analysis identified 587 putative WNT inducible enhancers near genes activated by WNT3A. One hundred and eight four WNT3A activated genes were found to have putative WNT inducible enhancers near them (Table 4.2). For several WNT3A targets including *Axin2*, *Inhbb*, *Bmper* and *Ptch1* we identified multiple putative WNT inducible enhancers near them. Figure 4.5 shows a highly conserved putative WNT inducible enhancer in *Ptch1* intronic region. A complete list of WNT inducible enhancers identified near WNT3A activated genes are given in Table 4.2.

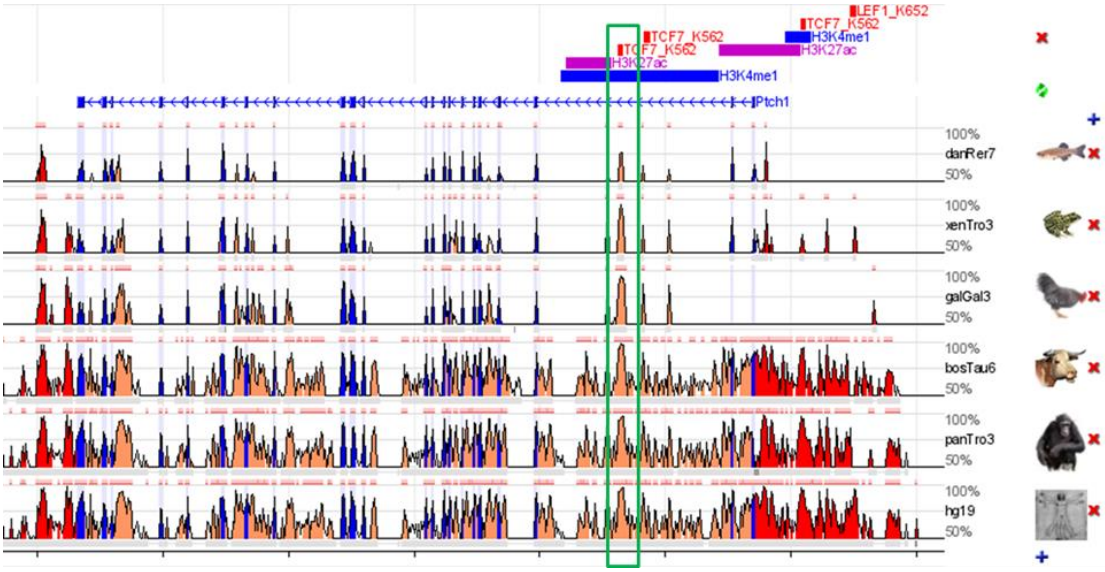

Figure 4.5: Putative WNT inducible enhancer in Ptch1 intronic region*. The enhancer was visualized in ECR browser. The TCF binding site in the enhancer region is marked in green rectangle. Genomic regions are color coded as follows: exons (blue); introns (salmon); intergenic regions (red). The predicted enhancer is highly conserved across multiple organisms. The height of the conservation plot at each position represents the number of nucleotides conserved in a windows of 100 nucleotides centered on that position.*

Subsequently, we experimentally validated WNT3A inducible enhancer activity of 5 predicted enhancers. About 500 bp regions around the TCF/LEF binding peaks in these enhancers were cloned into pGLuc Mini-TK 2 vector and transfected into MC3T3 pre-osteoblasts. TCF binding sites isolated from Topflash were used as positive control [342]. Enhancers predicted near *Pim1*, *Iyd* and *Errfi1* were identified as active osteoblasts enhancers (Figure 4.6). Compared to 'promoter only' constructs these enhancers showed more than 1.5-fold increase in reporter activity. Upon treatment with WNT3A *Pim1*, *Iyd*, and *Sema3f* enhancers showed significant increase in reporter activity compared to sham treated cells, suggesting that these are WNT3A inducible enhancers (Figure 4.6). Not much is known about the functions of these genes in osteoblasts. Further studies are required to understand how these genes and enhancers contribute to osteogenesis.

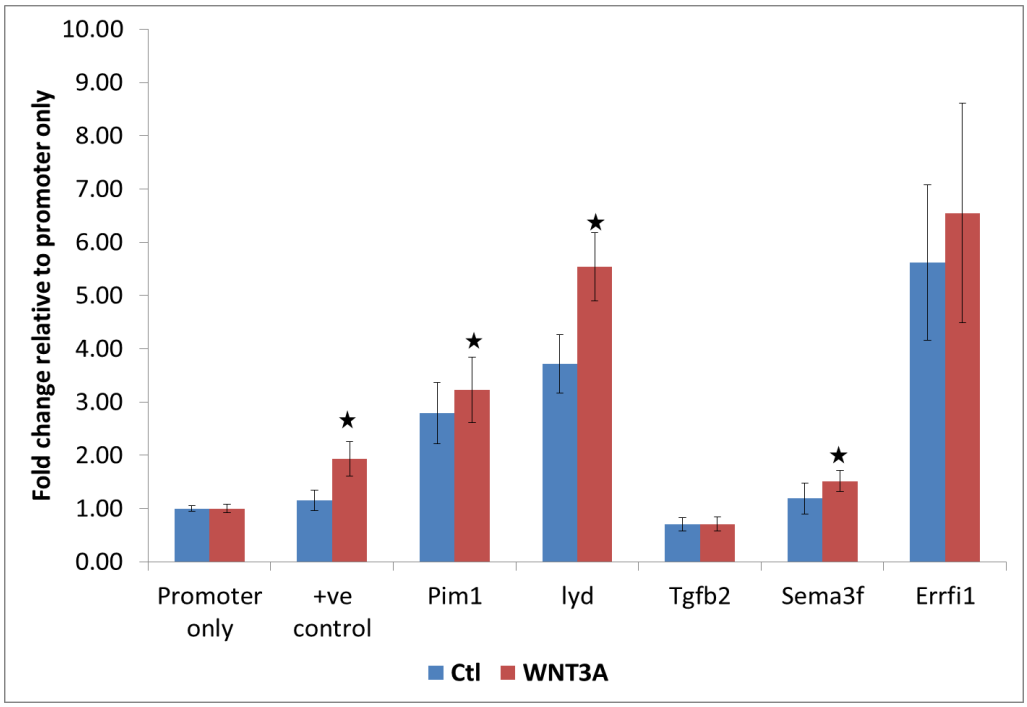

Figure 4.6: Enhancer validation. *Fold change in reporter expression in WNT3A treated (WNT3A) and sham treated (Ctl) cells are shown. Statistical significance was determined using a two sample t-test. WNT3A inducible enhancers with p value < 0.05 are highlighted with *.*

4.3.4 Motif analysis identifies AP-1 motifs as over-represented in TCF/LEF binding regulatory elements

Multiple transcription factors bind to same enhancer element. To identify enriched transcription factor binding motifs in the putative WNT inducible enhancers identified near WNT3A activated genes, a transcription factor recognition motif enrichment analysis was performed using HOMER. This analysis revealed that consensus AP-1 motifs (Figure 4.7) were over-represented in a these WNT inducible enhancers. Interestingly, promoter analysis of WNT3A activated genes also identified AP-1 as the most significantly enriched transcription factor binding motif.

Figure 4.7: AP-1 binding motif. *AP-1 binding motifs were over-represented in a large subset of WNT inducible enhancers. The sequence logo was generated using HOMER 4.7.2.*

4.4 Discussion

Recent genome-wide association studies have shown that single nucleotide polymorphisms (SNPs) that have been associated with risk for numerous diseases frequently lie in enhancer elements [343]. Variations in enhancer elements may influence the transcription of associated genes, thereby increasing the risk for many common diseases. Therefore, genome wide identification of enhancer elements is of great importance. In this study, we identified 36178 osteoblast enhancers by mapping H3K4me1 and H3K27ac ChIP-seq data to the mouse genome. A gene ontology analysis revealed that these enhancers regulate genes associated with biological processes such as '*extracellular matrix organization*', '*cell proliferation*' and '*cell adhesion*'. Interestingly, '*Positive regulation of WNT receptor signaling pathway*' was also one of the most significantly enriched ontology term associated with osteoblast enhancers. This suggests that distal regulatory elements play a huge role in regulating WNT signaling pathway in osteoblasts.

Our study showed that 83% (231/278) genes activated by WNT3A have TCF/LEF binding sites in their promoter or enhancers, suggesting that majority of WNT3A targets can be activated by the canonical signaling pathway. These genes include TCF7 and LEF1 transcription factors. Previous studies have experimentally validated WREs predicted near LEF1 and TCF7 promoters [163]. This confirms that the canonical WNT pathway regulates the transcription of TCF/LEF transcription factors. A motif analysis identified AP-1 binding motif as the most significantly enriched transcription factor binding motif in promoters of WNT3A targets and WNT inducible enhancers identified near WNT3A targets. AP-1 family transcription factors are activated by JNK pathway. WNT3A has been shown to activate JNK pathway in some contexts [63]. Previous studies have suggested that TCF and β-catenin physically interact with AP-1 transcription factors to regulate gene expression in cancer [344,345]. Interestingly, we also identified AP-1 family transcription factor *Fosl2* as a transcriptional target of WNT3A. FOSL2 has been shown to play a major role in regulating osteoblast differentiation. *Fosl2*-deficient osteoblasts displayed a differentiation defect [346] and mice lacking *Fosl2* in osteoblasts exhibited low bone mass [347] whereas *Fosl2*-overexpressing mice showed increased bone formation [346]. It is not known whether FOSL2 plays a role in regulating the expression of WNT3A targets identified in this study. Further studies are required to understand whether AP-1 transcription factors cooperate with TCF/LEF to regulate the expression of WNT3A targets in osteoblasts.

In conclusion, this study identified thousands of enhancer elements in osteoblasts and experimentally validated the enhancer activity of a few of those elements. Further experiments are required to understand how these enhancers regulate osteogenesis. This study also identified several putative WNT inducible enhancers and TCF/LEF targets in osteoblasts. Although further work is necessary to elucidate the connection between canonical WNT signaling and AP-1 transcription factors our study suggests that AP-1 transcription factors play a role in regulating WNT3A targets in osteoblasts.

Table 4.1: WNT3A activated genes with TCF/LEF binding sites in their promoter.

Genes			
Slc13a4	*Ier3*	*Tes*	*Nedd9*
Sema4f	*Ptch1*	*Irx3*	*Bmp4*
Sstr2	*Tspyl5*	*Hunk*	*Nfatc4*
Ndnf	*Pcdh10*	*Elfn1*	*Vgf*
Axin2	*Cdc42ep3*	*Pard6b*	*Itm2a*
Tmem100	*Insc*	*Actg2*	*Rapgef3*
Colec10	*Murc*	*Phldb2*	*Cthrc1*
C430002N11Rik	*Lurap1l*	*Sema3f*	*Wnt2b*
Aqp5	*Hdac9*	*Trp53i11*	*Adamts4*
Slc1a2	*Errfi1*	*Tmem26*	*Hes1*
Tgfb2	*Ankrd1*	*Sema5a*	*Sgms1*
Inhbb	*Nrcam*	*Pmepa1*	*Mtus1*
Nebl	*Thsd4*	*Osbpl3*	*Glipr1*
Bmp7	*Tiparp*	*Sh3rf1*	*Fjx1*
Apcdd1	*Fgf21*	*Cacna1g*	*Dbf4*
Kcnj2	*Syn1*	*Sync*	*Sfrp4*
Col7a1	*Spry1*	*Inhba*	*Maff*
Tnfrsf19	*Tgfb3*	*Fam184a*	*Pim1*
Enpp2	*Creld1*	*Prrx2*	*Arhgap6*
Prss46	*Plcxd2*	*Porcn*	*Timm8a1*
Rgcc	*Fzd1*	*Dpt*	*Stard13*
Tceal5	*Filip1l*	*Rnf122*	*Phlda1*
Etv4	*Fam185a*	*Gpn2*	*Limk2*
Gjb2	*Wif1*	*Cacnb4*	*Slc2a3*
Fhod3	*Rgs16*	*Csrp1*	*Sorbs1*
Gadd45g	*Crabp1*	*Fosl2*	*Chst1*
Arl4c	*Prickle1*	*Rnd3*	*Itga3*
Slitrk6	*Dusp1*	*Foxn3*	*Suox*
Aldh1a2	*Fgf18*	*Jak2*	*Rb1*
Ctnnd2	*Pgf*	*Tnfaip6*	*Irx5*
Mrgprf	*Fmnl2*	*Nrp2*	*Il16*
C1ql3	*Fam198b*	*Fam84b*	*D6Ertd527e*
Sfn	*Kank1*	*Artn*	*Slc20a1*
Cnn1	*Ppfibp2*	*Robo2*	*Zfp503*
Lif	*Fbln5*	*Stambpl1*	*Rdh10*
Specc1	*Hbegf*	*Egln3*	*Cyr61*
Cap2	*Ror1*	*Mrto4*	*Bmp2*
Tcf7	*Cyp26b1*	*Lin7a*	*Spire2*
Piezo2	*Serpine1*	*Kctd11*	*Fam131a*
Col26a1	*Galnt3*	*Fgfr1*	*Lepr*
Tec	*Lef1*	*Tcf4*	*Fgf13*
Pdgfa	*Ccnd1*	*Kcnj15*	*Fam65b*
Nkd1	*Nog*	*Unc13b*	*Mllt3*
Has2	*Scn3a*	*Pitpnc1*	
Stc1	*Bmpr1b*	*Zfp462*	
Tnfrsf12a	*Sh3bp4*	*Adk*	

Table 4.2: WNT inducible enhancers identified near WNT3A targets. *For all putative enhancers, the nearest gene is also given.*

Chromosome	Start	End	Nearest gene
chr2	102444823	102446053	Fjx1
chr9	60307509	60314013	Thsd4
chr1	150564691	150568423	Prg4
chr16	57571140	57572919	Filip1l
chr13	41349324	41350221	Nedd9
chr14	46435252	46439311	Bmp4
chr18	63366298	63367670	Piezo2
chr2	51135869	51149616	Rnd3
chr18	69468488	69471066	Tcf4
chr7	107663093	107667592	Ppfibp2
chr5	4753804	4760281	Fzd1
chr2	102782748	102783894	Slc1a2
chr12	35413969	35421060	Ahr
chr16	90497381	90498686	Hunk
chr1	62741648	62743857	Nrp2
chr15	32321623	32323948	Sema5a
chr5	32032676	32042208	Fosl2
chr9	23494989	23496155	Bmper
chr11	3346649	3351183	Limk2
chr2	51117351	51120272	Rnd3
chr16	57398852	57405648	Filip1l
chr5	151200333	151205156	Stard13
chr17	79112059	79113765	Qpct
chr4	54970782	54975577	Zfp462
chr8	91994069	92001840	Irx3
chr5	5004322	5008686	Fzd1
chr18	69701603	69702725	Tcf4
chr4	117973735	117979234	Artn
chr18	69660205	69662555	Tcf4
chr5	4591241	4593061	Fzd1
chrX	169023435	169025851	Arhgap6
chr4	55012083	55014984	Zfp462
chr2	50106931	50108929	Lypd6
chr2	102757096	102758555	Slc1a2
chr1	174897336	174899650	Grem2
chrX	169006516	169007342	Arhgap6
chr8	91776920	91778785	Irx3
chr16	57414527	57430665	Filip1l
chr19	34471677	34477948	Ch25h
chr19	36205919	36209945	Ankrd1
chr2	62379813	62381150	Dpp4
chr15	7884935	7887723	Gdnf
chr4	54467400	54472600	Zfp462
chr12	53916070	53919287	Egln3
chr3	145728038	145732102	Ddah1

chr5	*4493496*	*4499717*	*Fzd1*
chr3	*102497058*	*102499660*	*Ngf*
chr9	*60117078*	*60118162*	*Thsd4*
chr19	*36228240*	*36229424*	*Ankrd1*
chr12	*53781029*	*53783002*	*Egln3*
chr5	*151163200*	*151169790*	*Stard13*
chr4	*88013303*	*88016909*	*Mllt3*
chr9	*60405836*	*60408364*	*Thsd4*
chr2	*52700254*	*52703163*	*Cacnb4*
chr7	*83696565*	*83701583*	*Il16*
chr5	*32119267*	*32152007*	*Fosl2*
chr4	*100178817*	*100182991*	*Ror1*
chr3	*79902586*	*79905533*	*Fam198b*
chr1	*174908154*	*174909698*	*Grem2*
chr6	*137108814*	*137112413*	*Rerg*
chr1	*119418967*	*119421115*	*Inhbb*
chr13	*41328206*	*41346618*	*Nedd9*
chr1	*62441793*	*62448264*	*Nrp2*
chr15	*54351692*	*54355961*	*Colec10*
chr15	*93733475*	*93736406*	*Prickle1*
chr1	*119305965*	*119310492*	*Inhbb*
chr8	*91936653*	*91937754*	*Irx3*
chr3	*65494268*	*65495361*	*Tiparp*
chr13	*19628277*	*19629207*	*Sfrp4*
chr1	*62515997*	*62517670*	*Nrp2*
chr11	*108897305*	*108899282*	*Axin2*
chr5	*4526996*	*4538455*	*Fzd1*
chr3	*79906143*	*79909858*	*Fam198b*
chr12	*35526993*	*35536657*	*Ahr*
chr2	*52893490*	*52896968*	*Fmnl2*
chr18	*69438453*	*69441103*	*Tcf4*
chr1	*62746832*	*62753677*	*Nrp2*
chr8	*25322734*	*25327583*	*5430421F17Rik*
chr8	*25293427*	*25296772*	*5430421F17Rik*
chr8	*25364305*	*25371051*	*5430421F17Rik*
chr19	*34241985*	*34258143*	*Acta2*
chr1	*171257361*	*171264820*	*Adamts4*
chr14	*21191118*	*21191987*	*Adk*
chr18	*62170191*	*62171518*	*Adrb2*
chr18	*62146078*	*62151661*	*Adrb2*
chr12	*35514385*	*35518541*	*Ahr*
chr12	*35310892*	*35320566*	*Ahr*
chr12	*35460217*	*35461530*	*Ahr*
chr12	*35477222*	*35482973*	*Ahr*
chr12	*35332710*	*35334645*	*Ahr*
chr12	*35344913*	*35346047*	*Ahr*
chr13	*74245062*	*74246572*	*Ahrr*
chr9	*71287065*	*71289599*	*Aldh1a2*
chr9	*71317331*	*71318650*	*Aldh1a2*

chr19	*36178322*	*36179612*	*Ankrd1*
chr19	*36127089*	*36134951*	*Ankrd1*
chr15	*99582563*	*99587264*	*Aqp5*
chr1	*88649300*	*88656357*	*Arl4c*
chr1	*88667168*	*88669254*	*Arl4c*
chr18	*60870487*	*60904043*	*Arsi*
chr18	*60914582*	*60920176*	*Arsi*
chr4	*118013054*	*118020218*	*Artn*
chr4	*117995263*	*118001967*	*Artn*
chr4	*118029455*	*118030899*	*Artn*
chr2	*133443590*	*133444647*	*Bmp2*
chr2	*133437209*	*133438282*	*Bmp2*
chr5	*98761105*	*98763031*	*Bmp3*
chr14	*46384561*	*46390162*	*Bmp4*
chr2	*172811440*	*172812604*	*Bmp7*
chr2	*172778159*	*172779083*	*Bmp7*
chr9	*23155539*	*23159183*	*Bmper*
chr9	*23423189*	*23424494*	*Bmper*
chr9	*23188343*	*23192994*	*Bmper*
chr9	*23298427*	*23317396*	*Bmper*
chr9	*23354027*	*23356186*	*Bmper*
chr9	*23372470*	*23378310*	*Bmper*
chr9	*23471116*	*23475507*	*Bmper*
chr9	*23398954*	*23401033*	*Bmper*
chr9	*23248598*	*23255596*	*Bmper*
chr9	*23199201*	*23205476*	*Bmper*
chr3	*142278965*	*142280023*	*Bmpr1b*
chr9	*96747150*	*96804229*	*C430002N11Rik*
chr9	*96823365*	*96825597*	*C430002N11Rik*
chr11	*94466685*	*94475491*	*Cacna1g*
chr11	*94425552*	*94428911*	*Cacna1g*
chr2	*52622385*	*52625519*	*Cacnb4*
chr13	*46570960*	*46573857*	*Cap2*
chr4	*8211973*	*8213959*	*Car8*
chr4	*8252581*	*8254915*	*Car8*
chr7	*145028847*	*145034280*	*Ccnd1*
chr7	*144969402*	*144973279*	*Ccnd1*
chr7	*145025608*	*145027019*	*Ccnd1*
chr17	*79294594*	*79299676*	*Cdc42ep3*
chr17	*79414094*	*79425771*	*Cdc42ep3*
chr17	*79341912*	*79352456*	*Cdc42ep3*
chr17	*79336015*	*79341904*	*Cdc42ep3*
chr17	*79304685*	*79305727*	*Cdc42ep3*
chr17	*79277781*	*79278795*	*Cdc42ep3*
chr4	*11766043*	*11770541*	*Cdh17*
chr19	*34429997*	*34437339*	*Ch25h*
chr5	*136868617*	*136871154*	*Col26a1*
chr15	*54385197*	*54388460*	*Colec10*
chr9	*54783669*	*54788719*	*Crabp1*

chr9	*54799556*	*54807386*	*Crabp1*
chr9	*54776153*	*54777640*	*Crabp1*
chr6	*113478707*	*113490139*	*Creld1*
chr1	*135684151*	*135692636*	*Csrp1*
chr1	*135668071*	*135676674*	*Csrp1*
chr1	*135723522*	*135737288*	*Csrp1*
chr1	*135697095*	*135701183*	*Csrp1*
chr15	*39039544*	*39050195*	*Cthrc1*
chr15	*30555034*	*30557306*	*Ctnnd2*
chr6	*84582045*	*84584350*	*Cyp26b1*
chr3	*145612916*	*145616631*	*Cyr61*
chr3	*145673978*	*145695208*	*Cyr61*
chr3	*145661614*	*145664447*	*Cyr61*
chr3	*145646199*	*145658631*	*Cyr61*
chr3	*145645037*	*145646037*	*Cyr61*
chr6	*87178575*	*87193276*	*D6Ertd527e*
chr6	*87098719*	*87104141*	*D6Ertd527e*
chr3	*145699483*	*145708448*	*Ddah1*
chr3	*145831591*	*145850446*	*Ddah1*
chr3	*131918681*	*131920678*	*Dkk2*
chr2	*62422248*	*62423701*	*Dpp4*
chr1	*164626404*	*164633944*	*Dpt*
chr1	*164808717*	*164812134*	*Dpt*
chr17	*26501507*	*26517382*	*Dusp1*
chr17	*26526847*	*26538546*	*Dusp1*
chr17	*26496193*	*26499451*	*Dusp1*
chr11	*28811620*	*28813527*	*Efemp1*
chr11	*28951176*	*28953160*	*Efemp1*
chr12	*54185564*	*54195341*	*Egln3*
chr12	*53946841*	*53950721*	*Egln3*
chr12	*53886968*	*53890154*	*Egln3*
chr12	*53999655*	*54000993*	*Egln3*
chr12	*53752971*	*53753938*	*Egln3*
chr12	*54199297*	*54200559*	*Egln3*
chr12	*53864760*	*53866738*	*Egln3*
chr5	*139969072*	*139972491*	*Elfn1*
chr5	*139949039*	*139951749*	*Elfn1*
chr15	*54852522*	*54855365*	*Enpp2*
chr4	*150831615*	*150843912*	*Errfi1*
chr4	*150766547*	*150779257*	*Errfi1*
chr4	*150853652*	*150867313*	*Errfi1*
chr4	*150792851*	*150810455*	*Errfi1*
chr4	*150819586*	*150820904*	*Errfi1*
chr4	*150779291*	*150790110*	*Errfi1*
chr11	*101820008*	*101827995*	*Etv4*
chr11	*101789618*	*101791522*	*Etv4*
chr11	*101828048*	*101852719*	*Etv4*
chr6	*82029121*	*82031221*	*Eva1a*
chr16	*20698022*	*20704017*	*Fam131a*

chr3	*79973013*	*79981793*	*Fam198b*
chr3	*79987488*	*79997550*	*Fam198b*
chr3	*80002094*	*80008160*	*Fam198b*
chr3	*80054821*	*80057938*	*Fam198b*
chr13	*24535720*	*24538103*	*Fam65b*
chr13	*24678737*	*24679953*	*Fam65b*
chr13	*24644955*	*24649976*	*Fam65b*
chr13	*24655527*	*24658036*	*Fam65b*
chr12	*101798506*	*101799398*	*Fbln5*
chr8	*25540944*	*25547654*	*Fgfr1*
chr8	*25461962*	*25470329*	*Fgfr1*
chr8	*25438147*	*25442225*	*Fgfr1*
chr8	*25573306*	*25574632*	*Fgfr1*
chr18	*24721048*	*24725563*	*Fhod3*
chr18	*24971194*	*24973792*	*Fhod3*
chr16	*57534873*	*57538602*	*Filip1l*
chr16	*57524176*	*57533673*	*Filip1l*
chr16	*57382160*	*57384911*	*Filip1l*
chr16	*57546631*	*57558600*	*Filip1l*
chr16	*57513406*	*57516991*	*Filip1l*
chr16	*57573047*	*57574688*	*Filip1l*
chr16	*57495884*	*57497738*	*Filip1l*
chr16	*57433078*	*57436007*	*Filip1l*
chr16	*57466374*	*57469322*	*Filip1l*
chr16	*57559926*	*57566943*	*Filip1l*
chr2	*52936437*	*52939983*	*Fmnl2*
chr2	*52977459*	*52988865*	*Fmnl2*
chr2	*53047967*	*53060319*	*Fmnl2*
chr2	*53026892*	*53032776*	*Fmnl2*
chr2	*52871259*	*52875875*	*Fmnl2*
chr2	*52878729*	*52880758*	*Fmnl2*
chr2	*52883171*	*52892744*	*Fmnl2*
chr2	*53038154*	*53038892*	*Fmnl2*
chr2	*52804238*	*52805223*	*Fmnl2*
chr2	*52964666*	*52970837*	*Fmnl2*
chr2	*53012283*	*53014690*	*Fmnl2*
chr5	*32043111*	*32045841*	*Fosl2*
chr5	*32152035*	*32156493*	*Fosl2*
chr5	*31996026*	*31999245*	*Fosl2*
chr5	*32065792*	*32067537*	*Fosl2*
chr5	*32111145*	*32114612*	*Fosl2*
chr5	*31928778*	*31937445*	*Fosl2*
chr5	*32077363*	*32082390*	*Fosl2*
chr5	*32159174*	*32164869*	*Fosl2*
chr5	*32157513*	*32159116*	*Fosl2*
chr5	*32101549*	*32105660*	*Fosl2*
chr5	*32050678*	*32060472*	*Fosl2*
chr12	*99405331*	*99409234*	*Foxn3*
chr12	*99302446*	*99311297*	*Foxn3*

chr5	*4483990*	*4491544*	*Fzd1*
chr5	*4891929*	*4895733*	*Fzd1*
chr5	*4619593*	*4622519*	*Fzd1*
chr5	*4824787*	*4828031*	*Fzd1*
chr5	*4946996*	*4951666*	*Fzd1*
chr13	*51901423*	*51905525*	*Gadd45g*
chr2	*66062596*	*66064513*	*Galnt3*
chr15	*7929838*	*7933198*	*Gdnf*
chr15	*7875987*	*7879788*	*Gdnf*
chr15	*7771932*	*7773561*	*Gdnf*
chr15	*7857169*	*7865628*	*Gdnf*
chr2	*113763952*	*113767465*	*Grem1*
chr1	*174970341*	*174972685*	*Grem2*
chr1	*174844463*	*174848441*	*Grem2*
chr15	*56763898*	*56766523*	*Has2*
chr15	*56839066*	*56848319*	*Has2*
chr15	*56856242*	*56859143*	*Has2*
chr15	*56852882*	*56854073*	*Has2*
chr18	*36507047*	*36526638*	*Hbegf*
chr18	*36491236*	*36500596*	*Hbegf*
chr12	*34471002*	*34473802*	*Hdac9*
chr12	*34215121*	*34216115*	*Hdac9*
chr12	*34199560*	*34200649*	*Hdac9*
chr12	*34497437*	*34500538*	*Hdac9*
chr12	*34485280*	*34488649*	*Hdac9*
chr12	*34791390*	*34792392*	*Hdac9*
chr6	*58837644*	*58843373*	*Herc3*
chr16	*30055503*	*30070442*	*Hes1*
chr8	*79993656*	*79996899*	*Hhip*
chr17	*35802178*	*35803979*	*Ier3*
chr1	*72832045*	*72834625*	*Igfbp2*
chr1	*72772328*	*72775490*	*Igfbp2*
chr1	*72777392*	*72784972*	*Igfbp2*
chr7	*83669958*	*83672623*	*Il16*
chr7	*83710420*	*83727535*	*Il16*
chr7	*83765957*	*83767009*	*Il16*
chr7	*83736098*	*83743057*	*Il16*
chr13	*16659185*	*16662812*	*Inhba*
chr13	*16735517*	*16742409*	*Inhba*
chr13	*16755146*	*16765634*	*Inhba*
chr13	*16024911*	*16027982*	*Inhba*
chr13	*16007754*	*16024625*	*Inhba*
chr13	*16005811*	*16007721*	*Inhba*
chr13	*16711879*	*16723741*	*Inhba*
chr1	*119258913*	*119261070*	*Inhbb*
chr7	*114806405*	*114808192*	*Insc*
chr7	*114735923*	*114751400*	*Insc*
chr8	*91925392*	*91927157*	*Irx3*
chr8	*91712666*	*91713946*	*Irx3*

chr8	*91596494*	*91598629*	*Irx3*
chr8	*91767365*	*91771159*	*Irx3*
chr8	*92063536*	*92067439*	*Irx3*
chr8	*91568864*	*91578597*	*Irx3*
chr8	*91604616*	*91618439*	*Irx3*
chr8	*91948057*	*91949638*	*Irx3*
chr8	*91927257*	*91928499*	*Irx3*
chr8	*91888393*	*91890969*	*Irx3*
chr8	*91796911*	*91806877*	*Irx3*
chr8	*91897122*	*91903514*	*Irx3*
chr8	*92352690*	*92365301*	*Irx5*
chr8	*92487950*	*92490780*	*Irx5*
chr11	*95084119*	*95090308*	*Itga3*
chr2	*12316171*	*12318764*	*Itga8*
chr2	*12348938*	*12350119*	*Itga8*
chr8	*128679354*	*128681661*	*Itgb1*
chr8	*128651794*	*128658119*	*Itgb1*
chr10	*3572410*	*3574608*	*Iyd*
chr19	*25385957*	*25388323*	*Kank1*
chr19	*25373879*	*25375880*	*Kank1*
chr19	*25393771*	*25402212*	*Kank1*
chr11	*111052033*	*111058267*	*Kcnj2*
chr11	*111693250*	*111694899*	*Kcnj2*
chr11	*111746532*	*111748917*	*Kcnj2*
chr1	*132285213*	*132300989*	*Klhdc8a*
chr3	*130945592*	*130947987*	*Lef1*
chr3	*130933893*	*130936414*	*Lef1*
chr3	*130954954*	*130955913*	*Lef1*
chr3	*130949193*	*130953715*	*Lef1*
chr11	*4258182*	*4312989*	*Lif*
chr11	*4334690*	*4343261*	*Lif*
chr11	*3366216*	*3368520*	*Limk2*
chr7	*98569809*	*98578076*	*Lrrc32*
chr7	*98546901*	*98565878*	*Lrrc32*
chr7	*98479398*	*98508814*	*Lrrc32*
chr7	*98509006*	*98531862*	*Lrrc32*
chr4	*80951260*	*80952260*	*Lurap1l*
chr4	*80915633*	*80923169*	*Lurap1l*
chr4	*80948871*	*80951208*	*Lurap1l*
chr4	*80953375*	*80954246*	*Lurap1l*
chr7	*99293013*	*99300476*	*Map6*
chr4	*87982000*	*87986407*	*Mllt3*
chr4	*87932969*	*87935705*	*Mllt3*
chr10	*24227568*	*24229331*	*Moxd1*
chr10	*24395829*	*24400450*	*Moxd1*
chr7	*145298609*	*145306605*	*Mrgprf*
chr8	*41125366*	*41127792*	*Mtus1*
chr8	*41137934*	*41139470*	*Mtus1*
chr10	*109902312*	*109905363*	*Nav3*

chr10	*109985419*	*109987209*	*Nav3*
chr10	*110076074*	*110077825*	*Nav3*
chr13	*41509446*	*41513576*	*Nedd9*
chr13	*41529506*	*41533826*	*Nedd9*
chr13	*41365882*	*41367842*	*Nedd9*
chr13	*41444084*	*41452545*	*Nedd9*
chr13	*41472516*	*41478773*	*Nedd9*
chr13	*41514639*	*41522521*	*Nedd9*
chr13	*41455755*	*41462739*	*Nedd9*
chr13	*41320160*	*41324760*	*Nedd9*
chr13	*41350427*	*41360244*	*Nedd9*
chr13	*41465810*	*41469137*	*Nedd9*
chr14	*55833138*	*55835283*	*Nfatc4*
chr3	*102469449*	*102495325*	*Ngf*
chr3	*102353423*	*102369001*	*Ngf*
chr3	*102503698*	*102509810*	*Ngf*
chr3	*102524733*	*102531418*	*Ngf*
chr11	*46134021*	*46135387*	*Nipal4*
chr8	*88573489*	*88579301*	*Nkd1*
chr8	*88565899*	*88573136*	*Nkd1*
chr8	*88536351*	*88540760*	*Nkd1*
chr13	*73879678*	*73895239*	*Nkd2*
chr3	*51200651*	*51203712*	*Noct*
chr3	*51153908*	*51158114*	*Noct*
chr3	*50905204*	*50907009*	*Noct*
chr3	*50931405*	*50934321*	*Noct*
chr3	*51040928*	*51043915*	*Noct*
chr3	*51193679*	*51200204*	*Noct*
chr11	*89297193*	*89300531*	*Nog*
chr1	*62709366*	*62727620*	*Nrp2*
chr1	*62531128*	*62534206*	*Nrp2*
chr1	*62727821*	*62730924*	*Nrp2*
chr1	*62732371*	*62735066*	*Nrp2*
chr1	*62547397*	*62553912*	*Nrp2*
chr1	*62778579*	*62781271*	*Nrp2*
chr1	*62497570*	*62500755*	*Nrp2*
chr6	*50411886*	*50416075*	*Osbpl3*
chr6	*50372105*	*50385119*	*Osbpl3*
chr2	*168052154*	*168062734*	*Pard6b*
chr2	*168046806*	*168052072*	*Pard6b*
chr15	*78913108*	*78919690*	*Pdxp*
chr10	*111541442*	*111546780*	*Phlda1*
chr16	*45915951*	*45939958*	*Phldb2*
chr16	*45794681*	*45806529*	*Phldb2*
chr16	*45950228*	*45954265*	*Phldb2*
chr16	*45941808*	*45948808*	*Phldb2*
chr16	*45962039*	*45970890*	*Phldb2*
chr16	*45828455*	*45831676*	*Phldb2*
chr18	*63240758*	*63242310*	*Piezo2*

chr18	*63135440*	*63138021*	*Piezo2*
chr17	*29462955*	*29471763*	*Pim1*
chr17	*29436304*	*29438845*	*Pim1*
chr17	*29438948*	*29442795*	*Pim1*
chr17	*29456423*	*29462349*	*Pim1*
chr18	*66471825*	*66475035*	*Pmaip1*
chr2	*173227429*	*173278582*	*Pmepa1*
chr2	*173375315*	*173383622*	*Pmepa1*
chr2	*173304792*	*173309344*	*Pmepa1*
chr7	*107707476*	*107709293*	*Ppfibp2*
chr1	*150569350*	*150571826*	*Prg4*
chr1	*150459915*	*150461593*	*Prg4*
chr1	*150630334*	*150632677*	*Prg4*
chr1	*150502381*	*150503316*	*Prg4*
chr15	*93478261*	*93480587*	*Prickle1*
chr15	*93743525*	*93745201*	*Prickle1*
chr15	*93628346*	*93635143*	*Prickle1*
chr15	*93705662*	*93709425*	*Prickle1*
chr15	*93681123*	*93682529*	*Prickle1*
chr15	*93645247*	*93647722*	*Prickle1*
chr15	*93609763*	*93611469*	*Prickle1*
chr2	*30843751*	*30893674*	*Prrx2*
chr9	*96834164*	*96841331*	*Pxylp1*
chr9	*96850862*	*96854185*	*Pxylp1*
chr9	*96858341*	*96866137*	*Pxylp1*
chr17	*79092063*	*79094058*	*Qpct*
chr17	*79162848*	*79167701*	*Qpct*
chr17	*79098814*	*79100599*	*Qpct*
chr15	*97748082*	*97752242*	*Rapgef3*
chr1	*16227648*	*16229457*	*Rdh10*
chr6	*137153628*	*137157772*	*Rerg*
chr1	*153739559*	*153745018*	*Rgs16*
chr16	*74900572*	*74901677*	*Robo2*
chr16	*73646764*	*73647784*	*Robo2*
chr4	*100213849*	*100215145*	*Ror1*
chr4	*100128626*	*100129685*	*Ror1*
chr4	*100044582*	*100046295*	*Ror1*
chr7	*114168147*	*114173675*	*Rras2*
chr7	*114078996*	*114082988*	*Rras2*
chr7	*114178440*	*114185585*	*Rras2*
chr2	*65546136*	*65548258*	*Scn3a*
chr9	*107696684*	*107710355*	*Sema3f*
chr9	*107721995*	*107726101*	*Sema3f*
chr6	*82904684*	*82914621*	*Sema4f*
chr15	*32432654*	*32434325*	*Sema5a*
chr15	*32256990*	*32258696*	*Sema5a*
chr5	*137059182*	*137112383*	*Serpine1*
chr4	*133591769*	*133611771*	*Sfn*
chr19	*32271521*	*32273835*	*Sgms1*

chr19	*32339998*	*32343218*	*Sgms1*
chr19	*32354735*	*32357000*	*Sgms1*
chr19	*32186377*	*32187249*	*Sgms1*
chr19	*32228990*	*32232935*	*Sgms1*
chr19	*32283846*	*32286754*	*Sgms1*
chr19	*32279120*	*32283604*	*Sgms1*
chr19	*32193897*	*32202087*	*Sgms1*
chr19	*32177876*	*32183126*	*Sgms1*
chr1	*89115104*	*89126724*	*Sh3bp4*
chr1	*89067144*	*89075174*	*Sh3bp4*
chr1	*89076404*	*89082111*	*Sh3bp4*
chr8	*61193601*	*61194946*	*Sh3rf1*
chr11	*120955493*	*120966391*	*Slc16a3*
chr2	*102721600*	*102723604*	*Slc1a2*
chr2	*102675172*	*102676987*	*Slc1a2*
chr2	*129203257*	*129214614*	*Slc20a1*
chr18	*60478884*	*60485882*	*Smim3*
chr18	*60490116*	*60497510*	*Smim3*
chr19	*40453784*	*40457223*	*Sorbs1*
chr19	*40424437*	*40427714*	*Sorbs1*
chr19	*40432053*	*40434069*	*Sorbs1*
chr19	*40434202*	*40439139*	*Sorbs1*
chr19	*40377270*	*40378494*	*Sorbs1*
chr19	*40487012*	*40490332*	*Sorbs1*
chr19	*40508230*	*40514590*	*Sorbs1*
chr19	*40403897*	*40412035*	*Sorbs1*
chr19	*40475605*	*40480777*	*Sorbs1*
chr11	*62086200*	*62088541*	*Specc1*
chr3	*37640809*	*37643761*	*Spry1*
chr3	*37652795*	*37655264*	*Spry1*
chr19	*34191202*	*34201206*	*Stambpl1*
chr5	*151106388*	*151118943*	*Stard13*
chr5	*151250630*	*151253285*	*Stard13*
chr5	*151172117*	*151176574*	*Stard13*
chr5	*151134974*	*151137419*	*Stard13*
chr14	*69088219*	*69089958*	*Stc1*
chr10	*128668615*	*128669598*	*Suox*
chr7	*51966062*	*51974095*	*Svip*
chr7	*51964010*	*51965613*	*Svip*
chr2	*92943659*	*92950001*	*Syt13*
chr2	*92843123*	*92846981*	*Syt13*
chr18	*69414247*	*69419836*	*Tcf4*
chr18	*69516391*	*69525239*	*Tcf4*
chr18	*69672659*	*69676309*	*Tcf4*
chr18	*69589811*	*69600962*	*Tcf4*
chr18	*69399156*	*69404079*	*Tcf4*
chr18	*69662588*	*69668643*	*Tcf4*
chr18	*69631387*	*69633824*	*Tcf4*
chr18	*69500184*	*69502876*	*Tcf4*

chr18	*69604567*	*69616454*	*Tcf4*
chr18	*69343310*	*69353580*	*Tcf4*
chr18	*69572761*	*69577915*	*Tcf4*
chr18	*69640936*	*69647362*	*Tcf4*
chr18	*69639040*	*69640834*	*Tcf4*
chr11	*52272638*	*52274153*	*Tcf7*
chr5	*72846758*	*72858931*	*Tec*
chr6	*17105780*	*17112857*	*Tes*
chr6	*17113983*	*17116244*	*Tes*
chr6	*17070508*	*17076502*	*Tes*
chr6	*17080601*	*17084083*	*Tes*
chr1	*186693688*	*186706982*	*Tgfb2*
chr1	*186681043*	*186684357*	*Tgfb2*
chr1	*186673519*	*186677625*	*Tgfb2*
chr12	*86006400*	*86018020*	*Tgfb3*
chr12	*86019906*	*86029352*	*Tgfb3*
chr12	*86073239*	*86110951*	*Tgfb3*
chr9	*60023161*	*60025209*	*Thsd4*
chr9	*60053978*	*60065926*	*Thsd4*
chr9	*60202680*	*60211801*	*Thsd4*
chr9	*60101870*	*60111263*	*Thsd4*
chr9	*60075282*	*60077372*	*Thsd4*
chr9	*60350997*	*60355627*	*Thsd4*
chr9	*60078782*	*60085281*	*Thsd4*
chr9	*60452966*	*60455278*	*Thsd4*
chr10	*86293345*	*86312367*	*Timp3*
chr10	*86312685*	*86317524*	*Timp3*
chr10	*86326935*	*86342285*	*Timp3*
chr3	*65468019*	*65469851*	*Tiparp*
chr11	*90023864*	*90032394*	*Tmem100*
chr10	*68704301*	*68708447*	*Tmem26*
chr10	*68863255*	*68866375*	*Tmem26*
chr10	*68881261*	*68882748*	*Tmem26*
chr10	*68895967*	*68898764*	*Tmem26*
chr10	*68700722*	*68702470*	*Tmem26*
chr10	*68908911*	*68909873*	*Tmem26*
chr2	*52041982*	*52043499*	*Tnfaip6*
chr14	*61063126*	*61064957*	*Tnfrsf19*
chr14	*61016857*	*61017769*	*Tnfrsf19*
chr15	*33701193*	*33703672*	*Tspyl5*
chr4	*43208601*	*43210240*	*Unc13b*
chr5	*131164614*	*131167331*	*Wbscr17*
chr10	*121055036*	*121057430*	*Wif1*
chr3	*104992286*	*105006413*	*Wnt2b*
chr3	*104942295*	*104947499*	*Wnt2b*
chr3	*104937621*	*104941330*	*Wnt2b*
chr3	*104955922*	*104957082*	*Wnt2b*
chr4	*54875569*	*54879939*	*Zfp462*
chr4	*55002799*	*55007139*	*Zfp462*

chr4	*54525076*	*54528318*	*Zfp462*
chr4	*54963325*	*54968481*	*Zfp462*
chr4	*54975585*	*54982060*	*Zfp462*
chr14	*21981210*	*21996080*	*Zfp503*
chr6	*58846372*	*58848194*	*Herc3*
chr4	*100100523*	*100102032*	*Ror1*
chrX	*135983637*	*135984866*	*Arxes2*
chr5	*4916449*	*4918375*	*Fzd1*
chr12	*99293691*	*99299606*	*Foxn3*
chr10	*110058676*	*110059329*	*Nav3*
chr9	*22951881*	*22954208*	*Bmper*
chr13	*63562745*	*63569125*	*Ptch1*
chr5	*138986891*	*138997845*	*Pdgfa*
chr11	*108946319*	*108949690*	*Axin2*
chr11	*101804337*	*101809127*	*Etv4*
chr9	*23123854*	*23125178*	*Bmper*
chr9	*23338245*	*23349356*	*Bmper*
chr12	*85184799*	*85187278*	*Pgf*
chr5	*72807604*	*72810767*	*Tec*
chr3	*51073317*	*51075237*	*Noct*
chr15	*32328736*	*32330052*	*Sema5a*
chr1	*89205119*	*89207204*	*Sh3bp4*
chr11	*90080223*	*90081585*	*Tmem100*
chr2	*173278632*	*173284206*	*Pmepa1*
chr18	*69745331*	*69747560*	*Tcf4*
chr6	*17051799*	*17052677*	*Tes*
chr17	*79306731*	*79307729*	*Cdc42ep3*
chr1	*62621030*	*62623298*	*Nrp2*
chr16	*57499187*	*57501839*	*Filip1l*
chr12	*99224557*	*99228089*	*Foxn3*
chr13	*38786295*	*38787840*	*Eef1e1*
chr15	*7836697*	*7843604*	*Gdnf*
chr9	*60457305*	*60462095*	*Thsd4*
chr12	*34286284*	*34288298*	*Hdac9*
chr4	*54601210*	*54603294*	*Zfp462*
chr18	*63415018*	*63419118*	*Piezo2*
chr1	*62735592*	*62737533*	*Nrp2*
chr10	*24373314*	*24374255*	*Moxd1*
chr9	*23058554*	*23060095*	*Bmper*
chr13	*63550565*	*63554013*	*Ptch1*
chr3	*80047961*	*80049022*	*Fam198b*
chr17	*29446649*	*29450452*	*Pim1*
chr9	*60118271*	*60122731*	*Thsd4*
chr7	*114760606*	*114761671*	*Insc*
chr10	*111514780*	*111518832*	*Phlda1*
chr4	*81062108*	*81063336*	*Lurap1l*
chr1	*89134682*	*89136560*	*Sh3bp4*
chr2	*102758699*	*102761863*	*Slc1a2*
chr2	*12324002*	*12328269*	*Itga8*

chr19	*32328394*	*32329458*	*Sgms1*
chr1	*62678342*	*62680109*	*Nrp2*
chr8	*31110830*	*31114079*	*Rnf122*

Chapter 5

WNT16 Regulates the Expression of Canonical and Non-canonical WNT Targets in Osteoblasts

5.1 Introduction

Osteoporosis is a disease that affects millions of people worldwide, causing more than 9 million fractures annually [348]. Osteoporosis results from the imbalance in bone remodeling. Most current therapies for osteoporosis work by slowing down bone resorption, but the development of therapeutics that can also promote bone formation *de novo* would be of greater use in treating this condition [349], and would particularly help those who have lost a lot of bone mass. WNT signaling induces osteoblast-mediated bone formation and suppresses bone resorption by osteoclasts. Modulating WNT signaling pathway is emerging as a promising strategy in treating bone related diseases including osteoporosis [309, 350].

WNT16 is major WNT ligand involved in the regulation of postnatal bone homeostasis. Genome-wide association studies have identified WNT16 as a key gene associated with low bone mineral density, cortical thickness and fracture risk [88, 89, 351, 352]. WNT16 delivered in liposomes prevented inflammation induced bone loss [90]. Global deletion of *Wnt16* in mice resulted in spontaneous fractures as a result of decreased cortical thickness and high cortical porosity; however, the trabecular bone parameters were not significantly affected [90]. Consistent with these findings *Wnt16* was found to be highly expressed in the cortical bone compared to trabecular bone [90]. Inactivation of *Wnt16* in the osteoblast-lineage also resulted in lower cortical thickness, higher cortical porosity and spontaneous fractures at cortical bone sites. In contrast, the trabecular bone was unaffected [90]. However, transgenic mice overexpressing human *WNT16* in osteoblasts exhibited a significant increase in both cortical and trabecular bone mass [91], suggesting that WNT16 is sufficient to promote both cortical and trabecular bone mass, but its function is regionally restricted by its specific expression pattern.

The mechanism by which WNT16 regulates bone metabolism is not yet fully understood. Movérare-Skrtic *et al.* showed that the reduced cortical thickness observed in *Wnt16*$^{-/-}$ mice was a result of increased bone resorption [90]. WNT16 inhibited osteoclastogenesis both directly by acting on osteoclast progenitors and indirectly by increasing OPG expression in osteoblasts [90], suggesting WNT16 is a key negative regulator of osteoclastogenesis. Wergedal *et al.* showed that periosteal bone formation was reduced in the *Wnt16*$^{-/-}$ mice, suggesting that WNT16 may also have an anabolic role in bone. Jiang *et al.* showed that WNT16 is involved in intramembranous ossification [226]. These studies together suggest that WNT16 regulates bone formation and bone resorption and that this molecule might be targeted for therapeutic interventions to treat osteoporosis.

WNT ligands activate the β-catenin dependent canonical signaling pathway or β-catenin independent non-canonical pathways to regulate bone metabolism [10]. A

number of studies have suggested that WNT16 perform its functions by signaling through non-canonical pathways and that it does not activate canonical WNT signaling [353-355]. Few other studies have shown that WNT16 has the ability to signal through the canonical WNT cascade as well [226]. Movérare-Skrtic *et al.* showed that WNT16 signals through the canonical pathway and non-canonical JNK pathway in osteoblasts [90]. However, the effect of WNT16 on canonical WNT signaling activation in osteoblasts was milder than the effect of the classical canonical WNT ligand, WNT3A.

To effectively target WNT16 signaling to treat osteoporosis it is important to understand the mechanism by which WNT16 regulates bone metabolism. To understand the molecular mechanism by which WNT16 regulates osteoblastic gene expression and to identify target genes regulated by WNT16 in osteoblasts, we treated mouse calvarial osteoblasts with recombinant WNT16 and profiled the gene expression changes with RNA-seq. This study identified 603 genes regulated by WNT16. We also compared gene expression profiles of WNT16 treated osteoblasts to gene expression profiles of canonical WNT3A and non-canonical WNT5A treated osteoblasts. This analysis showed that a large number of WNT16 targets overlap with both WNT3A and WNT5A targets, suggesting that WNT16 activates both canonical and non-canonical WNT targets in osteoblasts.

5.2 Methods

5.2.1 Osteoblast isolation and culture

Osteoblasts were isolated from calvaria of neonates (4-5 days old) by serial digestion in Collagenase 1 and EDTA solutions. Osteoblast enriched fractions were centrifuged, washed with PBS, plated in 12 well plates at $2.6x10^5$ cells/well and cultured for 24 hours as described in Chapter 3. After 24 hours the media was changed to remove digestion debris and non-viable cells and these cultures were treated with 400ng/µl of recombinant WNT5A (R&D systems) or 800ng/µl of recombinant WNT16 (R&D systems).

5.2.2 Quantitative Real-time PCR (qRT-PCR)

Total RNA was purified using RNeasy Mini Kit (QIAGEN) according to manufacturer's protocol. Superscript III First-Strand Synthesis System (Invitrogen) was used with oligodT primers for reverse transcription according to manufacturer's protocol. Real time quantitative PCR was then performed with SYBR Select Master Mix (Applied Biosystems) using a Applied Biosystems 7900HT Fast Real-Time PCR System with the following cycling conditions: 50°C for 2 min for SYBR then 95 °C for 3 min (2 min for SYBR), followed by 40 cycles of 95 °C for 3 s (10 s for SYBR) and 30 s at 60 °C. Data was normalized to Gapdh and fold changes were calculated using the comparative Ct method [311]. Three independent replicates were analyzed per condition. Primers used for qRT-PCR are given in Table 5.1.

5.2.3 RNA-isolation and sequencing

Total RNA was purified using RNeasy Mini Kit (QIAGEN) according to manufacturer's protocol. RNA integrity was assessed using Bioanalyzer (Agilent). Poly(A)+-enriched cDNA libraries were generated using the Illumina TruSeq Sample

Preparation kit (Illumina) and checked for quality and quantity using Bioanalyzer. RNA-seq libraries were sequenced in NextSeq 550 sequencer (Illumina).

5.2.4 RNA-seq data analysis

RNA-seq data was analyzed as described in Chapter 3. Briefly, data quality was checked using FastQC (version 0.11.5) software. Sequence reads were aligned to the mouse reference genome (mm10) using TopHat (version 2.0.11) [245,251]. After read mapping, 'featureCounts' from Rsubread package (version 1.22.2) [257] was used to perform summarization of reads mapped to RefSeq genes and to generate gene-wise read counts. After generating read counts, low expressed genes were filtered from downstream analysis and genes with CPM value ≥ 2 in at least two libraries were retained. Subsequently, 'upper quartile' normalization was performed using the calcNormFactors function in edgeR (version 3.14.0) [261]. Differentially expressed genes were identified using 'limma' (version 3.28.12) after 'voom' [263] normalization. Genes with FDR [272] adjusted *p*-value <0.05 and fold change ≥ 1.5 were considered as significantly differentially expressed genes.

We also analyzed a published RNA-seq dataset profiling gene expression changes during differentiation of early pre-osteoblasts to mature osteoblasts as described in Chapter 3 [312] and used this data to assess how the expression of WNT16 targets change during osteoblast differentiation. Heatmaps were generated using heatmap.2 function in gplots (version 2.11.0) R package.

5.2.5 Functional Annotation

The functional analysis of differentially expressed genes was performed using functional annotation tool DAVID (version 6.8) [313]. Ontology [279] terms with *p*-value less than 0.01 were considered as significant.

5.2.6 Transcription factor binding motif enrichment analysis

Enriched transcription factor binding motif analysis was conducted using HOMER (version 4.7.2) [286]. Promoters of WNT target genes were analyzed using HOMER and enriched transcription factor binding motifs were identified (*p*-value < 0.001).

5.3 Results

5.3.1 Identification of canonical and non-canonical WNT targets in osteoblasts

WNT3A preferentially activates canonical signaling pathway whereas WNT5A activates non-canonical signaling pathways. Canonical WNT targets were identified by treating osteoblasts with recombinant WNT3A and measuring gene expression changes using RNA-seq. WNT3A up-regulated 278 genes and down-regulated 510 genes in osteoblasts. The results are discussed in detail in Chapter 3.

To identify non-canonical WNT targets, osteoblasts were treated with recombinant WNT5A and gene expression changes were quantified using RNA-seq. By comparing WNT5A treated osteoblasts to sham treated osteoblasts we identified 47 up-regulated genes and 84 down-regulated genes in WNT5A treated osteoblasts (Table 5.2).

Subsequently, a gene ontology analysis of WNT5A targets was performed using DAVID and the ontology analysis showed that genes up-regulated by WNT5A were associated with biological processes such as '*immune response*', '*cytokine-mediated signaling pathway*' and '*positive regulation of osteoclast development*'. Genes down-regulated by WNT5A were associated with '*muscle contraction*', '*positive regulation of cell-substrate adhesion*', '*extracellular matrix organization*', '*response to hypoxia*' and '*cellular calcium ion homeostasis*'. '*Positive regulation of osteoclast development*' was one of the significantly enriched gene ontology term associated with genes up-regulated by WNT5A. Previous studies have shown that osteoblast lineage specific deletion of *Wnt5a* using *Osx1-Cre* resulted in impaired bone formation and decreased osteoclastogenesis, suggesting that WNT5A plays a crucial role in osteoclastogenesis [69].

Next, we investigated the overlap between WNT5A targets and WNT3A targets identified in Chapter 3. Both WNT3A and WNT5A up-regulated the expression of four genes (*Prg4*, *Aqp5*, *Kcnj15* and *Cxcl14)* and down-regulated six genes including *Mybpc1*, *Egfl6*, *Col22a1*, *Adamts18*, *Cmya5* and *Lcn2*. Twenty one genes up-regulated by WNT3A (*Atp1a2*, *Nkd1*, *Tcf7*, *Pgf*, *Igfbp2*, *Nog*, *Tnfrsf19*, *Axin2*, *Ndnf* etc.) were down-regulated in response to WNT5A treatment. Twelve genes down-regulated by WNT3A including *Mmp13*, *Vdr*, *Ccl7*, *F13a1*, *Epas1*, *Gpx3* and *Gfra1* were up-regulated in WNT5A treated osteoblasts. Using qRT-PCR we validated the expression of three canonical WNT targets *Axin2*, *Igfbp2* and *Lef1* in WNT5A treated osteoblasts and confirmed that WNT5A down-regulated the expression of these genes (Figure 5.1).

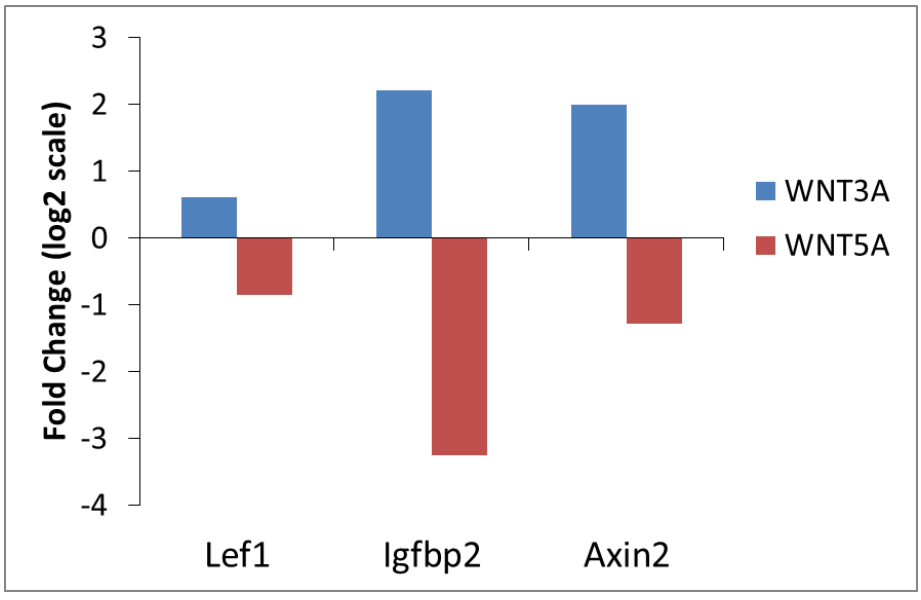

Figure 5.1: qRT-PCR validation of canonical WNT targets in WNT5A treated osteoblasts. *WNT5A down-regulated the expression of canonical WNT targets Lef1, Igfbp2 and Axin2. Fold changes relative to sham treated controls are given.*

5.3.2 Analysis of WNT16 regulated transcriptome in osteoblasts

Recombinant WNT16 up-regulated 180 genes and down-regulated 423 genes in osteoblasts (Table 5.2). We found that WNT16 up-regulated the expression of other WNT ligands *Wnt2b*, *Wnt7b* and *Wnt11* and several TGF-β/BMP signaling pathway members including *Bmp7*, *Tgfb2* and *Inhbb*. Previous studies have shown that TGF-β/BMP signaling also regulates bone formation and there exists a crosstalk between the TGF-β/BMP pathway and WNT signaling during osteoblast differentiation [356]. Our data suggests that WNT16 mediated up-regulation of TGF-β/BMP pathway genes may contribute to increased osteogenesis. Key genes down-regulated by WNT16 include '*Pparg*', the master regulator of adipogenesis [315], *Mef2c* transcription factor, a key negative regulator of bone metabolism [350] and, *Sfrp2*, a negative regulator of WNT signaling and bone metabolism. WN16 mediated down-regulation of these genes may also contribute to an increase in bone formation.

Next, we performed a gene ontology analysis of WNT16 targets using DAVID ontology analysis software and identified '*Regulation of cell proliferation*', '*Immune response*', '*Extracellular matrix organization*', '*Positive regulation of cell differentiation*' and '*Cell adhesion*' as some of the most significantly enriched biological processes associated with up-regulated genes. For down-regulated genes, '*Muscle contraction*', '*Immune system process*', '*Positive regulation of osteoblast differentiation*', '*Ossification*', and '*Bone mineralization*' were identified as some of the most significantly enriched biological processes (Figure 5.2).

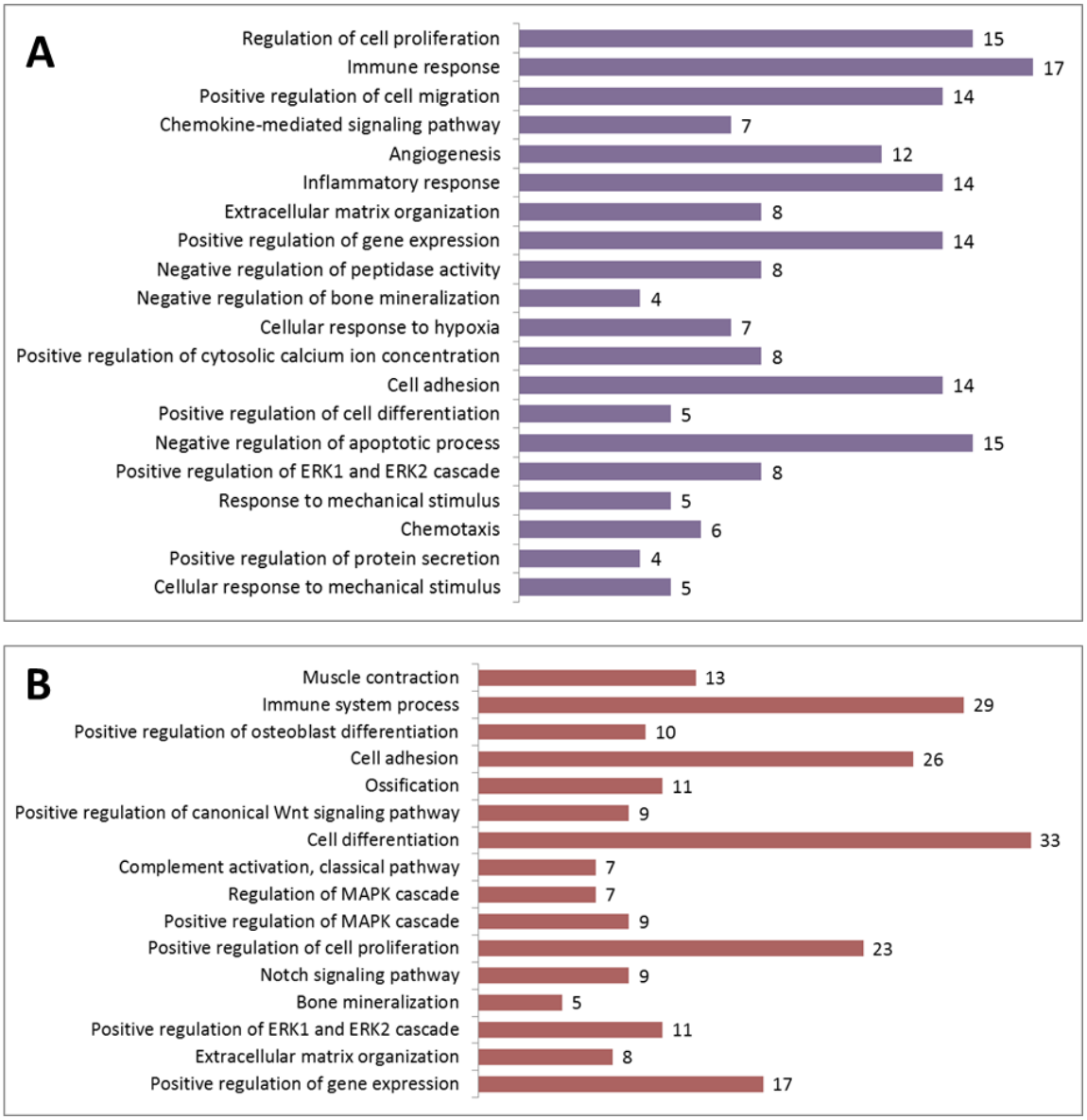

Figure 5.2: Enriched GO terms associated with WNT16 targets*. Enriched biological processes associated with up (**A**) and down-regulated genes (**B**). Number of genes associated with each category is also shown. Ontology analysis was performed using DAVID. Ontology terms with p-value <0.01 were considered as significant. Categories are arranged in the order of increasing p-values (from top to bottom).*

Gene ontology analysis suggested that WNT16 promotes cell proliferation and inhibits ossification. To further understand the role of WNT16 targets during osteogenic differentiation, we studied the expression of patterns of WNT16 targets during differentiations of early pre-osteoblasts to mature osteoblasts. Our study showed that a large number of genes up-regulated by WNT16 are highly expressed during early stages of osteoblast differentiation, when cell proliferation happens. We also found that the majority of the genes down-regulated by WNT16 are highly expressed during osteoblast

maturation/mineralization. This suggests that, similar to WNT3A, WNT16 may also promote early stages of osteogenesis and inhibit osteoblast maturation and mineralization (Figure 5.3 and Table 5.3).

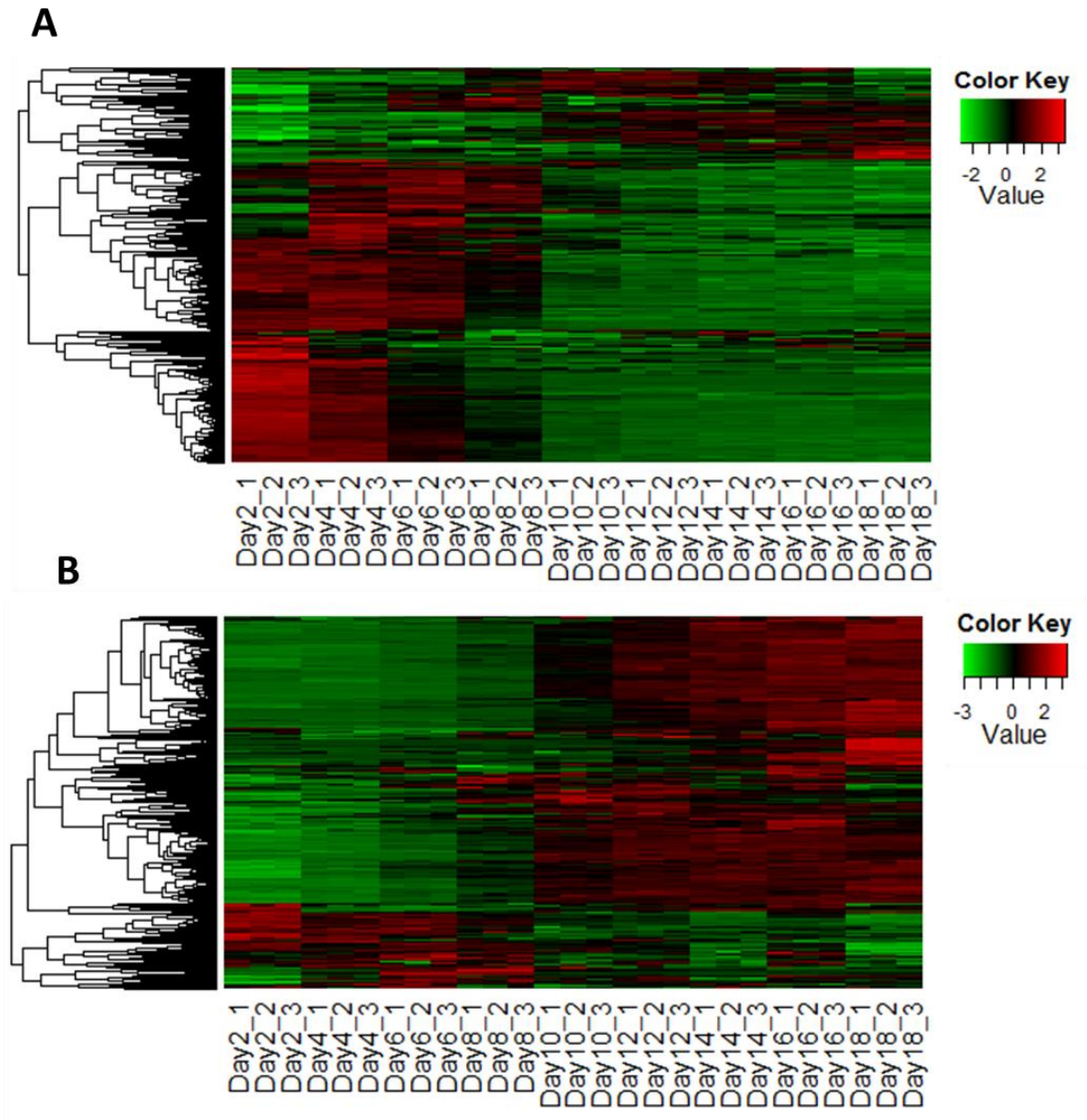

Figure 5.3: Expression profiles of WNT16 targets during the differentiation of pre-osteoblast to mature osteoblasts (Day 2 to Day 18). *Expression levels of WNT16 targets at different stages of osteoblast differentiation were determined using a public dataset as described in Section 3.2.6. Genes were clustered using hierarchical clustering and heatmaps were generated using gplots 2.11.* ***A****) Expression profiles of genes up-regulated by WNT16 in WT osteoblasts. A large number of genes up-regulated by WNT16 are highly expressed in early stage osteoblasts.* ***B****) Expression profiles of genes down-*

regulated by WNT16 in osteoblasts. Majority of the genes down-regulated by WNT16 are highly expressed in late stage osteoblasts.

5.3.3 WNT16 regulates canonical and non-canonical targets

Next, we evaluated the overlap between WNT16 targets and canonical WNT3A and non-canonical WNT5A targets. 37% (225/603) of the WNT16 targets overlapped with WNT3A targets and 14% (86/603) of the WNT16 targets overlapped with WNT5A targets. Only 10 WNT16 targets overlapped with both WNT3A and WNT5A targets (Figure 5.4). This suggests that WNT16 activates both canonical WNT3A and non-canonical WNT5A targets in osteoblasts.

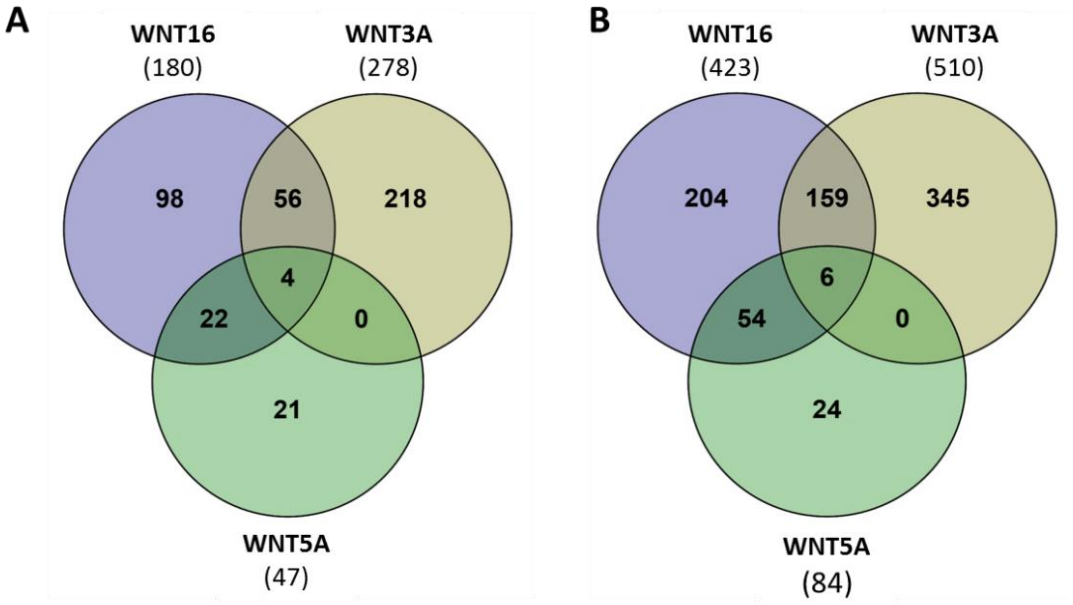

***Figure 5.4: Venn diagrams of genes differentially expressed in WNT16, WNT3A and WNT5A treated osteoblasts compared to sham-treated osteoblasts**. **A)** Overlap between up-regulated genes. **B)** Overlap between down-regulated genes.*

Subsequently, we analyzed promoters of genes activated by WNT16 to identify enriched transcription factor binding motifs. Interestingly, SMAD2, AP-1 and SMAD4 motifs were identified as the three most significantly enriched binding motifs. More than 90% of the WNT16 activated genes had SMAD binding sites in their promoter region and 58% had AP-1 binding sites. We also mapped TCF/LEF binding sites identified in Chapter 4 to WNT16 targets and found that 92 (51%) genes activated by WNT16 had TCF/LEF peaks in their promoters. The TGF-β/BMP signaling pathway activates SMAD transcription factors. This data suggests that SMADs may play a role in regulating the expression of at least some of the genes identified in this study.

5.4 Discussion

Studies have shown that targeting the WNT pathway is an effective strategy in treating osteoporosis as WNT signaling has the ability to promote bone formation and inhibit bone resorption [350]. WNT16 is a WNT ligand with both anabolic and anti-resorptive functions in bone. Therefore, identifying the target genes regulated by WNT16 and understanding the mechanism by which WNT16 regulates bone metabolism is of great importance.

In this study, we identified 603 genes regulated by WNT16 in osteoblasts. A large number of studies have suggested that WNT16 preferentially activates non-canonical WNT signaling to perform its functions. However, we found that WNT16 up-regulated canonical WNT targets such as *Axin2* and *Igfbp2* whereas non-canonical WNT5A down-regulated these genes. We also found that a large number of WNT16 targets overlap with canonical WNT3A targets and non-canonical WNT5A targets, suggesting that WNT16 activated canonical and non-canonical WNT signaling in osteoblasts.

More than 60% of the WNT16 targets identified in this study did not overlap with WNT3A targets. However, similar to WNT3A, a large number of genes up-regulated by WNT16 are highly expressed during early stages of osteoblast differentiation and the majority of genes down-regulated by WNT16 are highly expressed during osteoblast maturation and mineralization. This suggests that, like WNT3A, WNT16 may also promote osteoblast proliferation and inhibit maturation/ mineralization. This is consistent with the findings by Jiang *et al.* [226]. They found that MC3T3 cells transfected with an adenovirus containing WNT16 showed the formation of less mineralized nodules compared to control cells and canonical WNT inhibitor DKK1 abrogated the suppression of mineralization by WNT16, suggesting that WNT16 is a negative regulator of osteoblast maturation/ mineralization.

In this study, we identified *Mef2c* transcription factor as a gene down-regulated by WNT16 in osteoblasts. Our lab has previously shown that MEF2C regulates the expression of WNT inhibitor *Sost* in bone and osteoblast-lineage specific deletion of *Mef2c* results in high bone mass [350,357]. Recently, we found that targeted deletion of *Mef2c* in osteoclasts also results in high bone mass (unpublished data). Genome-wide association studies have identified MEF2C as a candidate gene associated with BMD [358]. These studies together suggest that MEF2C plays a key role in regulating both anabolic and catabolic responses in bone. However, very little is known about transcriptional regulation of MEF2C in bone. Our data suggests that WNT16 is a negative regulator of *Mef2c* and down-regulation *Mef2c* may contribute to WNT16 mediated anabolic responses.

A transcription factor binding motif enrichment analysis identified SMAD binding motifs as the most significantly enriched motifs in the promoters of genes up-regulated by WNT16. We also identified AP-1 and TCF/LEF binding sites in >50% genes activated by WNT16. Previous studies have shown that there exists a cross-talk between TGF-β/BMP signaling pathway and WNT signaling in bone [356,359]. It has also been shown that SMADs and AP-1 transcription factors function synergistically to

regulate gene expression [360-362]. It is likely that at least some of the WNT16 targets described herein may be regulated by a complex interplay between transcription factors. Further studies are required to understand the precise role of AP-1, TCF/LEF and SMAD transcription factors in regulating WNT16 target genes.

In summary, our study suggests that WNT16 is a negative regulator of osteoblast maturation and mineralization and a positive regulator of early stages of osteogenesis and, WNT16 mediates these effects by activating both canonical and non-canonical pathways. We also identified WNT16 as a negative regulator of *Mef2c* in osteoblasts.

Table 5.1: List of qRT-PCR primers.

	Forward	**Reverse**
Axin2	ATGAGTAGCGCCGTGTTAGTG	GGGCATAGGTTTGGTGGACT
Igfbp2	CAGACGCTACGCTGCTATCC	CTCCCTCAGAGTGGTCGTCA
Lef1	ATCACCTACAGCGACGAGCAC	TGGACATGGAAGTGTCGCCTG

Table 5.2: Genes differentially expressed in WNT16 and WNT5A treated osteoblasts. *WNT3A targets that overlap with WNT16 or WNT5A targets are also given. Fold changes are given in log2 scale (log FC). All genes listed in the table have a false discovery rate (FDR) adjusted p-value <0.05.*

Gene	**WNT16 (log FC)**	**WNT3A (log FC)**	**WNT5A (log FC)**
Prg4	*1.82*	*0.81*	*1.48*
Cxcl14	*0.61*	*0.89*	*1.15*
Kcnj15	*1.34*	*0.65*	*1.01*
Aqp5	*1.73*	*2.08*	*0.88*
Axin2	*1.00*	*2.71*	*-1.24*
Col7a1	*2.17*	*1.68*	
Sema4f	*2.00*	*2.99*	
Ccbe1	*1.95*	*1.78*	
Gm12505	*1.69*	*1.59*	
Prss46	*1.68*	*1.51*	
Slitrk6	*1.60*	*1.38*	
Wnt2b	*1.48*	*0.62*	
Has2	*1.40*	*1.10*	
Ptgs2	*1.39*	*1.08*	
E030011O05Rik	*1.34*	*1.17*	
Dynap	*1.29*	*1.58*	
Moxd1	*1.27*	*0.91*	
Grik3	*1.20*	*2.06*	
Sfn	*1.15*	*1.26*	
Dio2	*1.14*	*1.96*	
Grem1	*1.14*	*1.88*	

Ankrd1	*1.13*	*0.98*	
Inhba	*1.08*	*0.73*	
Sfrp4	*1.06*	*0.61*	
Bmp7	*1.06*	*1.72*	
Ier3	*1.04*	*1.05*	
Lrrc15	*1.04*	*1.03*	
Slc16a3	*1.01*	*0.82*	
Tgfb2	*0.99*	*1.91*	
Eva1a	*0.97*	*1.61*	
Bmpr1b	*0.93*	*0.80*	
Ch25h	*0.90*	*0.76*	
Syn1	*0.88*	*0.96*	
Kcnj2	*0.87*	*1.68*	
Errfi1	*0.86*	*0.98*	
Arl4c	*0.85*	*1.38*	
Timp3	*0.85*	*1.53*	
Wdr92	*0.82*	*0.60*	
Smim3	*0.82*	*0.87*	
Fhod3	*0.82*	*1.39*	
Lif	*0.79*	*1.23*	
Lrrc32	*0.79*	*0.88*	
Ngf	*0.78*	*1.35*	
Serpine1	*0.77*	*0.83*	
Hck	*0.77*	*1.15*	
Cnn1	*0.77*	*1.26*	
Tpd52	*0.74*	*0.63*	
Tec	*0.72*	*1.13*	
Slc20a1	*0.72*	*1.10*	
Vgf	*0.70*	*0.62*	
Rgcc	*0.70*	*1.49*	
Syt13	*0.70*	*2.05*	
Hhip	*0.69*	*2.03*	
Elfn1	*0.69*	*0.77*	
Gdnf	*0.67*	*0.66*	
Tnfaip6	*0.66*	*0.69*	
Nav3	*0.65*	*0.69*	
Pxylp1	*0.63*	*0.63*	
Inhbb	*0.59*	*1.87*	
Filip1l	*0.59*	*0.92*	
Il6	*1.71*		*1.73*
Gzme	*1.08*		*1.56*
Aspg	*0.90*	*-1.10*	*1.50*
Bdkrb1	*1.86*		*1.34*
Bdkrb2	*1.45*		*1.15*
Il20ra	*2.08*		*1.12*
Tnfsf11	*1.41*		*1.07*
Pcsk5	*1.37*		*1.06*
Cxcl1	*1.05*		*1.05*
Socs3	*0.89*		*1.01*

Spon1	*1.30*		*0.98*
Il4ra	*0.98*		*0.97*
Csgalnact1	*1.09*		*0.92*
Igfbp5	*1.31*		*0.87*
Tgfbi	*0.84*		*0.85*
Ptger4	*0.70*		*0.83*
Kcne4	*0.99*		*0.79*
Mmp3	*1.32*		*0.75*
F13a1	*1.23*	*-0.73*	*0.75*
Fgl2	*1.59*		*0.75*
Crabp2	*1.26*		*0.70*
Bcl3	*0.75*		*0.69*
Arg1	*2.96*		
Gm1045	*2.30*		
Adamts16	*2.14*		
Ctsw	*2.12*		
Cntn2	*2.11*		
Il11	*2.03*		
Acsbg1	*1.89*		
Cxcr6	*1.74*		
Lamb3	*1.71*		
Cxcl3	*1.54*		
Lamc3	*1.52*		
Pla1a	*1.46*		
Olfr1033	*1.43*		
Gjb3	*1.37*		
C1qtnf3	*1.33*		
Abcb1a	*1.26*		
Fcgr2b	*1.24*		
Enpp1	*1.24*		
Ccl6	*1.23*		
Lgr6	*1.23*		
Crct1	*1.20*		
Tfpi2	*1.19*		
Amer2	*1.17*		
Col5a3	*1.10*	*-0.92*	
Il1rl1	*1.09*		
1810011O10Rik	*1.07*		
Clec4n	*1.07*		
Chst11	*1.05*		
Vwa1	*1.05*		
Serpinb2	*1.04*		
Edn1	*1.03*		
Serinc2	*1.00*		
Lrrc4c	*1.00*		
Mfi2	*0.99*	*-1.87*	
Ccr1	*0.98*		
Tac1	*0.98*		
Parm1	*0.97*		

Xcr1	*0.96*		
Slc12a1	*0.87*		
Sema7a	*0.87*		
Anxa8	*0.86*		
Ppbp	*0.86*		
Slco4a1	*0.84*		
Procr	*0.84*		
Gldn	*0.83*		
Vegfc	*0.82*		
Wnt11	*0.81*		
Gja5	*0.81*		
Spock3	*0.81*		
Cacnb2	*0.78*		
Junb	*0.76*		
Wnt7b	*0.75*		
Nt5e	*0.75*		
Ano1	*0.75*		
Angpt4	*0.74*		
Ltbp2	*0.73*		
Slc16a2	*0.72*		
Ccl9	*0.72*		
Fstl3	*0.72*		
Itga5	*0.71*		
Tfr2	*0.71*		
Gng11	*0.71*		
Gem	*0.70*		
Atp8b4	*0.70*		
Hspb1	*0.69*		
Pkp2	*0.68*		
Ptgs2os	*0.67*		
Gcnt2	*0.67*		
Plod2	*0.67*		
Rnf19b	*0.67*		
Bhlhe40	*0.66*		
Crlf1	*0.66*		
Rasl11a	*0.66*		
Hk2	*0.66*		
Timp1	*0.66*		
Tmem243	*0.65*		
Has1	*0.64*		
Zbtb38	*0.64*		
Srpx2	*0.64*		
Gfpt2	*0.64*		
Bag2	*0.63*		
Klhl30	*0.63*		
Crem	*0.63*		
Ptk2b	*0.63*		
Nfatc2	*0.62*		
Sorcs2	*0.62*		

Medag	*0.62*		
Mcpt8	*0.62*		
Dyrk3	*0.61*		
Nav1	*0.61*		
Acan	*0.61*		
Sacs	*0.61*		
Stk26	*0.60*		
Pstpip1	*0.60*		
Slc2a1	*0.59*		
Apol9b	*0.59*		
Sgk1	*0.59*		
Hif1a	*0.59*		
Herc3		*1.57*	*-0.60*
Cdc42ep3		*1.00*	*-0.62*
Nkd1		*1.11*	*-0.63*
Tcf7		*1.20*	*-0.63*
Rapgef3	*-0.63*	*0.62*	*-0.64*
Pgf		*0.88*	*-0.65*
Itga8		*1.38*	*-0.67*
Nrcam		*0.98*	*-0.69*
Igfbp2		*2.18*	*-0.75*
Tmem100		*2.29*	*-0.75*
Nog		*0.82*	*-0.76*
Apcdd1		*1.69*	*-0.77*
Nipal4		*0.89*	*-0.91*
Atp1a2	*-0.90*	*1.38*	*-0.91*
5430421F17Rik	*-0.92*	*1.01*	*-0.92*
Tnfrsf19		*1.59*	*-1.01*
Insc		*1.00*	*-1.12*
Col26a1	*-0.91*	*1.13*	*-1.15*
Ndnf		*2.78*	*-1.34*
Tnfsf15		*2.01*	*-1.47*
Fam65b	*-0.60*	*0.64*	
Fam180a	*-0.61*	*1.24*	
Bmp2	*-0.61*	*0.80*	
Sema3f	*-0.64*	*0.76*	
Thsd4	*-0.72*	*0.98*	
Crabp1	*-0.74*	*0.91*	
Scn3a	*-0.97*	*0.81*	
Aldh1a7	*-1.09*	*1.08*	
Dpt	*-1.11*	*0.72*	
Nov	*-1.66*	*1.07*	
Mmp13		*-1.53*	*1.26*
Cxcl5			*1.01*
Gpr88		*-1.13*	*0.96*
Ptgfr		*-1.13*	*0.91*
Scn7a			*0.90*
Il13ra1			*0.85*
Xdh			*0.85*

Stac2			*0.82*
Vdr		*-0.77*	*0.81*
Ccl7		*-0.66*	*0.77*
1810041L15Rik		*-0.96*	*0.76*
Slc9b2			*0.75*
Epas1		*-0.92*	*0.72*
Crocc2			*0.71*
Gpx3		*-1.30*	*0.71*
Hpgd	*-0.63*	*-1.19*	*0.70*
Gfra1		*-1.40*	*0.68*
Nfkbiz			*0.65*
Gm10080			*0.64*
Pde4b			*0.64*
Cebpd			*0.61*
Npnt	*-1.00*		*-0.61*
Cryab			*-0.63*
Omd	*-1.16*		*-0.67*
Spta1	*-1.46*		*-0.70*
Ldb3			*-0.72*
Mybpc1	*-0.93*	*-1.00*	*-0.72*
Begain			*-0.72*
Egfl6	*-2.01*	*-1.61*	*-0.73*
Nptx1			*-0.74*
Myl1	*-1.14*		*-0.74*
Tspan18	*-0.72*		*-0.74*
Acta1	*-0.99*		*-0.75*
Itih5	*-0.70*		*-0.78*
Col22a1	*-0.96*	*-0.72*	*-0.78*
Myom1	*-0.89*		*-0.83*
Mylk4	*-1.18*		*-0.85*
Car2	*-0.64*		*-0.87*
Neb	*-0.90*		*-0.87*
Myh1	*-1.13*		*-0.88*
Ryr1	*-0.78*		*-0.91*
Actn3	*-1.23*		*-0.92*
Ankrd23	*-0.93*		*-0.92*
Asb2			*-0.92*
Adamts18	*-1.34*	*-1.20*	*-0.94*
Aldh1a1	*-1.74*		*-0.94*
Sh3bgr	*-0.60*		*-0.97*
Mb	*-1.30*		*-1.00*
Ttn	*-0.96*		*-1.01*
Prr5l	*-0.68*		*-1.02*
Obscn	*-0.92*		*-1.04*
S100a8	*-1.29*		*-1.05*
3110009E18Rik			*-1.10*
Tnnt3	*-1.45*		*-1.14*
Slc4a1			*-1.15*
Casq1	*-1.33*		*-1.18*

S100a9	*-1.32*		*-1.22*
Cmya5	*-1.31*	*-1.59*	*-1.23*
Tcap	*-1.69*		*-1.24*
Tnnc2	*-1.64*		*-1.27*
Ngp	*-0.93*		*-1.29*
Tnni2	*-1.60*		*-1.30*
Hba-a2	*-0.76*		*-1.31*
Smpd3	*-1.54*		*-1.34*
Lcn2	*-1.16*	*-1.53*	*-1.37*
Atp2a1	*-1.71*		*-1.38*
Ltf	*-1.18*		*-1.39*
Trdn	*-1.47*		*-1.41*
Myoz1	*-2.10*		*-1.42*
Hbb-bs	*-1.50*		*-1.44*
Ckm	*-1.98*		*-1.45*
Ckmt2	*-1.69*		*-1.46*
Alas2	*-0.90*		*-1.47*
Xirp2	*-1.49*		*-1.49*
Myot	*-1.49*		*-1.60*
Pygm	*-1.56*		*-1.61*
Eef1a2	*-2.01*		*-1.67*
Mybpc2	*-1.97*		*-1.71*
Myh2	*-2.34*		*-1.72*
Ibsp	*-1.66*		*-1.73*
Ampd1	*-2.16*		*-1.74*
Car3	*-1.89*		*-1.77*
Pvalb	*-2.01*		*-1.78*
Myh4	*-1.76*		*-1.82*
Phf19	*-0.59*		
Ptpn6	*-0.59*		
Synm	*-0.59*	*-1.43*	
Ablim1	*-0.59*		
Bcam	*-0.59*		
Ogn	*-0.59*		
Gbp7	*-0.59*	*-0.72*	
Hr	*-0.59*	*-0.92*	
Fam110b	*-0.60*		
Tmem204	*-0.60*		
AW551984	*-0.60*	*-0.78*	
Slc5a5	*-0.60*		
Mfsd6	*-0.60*		
Spi1	*-0.60*		
Klf4	*-0.60*		
Shank1	*-0.60*		
Cyth4	*-0.60*		
Stard8	*-0.60*		
Rnasel	*-0.60*	*-0.74*	
Hs3st3a1	*-0.61*	*-0.80*	
Rnf165	*-0.61*		

Klhdc8b	*-0.61*		
Gfra2	*-0.61*	*-0.96*	
1500009L16Rik	*-0.61*		
Hsd17b1	*-0.61*		
Ndst3	*-0.61*		
C1ra	*-0.61*	*-1.20*	
A230050P20Rik	*-0.61*		
Slc13a5	*-0.61*		
Il11ra1	*-0.61*	*-0.70*	
Tox	*-0.61*	*-0.68*	
Serpini1	*-0.61*		
Nid2	*-0.61*	*-0.68*	
Laptm5	*-0.61*		
Fgf10	*-0.62*		
Mylip	*-0.62*	*-0.75*	
Klf2	*-0.62*		
Paqr4	*-0.62*		
Vav1	*-0.62*		
Adrbk2	*-0.62*		
Zfp423	*-0.62*	*-1.01*	
Tdrkh	*-0.62*		
Rtn2	*-0.62*		
Lgr5	*-0.62*	*-0.93*	
Camk2a	*-0.62*		
Mmp28	*-0.62*		
Efnb1	*-0.63*		
Ptpn7	*-0.63*		
Mturn	*-0.63*		
Myod1	*-0.63*		
Hapln1	*-0.63*	*-0.90*	
Ddc	*-0.63*		
Enpp5	*-0.63*	*-0.86*	
Slc27a6	*-0.63*	*-0.65*	
Mgp	*-0.63*		
Nfam1	*-0.63*		
Ldb2	*-0.63*	*-0.60*	
Tmem51	*-0.63*		
Mboat1	*-0.64*		
Reps2	*-0.64*		
Scrn1	*-0.64*	*-0.92*	
Ankrd13d	*-0.64*		
Pcp4l1	*-0.64*	*-0.99*	
Grik5	*-0.64*		
Hcls1	*-0.64*		
Avil	*-0.64*		
Lonrf3	*-0.64*		
Pltp	*-0.65*		
Sepp1	*-0.65*	*-0.83*	
Ptchd4	*-0.65*		

Bche	*-0.65*	*-1.08*	
Cd36	*-0.65*		
Tmem106a	*-0.65*		
Sncaip	*-0.65*		
Trim21	*-0.65*	*-0.78*	
Tnfaip8l1	*-0.65*		
Fam160a1	*-0.65*	*-0.85*	
Glt28d2	*-0.65*		
Dlx5	*-0.66*	*-0.94*	
Bace2	*-0.66*		
Abcc3	*-0.66*		
Panx3	*-0.66*		
Itgb1bp2	*-0.66*		
Syne3	*-0.66*		
Trpv4	*-0.66*	*-0.79*	
Arhgef6	*-0.66*	*-0.61*	
Iqgap2	*-0.66*	*-0.97*	
Epha4	*-0.67*	*-0.81*	
Serpinb8	*-0.67*		
Cyb5r2	*-0.67*		
Ube2l6	*-0.67*	*-1.04*	
Adra1d	*-0.68*		
Mdk	*-0.68*		
Elmo1	*-0.68*	*-1.48*	
Angptl6	*-0.68*		
Thra	*-0.68*	*-0.59*	
Lonrf2	*-0.68*		
Scml2	*-0.68*		
Fam124a	*-0.68*	*-0.69*	
Khk	*-0.68*		
Prrg3	*-0.68*	*-0.67*	
Pgam2	*-0.68*		
Pdgfd	*-0.69*	*-1.13*	
Efnb3	*-0.69*		
Tmem88	*-0.69*		
Tlr13	*-0.69*		
Atp1b1	*-0.69*	*-0.97*	
Abca9	*-0.69*	*-1.06*	
Fzd5	*-0.69*	*-0.83*	
Dcn	*-0.69*	*-0.94*	
Cpq	*-0.69*		
Id4	*-0.69*	*-0.84*	
Clec11a	*-0.70*	*-0.98*	
Mamld1	*-0.70*	*-0.62*	
Soat2	*-0.70*		
Txlnb	*-0.70*		
Cpxm1	*-0.70*	*-0.95*	
Pik3ip1	*-0.70*	*-0.60*	
Tnfrsf14	*-0.70*		

Crispld1	*-0.70*	*-1.24*	
Naalad2	*-0.70*	*-0.92*	
Grip1	*-0.70*		
Kcnt2	*-0.70*		
Slfn5	*-0.71*	*-1.06*	
Kcnb1	*-0.71*		
Psmb8	*-0.71*	*-1.00*	
Fcer1g	*-0.71*		
Klhl41	*-0.72*		
Trim34a	*-0.72*	*-0.69*	
Capn5	*-0.72*		
Cd74	*-0.72*	*-1.02*	
Rassf2	*-0.72*	*-0.78*	
Emid1	*-0.72*		
4732491K20Rik	*-0.73*		
Coq8a	*-0.73*	*-0.61*	
Apod	*-0.73*	*-0.87*	
Parp14	*-0.73*	*-1.24*	
Tmem8	*-0.74*	*-1.07*	
Hey1	*-0.74*		
Atp1b2	*-0.74*		
Plcl1	*-0.74*		
Smyd1	*-0.74*		
Mfap2	*-0.74*		
Nfasc	*-0.74*	*-0.79*	
Calcrl	*-0.74*		
Gucy1b3	*-0.74*		
2700069I18Rik	*-0.74*		
Serpinb9	*-0.74*	*-0.95*	
Rdm1	*-0.75*		
Apobec1	*-0.75*		
D630003M21Rik	*-0.75*		
C1qa	*-0.75*		
Rab40b	*-0.76*		
Cpz	*-0.76*		
Cadm3	*-0.76*	*-0.96*	
Mtss1	*-0.76*		
Galnt5	*-0.76*	*-1.50*	
Dleu2	*-0.76*	*-0.75*	
Slc7a8	*-0.76*	*-0.61*	
Id1	*-0.76*		
Smarca1	*-0.77*	*-0.63*	
Meox2	*-0.77*	*-1.16*	
F2rl1	*-0.77*		
Erg	*-0.77*		
Prss16	*-0.77*		
Serpinb9b	*-0.78*		
Col8a2	*-0.78*	*-1.28*	
Gstm1	*-0.78*	*-0.66*	

Coro1a	*-0.78*		
Cmklr1	*-0.78*		
Dclk2	*-0.78*		
Agbl2	*-0.78*		
Prex2	*-0.79*		
Pcdhac2	*-0.79*		
Glt8d2	*-0.79*	*-1.32*	
Ifi204	*-0.79*	*-1.11*	
Slc1a6	*-0.79*		
Stk32c	*-0.79*		
Ntn3	*-0.80*		
Col15a1	*-0.80*		
Adm	*-0.80*		
Il31ra	*-0.80*		
Arc	*-0.80*		
Slc40a1	*-0.80*		
Lmod3	*-0.81*		
Gbp3	*-0.81*	*-1.24*	
1700020L24Rik	*-0.82*		
Srpx	*-0.82*		
Lgals9	*-0.82*	*-0.60*	
Il18	*-0.82*	*-0.78*	
Zcchc5	*-0.82*		
Prrt2	*-0.82*	*-0.69*	
Irgm2	*-0.82*	*-0.75*	
Ostn	*-0.83*	*-0.63*	
Col9a2	*-0.83*	*-1.46*	
Tcea3	*-0.83*	*-0.82*	
Ly6a	*-0.83*		
Mef2c	*-0.83*		
Ptgir	*-0.83*	*-1.13*	
Trim30d	*-0.83*		
Bst2	*-0.83*		
Ntrk3	*-0.83*		
Podn	*-0.84*	*-0.67*	
Aim1	*-0.84*	*-1.52*	
Mylpf	*-0.84*		
Gper1	*-0.84*		
Rhbdl1	*-0.84*		
Fabp3	*-0.84*		
Gramd2	*-0.84*		
Dock8	*-0.84*	*-1.23*	
Lbp	*-0.85*	*-1.61*	
Tbxa2r	*-0.85*	*-0.63*	
Rtn4rl1	*-0.85*		
Sorl1	*-0.86*	*-0.88*	
Smoc1	*-0.86*	*-2.15*	
Ntrk2	*-0.86*		
S100b	*-0.86*	*-1.19*	

Sybu	*-0.86*	*-0.81*	
Nrap	*-0.86*		
Ccdc3	*-0.86*		
Agtr1a	*-0.86*	*-0.90*	
Vstm4	*-0.87*		
Fabp4	*-0.87*		
Srsf12	*-0.87*	*-0.91*	
Acacb	*-0.87*		
Adam33	*-0.88*		
Fgf9	*-0.88*		
Uba7	*-0.88*	*-0.80*	
Cox6a2	*-0.88*		
Pdlim2	*-0.89*		
Rgs5	*-0.89*		
Lrrc75b	*-0.89*	*-1.08*	
Mme	*-0.89*	*-0.67*	
Ces2g	*-0.89*		
Chrdl1	*-0.90*	*-1.99*	
Gstt1	*-0.90*		
Cacng1	*-0.90*		
Diras2	*-0.91*	*-1.67*	
Fgfr2	*-0.91*		
Shisa2	*-0.91*		
Kcns1	*-0.91*	*-1.57*	
Aqp1	*-0.92*		
Adra1b	*-0.93*		
Hrc	*-0.93*		
Dock10	*-0.93*	*-0.68*	
Ptprv	*-0.93*	*-1.12*	
Sh3tc2	*-0.93*		
Dlg2	*-0.93*	*-0.79*	
C4b	*-0.94*	*-1.46*	
Npr3	*-0.94*	*-0.89*	
C1qb	*-0.94*		
Dio3	*-0.94*	*-2.20*	
Sparcl1	*-0.95*	*-1.29*	
Slc4a10	*-0.95*	*-1.06*	
C3	*-0.95*	*-1.56*	
Rnf144b	*-0.95*	*-0.59*	
Alpl	*-0.95*		
Pik3ap1	*-0.95*	*-0.63*	
Adam23	*-0.95*	*-1.49*	
Angptl1	*-0.95*		
1190005I06Rik	*-0.96*		
Camp	*-0.96*		
Serpinb6b	*-0.96*		
Il1rn	*-0.96*	*-0.98*	
S1pr3	*-0.97*	*-0.73*	
Spns2	*-0.97*	*-1.02*	

St3gal6	*-0.97*	*-1.02*	
Sh3rf3	*-0.97*		
Pcsk6	*-0.98*		
Cdkn1c	*-0.98*	*-1.51*	
Tgfa	*-0.98*		
Tmem35a	*-0.98*		
Myom2	*-0.99*		
Cygb	*-1.00*	*-1.26*	
Sned1	*-1.00*	*-1.80*	
Frem1	*-1.00*		
Pgm5	*-1.00*		
Ifih1	*-1.02*	*-0.87*	
Hfe2	*-1.03*		
Nrip2	*-1.04*		
Dhx58	*-1.04*	*-0.92*	
Xaf1	*-1.04*		
Unc45b	*-1.04*		
Sorbs2	*-1.04*	*-0.95*	
Dlk1	*-1.05*	*-0.71*	
C1qc	*-1.05*		
Serping1	*-1.07*	*-1.16*	
Mest	*-1.07*	*-0.94*	
Negr1	*-1.07*	*-1.38*	
Slc2a9	*-1.07*		
Mab21l3	*-1.08*		
Vit	*-1.08*	*-1.28*	
Rspo3	*-1.09*	*-2.40*	
Serpinb1a	*-1.09*	*-2.34*	
Rprm	*-1.09*		
Atp2a3	*-1.10*		
Ly6c1	*-1.10*		
Hgf	*-1.11*	*-2.79*	
Ggt5	*-1.11*	*-1.86*	
Rtp4	*-1.11*	*-0.73*	
Islr	*-1.12*	*-1.13*	
Epha5	*-1.14*	*-0.69*	
Angpt2	*-1.14*	*-0.86*	
Kcp	*-1.14*		
Ypel1	*-1.14*		
Olfml1	*-1.19*	*-1.43*	
Lect1	*-1.19*	*-2.86*	
Igtp	*-1.20*	*-0.94*	
Susd2	*-1.20*	*-0.97*	
1500015O10Rik	*-1.20*	*-0.98*	
Fmo1	*-1.21*	*-3.53*	
Palmd	*-1.23*	*-2.12*	
Kazald1	*-1.23*	*-1.13*	
Limch1	*-1.25*	*-1.20*	
Plekha4	*-1.27*	*-0.63*	

Spon2	*-1.27*		
Clca3a1	*-1.28*		
Chil3	*-1.28*		
Tmtc1	*-1.30*	*-1.47*	
Lpl	*-1.30*	*-1.07*	
Palm3	*-1.31*	*-1.29*	
Slfn8	*-1.32*	*-0.88*	
Pparg	*-1.36*	*-2.05*	
Pappa2	*-1.36*	*-0.90*	
Slc2a4	*-1.38*		
Mpo	*-1.39*		
Prelp	*-1.45*	*-0.86*	
Mylk2	*-1.49*		
Trim30a	*-1.50*	*-0.89*	
Cdsn	*-1.51*		
Abi3bp	*-1.57*	*-1.85*	
Gdf10	*-1.59*	*-1.54*	
Rcsd1	*-1.61*	*-0.93*	
Dner	*-1.61*	*-2.09*	
Sfrp2	*-1.63*	*-2.62*	
Gprin3	*-1.68*	*-3.03*	
Rspo2	*-1.71*	*-2.49*	
Slc26a7	*-1.73*		
Ackr4	*-1.75*		
Ifi44	*-1.75*	*-1.22*	
Agtr2	*-1.78*		
Shisa3	*-1.80*	*-1.00*	
Matn4	*-1.84*	*-2.38*	
Ucma	*-1.84*	*-4.58*	
Scara5	*-1.85*	*-2.71*	
Ifit3	*-1.87*		
Irf7	*-1.87*		
Prg2	*-1.88*		
Oasl2	*-1.94*		
Iigp1	*-1.97*		
Isg15	*-1.99*		
Ifit1	*-2.04*		

Table 5.3: Expression profiles of WNT16 targets during osteoblasts differentiation. *WNT16 targets showing high and low expression at early (day 2-day 6) and late stages (day 10-day 18) of osteoblast differentiation are shown. Gene expression was profiled during differentiation of early pre-osteoblasts to mature osteoblasts.*

Up-regulated genes with high expression at early stages				
Hyou1	Klhl11	Casc5	Tiam1	Ano1
Kif20b	Trip11	Bmper	Syt13	Wnt2b
Acaca	Ppp1r12b	Macf1	Dusp9	Cxcl14
Tpr	Syne1	Ier3	Slc25a30	Ptgs2os
Nupl1	Lrrk2	Slc16a3	Chd3	Fam132b
Senp5	Tfrc	Baz1a	Lrp8	Sacs
Rrp1b	Ftsj3	Zbed6	Ltbp1	Slc12a1
Eif3a	Tln2	Pla2g4a	Gan	Klhl30
Pdzd8	Ttc37	Pim1	Plat	Hbegf
Tpm1	Nhlrc3	Nexn	Tmem200a	Errfi1
Uba6	Sema3e	Tpd52	Adamts6	Fbn1
Diap3	Msn	Il6st	Gcnt4	Acan
Tmcc3	P4hb	Ncam1	Arl4c	Serinc2
Dna2	Bhlhe40	Bag2	Txnrd1	Il18rap
Exosc9	Chst11	Pgd	Skil	Ass1
Fancm	Aif1l	Adam12	Nes	Sema7a
Bpgm	Sh3rf1	Shroom4	Ptprb	Sync
Cep350	Arap2	Dpysl3	Zfp52	Grem1
Abl2	Herc1	Lox	Lpin3	Dynlt1b
Fosl2	Tubb5	Cit	Sh3bgrl2	Apol9b
Mina	Csrp1	Hells	Prkg2	Anxa8
Acsl4	Slc2a1	Tram2	Sgk1	Scn3a
Ranbp2	Pde4d	Dock5	Actg2	Pkp2
Tsr1	Ctps	Smim3	Chst2	Cnn1
Alkbh8	Clspn	Rictor	Tnfsf11	Slc20a1
Ddx3x	Lrig3	Plk2	Lrig1	Inhba
Mical2	Rbmx2	Ciapin1	Herc3	Tma7
Jun	Uhrf1bp1l	Ch25h	Spsb1	Tuba1c
Tbc1d1	Piga	Hsp90aa1	Csgalnact1	Grik3
Atm	Cdh3	Fstl3	D830031N03Rik	Lrp2
Adam19	Sdk1	Herc2	Gcnt2	Atp8b4
St3gal5	Utp20	Loxl3	Il4ra	Bmpr1b
Polr1b	Dyrk2	Tjp2	Zbtb38	Has2
Naa25	Hjurp	Tfr2	Fam198b	Enpp1
Usp34	Tiparp	Hk2	Inhbb	Rps15a-ps4
Actg1	Ddx21	Fbln2	Apex1	Serpine1
Gpr176	Ldlrad4	Mapk6	Cxadr	Lif
Eogt	Jade3	Lrrc8d	Il1rl2	Cdh10
Plcb4	Osbpl3	Wnt9a	Filip1l	Krt7

Slc4a7	Mtmr11	Socs3	Arsj	Il1rl1
Bdp1	Pmepa1	Csrnp1	Nqo1	Aqp5
Socs4	Nuak2	Nuak1	Ptar1	E030011O05Rik
Ammecr1	Wwc2	Plaur	Amer2	AI506816
Haus6	Wnk1	Map1b	Tes	Lrrc15
Smad7	Tjp1	Procr	Sulf1	Sema4f
Dhx9	Cep152	Adcy7	Ngf	Ankrd1
Kif21a	Ccne2	Pcdh19	Ltbp2	Gm1045
Rad54l2	Abcc1	Fzd6	Zfp462	Il11
Kri1	Thbs1	Dok1	Car12	Ptgs2
Cldn12	Glipr1	Zfp568	Nap1l2	Kcnj15
Slc38a1	Clcn5	Dst	Loxl2	Sfn
Ago3	Ptgs1	Mdn1	Fosl1	Col7a1
Uhmk1	Prepl	Igf2os	Loxl4	
Ahctf1	Lrrfip1	Tppp3	Ndufa8	
Up-regulated genes with low expression at early stages				
Pxdn	Brwd3	Galnt16	Nav3	Hmcn1
Zfp106	Adamts12	Cacna1c	Adamts15	Cth
Tspan11	Tgm2	Mfap1b	1810011O10Rik	Rgl1
Hmbox1	Wbscr17	Bnc2	Nt5e	Mcm9
Top1	Tgfb2	Adamts4	Hhip	Postn
Ash1l	Uprt	Nutf2	Lrrc17	Megf10
Nkiras2	Elk4	Mrps17	Igfbp5	Col6a3
Tet3	Tmem2	Arsi	4930539J05Rik	Axin2
Tbc1d16	Ermp1	Dnm3	Fgfbp1	Trim56
Ccdc80	Zfp382	Lsp1	Scube1	Tenm3
Pcdh7	Card10	Ccdc15	F13a1	Kcnj2
Itgb3	Kcne4	Crabp2	Cntn2	Medag
Itpr2	Ralgps1	Bmp7	Eln	Olfr1033
Foxp1	Plod2	Timp3	Pcsk5	Serpina3n
Rassf8	Lrch2	Dpep1	Moxd1	
Rest	Nav1	Tnfaip6	Adamts16	
Gm13498	Ccbe1	C1qtnf3	Spon1	
Down-regulated genes with high expression at late stages				
Cldn19	Slc7a8	Itgb3bp	Ccdc23	Lrp3
Lcn2	Smpdl3a	Angpt2	Grn	C1s1
S100a8	Mlip	Peli2	Creg1	Pnrc1
Tusc5	Rassf4	Comp	Ndufa4l2	Fth1
Matn1	Bri3	Sorbs2	Pelo	Fam102a
Dner	Lonrf3	Rnasel	Adamts2	Sesn1
Rspo2	Islr	Ramp2	Fam19a5	Nr2f1
Tnfsf12	Col15a1	Fbln7	Cuta	Gas1
Lyz1	Prkcb	Vegfb	Ndufb11	Grina
Smpd3	Mab21l2	Cpxm1	Pink1	Rras
1700096K18Rik	Npnt	Adrbk2	Tspan7	Cnpy2

AI607873	Smim1	Elmo1	Fzd8	Pigp
Matn4	Panx3	Prex2	Vstm4	Nrip2
Sfrp2	Cd36	Hcfc1r1	Abhd14b	Ptn
Fxyd1	Sparcl1	Srpx	Serf1	Podn
Pparg	Mamstr	Rab40b	Tcn2	Dzip1
Mia	Ang	Ptgis	Capn5	Smim19
Adh1	Cp	Pik3ip1	Smoc2	Cmtm3
Kazald1	Fabp3	Tcea3	Rnf167	Snhg18
P2rx6	Tmem8	Ptprv	Wbp1	Serf2
Lpl	Chn2	Cadm1	Ppfibp2	Eif3f
Gdf10	Sepp1	Cxcl12	Rnase4	Rnf130
Slpi	Aoc3	Gper1	Gm2a	Dnase1l1
Chrdl1	AA388235	Foxred2	Ifitm2	Ifi27
Mt1	Pou3f3	Pyroxd2	Coq10a	Fam20c
Klf15	Id3	Uap1l1	Sncaip	Jag1
Abi3bp	Bace2	Lrrc51	Fcgrt	Atraid
Slc25a45	Susd5	Epb4.1l4b	Ppp1r3b	Fam46a
Prelp	Lgals3	Tspan12	Appl2	Arhgef6
Fzd9	Prrg3	Tcf7l1	Ctsf	1110059G10Rik
Ibsp	Ypel1	Tbkbp1	B2m	Mxd4
Lcp1	Fam213a	Ostn	Pcgf2	Gstm5
Fam198a	Cxx1b	Cfh	C1ra	Mtss1l
Negr1	Pdlim2	1810026B05Rik	Fam26e	Serpine2
Atoh8	Gstt1	Gpm6b	Ptms	Itm2b
Serping1	Gamt	Gpr137b	1500012F01Rik	Thra
Alpl	Fmo1	Dcn	Csad	Tapbp
Lect1	Prrt2	Pgm5	Adamts9	Ggh
Omd	Rcsd1	Hvcn1	Nagpa	Il11ra1
Ms4a7	Trnp1	Copz2	Eny2	Iscu
Cd68	Scrn1	Mef2c	Tmem8b	Tcta
Gpnmb	Lrrc75b	Lgals9	Tmem150a	Map1lc3a
Mme	Diras2	Gnptg	Atp5sl	Gstm2
Id1	Vkorc1	Tmem42	Nudt16l1	Ctsa
Spns2	Bmp2	Dpp7	Pltp	Etfb
Spa17	Tmem107	Hexa	Mrps6	Glt8d1
1500015O10Rik	Cpz	Uba7	Amdhd2	Dirc2
Tle2	Qpct	2410006H16Rik	Tmem246	
Down-regulated genes with low expression at late stages				
Mir703	Gnb2l1	Irf9	Lamp1	Tomm6
Ly6c1	Slc9a3r1	Atf5	Chchd7	Slc13a5
Klf2	Tmem179b	Rps29	Lyrm4	Emilin2
Fabp5	Dcxr	Krtcap2	Rplp1	Pla2r1
Rps5	0610012G03Rik	Ppcdc	Bola3	Ndufa3
Dhx58	Prickle3	Rps19	Trappc2l	Cstb
Fam124a	Crip2	Mgmt	Slc36a1	Cox8a

Ifi204	Rsrp1	Atp5e	Galk2	Tbca
Uxt	Ly6a	Lxn	Rpl38	Ndufb2
Bst2	Fam173a	Timm10b	Ndn	Rpl37a
Tmem88	Atp5k	Rpl28	Hint1	Rps18
Cdsn	Ywhah	Rps20	Rps28	Ctdnep1
Eif1				

Chapter 6

Conclusion

A large number of studies have contributed to our current understanding of WNT signaling pathway in bone and this pathway has emerged as a major regulator of bone development and metabolism. It has been proposed that targeting the WNT pathway is a potential therapeutic strategy for osteoporosis and other bone disorders. Given the complexity of WNT signaling pathway, it is important to identify the functions of individual pathway components and delineate the crosstalk between WNT signaling with other signaling pathways in order to develop specific and effective therapies. Although substantial amount of information is available regarding the role of WNT signaling in bone development and remodeling, relatively little is known about the specific functions of different WNT pathway members in bone or the target genes regulated by WNT signaling.

I studied the functions of WNT ligands WNT3A, WNT5A and WNT16 and WNT co-receptors LRP5 and LRP6 in osteoblasts and identified more than 1000 WNT target genes, many of which have never been described before in this context. This study provides the first account of WNT regulated transcriptome in primary osteoblasts.

In Chapter 3, I examined the role of WNT3A in osteoblasts. Using RNA-seq I identified 788 genes regulated by WNT3A. These genes included several members of WNT, TGF-β/BMP and MAPK signaling pathways, suggesting that there exists a crosstalk between theses pathways during osteoblast differentiation. Future studies could focus on understanding how these pathways coordinately regulate bone metabolism. For example, treating TGF-β or BMP receptor knockout osteoblasts with recombinant WNT3A and performing gene expression studies will reveal whether TGF-β/BMP also play a role in transcriptional regulation of genes identified in this study. My study also showed that WNT3A is a positive regulator of early stages of osteoblast differentiation and a negative regulator of later stages of osteoblast differentiation. Treatment with recombinant WNT3A resulted in enhanced osteoblasts proliferation, *in vitro;* as well as increased calvarial thickness and decreased mineralization, *in vivo*. These findings suggests that prolonged activation of WNT3A signaling may negatively affect bone mass.

LRP5 and LRP6 are two WNT co-receptors that play a major role in bone development and metabolism. Both LRP5 and LRP6 are required for normal postnatal bone homeostasis. However, their specific functions during osteogenesis are not well understood. My study showed that LRP5 and LRP6 regulate different set of target genes in osteoblasts. Of the 249 genes differentially expressed in *Lrp5*$^{-/-}$ osteoblasts compared to *WT* osteoblasts only 28 genes overlapped with genes differentially expressed in *Lrp6*$^{-/-}$ osteoblasts compared to controls. I also studied the role of LRP5 and LRP6 in mediating WNT3A signaling and identified LRP6 as the key mediator of WNT3A signaling in osteoblasts. WNT3A up- or down-regulated ~73% of its target genes independent of LRP5 whereas only ~14% of WNT3A targets were differentially expressed in osteoblasts

lacking LRP6, in response to WNT3A treatment. However, it is known that loss of function mutations in *LRP5* greatly impairs bone formation [35, 39], suggesting that LRP5 has a significant role in regulating bone metabolism. It is likely that LRP5 may play a significant role in mediating signaling by other canonical WNT ligands such as WNT1 and WNT10B. Goel *et al*. have shown that both LRP5 and LRP6 are required for responsiveness to WNT1/9B/10B in mammary epithelial cells [363]. To understand whether LRP5 plays a role in canonical WNT signaling mediated by other WNT ligands we assayed β-catenin activation in WT and $Lrp5^{-/-}$ osteoblasts treated with recombinant WNT1 and WNT10B; however, the data was inconclusive, possibly due to the low activity of recombinant WNT1 and WNT10B. Unavailability of animal models overexpressing WNTs or biologically active recombinant WNT proteins limited our ability to study the functions of majority of WNT proteins in osteoblasts.

In Chapter 4, by mapping TCF/LEF binding sites identified using ChIP-seq to the genes activated by WNT3A I identified several putative TCF/LEF targets. My study showed that 83% (231/278) of WNT3A activated genes harbor TCF/LEF binding sites in their vicinity. By integrating RNA-seq and ChIP-seq data I also identified 587 putative WNT inducible enhancers near WNT3A activated genes. A detailed characterization of these enhancers will further our understanding of WNT mediated transcription regulation in osteoblasts. A motif enrichment analysis revealed that consensus AP-1 motifs were over-represented in a large subset of WNT inducible enhancers and promoters of WNT3A targets. Interestingly, my study also identified AP-1 family transcription factor *Fosl2* as a WNT3A target. Future work could focus on understanding whether there exists a crosstalk between WNT/β-catenin pathway and JNK pathway during osteoblast differentiation. Methods such as rapid immunoprecipitation mass spectrometry of endogenous proteins (RIME) [364] can be used to identify whether transcription factors activated by JNK pathway interact with canonical WNT pathway activated transcription factors TCF/LEF or β-catenin to regulate gene expression in osteoblasts.

In Chapter 5, I investigated the function of WNT16 in osteoblasts and identified 603 genes regulated by WNT16. I also compared gene expression profiles of WNT16 treated osteoblasts to gene expression profiles of canonical WNT3A and non-canonical WNT5B treated osteoblasts and found that 37% (225/603) of the WNT16 targets overlapped with WNT3A targets and 14% (86/603) with WNT5A targets. This suggests that WNT16 activates canonical and non-canonical WNT targets. My study identified *Mef2c* transcription factor, a major positive regulator of *Sost*, as a gene down-regulated by WNT16 in osteoblasts. Our lab has shown that mice lacking *Mef2c* in osteoblasts or osteoclasts exhibit high bone mass. These studies suggest that MEF2C plays a key role in regulating both anabolic and catabolic responses in bone. However, very little is known about transcriptional regulation of *Mef2c* in bone. My study has identified WNT16 as a negative regulator of *Mef2c* in osteoblasts.

Similar to WNT3A, WNT16 also up-regulated genes associated with early stages of osteoblast differentiation and down-regulated regulators of osteoblasts maturation and mineralization. From the pharmacological point of view, the fact that WNT3A and

WNT16 promote early stages of osteoblast differentiation and inhibit osteoblast maturation/mineralization has important implications. Activation of WNT3A and WNT16 signaling in early stage osteoblasts may promote bone formation; however, long term activation may have detrimental effects on bone mass.

One weakness of my study is that I did not use purified osteoblasts for this study. The population of cells we isolated from calvaria may also contain other cell types including fibroblasts and osteoclasts at a very small quantity. Performing similar studies on purified osteoblasts will provide more accurate results. Another weakness is that the gene expression analysis was performed after treating osteoblasts with WNTs for 24 hours. Some of the target genes identified in this study may not be direct WNT targets as transcription factors and other signaling proteins activated by WNT may also influence gene expression in these cells. Performing gene expression studies at an early time point or treating cells with a translation blocker along with recombinant WNT treatment will allow the identification of more primary WNT targets.

My study was heavily dependent on high -throughput sequencing technologies. Using RNA-seq, I identified more than thousand genes regulated by WNTs in osteoblasts which may include some false positives as well. There are several tools available for RNA-seq data analysis (discussed in chapter 2). Previous studies have suggested that no one data analysis pipeline outperforms other pipelines in every aspect. In my study, I used TopHat2 for read alignment, featureCounts for read quantification and limma for differential gene expression analysis. Read aligner STAR has been shown to outperform TopHat2 in several aspects even though the memory requirement is significantly higher than TopHat2 [253]. Similarly, EdgeR and DEseq2 have been shown to perform well in identifying differentially expressed genes [270]. Analyzing my data with alternative pipelines (for example: STAR-featureCounts-EdgeR/DEseq2) and selecting differentially expressed genes commonly identified by these pipelines may reduce the number of false positives, but at the expense of missing some true positives. Alternatively, an extensive validation of the WNT targets can be performed using techniques such as q-RT PCR. Alternative pipelines exist for ChIP-seq data analysis as well. For ChIP-seq studies also, analyzing data using alternative pipelines (for example: BWA for read alignment and SISSRS for peak calling) and selecting peaks called by multiple pipelines may reduce the number of false positive discoveries.

Altogether, the work presented in this thesis provides new insights into WNT signaling pathway in the context of bone metabolism. This study has identified several WNT targets that may have the potential to promote bone formation. Future studies aimed at understanding the precise mechanism by which these genes regulate bone metabolism will enhance our understanding of the WNT signaling pathway and the molecular mechanisms that regulate bone metabolism in general.

References

1. Clevers, H., et al. (2012). "Wnt/beta-catenin signaling and disease." Cell 149(6): 1192-1205.
2. Qian, J., et al. (2003). "Mouse Wnt9b transforming activity, tissue-specific expression, and evolution." Genomics 81(1): 34-46.
3. MacDonald, B. T., et al. (2009). "Wnt/beta-catenin signaling: components, mechanisms, and diseases." Dev Cell 17(1): 9-26.
4. van Amerongen, R., et al. (2009). "Towards an integrated view of Wnt signaling in development." Development 136(19): 3205-3214.
5. Zimmerman, Z. F., et al. (2013). "Activation of Wnt/beta-catenin signaling increases apoptosis in melanoma cells treated with trail." PLoS One 8(7): e69593.
6. Teo, J. L., et al. (2010). "The Wnt signaling pathway in cellular proliferation and differentiation: A tale of two coactivators." Adv Drug Deliv Rev 62(12): 1149-115
7. Maupin, K. A., et al. (2013). "A Comprehensive Overview of Skeletal Phenotypes Associated with Alterations in Wnt/beta-catenin Signaling in Humans and Mice." Bone Res 1(1): 27-71.
8. Baron, R., et al. (2013). "WNT signaling in bone homeostasis and disease: from human mutations to treatments." Nat Med 19(2): 179-192.
9. Hoeppner, L. H., et al. (2009). "Wnt signaling as a therapeutic target for bone diseases." Expert Opin Ther Targets 13(4): 485-496.
10. Niehrs, C. (2012). "The complex world of WNT receptor signalling." Nat Rev Mol Cell Biol 13(12): 767-779.
11. Zhang, L., et al. (2012). "Fas-associated factor 1 is a scaffold protein that promotes beta-transducin repeat-containing protein (beta-TrCP)-mediated beta-catenin ub
12. Gao, C., et al. (2014). "Regulation of Wnt/beta-catenin signaling by posttranslational modifications." Cell Biosci 4(1): 13.
13. van Amerongen, R., et al. (2008). "Alternative wnt signaling is initiated by distinct receptors." Sci Signal 1(35): re9.
14. Lerner, U. H., et al. (2015). "The WNT system: background and its role in bone." J Intern Med 277(6): 630-649.
15. De, A. (2011). "Wnt/Ca2+ signaling pathway: a brief overview." Acta Biochim Biophys Sin (Shanghai) 43(10): 745-756.
16. Cui, J., et al. (2007). "JNK pathway: diseases and therapeutic potential." Acta Pharmacol Sin 28(5): 601-608.
17. Bootman, M. D. (2012). "Calcium signaling." Cold Spring Harb Perspect Biol 4(7): a011171.
18. Kestler, H. A., et al. (2011). "Generating a Wnt switch: it's all about the right

dosage." J Cell Biol 193(3): 431-433.

19. Nalesso, G., et al. (2011). "WNT-3A modulates articular chondrocyte phenotype by activating both canonical and noncanonical pathways." J Cell Biol 193(3): 551-564.
20. Bernardi, H., et al. (2011). "Wnt4 activates the canonical beta-catenin pathway and regulates negatively myostatin: functional implication in myogenesis." Am J Physiol Cell Physiol 300(5): C1122-1138.
21. Mikels, A. J., et al. (2006). "Purified Wnt5a protein activates or inhibits beta-catenin-TCF signaling depending on receptor context." PLoS Biol 4(4): e115.
22. Kikuchi, A., et al. (2011). "New insights into the mechanism of Wnt signaling pathway activation." Int Rev Cell Mol Biol 291: 21-71.
23. Clarke, B. (2008). "Normal bone anatomy and physiology." Clin J Am Soc Nephrol 3 Suppl 3: S131-139.
24. Regard, J. B., et al. (2012). "Wnt signaling in bone development and disease: making stronger bone with Wnts." Cold Spring Harb Perspect Biol 4(12).
25. Zhang, C. (2010). "Transcriptional regulation of bone formation by the osteoblast-specific transcription factor Osx." J Orthop Surg Res 5: 37.
26. Feng, X., et al. (2011). "Disorders of bone remodeling." Annu Rev Pathol 6: 121-145.
27. Hadjidakis, D. J., et al. (2006). "Bone remodeling." Ann N Y Acad Sci 1092: 385-396.
28. Zhou, X., et al. (2014). "Chondrocytes transdifferentiate into osteoblasts in endochondral bone during development, postnatal growth and fracture healing in mice." PLoS Genet 10(12): e1004820.
29. Long, F., et al. (2013). "Development of the endochondral skeleton." Cold Spring Harb Perspect Biol 5(1): a008334.
30. Rochefort, G. Y., et al. (2010). "Osteocyte: the unrecognized side of bone tissue." Osteoporos Int 21(9): 1457-1469.
31. Imai, Y., et al. (2013). "Nuclear receptors in bone physiology and diseases." Physiol Rev 3(2):481-523.
32. Boyce, B. F., et al. (2007). "Biology of RANK, RANKL, and osteoprotegerin." Arthritis Res Ther 9 Suppl 1: S1.
33. Sims, N. A., et al. (2015). "Coupling Signals between the Osteoclast and Osteoblast: How are Messages Transmitted between These Temporary Visitors to the Bone Surface?" Front Endocrinol (Lausanne) 6: 41.
34. Augustine, M., et al. (2013). "Parathyroid hormone and parathyroid hormone-related protein analogs as therapies for osteoporosis." Curr Osteoporos Rep 11(4): 400-406.
35. Gong, Y., et al. (2001). "LDL receptor-related protein 5 (LRP5) affects bone

accrual and eye development." Cell 107(4): 513-523.

36. Little, R. D., et al. (2002). "A mutation in the LDL receptor-related protein 5 gene results in the autosomal dominant high-bone-mass trait." Am J Hum Genet 70(1): 11-19.

37. Korvala, J., et al. (2012). "Mutations in LRP5 cause primary osteoporosis without features of OI by reducing Wnt signaling activity." BMC Med Genet 13: 26.

38. Mani, A., et al. (2007). "LRP6 mutation in a family with early coronary disease and metabolic risk factors." Science 315(5816): 1278-1282.

39. Boyden, L. M., et al. (2002). "High bone density due to a mutation in LDL-receptor-related protein 5." N Engl J Med 346(20): 1513-1521.

40. Brunkow, M. E., et al. (2001). "Bone dysplasia sclerosteosis results from loss of the SOST gene product, a novel cystine knot-containing protein." Am J Hum Genet 68(3): 577-589.

41. Balemans, W., et al. (2002). "Identification of a 52 kb deletion downstream of the SOST gene in patients with van Buchem disease." J Med Genet 39(2): 91-97.

42. Spencer, G. J., et al. (2006). "Wnt signalling in osteoblasts regulates expression of the receptor activator of NFkappaB ligand and inhibits osteoclastogenesis in vitro." J Cell Sci 119(Pt 7): 1283-1296.

43. Witte, F., et al. (2009). "Comprehensive expression analysis of all Wnt genes and their major secreted antagonists during mouse limb development and cartilage differentiation." Gene Expr Patterns 9(4): 215-223.

44. Tan, S. H., et al. (2014). "Wnts produced by Osterix-expressing osteolineage cells regulate their proliferation and differentiation." Proc Natl Acad Sci U S A 111(49): E5262-5271.

45. Mak, W., et al. (2009). "Biphasic glucocorticoid-dependent regulation of Wnt expression and its inhibitors in mature osteoblastic cells." Calcif Tissue Int 85(6): 538-545.

46. Monroe, D. G., et al. (2012). "Update on Wnt signaling in bone cell biology and bone disease." Gene 492(1): 1-18.

47. Fahiminiya, S., et al. (2013). "Mutations in WNT1 are a cause of osteogenesis imperfecta." J Med Genet 50(5): 345-348.

48. Keupp, K., et al. (2013). "Mutations in WNT1 cause different forms of bone fragility." Am J Hum Genet 92(4): 565-574.

49. Colaianni, G., et al. (2015). "CELLULAR MECHANISMS OF BONE REGENERATION: ROLE OF WNT-1 IN BONE-MUSCLE INTERACTION DURING PHYSICAL ACTIVITY39." J Biol Regul Homeost Agents 29(4 Suppl): 39-45.

50. Laine, C. M., et al. (2013). "WNT1 mutations in early-onset osteoporosis and osteogenesis imperfecta." N Engl J Med 368(19): 1809-1816.

51. Weivoda, M. M., et al. (2016). "Osteoclast TGF-beta Receptor Signaling Induces Wnt1 Secretion and Couples Bone Resorption to Bone Formation." J Bone Miner Res 31(1): 76-85.

52. Niemann, S., et al. (2004). "Homozygous WNT3 mutation causes tetra-amelia in a large consanguineous family." Am J Hum Genet 74(3): 558-563.

53. Hsu, Y. H., et al. (2012). "Clinical review: Genome-wide association studies of skeletal phenotypes: what we have learned and where we are headed." J Clin Endocrinol Metab 97(10): E1958-1977.

54. Katoh, M. (2002). "WNT3-WNT14B and WNT3A-WNT14 gene clusters (Review)." Int J Mol Med 9(6): 579-584.

55. Takada, I., et al. (2007). "A histone lysine methyltransferase activated by non-canonical Wnt signalling suppresses PPAR-gamma transactivation." Nat Cell Biol 9(11): 1273-1285.

56. Boland, G. M., et al. (2004). "Wnt 3a promotes proliferation and suppresses osteogenic differentiation of adult human mesenchymal stem cells." J Cell Biochem 93(6): 1210-1230.

57. Minear, S., et al. (2010). "Wnt proteins promote bone regeneration." Sci Transl Med 2(29): 29ra30.

58. Karner, C. M., et al. (2016). "Wnt Protein Signaling Reduces Nuclear Acetyl-CoA Levels to Suppress Gene Expression during Osteoblast Differentiation." J Biol Chem 291(25): 13028-13039.

59. Santiago, F., et al. (2012). "Noncanonical Wnt signaling promotes osteoclast differentiation and is facilitated by the human immunodeficiency virus protease inhibitor ritonavir." Biochem Biophys Res Commun 417(1): 223-230.

60. Almeida, M., et al. (2005). "Wnt proteins prevent apoptosis of both uncommitted osteoblast progenitors and differentiated osteoblasts by beta-catenin-dependent and -independent signaling cascades involving Src/ERK and phosphatidylinositol 3-kinase/AKT." J Biol Chem 280(50): 41342-41351.

61. Weivoda, M. M., et al. (2016). "Wnt Signaling Inhibits Osteoclast Differentiation by Activating Canonical and Noncanonical cAMP/PKA Pathways." J Bone Miner Res 31(1): 65-75.

62. Tu, X., et al. (2007). "Noncanonical Wnt signaling through G protein-linked PKCdelta activation promotes bone formation." Dev Cell 12(1): 113-127.

63. Qiu, W., et al. (2011). "Activation of non-canonical Wnt/JNK pathway by Wnt3a is associated with differentiation fate determination of human bone marrow stromal (mesenchymal) stem cells." Biochem Biophys Res Commun 413(1): 98-104.

64. Yu, B., et al. (2014). "Wnt4 signaling prevents skeletal aging and inflammation by inhibiting nuclear factor-kappaB." Nat Med 20(9): 1009-1017.

65. Chang, J., et al. (2007). "Noncanonical Wnt-4 signaling enhances bone regeneration

of mesenchymal stem cells in craniofacial defects through activation of p38 MAPK." J Biol Chem 282(42): 30938-30948.

66. Person, A. D., et al. (2010). "WNT5A mutations in patients with autosomal dominant Robinow syndrome." Dev Dyn 239(1): 327-337.

67. Yamaguchi, T. P., et al. (1999). "A Wnt5a pathway underlies outgrowth of multiple structures in the vertebrate embryo." Development 126(6): 1211-1223.

68. Oishi, I., et al. (2003). "The receptor tyrosine kinase Ror2 is involved in non-canonical Wnt5a/JNK signalling pathway." Genes Cells 8(7): 645-654.

69. Maeda, K., et al. (2012). "Wnt5a-Ror2 signaling between osteoblast-lineage cells and osteoclast precursors enhances osteoclastogenesis." Nat Med 18(3): 405-412.

70. Keller, K. C., et al. (2016). "Wnt5a Supports Osteogenic Lineage Decisions in Embryonic Stem Cells." Stem Cells Dev 25(13): 1020-1032.

71. Okamoto, M., et al. (2014). "Noncanonical Wnt5a enhances Wnt/beta-catenin signaling during osteoblastogenesis." Sci Rep 4: 4493.

72. Yang, Y., et al. (2003). "Wnt5a and Wnt5b exhibit distinct activities in coordinating chondrocyte proliferation and differentiation." Development 130(5): 1003-1015.

73. Parr, B. A., et al. (1995). "Dorsalizing signal Wnt-7a required for normal polarity of D-V and A-P axes of mouse limb." Nature 374(6520): 350-353.

74. Eyaid, W., et al. (2011). "A novel homozygous missense mutation (c.610G>A, p.Gly204Ser) in the WNT7A gene causes tetra-amelia in two Saudi families." Am J Med Genet A 155a(3): 599-604.

75. Kirikoshi, H., et al. (2001). "Molecular cloning and characterization of human WNT7B." Int J Oncol 19(4): 779-783.

76. Chen, J., et al. (2014). "WNT7B promotes bone formation in part through mTORC1." PLoS Genet 10(1): e1004145.

77. Hu, H., et al. (2005). "Sequential roles of Hedgehog and Wnt signaling in osteoblast development." Development 132(1): 49-60.

78. Saitoh, T., et al. (2001). "Proto-oncogene WNT10B is up-regulated by tumor necrosis factor alpha in human gastric cancer cell line MKN45." Int J Oncol 19(6): 1187-1192.

79. Cawthorn, W. P., et al. (2012). "Wnt6, Wnt10a and Wnt10b inhibit adipogenesis and stimulate osteoblastogenesis through a beta-catenin-dependent mechanism." Bone 50(2): 477-489.

80. Kang, S., et al. (2007). "Wnt signaling stimulates osteoblastogenesis of mesenchymal precursors by suppressing CCAAT/enhancer-binding protein alpha and peroxisome proliferator-activated receptor gamma." J Biol Chem 282(19): 14515-14524.

81. Bennett, C. N., et al. (2005). "Regulation of osteoblastogenesis and bone mass by

Wnt10b." Proc Natl Acad Sci U S A 102(9): 3324-3329.

82. Bennett, C. N., et al. (2007). "Wnt10b increases postnatal bone formation by enhancing osteoblast differentiation." J Bone Miner Res 22(12): 1924-1932.

83. Stevens, J. R., et al. (2010). "Wnt10b deficiency results in age-dependent loss of bone mass and progressive reduction of mesenchymal progenitor cells." J Bone Miner Res 25(10): 2138-2147.

84. Blattner, A., et al. (2010). "Homozygous nonsense mutation in WNT10B and sporadic split-hand/foot malformation (SHFM) with autosomal recessive inheritance." Am J Med

85. Yu, P., et al. (2016). "Mutations in WNT10B Are Identified in Individuals with Oligodontia." Am J Hum Genet 99(1): 195-201.

86. Liu, S., et al. (2014). "Overexpression of Wnt11 promotes chondrogenic differentiation of bone marrow-derived mesenchymal stem cells in synergism with TGF-beta." Mol Cell Biochem 390(1-2): 123-131.

87. Friedman, M. S., et al. (2009). "Wnt11 promotes osteoblast maturation and mineralization through R-spondin 2." J Biol Chem 284(21): 14117-14125.

88. Estrada, K., et al. (2012). "Genome-wide meta-analysis identifies 56 bone mineral density loci and reveals 14 loci associated with risk of fracture." Nat Genet 44(5): 491-501.

89. Zheng, H. F., et al. (2012). "WNT16 influences bone mineral density, cortical bone thickness, bone strength, and osteoporotic fracture risk." PLoS Genet 8(7): e1002745.

90. Moverare-Skrtic, S., et al. (2014). "Osteoblast-derived WNT16 represses osteoclastogenesis and prevents cortical bone fragility fractures." Nat Med 20(11): 1279-1288.

91. Alam, I., et al. (2016). "Osteoblast-Specific Overexpression of Human WNT16 Increases Both Cortical and Trabecular Bone Mass and Structure in Mice." Endocrinology 157(2): 722-736.

92. Proffitt, K. D., et al. (2012). "Precise regulation of porcupine activity is required for physiological Wnt signaling." J Biol Chem 287(41): 34167-34178.

93. Port, F., et al. (2010). "Wnt trafficking: new insights into Wnt maturation, secretion and spreading." Traffic 11(10): 1265-1271.

94. Stevenson, D. A., et al. (2014). "Goltz syndrome and PORCN mosaicism." Int J Dermatol 53(12): 1481-1484.

95. Barrott, J. J., et al. (2011). "Deletion of mouse Porcn blocks Wnt ligand secretion and reveals an ectodermal etiology of human focal dermal hypoplasia/Goltz syndrome." Proc Natl Acad Sci U S A 108(31): 12752-12757.

96. Liu, W., et al. (2012). "Deletion of Porcn in mice leads to multiple developmental defects and models human focal dermal hypoplasia (Goltz syndrome)." PLoS One

7(3): e32331.

97. Banziger, C., et al. (2006). "Wntless, a conserved membrane protein dedicated to the secretion of Wnt proteins from signaling cells." Cell 125(3): 509-522.

98. Styrkarsdottir, U., et al. (2010). "European bone mineral density loci are also associated with BMD in East-Asian populations." PLoS One 5(10): e13217.

99. Rivadeneira, F., et al. (2009). "Twenty bone-mineral-density loci identified by large-scale meta-analysis of genome-wide association studies." Nat Genet 41(11): 1199-1206.

100. Fu, J., et al. (2009). "Reciprocal regulation of Wnt and Gpr177/mouse Wntless is required for embryonic axis formation." Proc Natl Acad Sci U S A 106(44): 18598-18603.

101. Zhu, X., et al. (2012). "Wls-mediated Wnts differentially regulate distal limb patterning and tissue morphogenesis." Dev Biol 365(2): 328-338.

102. Wan, Y., et al. (2013). "Osteoblastic Wnts differentially regulate bone remodeling and the maintenance of bone marrow mesenchymal stem cells." Bone 55(1): 258-267.

103. Zhong, Z., et al. (2012). "Wntless functions in mature osteoblasts to regulate bone mass." Proc Natl Acad Sci U S A 109(33): E2197-2204.

104. Huang, H. C., et al. (2004). "The Frizzled family: receptors for multiple signal transduction pathways." Genome Biol 5(7): 234.

105. Albers, J., et al. (2013). "Canonical Wnt signaling inhibits osteoclastogenesis independent of osteoprotegerin." J Cell Biol 200(4): 537-549.

106. Drake, R., et al. (1990). "Evidence for the involvement of a 35-kDa membrane protein in the synthesis of glucosylphosphoryldolichol." Biosci Rep 10(1): 61-68.

107. Albers, J., et al. (2011). "Control of bone formation by the serpentine receptor Frizzled-9." J Cell Biol 192(6): 1057-1072.

108. He, X., et al. (2004). "LDL receptor-related proteins 5 and 6 in Wnt/beta-catenin signaling: arrows point the way." Development 131(8): 1663-1677.

109. Riddle, R. C., et al. (2013). "Lrp5 and Lrp6 exert overlapping functions in osteoblasts during postnatal bone acquisition." PLoS One 8(5): e63323.

110. Niziolek, P. J., et al. (2011). "High-bone-mass-producing mutations in the Wnt signaling pathway result in distinct skeletal phenotypes." Bone 49(5): 1010-1019.

111. Pinson, K. I., et al. (2000). "An LDL-receptor-related protein mediates Wnt signalling in mice." Nature 407(6803): 535-538.

112. Kato, M., et al. (2002). "Cbfa1-independent decrease in osteoblast proliferation, osteopenia, and persistent embryonic eye vascularization in mice deficient in Lrp5, a Wnt coreceptor." J Cell Biol 157(2): 303-314.

113. Sawakami, K., et al. (2006). "The Wnt co-receptor LRP5 is essential for skeletal

mechanotransduction but not for the anabolic bone response to parathyroid hormone treatment." J Biol Chem 281(33): 23698-23711.

114. Niziolek, P. J., et al. (2012). "Mechanotransduction in bone tissue: The A214V and G171V mutations in Lrp5 enhance load-induced osteogenesis in a surface-selective manner." Bone 51(3): 459-465.
115. Holmen, S. L., et al. (2004). "Decreased BMD and limb deformities in mice carrying mutations in both Lrp5 and Lrp6." J Bone Miner Res 19(12): 2033-2040.
116. Joeng, K. S., et al. (2011). "Lrp5 and Lrp6 redundantly control skeletal development in the mouse embryo." Dev Biol 359(2): 222-229.
117. Frey, J. L., et al. (2015). "Wnt-Lrp5 signaling regulates fatty acid metabolism in the osteoblast." Mol Cell Biol 35(11): 1979-1991.
118. Zilberberg, A., et al. (2004). "The low density lipoprotein receptor-1, LRP1, interacts with the human frizzled-1 (HFz1) and down-regulates the canonical Wnt signaling pathway." J Biol Chem 279(17): 17535-17542.
119. Choi, H. Y., et al. (2009). "Lrp4, a novel receptor for Dickkopf 1 and sclerostin, is expressed by osteoblasts and regulates bone growth and turnover in vivo." PLoS One 4(11): e7930.
120. Leupin, O., et al. (2011). "Bone overgrowth-associated mutations in the LRP4 gene impair sclerostin facilitator function." J Biol Chem 286(22): 19489-19500.
121. Zhang, J., et al. (2012). "LRP8 mediates Wnt/beta-catenin signaling and controls osteoblast differentiation." J Bone Miner Res 27(10): 2065-2074.
122. Green, J., et al. (2014). "The role of Ryk and Ror receptor tyrosine kinases in Wnt signal transduction." Cold Spring Harb Perspect Biol 6(2).
123. Grumolato, L., et al. (2010). "Canonical and noncanonical Wnts use a common mechanism to activate completely unrelated coreceptors." Genes Dev 24(22): 2517-2530.
124. Sato, A., et al. (2010). "Wnt5a regulates distinct signalling pathways by binding to Frizzled2." Embo j 29(1): 41-54.
125. Afzal, A. R., et al. (2003). "One gene, two phenotypes: ROR2 mutations in autosomal recessive Robinow syndrome and autosomal dominant brachydactyly type B." Hum Mutat 22(1): 1-11.
126. Raz, R., et al. (2008). "The mutation ROR2W749X, linked to human BDB, is a recessive mutation in the mouse, causing brachydactyly, mediating patterning of joints and modeling recessive Robinow syndrome." Development 135(9): 1713-1723.
127. Tamhankar, P. M., et al. (2014). "Identification of novel ROR2 gene mutations in Indian children with Robinow syndrome." J Clin Res Pediatr Endocrinol 6(2): 79-83.
128. Takeuchi, S., et al. (2000). "Mouse Ror2 receptor tyrosine kinase is required for the

heart development and limb formation." Genes Cells 5(1): 71-78.

129. DeChiara, T. M., et al. (2000). "Ror2, encoding a receptor-like tyrosine kinase, is required for cartilage and growth plate development." Nat Genet 24(3): 271-274.

130. Nomi, M., et al. (2001). "Loss of mRor1 enhances the heart and skeletal abnormalities in mRor2-deficient mice: redundant and pleiotropic functions of mRor1 and mRor2 receptor tyrosine kinases." Mol Cell Biol 21(24): 8329-8335.

131. Lyashenko, N., et al. (2010). "Mice lacking the orphan receptor ror1 have distinct skeletal abnormalities and are growth retarded." Dev Dyn 239(8): 2266-2277.

132. Liu, Y., et al. (2007). "The orphan receptor tyrosine kinase Ror2 promotes osteoblast differentiation and enhances ex vivo bone formation." Mol Endocrinol 21(2): 376-387.

133. Halford, M. M., et al. (2001). "Revelations of the RYK receptor." Bioessays 23(1): 34-45.

134. Halford, M. M., et al. (2000). "Ryk-deficient mice exhibit craniofacial defects associated with perturbed Eph receptor crosstalk." Nat Genet 25(4): 414-418.

135. Andre, P., et al. (2012). "The Wnt coreceptor Ryk regulates Wnt/planar cell polarity by modulating the degradation of the core planar cell polarity component Vangl2." J Biol Chem 287(53): 44518-44525.

136. McEwen, A. E., et al. (2012). "Signaling from the adherens junction." Subcell Biochem 60: 171-196.

137. Holmen, S. L., et al. (2005). "Essential role of beta-catenin in postnatal bone acquisition." J Biol Chem 280(22): 21162-21168.

138. Day, T. F., et al. (2005). "Wnt/beta-catenin signaling in mesenchymal progenitors controls osteoblast and chondrocyte differentiation during vertebrate skeletogenesis." Dev Cell 8(5): 739-750.

139. Hill, T. P., et al. (2005). "Canonical Wnt/beta-catenin signaling prevents osteoblasts from differentiating into chondrocytes." Dev Cell 8(5): 727-738.

140. Rodda, S. J., et al. (2006). "Distinct roles for Hedgehog and canonical Wnt signaling in specification, differentiation and maintenance of osteoblast progenitors." Development 133(16): 3231-3244.

141. Glass, D. A., 2nd, et al. (2005). "Canonical Wnt signaling in differentiated osteoblasts controls osteoclast differentiation." Dev Cell 8(5): 751-764.

142. Kramer, I., et al. (2010). "Osteocyte Wnt/beta-catenin signaling is required for normal bone homeostasis." Mol Cell Biol 30(12): 3071-3085.

143. Chen, J., et al. (2013). "beta-catenin promotes bone formation and suppresses bone resorption in postnatal growing mice." J Bone Miner Res 28(5): 1160-1169.

144. Kang, K. S., et al. (2016). "Postnatal beta-catenin deletion from Dmp1-expressing osteocytes/osteoblasts reduces structural adaptation to loading, but not periosteal

load-induced bone formation." Bone 88: 138-145.

145. Zhao, L., et al. (2013). "Inactivation of Lrp5 in osteocytes reduces young's modulus and responsiveness to the mechanical loading." Bone 54(1): 35-43.

146. Wei, W., et al. (2011). "Biphasic and dosage-dependent regulation of osteoclastogenesis by beta-catenin." Mol Cell Biol 31(23): 4706-4719.

147. Li, J., et al. (2016). "Different bone remodeling levels of trabecular and cortical bone in response to changes in Wnt/beta-catenin signaling in mice." J Orthop Res.

148. Yu, H. M., et al. (2005). "The role of Axin2 in calvarial morphogenesis and craniosynostosis." Development 132(8): 1995-2005.

149. Jho, E. H., et al. (2002). "Wnt/beta-catenin/Tcf signaling induces the transcription of Axin2, a negative regulator of the signaling pathway." Mol Cell Biol 22(4): 1172-1183.

150. Dao, D. Y., et al. (2010). "Axin2 regulates chondrocyte maturation and axial skeletal development." J Orthop Res 28(1): 89-95.

151. Yan, Y., et al. (2009). "Axin2 controls bone remodeling through the beta-catenin-BMP signaling pathway in adult mice." J Cell Sci 122(Pt 19): 3566-3578.

152. Miclea, R. L., et al. (2010). "APC mutations are associated with increased bone mineral density in patients with familial adenomatous polyposis." J Bone Miner Res 25(12): 2624-2632.

153. Yerges, L. M., et al. (2009). "High-density association study of 383 candidate genes for volumetric BMD at the femoral neck and lumbar spine among older men." J Bone Miner Res 24(12): 2039-2049.

154. Fodde, R., et al. (1994). "A targeted chain-termination mutation in the mouse Apc gene results in multiple intestinal tumors." Proc Natl Acad Sci U S A 91(19): 8969-8973.

155. Miclea, R. L., et al. (2009). "Adenomatous polyposis coli-mediated control of beta-catenin is essential for both chondrogenic and osteogenic differentiation of skeletal precursors." BMC Dev Biol 9: 26.

156. Doble, B. W., et al. (2003). "GSK-3: tricks of the trade for a multi-tasking kinase." J Cell Sci 116(Pt 7): 1175-1186.

157. Hoeflich, K. P., et al. (2000). "Requirement for glycogen synthase kinase-3beta in cell survival and NF-kappaB activation." Nature 406(6791): 86-90.

158. Itoh, S., et al. (2012). "GSK-3alpha and GSK-3beta proteins are involved in early stages of chondrocyte differentiation with functional redundancy through RelA protein phosphorylation." J Biol Chem 287(35): 29227-29236.

159. Noh, T., et al. (2009). "Lef1 haploinsufficient mice display a low turnover and low bone mass phenotype in a gender- and age-specific manner." PLoS One 4(5): e5438.

160. Kugimiya, F., et al. (2007). "GSK-3beta controls osteogenesis through regulating Runx2 activity." PLoS One 2(9): e837.

161. Clement-Lacroix, P., et al. (2005). "Lrp5-independent activation of Wnt signaling by lithium chloride increases bone formation and bone mass in mice." Proc Natl Acad Sci U S A 102(48): 17406-17411.

162. Galli, C., et al. (2013). "GSK3b-inhibitor lithium chloride enhances activation of Wnt canonical signaling and osteoblast differentiation on hydrophilic titanium surfaces." Clin Oral Implants Res 24(8): 921-927.

163. Cadigan, K. M., et al. (2012). "TCF/LEFs and Wnt signaling in the nucleus." Cold Spring Harb Perspect Biol 4(11).

164. Kahler, R. A., et al. (2006). "Lymphocyte enhancer-binding factor 1 (Lef1) inhibits terminal differentiation of osteoblasts." J Cell Biochem 97(5): 969-983.

165. Kahler, R. A., et al. (2003). "Lymphoid enhancer factor-1 and beta-catenin inhibit Runx2-dependent transcriptional activation of the osteocalcin promoter." J Biol Chem 278(14): 11937-11944.

166. Hoeppner, L. H., et al. (2009). "Runx2 and bone morphogenic protein 2 regulate the expression of an alternative Lef1 transcript during osteoblast maturation." J Cell Physiol 221(2): 480-489.

167. Hoeppner, L. H., et al. (2011). "Lef1DeltaN binds beta-catenin and increases osteoblast activity and trabecular bone mass." J Biol Chem 286(13): 10950-10959.

168. Camp, N. D., et al. (2012). "Wilms tumor gene on X chromosome (WTX) inhibits degradation of NRF2 protein through competitive binding to KEAP1 protein." J Biol Chem 287(9): 6539-6550.

169. Moisan, A., et al. (2011). "The WTX tumor suppressor regulates mesenchymal progenitor cell fate specification." Dev Cell 20(5): 583-596.

170. Huang, H., et al. (2008). "Wnt/beta-catenin signaling: new (and old) players and new insights." Curr Opin Cell Biol 20(2): 119-125.

171. Holman, S. K., et al. (2011). "The male phenotype in osteopathia striata congenita with cranial sclerosis." Am J Med Genet A 155a(10): 2397-2408.

172. Perdu, B., et al. (2011). "Two novel WTX mutations underscore the unpredictability of male survival in osteopathia striata with cranial sclerosis." Clin Genet 80(4): 383-388.

173. Bovolenta, P., et al. (2008). "Beyond Wnt inhibition: new functions of secreted Frizzled-related proteins in development and disease." J Cell Sci 121(Pt 6): 737-746.

174. Bodine, P. V., et al. (2004). "The Wnt antagonist secreted frizzled-related protein-1 is a negative regulator of trabecular bone formation in adult mice." Mol Endocrinol 18(5): 1222-1237.

175. Yao, W., et al. (2010). "Overexpression of secreted frizzled-related protein 1

inhibits bone formation and attenuates parathyroid hormone bone anabolic effects." J Bone Miner Res 25(2): 190-199.

176. Hausler, K. D., et al. (2004). "Secreted frizzled-related protein-1 inhibits RANKL-dependent osteoclast formation." J Bone Miner Res 19(11): 1873-1881.

177. Oshima, T., et al. (2005). "Myeloma cells suppress bone formation by secreting a soluble Wnt inhibitor, sFRP-2." Blood 106(9): 3160-3165.

178. Lories, R. J., et al. (2007). "Articular cartilage and biomechanical properties of the long bones in Frzb-knockout mice." Arthritis Rheum 56(12): 4095-4103.

179. Nakanishi, R., et al. (2008). "Osteoblast-targeted expression of Sfrp4 in mice results in low bone mass." J Bone Miner Res 23(2): 271-277.

180. Nakanishi, R., et al. (2006). "Secreted frizzled-related protein 4 is a negative regulator of peak BMD in SAMP6 mice." J Bone Miner Res 21(11): 1713-1721.

181. Haraguchi, R., et al. (2016). "sFRP4-dependent Wnt signal modulation is critical for bone remodeling during postnatal development and age-related bone loss." Sci Rep 6: 25198.

182. Niehrs, C. (2006). "Function and biological roles of the Dickkopf family of Wnt modulators." Oncogene 25(57): 7469-7481.

183. Mukhopadhyay, M., et al. (2001). "Dickkopf1 is required for embryonic head induction and limb morphogenesis in the mouse." Dev Cell 1(3): 423-434.

184. Morvan, F., et al. (2006). "Deletion of a single allele of the Dkk1 gene leads to an increase in bone formation and bone mass." J Bone Miner Res 21(6): 934-945.

185. Yao, G. Q., et al. (2011). "Targeted overexpression of Dkk1 in osteoblasts reduces bone mass but does not impair the anabolic response to intermittent PTH treatment in mice." J Bone Miner Metab 29(2): 141-148.

186. Tian, E., et al. (2003). "The role of the Wnt-signaling antagonist DKK1 in the development of osteolytic lesions in multiple myeloma." N Engl J Med 349(26): 2483-2494.

187. Heath, D. J., et al. (2009). "Inhibiting Dickkopf-1 (Dkk1) removes suppression of bone formation and prevents the development of osteolytic bone disease in multiple myeloma." J Bone Miner Res 24(3): 425-436.

188. Li, X., et al. (2005). "Dkk2 has a role in terminal osteoblast differentiation and mineralized matrix formation." Nat Genet 37(9): 945-952.

189. Hiramitsu, S., et al. (2013). "The effects of Dickkopf-4 on the proliferation, differentiation, and apoptosis of osteoblasts." Endocrinology 154(12): 4618-4626.

190. Aslan, H., et al. (2006). "Advanced molecular profiling in vivo detects novel function of dickkopf-3 in the regulation of bone formation." J Bone Miner Res 21(12): 1935-1945.

191. Li, X., et al. (2005). "Sclerostin binds to LRP5/6 and antagonizes canonical Wnt

signaling." J Biol Chem 280(20): 19883-19887.

192. Balemans, W., et al. (2001). "Increased bone density in sclerosteosis is due to the deficiency of a novel secreted protein (SOST)." Hum Mol Genet 10(5): 537-543.

193. Li, X., et al. (2008). "Targeted deletion of the sclerostin gene in mice results in increased bone formation and bone strength." J Bone Miner Res 23(6): 860-869.

194. Winkler, D. G., et al. (2003). "Osteocyte control of bone formation via sclerostin, a novel BMP antagonist." Embo j 22(23): 6267-6276.

195. Loots, G. G., et al. (2005). "Genomic deletion of a long-range bone enhancer misregulates sclerostin in Van Buchem disease." Genome Res 15(7): 928-935.

196. Lin, C., et al. (2009). "Sclerostin mediates bone response to mechanical unloading through antagonizing Wnt/beta-catenin signaling." J Bone Miner Res 24(10): 1651-1661.

197. Tu, X., et al. (2012). "Sost downregulation and local Wnt signaling are required for the osteogenic response to mechanical loading." Bone 50(1): 209-217.

198. Silva, B. C., et al. (2015). "Parathyroid hormone: anabolic and catabolic actions on the skeleton." Curr Opin Pharmacol 22: 41-50.

199. Kramer, I., et al. (2010). "Parathyroid hormone (PTH)-induced bone gain is blunted in SOST overexpressing and deficient mice." J Bone Miner Res 25(2): 178-189.

200. van Bezooijen, R. L., et al. (2004). "Sclerostin is an osteocyte-expressed negative regulator of bone formation, but not a classical BMP antagonist." J Exp Med 199(6): 805-814.

201. Sutherland, M. K., et al. (2004). "Sclerostin promotes the apoptosis of human osteoblastic cells: a novel regulation of bone formation." Bone 35(4): 828-835.

202. Wijenayaka, A. R., et al. (2011). "Sclerostin stimulates osteocyte support of osteoclast activity by a RANKL-dependent pathway." PLoS One 6(10): e25900.

203. Nolan, K., et al. (2014). "The DAN family: modulators of TGF-beta signaling and beyond." Protein Sci 23(8): 999-1012.

204. Ellies, D. L., et al. (2014). "Wise regulates bone deposition through genetic interactions with Lrp5." PLoS One 9(5): e96257.

205. Ahn, Y., et al. (2013). "Lrp4 and Wise interplay controls the formation and patterning of mammary and other skin appendage placodes by modulating Wnt signaling." Development 140(3): 583-593.

206. Collette, N. M., et al. (2013). "Sost and its paralog Sostdc1 coordinate digit number in a Gli3-dependent manner." Dev Biol 383(1): 90-105.

207. Collette, N. M., et al. (2016). "Sostdc1 deficiency accelerates fracture healing by promoting the expansion of periosteal mesenchymal stem cells." Bone 88: 20-30.

208. He, J. W., et al. (2011). "Contribution of the sclerostin domain-containing protein 1 (SOSTDC1) gene to normal variation of peak bone mineral density in Chinese

women and men." J Bone Miner Metab 29(5): 571-581.

209. Kakugawa, S., et al. (2015). "Notum deacylates Wnt proteins to suppress signalling activity." Nature 519(7542): 187-192.

210. Tarver, J. E., Jr., et al. (2016). "Stimulation of cortical bone formation with thienopyrimidine based inhibitors of Notum Pectinacetylesterase." Bioorg Med Chem Lett 26(6): 1525-1528.

211. Schulze, J., et al. (2010). "Negative regulation of bone formation by the transmembrane Wnt antagonist Kremen-2." PLoS One 5(4): e10309.

212. Mao, B., et al. (2002). "Kremen proteins are Dickkopf receptors that regulate Wnt/beta-catenin signalling." Nature 417(6889): 664-667.

213. Ellwanger, K., et al. (2008). "Targeted disruption of the Wnt regulator Kremen induces limb defects and high bone density." Mol Cell Biol 28(15): 4875-4882.

214. Nam, J. S., et al. (2006). "Mouse cristin/R-spondin family proteins are novel ligands for the Frizzled 8 and LRP6 receptors and activate beta-catenin-dependent gene expression." J Biol Chem 281(19): 13247-13257.

215. Binnerts, M. E., et al. (2007). "R-Spondin1 regulates Wnt signaling by inhibiting internalization of LRP6." Proc Natl Acad Sci U S A 104(37): 14700-14705.

216. Lu, W., et al. (2008). "R-spondin1 synergizes with Wnt3A in inducing osteoblast differentiation and osteoprotegerin expression." FEBS Lett 582(5): 643-650.

217. Jin, Y. R., et al. (2011). "The canonical Wnt signaling activator, R-spondin2, regulates craniofacial patterning and morphogenesis within the branchial arch through ectodermal-mesenchymal interaction." Dev Biol 352(1): 1-13.

218. Zhu, C., et al. (2016). "LGR4 acts as a key receptor for R-spondin 2 to promote osteogenesis through Wnt signaling pathway." Cell Signal 28(8): 989-1000.

219. Duncan, E. L., et al. (2011). "Genome-wide association study using extreme truncate selection identifies novel genes affecting bone mineral density and fracture risk." PLoS Genet 7(4): e1001372.

220. Carmon, K. S., et al. (2011). "R-spondins function as ligands of the orphan receptors LGR4 and LGR5 to regulate Wnt/beta-catenin signaling." Proc Natl Acad Sci U S A 108(28): 11452-11457.

221. de Lau, W., et al. (2011). "Lgr5 homologues associate with Wnt receptors and mediate R-spondin signalling." Nature 476(7360): 293-297.

222. Luo, J., et al. (2009). "Regulation of bone formation and remodeling by G-protein-coupled receptor 48." Development 136(16): 2747-2756.

223. Hatakeyama, J., et al. (2014). "Vangl1 and Vangl2: planar cell polarity components with a developing role in cancer." Endocr Relat Cancer 21(5): R345-356.

224. Wang, B., et al. (2011). "Disruption of PCP signaling causes limb morphogenesis and skeletal defects and may underlie Robinow syndrome and brachydactyly type

B." Hum Mol Genet 20(2): 271-285.

225. Galea, G. L., et al. (2015). "Planar cell polarity aligns osteoblast division in response to substrate strain." J Bone Miner Res 30(3): 423-435.

226. Jiang, Z., et al. (2014). "Wnt16 is involved in intramembranous ossification and suppresses osteoblast differentiation through the Wnt/beta-catenin pathway." J Cell Physiol 229(3): 384-392.

227. Goodwin, S., et al. (2016). "Coming of age: ten years of next-generation sequencing technologies." Nat Rev Genet 17(6): 333-351.

228. Buermans, H. P., et al. (2014). "Next generation sequencing technology: Advances and applications." Biochim Biophys Acta 1842(10): 1932-1941.

229. van Dijk, E. L., et al. (2014). "Ten years of next-generation sequencing technology." Trends Genet 30(9): 418-426.

230. Metzker, M. L. (2010). "Sequencing technologies - the next generation." Nat Rev Genet 11(1): 31-46.

231. Liu, L., et al. (2012). "Comparison of next-generation sequencing systems." J Biomed Biotechnol 2012: 251364.

232. Zhao, W., et al. (2014). "Comparison of RNA-Seq by poly (A) capture, ribosomal RNA depletion, and DNA microarray for expression profiling." BMC Genomics 15: 419.

233. Ewing, B., et al. (1998). "Base-calling of automated sequencer traces using phred. I. Accuracy assessment." Genome Res 8(3): 175-185.

234. Cock, P. J., et al. (2010). "The Sanger FASTQ file format for sequences with quality scores, and the Solexa/Illumina FASTQ variants." Nucleic Acids Res 38(6): 1767-1

235. Conesa, A., et al. (2016). "A survey of best practices for RNA-seq data analysis." Genome Biol 17: 13.

236. Wang, L., et al. (2012). "RSeQC: quality control of RNA-seq experiments." Bioinformatics 28(16): 2184-2185.

237. DeLuca, D. S., et al. (2012). "RNA-SeQC: RNA-seq metrics for quality control and process optimization." Bioinformatics 28(11): 1530-1532.

238. Kroll, K. W., et al. (2014). "Quality Control for RNA-Seq (QuaCRS): An Integrated Quality Control Pipeline." Cancer Inform 13(Suppl 3): 7-14.

239. http://www.bioinformatics.babraham.ac.uk/projects/fastqc/

240. Ruffalo, M., et al. (2012). "Accurate estimation of short read mapping quality for next-generation genome sequencing." Bioinformatics 28(18): i349-i355.

241. Bolger, A. M., et al. (2014). "Trimmomatic: a flexible trimmer for Illumina sequence data." Bioinformatics 30(15): 2114-2120.

242. Langmead, B., et al. (2012). "Fast gapped-read alignment with Bowtie 2." Nat Methods 9(4): 357-359.

243. Li, H., et al. (2009). "Fast and accurate short read alignment with Burrows-Wheeler transform." Bioinformatics 25(14): 1754-1760.

244. Liao, Y., et al. (2013). "The Subread aligner: fast, accurate and scalable read mapping by seed-and-vote." Nucleic Acids Res 41(10): e108.

245. Trapnell, C., et al. (2009). "TopHat: discovering splice junctions with RNA-Seq." Bioinformatics 25(9): 1105-1111.

246. Dobin, A., et al. (2013). "STAR: ultrafast universal RNA-seq aligner." Bioinformatics 29(1): 15-21.

247. Wu, T. D., et al. (2010). "Fast and SNP-tolerant detection of complex variants and splicing in short reads." Bioinformatics 26(7): 873-881.

248. Wang, K., et al. (2010). "MapSplice: accurate mapping of RNA-seq reads for splice junction discovery." Nucleic Acids Res 38(18): e178.

249. Muhamad, F.N., et al. (2015). "Reducing the search spaceand time complexity of needleman-wunsch algorithm (global alignment) andsmith-waterman algorithm (local alignment) for dna sequence alignment." JurnalTeknologi 77(20)

250. Loytynoja, A. (2012). "Alignment methods: strategies, challenges, benchmarking, and comparative overview." Methods Mol Biol 855: 203-235.

251. Kim, D., et al. (2013). "TopHat2: accurate alignment of transcriptomes in the presence of insertions, deletions and gene fusions." Genome Biol 14(4): R36.

252. Wu, T. D., et al. (2016). "GMAP and GSNAP for Genomic Sequence Alignment: Enhancements to Speed, Accuracy, and Functionality." Methods Mol Biol 1418: 283-334.

253. Engstrom, P. G., et al. (2013). "Systematic evaluation of spliced alignment programs for RNA-seq data." Nat Methods 10(12): 1185-1191.

254. Kent, W. J., et al. (2002). "The human genome browser at UCSC." Genome Res 12(6): 996-1006.

255. Trapnell, C., et al. (2012). "Differential gene and transcript expression analysis of RNA-seq experiments with TopHat and Cufflinks." Nat Protoc 7(3): 562-578.

256. Anders, S., et al. (2015). "HTSeq--a Python framework to work with high-throughput sequencing data." Bioinformatics 31(2): 166-169.

257. Liao, Y., et al. (2014). "featureCounts: an efficient general purpose program for assigning sequence reads to genomic features." Bioinformatics 30(7): 923-930.

258. Nicolae, M., et al. (2011). "Estimation of alternative splicing isoform frequencies from RNA-Seq data." Algorithms Mol Biol 6(1): 9.

259. Li, B., et al. (2011). "RSEM: accurate transcript quantification from RNA-Seq data with or without a reference genome." BMC Bioinformatics 12: 323.

260. Anders, S., et al. (2010). "Differential expression analysis for sequence count data." Genome Biol 11(10): R106.

261. Robinson, M. D., et al. (2010). "edgeR: a Bioconductor package for differential expression analysis of digital gene expression data." Bioinformatics 26(1): 139-140.

262. Ritchie, M. E., et al. (2015). "limma powers differential expression analyses for RNA-sequencing and microarray studies." Nucleic Acids Res 43(7): e47.

263. Law, C. W., et al. (2014). "voom: Precision weights unlock linear model analysis tools for RNA-seq read counts." Genome Biol 15(2): R29.

264. Law, C. W, et al.(2016) . "RNA-seq analysis is easy as 1-2-3 with limma, Glimma and edgeR". F1000Research 5:1408

265. Rapaport, F., et al. (2013). "Comprehensive evaluation of differential gene expression analysis methods for RNA-seq data." Genome Biol 14(9): R95.

266. Dillies, M. A., et al. (2013). "A comprehensive evaluation of normalization methods for Illumina high-throughput RNA sequencing data analysis." Brief Bioinform 14(6): 671-683.

267. Robinson, M. D., et al. (2010). "A scaling normalization method for differential expression analysis of RNA-seq data." Genome Biol 11(3): R25.

268. Bullard, J. H., et al. (2010). "Evaluation of statistical methods for normalization and differential expression in mRNA-Seq experiments." BMC Bioinformatics 11: 94.

269. Hardcastle, T. J., et al. (2010). "baySeq: empirical Bayesian methods for identifying differential expression in sequence count data." BMC Bioinformatics 11: 422.

270. Seyednasrollah, F., et al. (2015). "Comparison of software packages for detecting differential expression in RNA-seq studies." Brief Bioinform 16(1): 59-70.

271. Tarazona, S., et al. (2011). "Differential expression in RNA-seq: a matter of depth." Genome Res 21(12): 2213-2223.

272. Benjamini, Y., et al. (1995). "Controlling the false discovery rate: a practical and powerful approach to multiple testing." Journal of the royal statistical society. Series B (Methodological) 289-300

273. Huang, D. W., et al. (2007). "The DAVID Gene Functional Classification Tool: a novel biological module-centric algorithm to functionally analyze large gene lists." Genome Biol 8(9): R183.

274. Subramanian, A., et al. (2005). "Gene set enrichment analysis: a knowledge-based approach for interpreting genome-wide expression profiles." Proc Natl Acad Sci U S A 102(43): 15545-15550.

275. Eden, E., et al. (2009). "GOrilla: a tool for discovery and visualization of enriched GO terms in ranked gene lists." BMC Bioinformatics 10: 48.

276. Ernst, J., et al. (2006). "STEM: a tool for the analysis of short time series gene expression data." BMC Bioinformatics 7: 191.

277. Chen, J., et al. (2009). "ToppGene Suite for gene list enrichment analysis and candidate gene prioritization." Nucleic Acids Res 37(Web Server issue): W305-311.

278. Kanehisa, M., et al. (2000). "KEGG: kyoto encyclopedia of genes and genomes." Nucleic Acids Res 28(1): 27-30.

279. Ashburner, M., et al. (2000). "Gene ontology: tool for the unification of biology. The Gene Ontology Consortium." Nat Genet 25(1): 25-29.

280. Park, P. J. (2009). "ChIP-seq: advantages and challenges of a maturing technology." Nat Rev Genet 10(10): 669-680.

281. Buecker, C., et al. (2012). "Enhancers as information integration hubs in development: lessons from genomics." Trends Genet 28(6): 276-284.

282. (2012). "An integrated encyclopedia of DNA elements in the human genome." Nature 489(7414): 57-74.

283. Kundaje, A., et al. (2015). "Integrative analysis of 111 reference human epigenomes." Nature 518(7539): 317-330.

284. McLean, C. Y., et al. (2010). "GREAT improves functional interpretation of cis-regulatory regions." Nat Biotechnol 28(5): 495-501.

285. Yu, G., et al. (2015). "ChIPseeker: an R/Bioconductor package for ChIP peak annotation, comparison and visualization." Bioinformatics 31(14): 2382-2383.

286. Heinz, S., et al. (2010). "Simple combinations of lineage-determining transcription factors prime cis-regulatory elements required for macrophage and B cell identities." Mol Cell 38(4): 576-589.

287. Bailey, T. L., et al. (2015). "The MEME Suite." Nucleic Acids Res 43(W1): W39-49.

288. Liu, X. S., et al. (2002). "An algorithm for finding protein-DNA binding sites with applications to chromatin-immunoprecipitation microarray experiments." Nat Biotechnol 20(8): 835-839.

289. Zambelli, F., et al. (2013). "PscanChIP: Finding over-represented transcription factor-binding site motifs and their correlations in sequences from ChIP-Seq experiments." Nucleic Acids Res 41(Web Server issue): W535-543.

290. Hatem, A., et al. (2013). "Benchmarking short sequence mapping tools." BMC Bioinformatics 14: 184.

291. Hurgobin, B. (2016). "Short Read Alignment Using SOAP2." Methods Mol Biol 1374: 241-252.

292. http://bowtie-bio.sourceforge.net/index.shtml

293. Zhang, Y., et al. (2008). "Model-based analysis of ChIP-Seq (MACS)." Genome Biol 9(9): R137.

294. Rozowsky, J., et al. (2009). "PeakSeq enables systematic scoring of ChIP-seq

experiments relative to controls." Nat Biotechnol 27(1): 66-75.

295. Jothi, R., et al. (2008). "Genome-wide identification of in vivo protein-DNA binding sites from ChIP-Seq data." Nucleic Acids Res 36(16): 5221-5231.

296. Valouev, A., et al. (2008). "Genome-wide analysis of transcription factor binding sites based on ChIP-Seq data." Nat Methods 5(9): 829-834.

297. Zang, C., et al. (2009). "A clustering approach for identification of enriched domains from histone modification ChIP-Seq data." Bioinformatics 25(15): 1952-1958.

298. Wilbanks, E. G., et al. (2010). "Evaluation of algorithm performance in ChIP-seq peak detection." PLoS One 5(7): e11471.

299. Cheng, J., et al. (2014). "A role for H3K4 monomethylation in gene repression and partitioning of chromatin readers." Mol Cell 53(6): 979-992.

300. Young, M. D., et al. (2011). "ChIP-seq analysis reveals distinct H3K27me3 profiles that correlate with transcriptional activity." Nucleic Acids Res 39(17): 7415-7427

301. Neph, S., et al. (2012). "BEDOPS: high-performance genomic feature operations." Bioinformatics 28(14): 1919-1920.

302. Bailey, T. L., et al. (2009). "MEME SUITE: tools for motif discovery and searching." Nucleic Acids Res 37(Web Server issue): W202-208.

303. Bailey, T. L. (2011). "DREME: motif discovery in transcription factor ChIP-seq data." Bioinformatics 27(12): 1653-1659.

304. Ayturk, U. M., et al. (2013). "An RNA-seq protocol to identify mRNA expression changes in mouse diaphyseal bone: applications in mice with bone property altering Lrp5 mutations." J Bone Miner Res 28(10): 2081-2093.

305. Kelly, N. H., et al. (2016). "Transcriptional profiling of cortical versus cancellous bone from mechanically-loaded murine tibiae reveals differential gene expression." Bone 86: 22-29.

306. Meyer, M. B., et al. (2014). "The RUNX2 cistrome in osteoblasts: characterization, down-regulation following differentiation, and relationship to gene expression." J Biol Chem 289(23): 16016-16031.

307. St John, H. C., et al. (2014). "The osteoblast to osteocyte transition: epigenetic changes and response to the vitamin D3 hormone." Mol Endocrinol 28(7): 1150-1165.

308. Meyer, M. B., et al. (2016). "Epigenetic Plasticity Drives Adipogenic and Osteogenic Differentiation of Marrow-derived Mesenchymal Stem Cells." J Biol Chem 291(34): 17829-17847.

309. Khosla, S., et al. (2008). "Building bone to reverse osteoporosis and repair fractures." J Clin Invest 118(2): 421-428.

310. Bellows, C. G., et al. (1986). "Phenotypic differences in subclones and long-term

cultures of clonally derived rat bone cell lines." J Cell Biochem 31(2): 153-169.

311. Livak, K. J., et al. (2001). "Analysis of relative gene expression data using real-time quantitative PCR and the 2(-Delta Delta C(T)) Method." Methods 25(4): 402-408.

312. Kemp, J. P., et al. (2014). "Phenotypic dissection of bone mineral density reveals skeletal site specificity and facilitates the identification of novel loci in the genetic regulation of bone mass attainment." PLoS Genet 10(6): e1004423.

313. Huang da, W., et al. (2009). "Systematic and integrative analysis of large gene lists using DAVID bioinformatics resources." Nat Protoc 4(1): 44-57.

314. Bouxsein, M. L., et al. (2010). "Guidelines for assessment of bone microstructure in rodents using micro-computed tomography." J Bone Miner Res 25(7): 1468-1486.

315. Spiegelman, B. M., et al. (1997). "PPAR gamma and the control of adipogenesis." Biochimie 79(2-3): 111-112.

316. Bi, W., et al. (1999). "Sox9 is required for cartilage formation." Nat Genet 22(1): 85-89.

317. Shahnazari, M., et al. (2013). "CXCL12/CXCR4 signaling in the osteoblast regulates the mesenchymal stem cell and osteoclast lineage populations." Faseb j 27(9): 3505-3513.

318. He, X., et al. (2016). "TLR4 Activation Promotes Bone Marrow MSC Proliferation and Osteogenic Differentiation via Wnt3a and Wnt5a Signaling." PLoS One 11(3): e0149876.

319. Zhan, Q., et al. (2015). "Activation of TLR3 induces osteogenic responses in human aortic valve interstitial cells through the NF-kappaB and ERK1/2 pathways." Int J Biol Sci 11(4): 482-493.

320. Liu, G., et al. (2009). "Canonical Wnts function as potent regulators of osteogenesis by human mesenchymal stem cells." J Cell Biol 185(1): 67-75.

321. Zhou, H., et al. (2009). "Glucocorticoid-dependent Wnt signaling by mature osteoblasts is a key regulator of cranial skeletal development in mice." Development 136(3): 427-436.

322. Jackson, A., et al. (2005). "Gene array analysis of Wnt-regulated genes in C3H10T1/2 cells." Bone 36(4): 585-598.

323. Abe, E., et al. (2000). "Essential requirement of BMPs-2/4 for both osteoblast and osteoclast formation in murine bone marrow cultures from adult mice: antagonism by noggin." J Bone Miner Res 15(4): 663-673.

324. Su, J. L., et al. (2010). "CYR61 regulates BMP-2-dependent osteoblast differentiation through the {alpha}v{beta}3 integrin/integrin-linked kinase/ERK pathway." J Biol Chem 285(41): 31325-31336.

325. Qiu, W., et al. (2010). "Tumor necrosis factor receptor superfamily member 19 (TNFRSF19) regulates differentiation fate of human mesenchymal (stromal) stem cells through canonical Wnt signaling and C/EBP." J Biol Chem 285(19): 14438-

14449.

326. Jullien, N., et al. (2012). "Downregulation of ErbB3 by Wnt3a contributes to wnt-induced osteoblast differentiation in mesenchymal cells." J Cell Biochem 113(6): 2047-2056.

327. Jin, Z., et al. (2015). "HDAC9 Inhibits Osteoclastogenesis via Mutual Suppression of PPARgamma/RANKL Signaling." Mol Endocrinol 29(5): 730-738.

328. Daniels, D. L., et al. (2005). "Beta-catenin directly displaces Groucho/TLE repressors from Tcf/Lef in Wnt-mediated transcription activation." Nat Struct Mol Biol 12(4): 364-371.

329. Yavropoulou, M. P., et al. (2007). "The role of the Wnt signaling pathway in osteoblast commitment and differentiation." Hormones (Athens) 6(4): 279-294.

330. Pike, J. W., et al. (2015). "Epigenetic histone modifications and master regulators as determinants of context dependent nuclear receptor activity in bone cells." Bone 81: 757-764.

331. Dose, M., et al. (2014). "beta-Catenin induces T-cell transformation by promoting genomic instability." Proc Natl Acad Sci U S A 111(1): 391-396.

332. Wu, J. Q., et al. (2012). "Tcf7 is an important regulator of the switch of self-renewal and differentiation in a multipotential hematopoietic cell line." PLoS Genet 8(3): e1002565.

333. Chen, C., et al. (2014). "Genome-wide ChIP-seq analysis of TCF4 binding regions in colorectal cancer cells." Int J Clin Exp Med 7(11): 4253-4259.

334. Watanabe, K., et al. (2014). "Integrative ChIP-seq/microarray analysis identifies a CTNNB1 target signature enriched in intestinal stem cells and colon cancer." PLoS One 9(3): e92317.

335. Zentner, G. E., et al. (2011). "Epigenetic signatures distinguish multiple classes of enhancers with distinct cellular functions." Genome Res 21(8): 1273-1283.

336. Creyghton, M. P., et al. (2010). "Histone H3K27ac separates active from poised enhancers and predicts developmental state." Proc Natl Acad Sci U S A 107(50): 21931-21936.

337. Calo, E., et al. (2013). "Modification of enhancer chromatin: what, how, and why?" Mol Cell 49(5): 825-837.

338. Barrett, T., et al. (2013). "NCBI GEO: archive for functional genomics data sets--update." Nucleic Acids Res 41(Database issue): D991-995.

339. Kuhn, R. M., et al. (2013). "The UCSC genome browser and associated tools." Brief Bioinform 14(2): 144-161.

340. Robinson, J. T., et al. (2011). "Integrative genomics viewer." Nat Biotechnol 29(1): 24-26.

341. Ovcharenko, I., et al. (2004). "ECR Browser: a tool for visualizing and accessing

data from comparisons of multiple vertebrate genomes." Nucleic Acids Res 32(Web Server issue): W280-286.

342. Chen, R. H., et al. (2000). "Wnt signaling to beta-catenin involves two interactive components. Glycogen synthase kinase-3beta inhibition and activation of protein kinase C." J Biol Chem 275(23): 17894-17899.

343. Corradin, O., et al. (2014). "Enhancer variants: evaluating functions in common disease." Genome Med 6(10): 85.

344. Nateri, A. S., et al. (2005). "Interaction of phosphorylated c-Jun with TCF4 regulates intestinal cancer development." Nature 437(7056): 281-285.

345. Toualbi, K., et al. (2007). "Physical and functional cooperation between AP-1 and beta-catenin for the regulation of TCF-dependent genes." Oncogene 26(24): 3492-3502.

346. Bozec, A., et al. (2010). "Fra-2/AP-1 controls bone formation by regulating osteoblast differentiation and collagen production." J Cell Biol 190(6): 1093-1106.

347. Bozec, A., et al. (2013). "Osteoblast-specific expression of Fra-2/AP-1 controls adiponectin and osteocalcin expression and affects metabolism." J Cell Sci 126(Pt 23): 5432-5440.

348. Johnell, O., et al. (2006). "An estimate of the worldwide prevalence and disability associated with osteoporotic fractures." Osteoporos Int 17(12): 1726-1733.

349. Canalis, E. (2013). "Wnt signalling in osteoporosis: mechanisms and novel therapeutic approaches." Nat Rev Endocrinol 9(10): 575-583.

350. Sebastian, A., et al. (2016). "Transcriptional control of Sost in bone." Bone.

351. Niu, T., et al. (2016). "Identification of IDUA and WNT16 Phosphorylation-Related Non-Synonymous Polymorphisms for Bone Mineral Density in Meta-Analyses of Genome-Wide Association Studies." J Bone Miner Res 31(2): 358-368.

352. Medina-Gomez, C., et al. (2012). "Meta-analysis of genome-wide scans for total body BMD in children and adults reveals allelic heterogeneity and age-specific effects at the WNT16 locus." PLoS Genet 8(7): e1002718.

353. Hendrickx, G., et al. (2014). "Variation in the Kozak sequence of WNT16 results in an increased translation and is associated with osteoporosis related parameters." Bone 59: 57-65.

354. Green, J. L., et al. (2013). "Use of a molecular genetic platform technology to produce human Wnt proteins reveals distinct local and distal signaling abilities." PLoS One 8(3): e58395.

355. Teh, M. T., et al. (2007). "Role for WNT16B in human epidermal keratinocyte proliferation and differentiation." J Cell Sci 120(Pt 2): 330-339.

356. Wu, M., et al. (2016). "TGF-beta and BMP signaling in osteoblast, skeletal development, and bone formation, homeostasis and disease." Bone Res 4: 16009.

357. Collette, N. M., et al. (2012). "Targeted deletion of Sost distal enhancer increases bone formation and bone mass." Proc Natl Acad Sci U S A 109(35): 14092-14097.

358. Zheng, H. F., et al. (2013). "Meta-analysis of genome-wide studies identifies MEF2C SNPs associated with bone mineral density at forearm." J Med Genet 50(7): 473-478.

359. Warner, D. R., et al. (2005). "Cross-talk between the TGFbeta and Wnt signaling pathways in murine embryonic maxillary mesenchymal cells." FEBS Lett 579(17): 3539-3546.

360. Wong, C., et al. (1999). "Smad3-Smad4 and AP-1 complexes synergize in transcriptional activation of the c-Jun promoter by transforming growth factor beta." Mol Cell Biol 19(3): 1821-1830.

361. Liberati, N. T., et al. (1999). "Smads bind directly to the Jun family of AP-1 transcription factors." Proc Natl Acad Sci U S A 96(9): 4844-4849.

362. Zhang, Y., et al. (1998). "Smad3 and Smad4 cooperate with c-Jun/c-Fos to mediate TGF-beta-induced transcription." Nature 394(6696): 909-913.

363. Goel, S., et al. (2012). "Both LRP5 and LRP6 receptors are required to respond to physiological Wnt ligands in mammary epithelial cells and fibroblasts." J Biol Chem

364. Mohammed, H., et al. (2016). "Rapid immunoprecipitation mass spectrometry of endogenous proteins (RIME) for analysis of chromatin complexes." Nat Protoc 11(2): 316-3